



Universiteit
Leiden
The Netherlands

Calcium-dependent regulation of auxin transport in plant development

Wei, X.

Citation

Wei, X. (2024, January 11). *Calcium-dependent regulation of auxin transport in plant development*. Retrieved from <https://hdl.handle.net/1887/3677385>

Version: Publisher's Version

License: [Licence agreement concerning inclusion of doctoral thesis in the Institutional Repository of the University of Leiden](#)

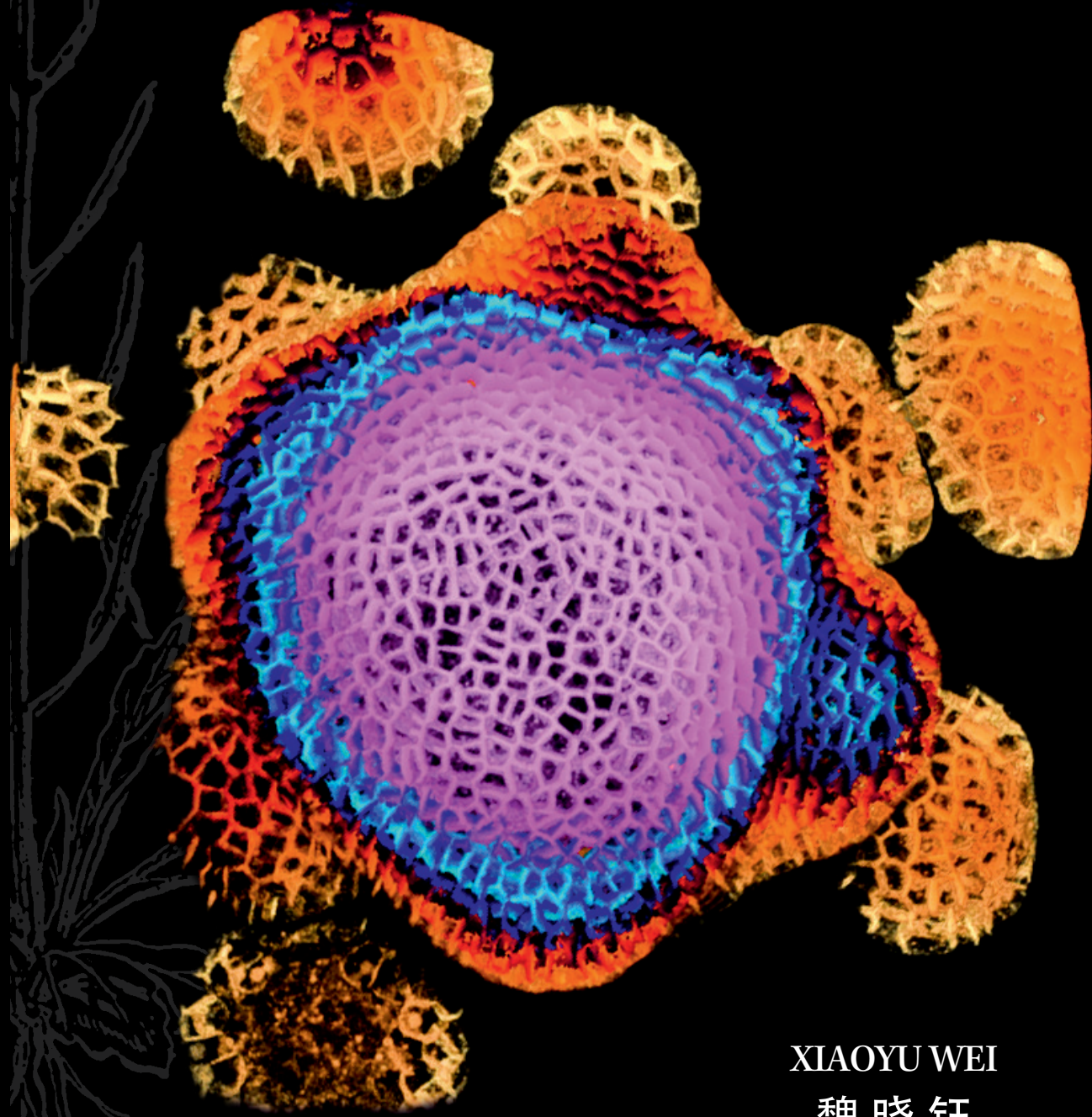
Downloaded from: <https://hdl.handle.net/1887/3677385>

Note: To cite this publication please use the final published version (if applicable).

Calcium-dependent regulation of auxin transport in plant development

Calcium-dependent regulation of auxin transport in plant development

XIAOYU WEI 2024



XIAOYU WEI
魏晓钰

Calcium-dependent regulation of auxin transport in plant development

Xiaoyu Wei

魏 晓 钰

© 2024 Xiaoyu Wei, Leiden, The Netherlands.

This work was supported by the China Scholarship Council.

Front cover: Inflorescence meristem of *Arabidopsis pid* mutant expressing “untouchable” PID

Cover design: Xiaoyu Wei, Sandra Tukker

ISBN: 978-94-6483-650-9

Printed by: Ridderprint, www.ridderprint.nl

Calcium-dependent regulation of auxin transport in plant development

Proefschrift

ter verkrijging van
de graad van doctor aan de Universiteit Leiden,
op gezag van rector magnificus prof.dr.ir. H. Bijl,
volgens besluit van het college voor promoties
te verdedigen op donderdag 11 januari 2024
klokke 10:00 uur

door

Xiaoyu Wei

Geboren te Yan'an (Shaanxi, China)

in 1989

Promotor:

Prof. dr. R. Offringa

Co-promotor:

Prof. dr. P.J.J. Hooykaas

Promotiecommissie:

Prof. dr. A.H. Meijer

Prof. dr. J. Memelink

Dr. S. Balazadeh

Prof. dr. R.M.H. Merks

Dr. M. Geisler, University of Fribourg

Prof. dr. ir. J.H.B. Sprakel, Wageningen University & Research

Contents

Chapter 1

The role of calcium as second messenger in auxin transport and signaling	7
--	---

Chapter 2

CALMODULIN-LIKE 12/TOUCH 3 and closely related calmodulins and calmodulin-like proteins redundantly interact with the PINOID kinase	67
---	----

Chapter 3

PINOID plasma membrane association and CALMODULIN-LIKE 12/TOUCH 3 binding converge on an amphipathic alpha-helix in the kinase insertion domain	99
---	----

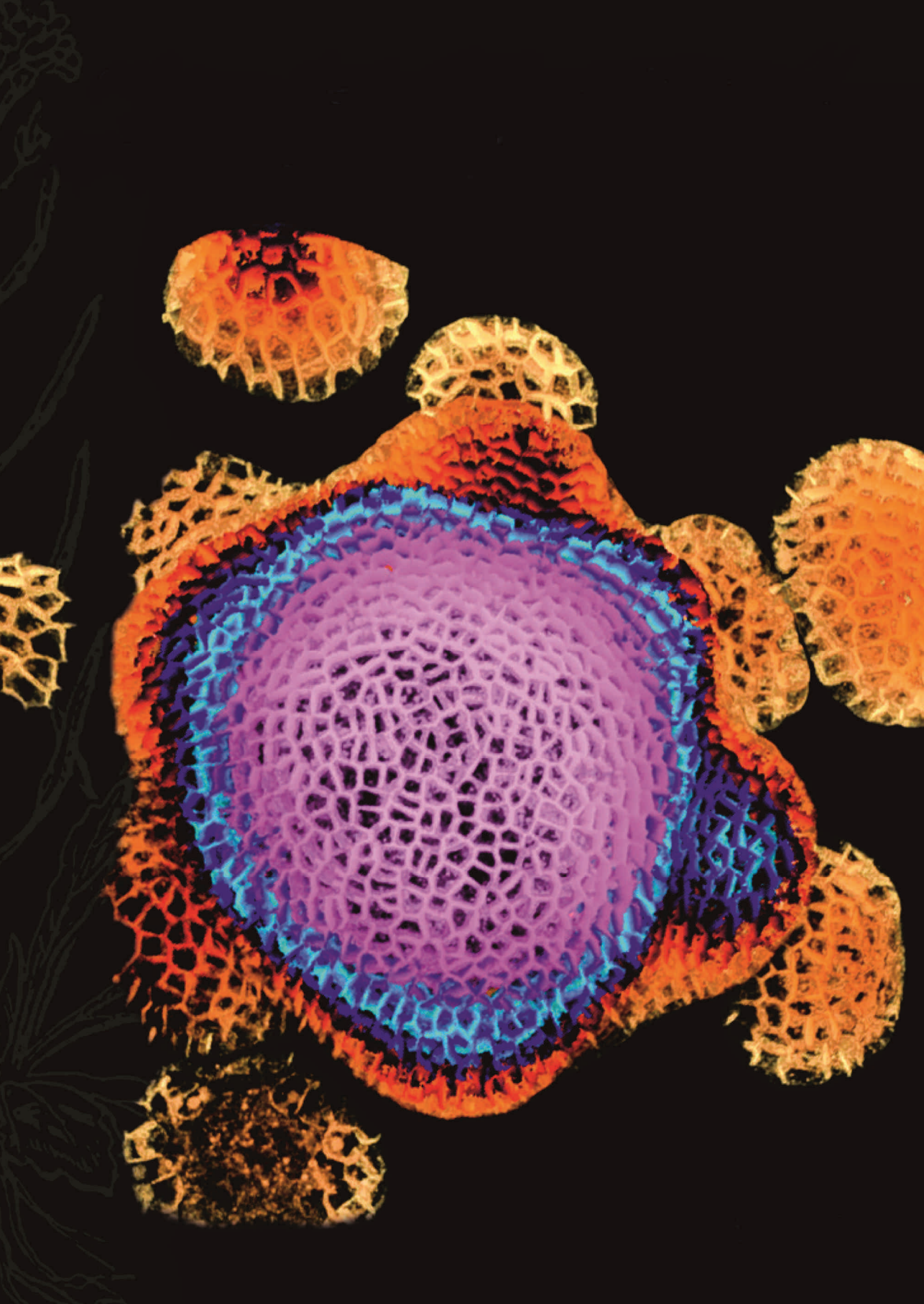
Chapter 4

Calcium-regulated PINOID kinase activity is required for a robust spiral phyllotaxis in the Arabidopsis inflorescence	141
---	-----

Summary	173
---------	-----

Samenvatting	181
--------------	-----

Curriculum Vitae	187
------------------	-----



Chapter 1

The role of calcium as second messenger in auxin transport and signaling

(Introduction)

Xiaoyu Wei¹ and Remko Offringa¹

¹ Plant Developmental Genetics, Institute of Biology Leiden, Leiden University, Sylviusweg 72, 2333 BE, Leiden, Netherlands

1. The phytohormone auxin is a pivotal regulator of plant growth, development and adaptation to the environment

Auxin was the first hormone to be discovered. Its existence was already predicted by Charles Darwin and his son in their book *The Power of Movement in Plants* in 1880 (Darwin and Darwin, 1880), and demonstrated later by Went through his coleoptile bending experiments in 1926 (Went, 1926), and its chemical structure, indole-3-acetic acid (IAA), was determined in the 1930s (Kögl et al., 1934). Intensive research has since revealed that auxin is involved in nearly every aspect of plant growth and development.

Auxin plays a crucial role in various developmental processes, including embryogenesis (Winnicki, 2020), organogenesis in the root (Benková et al., 2003; Cavallari et al., 2021) and in the shoot (Benková et al., 2003), which includes phyllotaxis (Bohn-Courseau, 2010; Sassi and Vernoux, 2013), organ patterning (Qi et al., 2014) and morphogenesis (Chitwood et al., 2012; Heisler and Byrne, 2020). It has a broad role in plant growth and development, as it regulates basic cellular processes, such as cell division, cell expansion, and cell differentiation (Perrot-Rechenmann, 2010; Ding and Friml, 2010; Du et al., 2020).

Auxin also is a major determinant in a plant's response to the environment. Due to their sessile nature, plants have evolved a remarkable capacity for morphological plasticity in response to changing and often unfavourable environments. They modify their growth and development through the perception and integration of exogenous signals, utilizing auxin as a coordinative signal. The exogenous signals include light (Halliday et al., 2009; Hohm et al., 2013), gravity (Baster et al., 2013), obstacles (Lee et al., 2020), salinity (Wang et al., 2019), mechanical stress (Nakayama et al., 2012) and osmotic stress (Naser and Shani, 2016), among others. In addition, auxin interplays with other endogenous signals, such as the plant hormones cytokinins, brassinosteroids, ethylene, abscisic acid, gibberellins, jasmonic acid and strigolactones, or important compounds such as nitrate, phosphate, polyamines and sugars

(Saini et al., 2013; Mroue et al., 2018). Through these interactions, auxin specifies organ orientation and positioning by regulating cell growth and division.

Auxin action is primarily achieved through differential concentrations, which are established and maintained by a combination of biosynthesis, homeostasis, degradation and transport, and eventually by its perception and signal transduction. In this chapter, we will focus on the mechanisms of auxin perception and signaling, the differential distribution of this hormone by its polar transport and the involvement of Ca^{2+} signaling in these processes.

2. Auxin perception and signalling

The asymmetric distribution of auxin in tissues is primarily established through local auxin synthesis and polar auxin transport (PAT). This spatial distribution of auxin is then translated into varying intensities of auxin signaling, which in turn determines the rate of cell division, cell expansion and cell differentiation, ultimately influencing the growth and developmental responses of a plant (Chen, 2001; Benková et al., 2003; Paciorek and Friml, 2006; Yu et al., 2022b). Auxin perception and signal transduction occur through different signaling pathways, known as the canonical and non-canonical pathways (Figure 1).

The TRANSPORT INHIBITOR RESPONSE 1/AUXIN SIGNALING F-BOX proteins (TIR1/AFB), the AUXIN/INDOLE-3-ACETIC ACID (Aux/IAA) transcriptional repressor proteins, and the AUXIN RESPONSE FACTOR (ARF) transcription factors together form the canonical auxin signaling pathway (Reviewed in Yu et al., 2022b). Briefly, intracellular auxin acts like a “molecular glue” and promotes the association of TIR1/AFBs, which are components of the ubiquitin-ligase (E3) complex SKP1-CUL-FBP (SCF), and Aux/IAAs via hydrophobic interaction forces, forming an E2-SCF^{TIR1/AFB}-Aux/IAA complex. Aux/IAAs are subsequently polyubiquitinated and degraded by the 26S

proteasome, thus releasing their inhibition of ARF transcription factors and leading to activation of auxin-dependent transcription.

Despite the canonical TIR1/AFB-Aux/IAA-ARF pathway explaining the main auxin responses, accumulating evidence challenges its exclusivity. For example, exogenous auxin treatment can trigger an increase in cytosolic Ca^{2+} $[\text{Ca}^{2+}]_{\text{cyt}}$ within 7-14 seconds (Monshausen et al., 2011) and reduce elongation growth within 30 seconds in the *Arabidopsis thaliana* (*Arabidopsis*) primary root (Fendrych et al., 2018), which is too fast for the canonical, transcription-mediated pathway of auxin signaling. Moreover, auxin-inhibited clathrin-mediated PIN endocytosis was shown to be TIR1-independent (Paciorek et al., 2005), suggesting the existence of non-canonical pathways that are important in the coordination of plant growth and development. Notably, a recent study showed that TIR1/AFBs possess adenylate cyclase (AC) activity and stimulates cAMP production, which is crucial in regulation of root growth and transcriptional response, indicating that TIR1/AFBs translate auxin signaling in a dual way (Qi et al., 2022; Figure 1).

Arabidopsis AUXIN BINDING PROTEIN1 (ABP1) has long been reported and is believed to be an auxin receptor responsible for rapid, non-transcriptional signaling events at the cell surface, regulating clathrin-mediated endocytosis to affect PIN distribution, cell expansion, and cytoskeletal rearrangements (Yu et al., 2022b). However, recent findings and studies have raised questions about its importance as an auxin receptor, with some studies claiming that “ABP1 is not required for either auxin signaling or *Arabidopsis* development” due to the fact that verified *abp1* knockout alleles do not show obvious growth defects or auxin insensitivity (Gao et al., 2015; Dai et al., 2015; Michalko et al., 2015; Gelová et al., 2021). Meanwhile, new evidence supporting ABP1 as auxin receptor has been reported. ER-localized ABP1 can be secreted to the apoplast and can interact with the extracellular domain of the plasma membrane (PM)-localized receptor-like kinase TRANSMEMBRANE KINASE 1 (TMK1) in an auxin-dependent manner. This interaction is required for a subset of rapid cellular effects, such as an auxin-

The role of calcium as second messenger in auxin transport and signaling

induced ultrafast global phospho-response, activation of H⁺-ATPases and accelerated cytoplasmic streaming, and development mediated by auxin canalization (Friml et al., 2022). Therefore, the role of ABP1 in auxin signaling is much more complicated than previously thought, and further investigation is needed.

Another non-canonical auxin signaling pathway, dependent on the ubiquitin-proteasome system, has been shown by the complex of the Arabidopsis S-Phase Kinase-Associated Protein 2A (SKP2A), E2FC and dimerization partner of E2FB (DPB). Similar to TIR1/AFBs, SKP2A is an F-box protein subunit of the SCF ubiquitin ligase. The binding of auxin promotes the ubiquitin-mediated degradation of the cell cycle repressors E2FC and DPB, thus promoting cell cycle progression (Jurado et al., 2010).

Additionally, another non-canonical pathway dependent on ARFs has been revealed by the variant ARF3, also known as ETTIN (ETT). Unlike the typical Aux/IAA interaction domain, ARF3 harbors a long and intrinsically disordered C-terminal domain – the ETT-specific domain. This domain enables ARF3 to interact with a set of alternative transcriptional regulators that determine plant shape and pattern, such as INDEHISCENT (IND), REPLUMLESS (RPL), BREVIPEDICELLUS (BP), ABERRANT TESTA SHAPE (ATS), PLETHORA5 (PLT5), KNOTTED-LIKE FROM ARABIDOPSIS THALIANA1/3 (KNAT1/3), BABYBOOM (BBM), TEOSINTE BRANCHED1(TB1)/BRANCHED1 (BRC1), CYCLOIDEA AND PCF4/18 (TCP4/18) and TOPLESS (TPL) (Simonini et al., 2016; Simonini et al., 2018; Kuhn et al., 2020). IAA can bind directly to this domain, thus disrupting these interactions and thereby affecting the expression of a group of genes involved in different growth and development processes (Simonini et al., 2016; Kuhn et al., 2020; Figure 1).

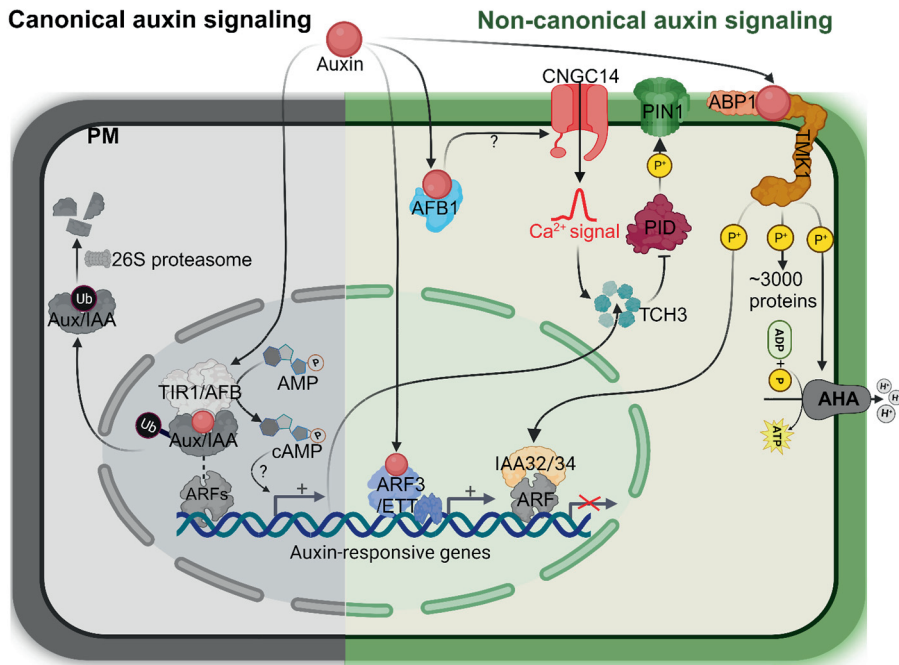


Figure 1. Canonical and non-canonical auxin signaling. Left: canonical nuclear TIR1/AFB-Aux/IAA-ARFs pathway. Right: non-canonical auxin signaling. Details are described in the main text. PM: Plasma membrane.

Similarly to ARF3, there are also nonconformists among the Aux/IAAs. For example, IAA33, lacking the domains I and II that are essential for TIR1/AFB-binding, can be induced by auxin and stabilized by auxin via MITOGEN-ACTIVATED PROTEIN KINASE 14 (MPK14) on the one hand. On the other hand, it can compete with IAA5 to interact and thus release the repression of ARF10/16, helping to maintain the root stem cell (Ding and Friml, 2010; Lv et al., 2020). IAA32 and IAA34, lacking the canonical domain II, are targeted and phosphorylated in the nucleus by the C-terminal kinase domain of TMK1, which is cleaved off from TMK1 after auxin treatment, regulating differential growth of the apical hook (Cao et al., 2019; Figure 1). The other two noncanonical Aux/IAAs also lacking the canonical domain II are IAA20 and IAA30 (Dreher et al., 2006). Overexpression of IAA20 and IAA30 shows similar auxin-related aberrant

phenotypes: affected gravitropic growth, malformed vasculature of cotyledons and collapse of the root apical meristem (Sato and Yamamoto, 2008; Muller et al., 2016). Furthermore, their double mutant *iaa20/30* forms ectopic protoxylem (Muller et al., 2016). Hence, it is likely that IAA20 and IAA30 may also have a potential to play some roles in auxin signaling.

Overall, the understanding of auxin signaling has expanded beyond the canonical TIR1/AFB-Aux/IAA-ARFs pathway, with accumulating evidence supporting the existence and importance of non-canonical pathways. Further investigations are needed to fully elucidate the intricate mechanisms underlying auxin signaling and its roles in plant growth and development.

3. Polar auxin transport driven by PIN proteins

3.1 Mechanisms of auxin distribution

Auxin functions through the development of gradients and concentration maxima and minima within developing tissues, providing positional cues for diverse developmental processes (Geisler, 2021). It is primarily synthesized in the shoot and redistributed throughout the plant by two distinct, but interconnected, transport systems: fast passive transport in the phloem and slow cell-to-cell PAT. Phloem transport delivers auxin from its synthesis sites to recipient organs, while PAT distributes auxin in a precise manner to establish and maintain local auxin gradients and maxima/minima mainly in developing tissues or in response to exogenous and endogenous signals (Adamowski and Friml, 2015).

At the cellular level, the chemiosmotic hypothesis explains PAT based on the chemical properties of the principal auxin form, IAA (Rubery and Sheldrake, 1973; Raven, 1975; Goldsmith, 1977; Figure 2). As IAA is a weak acid, a portion exists in a protonated state (IAAH) in the slightly acidic pH of the apoplast (pH 5.5), becoming hydrophobic and able to passively diffuse through the PM. Once inside the neutral cytoplasm (pH 7.0), auxin becomes deprotonated (IAA^-) and unable to

pass the PM easily by diffusion, thus getting “trapped” inside the cell. For auxin to be transported out of the cell, the action of efflux carriers is required, and these efflux transporters need to be polarly localized at the PM to control the directionality of auxin flow.

3.2 PIN efflux carriers

According to the chemiosmotic hypothesis, the directionality of intercellular auxin transport depends on the polar subcellular localization of different types of auxin transporters. In Arabidopsis, four main classes of auxin transporters have been identified: the PIN-FORMED (PIN) efflux carriers, the PIN-likes (PILS), the AUXIN RESISTANT 1 (AUX1) and AUX1-LIKE (LAX) influx transporters, and the ATP-binding cassette B (ABCB)-type transporters (reviewed by Grones and Friml, 2015, and Geisler, 2021; Figure 2). Apart from these four major classes, some proteins from other transporter families have been reported to transport auxin, such as NITRATE TRANSPORTER 1.1 (NRT1.1) and WALLS ARE THIN 1 (WAT1) (reviewed in Geisler 2021; Figure 2). Among these transporters, the PIN efflux carriers play a crucial role, as they are rate-limiting for PAT, and their asymmetric localization within cells determines the directionality of intercellular auxin flow and thus the position of the auxin maximum or minimum formed (Petrášek et al., 2006; Wiśniewska et al., 2006; Prasad and Dhonukshe, 2013).

The PIN proteins are a plant-specific family of transmembrane (TM) proteins, named after the pin-shaped inflorescence of the Arabidopsis *pin formed 1* (*pin1*) mutant. They consist of two hydrophobic TM regions, interrupted by a short or long hydrophilic loop (HL) (Okada et al., 1991; Viaene et al., 2013). A recent biophysical study showed that of PINs form a homodimer structure, each monomer composed of a transport and scaffold domain with a clearly defined auxin binding site (Ung et al., 2022). And a proline–proline crossover next to the binding site is crucial for structural changes during auxin transport, which is independent of proton and ion gradients. In Arabidopsis, eight PINs have been identified, which

The role of calcium as second messenger in auxin transport and signaling

are divided into “long” (PIN1-4, 6 and 7) and “short” (PIN 5 and 8) PINs based on the length of their HL (Křeček et al., 2009; Viaene et al., 2013). The long PINs (PIN1-4 and 7) predominantly show polar PM-localization, determining the direction of auxin flow (Petrásek et al., 2006; Zažímalová et al., 2010; Adamowski and Friml, 2015). In contrast, the short PINs (PIN5 and 8) do not localize at the PM but reside at the endoplasmic reticulum (ER), where they mediate auxin flow between the cytoplasm and ER to regulate subcellular auxin homeostasis (Mravec et al., 2009; Bosco et al., 2012a; Dal Bosco et al., 2012b; Ding et al., 2012; Figure 1). PIN6 is considered as a member of the long PIN subfamily due to its high sequence similarity in the TM regions, the presence of an HL that is only partially reduced in size (Křeček et al., 2009), and its phosphorylation state-dependent localization at both the PM and ER (Simon et al., 2016; Ditengou et al., 2018; Sisi and Růžicka, 2020).

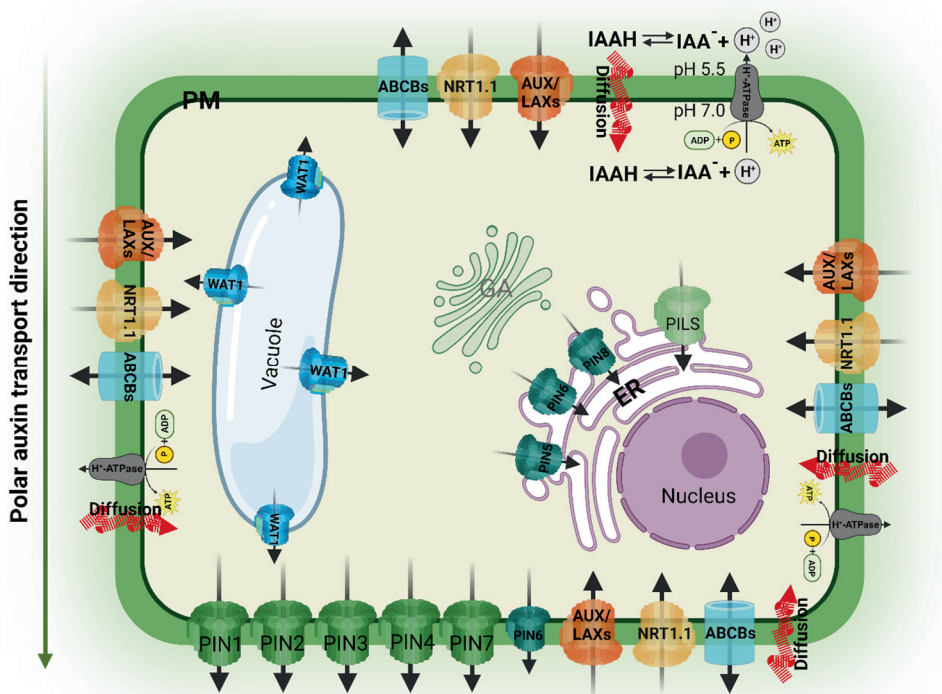


Figure 2. Mechanisms of subcellular auxin distribution and cell-to-cell PAT and the auxin transporters involved. Schematic representation of a cell in a row, indicating passive auxin diffusion and the different auxin transporters involved in subcellular auxin distribution and PAT. The direction auxin diffusion and (polar) auxin transport is indicated by arrows. ER: Endoplasmic reticulum; GA: Golgi apparatus; PM: Plasma membrane.

3.3 Polar auxin transport regulated plant growth and development

PIN-driven PAT (primarily through the long PINs PIN1-4 and 7) plays a crucial role in modulating auxin-dependent plant growth and development and a plant's response to exogenous and endogenous signals.

In *Arabidopsis*, during embryogenesis, PIN1, 3, 4, and 7 are expressed in different places and at different times, mediating the dynamic and shifting pattern of auxin accumulation. This contributes to the establishment of apical-basal polarity and induces the formation of primordia for aerial and underground organs (Friml et al., 2003). Single mutations in these PINs cause developmental defects in early embryogenesis, with aberrations becoming increasingly severe in multiple mutant combinations (Friml et al., 2002; Friml et al., 2003; Blilou et al., 2005; Vieten et al., 2005; Jenik and Barton, 2005).

During seedling development, at the root tip, PIN1, PIN2, PIN3, PIN4, and PIN7 work together to establish a local “reflux loop” (or “reverse fountain”) of auxin, generating a symmetrical auxin gradient with a maximum close to the root tip. This gradient maintains root stem cell activity, root growth and patterning (Friml et al., 2002a; Friml et al., 2003; Blilou et al., 2005; Kleine-Vehn et al., 2010; Wabnik et al., 2011). For apical hook formation, PIN1, 3, 4 and 7 cooperate in regulating the dynamic, asymmetric distribution of auxin, resulting in differential growth at the apical hook (Žádníková et al., 2010). PIN1-driven PAT also plays a major role in lateral roots initiation (Benková et al., 2003), vascular tissue differentiation and regeneration (Galweiler et al., 1998; Mattsson et al., 1999; Scarpella et al., 2010; Marcos and Berleth, 2014; Mazur et al., 2016), leaf and flower positioning (phyllotaxis) and organogenesis (Okada et al., 1991; Reinhardt et al., 2000, 2003; Aloni et al., 2003; Qi et al., 2014; Deb et al., 2015; Xiong and Jiao, 2019).

The role of calcium as second messenger in auxin transport and signaling

The dynamic polar subcellular localization of PIN proteins enables them to redirect auxin flow and form auxin gradients, leading to differential cell elongation and organ bending in response to endogenous and external signals. Gravity is a fundamental environmental signal that modulates plant growth through gravitropism. PIN2 is the main player mediating auxin transport in root gravitropism, as indicated by the strong agravitropic phenotype of *Arabidopsis pin2* mutant roots (Luschnig et al., 1998). PIN2 transports auxin from the root tip, where gravity is perceived, to the elongation zone, where growth is regulated (Abas et al., 2006; Sukumar et al., 2009; Lešková et al., 2020). PIN3 and PIN7 are also required for root gravitropism, polarly localizing at lower sides of columella cells to transport auxin towards the lower side of the root tip after gravistimulation (Friml et al., 2002b; Kleine-Vehn et al., 2010; Wang et al., 2015a, Ruiz Rosquete et al., 2018).

Light is another essential environmental signal for plant development. In etiolated hypocotyls, PIN3 apolarly localizes in endodermal cells, but with unilateral blue light stimulation, PIN3 gradually polarizes to and is stabilized at the endodermal cell sides away from the light source. This directs auxin flow to the shaded side of the hypocotyl, resulting in shoot growth toward the light source (positive phototropic response) (Ding et al., 2011). Conversely, *Arabidopsis* roots exhibit a negative phototropic response. In dark grown roots, PIN1 and PIN2 become less polarized at the PM and show internalized localization in intracellular compartments. PIN2 was proposed to stabilize at the PM at the light side and to be removed from the PM at the shaded side of the root through vacuole-targeted degradation (Wan et al., 2012), while PIN3 was reported to polarize to the lateral membranes towards the light in the root columella cells at the root tip. As a result, auxin was proposed to accumulate at the illuminated root side to promote growth, causing roots to grow away from the light (negative phototropic response) (Zhang et al., 2013). However, this does not fit with the observation that elevated auxin levels at the lower side of the root during the root gravitropic response trigger the

opposite (positive gravitropic) growth response. More recently, evidence was provided that the positive phototropic response of the root does not require an asymmetric auxin distribution, and that the elevated auxin levels observed at the illuminated side only appear after the first phototropic root bending, probably caused by the counteracting positive gravitropic response (Kimura et al., 2018). The exact mechanism of root phototropism still remains to be established.

PIN-driven PAT also plays a role in response to abiotic stress. For example, salinity induces internalization of PIN2 from the PM at the side of the root proximal to the area of high salt concentration, and therefore differential PIN2 distribution redirects auxin flow to the root side without salt, resulting in the root growing away from the high salt concentration area (Galvan-Ampudia et al., 2013). In addition to responding to environmental signals, PIN-driven PAT is also involved in responses to endogenous signals, such as auxin (Sauer et al., 2006; Baster et al., 2013; Han et al., 2021), cytokinins (Šimášková et al., 2015; Marhavý et al., 2014), gibberellins (Mäkilä et al., 2023; Willige et al., 2011), strigolactones (Zhang et al., 2020), brassinosteroids (Retzer et al., 2019) and phospholipids (Ischebeck et al., 2013; Tejos et al., 2014).

3.4 The establishment of PIN polarity

Mounting evidence suggests that subcellular trafficking of PIN proteins is the primary mechanism for the establishment and maintenance of PIN polarity (Adamowski and Friml, 2015). PIN proteins undergo continuous and dynamic cycling between their PM polar domain and endosomal compartments (Kleine-Vehn and Friml, 2008; Grunewald and Friml, 2010; Marhava, 2022). The newly synthesized PINs enter the endomembrane system through the endoplasmic reticulum (ER), where they are folded and glycosylated before being transported to the Golgi apparatus. They undergo further modifications after moving to the trans-Golgi network (TGN) and are then sorted to the PM (Grunewald and Friml, 2010). As the secretion of newly synthesized PIN1 from the TGN to the PM has been

suggested to be non-polar (Dhonukshe et al., 2008), we will mainly focus on the post-secretion regulation of PIN proteins. During developmental processes or in response to endogenous and exogenous signals, PIN proteins can be endocytosed, trafficked to the trans-Golgi network (TGN)/early endosome (EE), and then transported to different polar domains at the PM by exocytosis or directed to the vacuole for degradation by multivesicular bodies (MVB). These processes determine the abundance and polarity of PINs at the PM (Cheng and Wang, 2022).

3.5 PIN phosphorylation and auxin transport polarity and activity

The polarity and activity of PIN proteins at the PM have been reported to be regulated by post-translationally modifications through phosphorylation at various residues in the central PIN hydrophilic loop (PIN HL) (reviewed in Bassukas et al., 2022). This strongly indicates that not only the trafficking of PIN per se, but also the specific polarity signals within the protein, determine the localization and activity of the protein at distinct polar domains (Grunewald and Friml, 2010). Consistently, an increasing number of protein kinases have been shown to be capable of phosphorylating multiple sites within the PIN sequences, suggesting that the PIN polarity and activity signals are related to the phosphorylation status of these proteins.

3.5.1 PID/WAG AGC3 kinases

Among the known PIN phosphorylating protein kinases, PINOID (PID) is one of the most well-characterized regulators of PIN polarity. PID, together with its homologs WAG1, WAG2 and AGC3-4 compose the AGC3 subfamily of the plant-specific AGCVIII group of kinases. These kinases are related to and thus are named after the protein kinase A, protein kinase G and the Ca^{2+} -activated protein kinase C group of kinases found in other eukaryotic organisms (Rademacher and Offringa, 2012). PID, WAG1 and WAG2 instruct apical asymmetric PIN localisation by phosphorylating the serine (S) residue in three conserved TPRXS

motifs (S1-S3: S231, 252, and 290 in PIN1) within the PIN-HL (Michniewicz et al., 2007; Dhonukshe et al., 2010; Huang et al., 2010). *Arabidopsis pid* single or *pid*, *wag1*, *wag2* multiple mutants exhibit an increasing preference for basal PIN localization, resulting in either defects in cotyledon initiation during embryogenesis (Bennett et al., 1995; Cheng et al., 2008), the development of a pin-shaped inflorescence phenocopying that of the *pin-formed 1 (pin1)* mutant (Bennett et al., 1995; Reinhardt et al., 2003; Friml et al., 2004), or agravitropic root growth (Dhonukshe et al., 2010). By contrast, overexpression of these kinases leads to a basal-to-apical switch of PIN1, PIN4 and PIN2 in the root meristem, causing depletion of the auxin maximum and leading to agravitropic root growth and eventually collapse of the root meristem (Benjamins et al., 2001; Friml et al., 2004). The remarkable change of PIN polarity in loss- or gain-of-function mutants of the *PID* and *WAG* genes, is mirrored by PIN polarity changes observed in plants expressing the engineered phosphomimic (resulting in apical/shootward localization) and phospho-dead (resulting in basal/rootward localization) versions of PIN proteins (Huang et al., 2010; Dhonukshe et al., 2010). Moreover, the mutants defective in subunits of the antagonistically acting trimeric phosphatases, which includes the protein phosphatase 2A (PP2A) (Michniewicz et al., 2007), PP1 (Guo et al., 2015), and PP6 (Dai et al., 2012), exhibit similar apical/rootward localization of PIN proteins as *PID/WAG* overexpression lines. These findings show a direct correlation between *PID/WAG*-mediated phosphorylation and apical localization of PINs. Notably, in addition to their role in directing a PIN basal-to-apical shift, phosphorylation conducted by *PID* or *WAG2* also enhanced the transport activity of PINs in the *Xenopus* oocytes system (Zourelidou et al., 2014). However, phosphorylated PIN1 at S1-S3 sites have also been detected with phosphosite-specific antibodies at the basal as well as the apical side of the PM in different root cell types, in embryos, and shoot apical meristems, or even in the *pid* mutant (Weller et al., 2017), indicating that a more complex model is required to explain the effects of PIN phosphorylation on their polar localization and activity.

3.5.2 AGC1 kinases

Apart from the AGC3 kinases, the AGC1 clade kinase D6 PROTEIN KINASE (D6PK) and three related D6PK-LIKE1-3 were found to phosphorylate S1-S5 of PINs, but preferably S4-S5 (Zourelidou et al., 2014). D6PK acts redundantly with PID/WAGs in phosphorylating S1-S3, suggesting that these kinases share some functional redundancy (Zourelidou et al., 2009; Zourelidou et al., 2014). However, in D6PK loss-of-function and overexpression plants, unlike PID or WAG loss-of-function and overexpression plants, the PIN polarity does not change (Zourelidou et al., 2009). D6PK colocalizes with PIN1, PIN2 and PIN4 at the basal (rootward) PM of *Arabidopsis* root cells, where it rather regulates the rate of PAT (Zourelidou et al., 2009; Barbosa et al., 2014). D6PK and D6PKL1-3 play a crucial role in hypocotyl phototropism and gravitropism, shade-avoidance, as well as lateral root and shoot differentiation (Zourelidou et al., 2009; Willige et al., 2013; Kohnen et al., 2016). An additional AGC1 kinase that was found to phosphorylate and activate PIN proteins to regulate PAT is PROTEIN KINASE ASSOCIATED WITH BREVIS RADIX (PAX) (Marhava et al., 2018). PAX is specifically expressed in the protophloem and activates PIN-mediated auxin efflux, whereas its auxin-sensing repressor BREVIS RADIX (BRX), which is a PM-associated, polarly localized protein that is specifically expressed in the protophloem, strongly dampens this stimulation by inhibiting PAX activity. PAX and BRX act together as a molecular rheostat to regulate protophloem development and root patterning (Marhava et al., 2018). Notably, the PHOSPHOINOSITIDE-DEPENDENT PROTEIN KINASE 1 (PDK1) was found to phosphorylate the activation loops of PAX and D6PK to activate these protein kinases (Zegzouti et al., 2006; Xiao and Offringa, 2020; Tan et al., 2020).

3.5.3 MAPKs and RLKs

Besides the AGC kinases, PIN proteins are also regulated through phosphorylation by MITOGEN-ACTIVATED PROTEIN KINASES (MAPKs) and RECEPTOR-LIKE PROTEIN KINASES (RLKs).

MAPKs are a conserved family of protein kinases found in all eukaryotes. They function in a signal transduction cascade that is designed to transduce and amplify signals through sequential phosphorylation: MAPKs are activated through phosphorylation by MAPK KINASES (MAPKKs), which are again activated through phosphorylation by MAPKK KINASES (MAPKKKs) (Enders et al., 2017; Lin et al., 2021). In plants, their signaling has been mostly linked to responses to high salinity, drought, extreme temperature and insect and pathogen infections (Lin et al., 2021). More recently, the MAPKs MPK4 and MPK6 were found to phosphorylate the threonines (T) within the three TPRXS motifs that were also targets of the AGC kinases (Dory et al., 2018). MAP KINASE KINASE 7 (MKK7) acts upstream of MPK6. Induction of expression of their upstream activator MAPK KINASE 7 (MKK7) or activation of the MAPK pathway by application of the pathogen-derived flg22 peptide was found to alter the trafficking of PIN1, resulting in MPK6-dependent intracellular accumulation of PIN1 in root cells (Dory et al., 2018). Furthermore, the MKK7-MPK6 cascade was reported to lead to phosphorylation of Ser 337 in the PIN1-HL, to regulate the basal localization of PIN1 in xylem parenchyma cells and PAT in the primary stem, thereby controlling shoot branching (Zhang et al., 2010; Jia et al., 2016).

RLKs belong to a large family of PM localized kinases. They consist of a ligand-binding extracellular domain, a single transmembrane domain, and a cytoplasmic kinase domain. The auxin-regulated RLKs CANALIZATION-RELATED AUXIN-REGULATED MALECTIN-TYPE (CAMEL) together with CANALIZATION-RELATED RLK (CANAR) interact with and phosphorylate PIN1, possibly at T129, T234, S240, T257, and S408, which are not shared by any previously reported protein kinases (Hajny et al., 2020). PIN1 subcellular trafficking and basal polarization are impaired in *Arabidopsis camel* or *canar* loss-of-function mutants

The role of calcium as second messenger in auxin transport and signaling causing defects in leaf venation and vasculature regeneration after wounding (Hajny et al., 2020).

4. Calcium signalling and its involvement in auxin action

4.1 Ca^{2+} is a ubiquitous second messenger for both plant development and early stress responses

The divalent cation calcium (Ca^{2+}) is a crucial component of the plant growth system, playing a vital role in the formation of cell walls, cell membranes and various cellular processes (Hepler and Wayne, 1985; Eklund and Eliasson, 1990; Xu and Heath, 1998). Additionally, Ca^{2+} acts as a ubiquitous second messenger, translating environmental challenges and developmental cues into signal-specific changes in the concentration of cytosolic Ca^{2+} ($[\text{Ca}^{2+}]_{\text{cyt}}$), referred to as the ‘calcium signature’ (Verret et al., 2010).

To decipher the diverse stimuli-induced Ca^{2+} signatures, plants have evolved an extensive array of Ca^{2+} sensors (Roberts and Harmon, 1992; Vogel, 1994). The majority of the Ca^{2+} sensors are sensor relay proteins, which include Calmodulins (CaMs), Calmodulin-like proteins (CMLs) and Calcineurin B-like proteins (CBLs) (Sanders et al., 2002; Hashimoto and Kudla, 2011). The Arabidopsis CaM/CMLs family harbours seven *CaM* genes and 50 *CMLs* (McCormack and Braam, 2003). While lacking other identifiable functional domains, the CaM/CMLs possess a varying number of Ca^{2+} binding domains called “EF hands”. They function by altering downstream target activities through Ca^{2+} -dependent protein–protein interactions (Hashimoto and Kudla, 2011). Similarly, CBLs act as sensor relay proteins due to their lack of enzymatic activity. They can interact with a specific family of proteins known as CBL-interacting protein kinases (CIPKs), playing a crucial role in response to wounding, cold, drought, salt stress, regulation of ABA sensitivity and biosynthesis, and nutrient sensing (Luan et al., 2002). In contrast, calcium-dependent protein kinases (CDPKs) are sensor-responders. They contain

both a Ca^{2+} sensing domain with EF-hand motifs and a protein kinase domain. Binding of Ca^{2+} results in activation of the kinase domain leading to the subsequent phosphorylation of target proteins (Hashimoto and Kudla, 2011).

In conclusion, Ca^{2+} serves as a pivotal messenger in plant development and early stress responses, with specialized sensors, such as CaM/CMLs, CBLs, and CDPKs, enabling plants to interpret and respond to various environmental and developmental cues.

4.2 Calcium as second messenger in auxin signalling

Over the past decade, the growth in genetic studies and related technology development provide an abundant amount of evidence showing that certain rapid auxin responses cannot be fully explained by the nuclear canonical TIR1/AFB-Aux/IAA-ARFs pathway. Instead, they suggest the involvement of new pathways that rely on TIR1/AFBs receptors localized outside the nucleus and/or TMK receptors localized to the PM (reviewed in McLaughlin et al., 2021, Pérez-Henríquez and Yang, 2023). For instance, auxin rapidly inhibits root growth within 30 seconds, which is too rapid to depend on transcriptional regulation. However, its dependence on TIR1/AFB signalling suggests the existence of an extranuclear TIR1/AFB-dependent signalling pathway (Fendrych et al., 2018). Indeed, recent studies have shown that all six TIR1/AFBs exhibit both nuclear and cytoplasmic subcellular localization in Arabidopsis root cells, with specifically AFB1 being predominantly located in the cytoplasm (Prigge et al., 2020). Consistent with these finding, AFB1 was reported to mediate the rapid root growth inhibition, as the single *afb1* loss-of-function mutant shows a significant defect in rapid root growth inhibition (Fendrych et al., 2018; Prigge et al., 2020; Serre et al., 2021).

Ca^{2+} signalling is one of the earliest responses to auxin (Hasenstein and Evans, 1986; Gehring et al., 1990; Shishova and Lindberg, 2004; Monshausen et al., 2011). The auxin induced rapid inhibition on root growth is accompanied by a CYCLIC

NUCLEOTIDE-GATED CHANNEL 14 (CNGC14)-dependent transient increase in $[Ca^{2+}]_{\text{cyt}}$. Inhibition of root growth is significantly delayed in the *cngc14* loss-of-function mutant, indicating the involvement of Ca^{2+} signalling in rapid auxin response (Dindas et al., 2018; Shih et al., 2015). Moreover, auxin triggered transient increase in $[Ca^{2+}]_{\text{cyt}}$ requires TIR1/AFB-based auxin signalling (Dindas et al., 2018). A recent study has shown that the cytoplasmic AFB1 induces this non-genomic rapid auxin response, and that AFB1 is dependent on and acts upstream of CNGC14-mediated Ca^{2+} signalling, mediating the rapid root growth inhibition (Dubey et al., 2023).

4.3 Calcium signalling involved in polar auxin transport

The first reports linking Ca^{2+} signalling to PAT date back several decades. In 1973, Dela Fuente and Leopold (1973) found that PAT in sunflower stem sections was significantly suppressed by washing with the Ca^{2+} chelator ethylenediaminetetraacetate (EDTA), but could be restored by subsequent application of $CaCl_2$. Additionally, PAT was observed to be dampened under low Ca^{2+} conditions (Dela Fuente, 1984). Further studies by Lee et al. (1984) reported that gravistimulation induces polar movement of calcium across the root tip of maize and pea from the upper side to the lower side, coinciding with the basipetal movement of auxin. Subsequent research confirmed these findings and suggested that gravity-induced increase in $[Ca^{2+}]_{\text{cyt}}$ constitutes an upstream event of PAT (Plieth and Trewavas, 2002; Toyota et al., 2008).

Ca^{2+} signalling plays a regulatory role in various processes involving PAT, including phototropism (Baum et al., 1999; Harada et al., 2003; Harada and Shimazaki, 2007; Zhao et al., 2013), response to inositol trisphosphate (Zhang et al., 2011), coping with toxic heavy metals (Li et al., 2016), shoot apical meristem (SAM) development (Li et al., 2019), and maintenance of the quiescent center (QC) in the root meristem (Goh et al., 2012). These findings highlight the crucial interplay between auxin and Ca^{2+} in plant physiological processes.

As previously mentioned, the asymmetrically distributed PIN proteins provide directionality in and perform the rate-limiting step in PAT (Petrášek et al., 2006; Wiśniewska et al., 2006). PIN-driven PAT can be regulated at multiple levels, including transcription, protein degradation, subcellular trafficking, polarity, and activity (Cheng and Wang, 2022). Since the direct involvement of Ca^{2+} signalling in PIN transcription and protein degradation is scarcely reported, this discussion will mainly focus on how Ca^{2+} signalling translates environmental challenges and developmental cues into alterations in PIN polarity, activity, and subcellular trafficking, subsequently leading to changes in plant growth and development.

4.4 Ca^{2+} signalling in the regulation of PIN subcellular trafficking

Ca^{2+} has been reported to play a role in regulating both protein endocytosis and exocytosis, including PIN proteins, thereby affecting protein abundance and polarity at the PM (Figure 3).

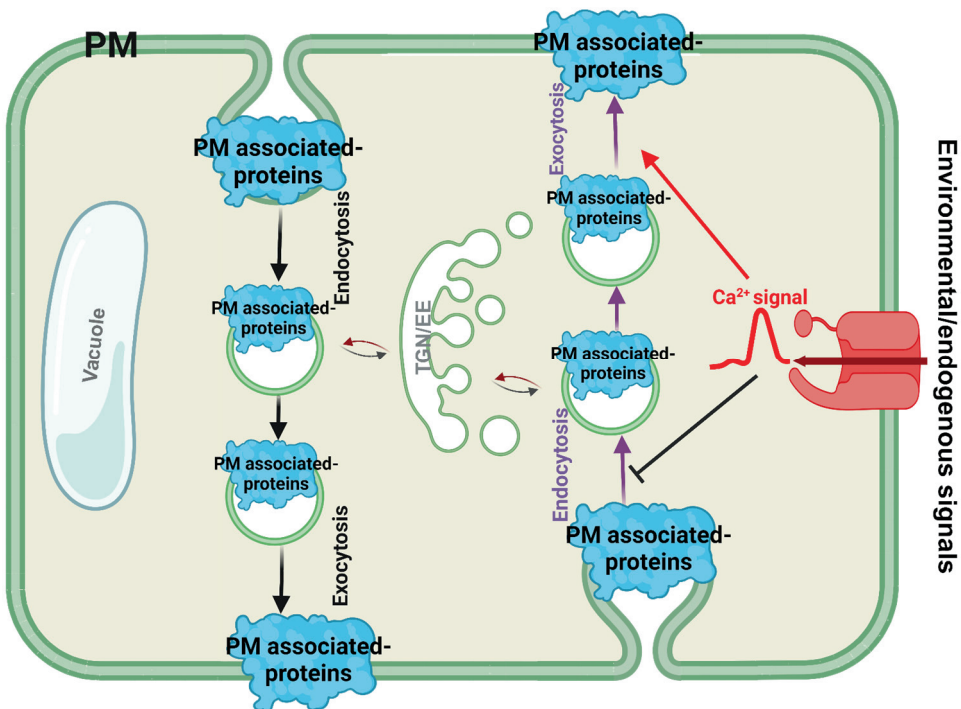


Figure 3. Schematic depiction of the effect of endogenous and environmental signal-induced elevated $[Ca^{2+}]_{cyt}$ on protein exocytosis and endocytosis. Elevation in the $[Ca^{2+}]_{cyt}$ has an inhibitory effect on endocytosis and a stimulating effect on exocytosis. TGN/EE: Trans-golgi network /early endosome; PM: Plasma membrane.

4.4.1 Effect of Ca^{2+} signalling on endocytosis

The PM localized PIN proteins are constitutively internalized via clathrin-mediated endocytosis. The involvement of Ca^{2+} signals in the regulation of endocytosis has been reported both in animals and plants. In synaptic terminals of retinal bipolar neurons, elevated $[Ca^{2+}]_{cyt}$ strongly inhibits endocytosis, as indicated by Ca^{2+} -induced increases in membrane capacitance (Von Gersdorff and Matthews, 1994). In muscle cells, rapid influx of Ca^{2+} accelerates exocytosis of the Glucose Transporter type 4 protein (GLUT4), but slows down its endocytosis (Li et al., 2014). Moreover, caffeine-induced Ca^{2+} release on sarcoplasmic reticulum was shown to inhibit endocytosis (Page et al., 1994).

TPLATE is a plant-specific interactor of clathrin (Van Damme et al., 2011). It is part of a unique multi-subunit protein complex (the TPLATE complex, TPC) that acts in concert with the adaptor protein complex 2 (AP2 complex), dynamin-related proteins and clathrin, to regulate plant growth via its role as a major adaptor module for clathrin-mediated endocytosis (Gadeyne et al., 2014). Several TPC subunits contain Ca^{2+} binding EF hand motifs, suggesting a role for Ca^{2+} -dependent regulation; however, further validation is needed (Day et al., 2002; Bar et al., 2008; Gadeyne et al., 2014). Treatment with caffeine, which increases the $[Ca^{2+}]_{cyt}$ by inducing intracellular Ca^{2+} store leaks, was found to inhibit endocytosis by dislodging TPLATE and CLATHRIN LIGHT CHAIN2 from the cell plate during cytokinesis, which is consistent with findings in animals that high $[Ca^{2+}]_{cyt}$ inhibits endocytosis (Page et al., 1994; Van Damme et al., 2011).

4.4.2 Effect of Ca^{2+} signalling on exocytosis

Following endocytosis, vesicles containing PIN proteins can be directed to recycling endosomes (RE) and from there PIN cargo is delivered back to the PM. Ca^{2+} is well known for its role in activation of exocytosis in both animal and plant cells. The paradigm for the role of Ca^{2+} in exocytosis is in neurotransmission, where a local elevation in the $[\text{Ca}^{2+}]_{\text{cyt}}$ in the axon termini triggers the exocytosis of neurotransmitter-filled vesicles to activate downstream neurons (Benarroch, 2013). Ca^{2+} also triggers granule exocytosis in mast cells, and hormone exocytosis in endocrine cells (reviewed in Pang and Südhof, 2010). The direct activation effect of elevation of $[\text{Ca}^{2+}]_{\text{cyt}}$ on exocytosis in plants was demonstrated by Ca^{2+} -induced increases of membrane capacitance in protoplasts from barley aleurone (Homann and Tester, 1997), maize coleoptiles or root caps (Sutter et al., 2000; Carroll et al., 1998) or tobacco leaves (Sutter et al., 2012).

The stimulating effect of Ca^{2+} on exocytosis is mediated by specific Ca^{2+} sensing proteins, named SYNAPTOTAGMINS (SYTs). SYTs function as the primary Ca^{2+} sensors to stimulate exocytosis in mammalian cells. SYT1, SYT2, and SYT9 function as Ca^{2+} -sensors in synaptic exocytosis, SYT1 and SYT7 are major Ca^{2+} sensors in endocrine large dense-core vesicle exocytosis, SYT2 functions as the major Ca^{2+} sensor for exocytosis in mast cells, SYT4 functions in postsynaptic exocytosis in *Drosophila*, and SYT7 mediates Ca^{2+} -triggered lysosome exocytosis in fibroblasts (Pang and Südhof, 2010). SYTs contain a N-terminal transmembrane region, and two C-terminal Ca^{2+} -binding C2-domains that act via Ca^{2+} -dependent interactions with both the fusing phospholipid membranes and the membrane fusion machinery (Pang and Südhof, 2010). In plants, calcium-dependent candidate regulators of exocytosis include CaMs, CDPKs, NADPH oxidases (NOX), actin-binding proteins, ANNEXINS (ANNs) and SYNAPTOTAGMINS (SYTs) (Žárský et al., 2009). The SYNAPTOTAGMIN family in *Arabidopsis* has five members (Craxton, 2004). SYT1 is indispensable for maintaining PM integrity under salt or freezing stress, likely by facilitating the process of exocytotic membrane resealing (Schapire et al., 2008). SYT2 participates in pollen germination and pollen tube

growth (Wang et al., 2015b). SYT3 and SYT1 act redundantly in preventing PM damage and promoting abiotic stress resistance (Ruiz-Lopez et al., 2021). SYT4/5 contribute to Arabidopsis immunity to *Pseudomonas syringae* DC3000 (Kim et al., 2022). However, involvement of SYTs in exocytosis in plants needs further study. ANNEXINs were initially identified in animal cells and named for their ability to "annex" or bring together membranes. They were initially proposed to be involved in membrane fusion processes (Clark et al., 2012). ANNEXINS are composed of two principal domains: the divergent NH₂-terminal "head" and the conserved COOH-terminal protein core, which contains a conserved Ca²⁺- and membrane-binding motif (Gerke and Moss, 2002). Root cells of Arabidopsis seedlings ectopically expressing ZmANN33 or ZmANN35 show a more intact PM after chilling stress, which is likely due to the accelerated exocytotic process (He et al., 2019). Arabidopsis ANN5 plays a role in the maintenance of membrane integrity in pollen grains exposed to osmotic or ionic imbalances (Lichocka et al., 2022). Overexpression of ANN5 leads to increased resistance of pollen germination and pollen tube growth to the exocytosis-inhibiting fungal toxin Brefeldin A (BFA), and this effect is modulated by Ca²⁺ fluctuations that occur within pollen cells (Zhu et al., 2014).

4.5 Calcium signalling in the regulation of PIN polarity/activity

The shift in PIN polarity might result from other regulators that interact with PID/WAGs, enhancing the efficiency of this polarity shift. Several regulators of PID or WAGs have been identified. The PHOSPHOLIPASE D (PLD)-derived phosphatidic acid (PA) has been reported to bind to the PID insertion domain (ID) in the catalytic domain to promote PID-mediated PIN2 phosphorylation and subsequent root growth under salt stress (Wang et al., 2019). The 3-PHOSPHOINOSITIDE-DEPENDENT PROTEIN KINASE-1 (PDK1) was initially reported to interact with PID through the C-terminal PDK1-interacting-fragment (PIF) domain and promote PID kinase activity by phosphorylating the

activation segment of PID (Zegzouti et al., 2006). However, Xiao and Offringa (2020) have shown that both PID functionality and its subcellular localization do not depend on PDK1 function. Instead, PDK1 plays a more important role in regulation of PAT by phosphorylating and activating the AGC1 kinases PAX and D6PK (Xiao and Offringa, 2020; Tan et al., 2020; Figure 3). Some other regulators, like BTB and TAZ domain scaffold protein 1 (BT1/PBP2) (Benjamins et al., 2003; Robert et al., 2009) and 14-3-3 (Xiao, 2019), were also reported to interact with PID, however these interactions have mainly been shown by *in vitro* biochemical assays and their biological function is yet to be determined.

The first molecular clue that Ca^{2+} signaling is involved in regulating PIN-driven PAT was provided by the finding that PID interacts with the CALMODULIN-LIKE 12/TOUCH 3 (CML12/TCH3) and the EF hand containing PID-BINDING PROTEIN 1 (PBP1) in a Ca^{2+} -dependent manner (Benjamins et al., 2003). Later, CML12/TCH3 was also found to interact with WAG2 (Fan, 2014). CML12/TCH3 is a negative regulator of PID kinase activity both *in vitro*, as shown by phosphorylation assays, and *in planta* where *TCH3* overexpression reduces *PID* overexpression induced root meristem collapse (Robert, 2008; Galván-Ampudia, 2009). Consistently, Zhang et al. (2011) showed that modulation of PIN polarity by the inositol trisphosphate (InsP3)-mediated increase of $[\text{Ca}^{2+}]_{\text{cyt}}$ is PID/WAG-dependent. Elevating InsP3 or $[\text{Ca}^{2+}]_{\text{cyt}}$ levels interfered with apical localization of PIN2 in young cortex cells of *35S::PID* seedlings, thereby delaying the *35S::PID*-mediated root apical meristem collapse, whereas treatments decreasing $[\text{Ca}^{2+}]_{\text{cyt}}$ enhanced the root collapse of *35S::PID* plants and affected the basal PIN2 polarity in young epidermal cells of *pid wag1 wag2* roots (Zhang et al., 2011).

Apart from PID and WAG2, no involvement in Ca^{2+} -dependent regulation has been reported for the other kinases phosphorylating PIN proteins, as discussed above. Below a few other kinases are presented that do seem to play a role in Ca^{2+} -dependent regulation of PAT.

4.5.1 CRKs

The CDPK-RELATED KINASE5 (CRK5), a member of the Arabidopsis Ca^{2+} /calmodulin-dependent kinase-related kinase family (CRKs) (Harper et al., 2004), was reported to phosphorylate PINs to regulate plant development (Rigo et al., 2013). In Arabidopsis, the CRK family consist of eight highly conserved members. They share a conserved C-terminal CaM-binding domain, but have sequence divergence in their N-terminus except for two conserved domains that are responsible for membrane-association (Harper et al., 2004; Leclercq et al., 2005;. Rigo et al., 2013).

CRKs are Ca^{2+} responsive kinases. In *Nicotiana tabacum*, the biochemical activity of NtCPK5 is calcium-dependent (Wang et al., 2005). In Arabidopsis, biochemical studies have shown that the autophosphorylation activity of CRK1 and CRK3 is remarkably increased (up to 10-fold) in the presence of CaM and Ca^{2+} , whereas their substrate phosphorylation activity is only two- to threefold increased (Wang et al., 2004; Du et al., 2005). Regarding CRK5, its autophosphorylation and trans-phosphorylation activity were found to be similar in the presence or absence of CaM and Ca^{2+} (Rigo et al., 2013). This might be because CRK5 requires some yet undefined Ca^{2+} binding partners, as suggested previously (Harmon, 2003; Du et al., 2005). CRK5 was found to phosphorylate PIN1, 2, 3, 4, and 7 *in vitro*, but the phosphorylation sites have not yet been identified (Rigo et al., 2013; Baba et al., 2019a; Baba et al., 2019b). CRK5 has been reported to mediate phosphorylation of PIN proteins in various developmental processes. For instance, CRK5 was found to phosphorylate PIN2 to regulate root gravitropism and lateral root formation (Rigo et al., 2013), PIN3 to mediate apical hook development (Baba et al., 2019b) and PIN1 to coordinate embryonic development (Baba et al., 2019a). In *crk5* loss-of-function mutants, apical (shootward) localization of PIN2 in root epidermis cells is reduced and the protein shows mixed apolar and apical localization in the cortex of the root transition zone. CRK5 phosphorylation may thus control PIN2 polarity, stability and/or degradation (Rigo et al., 2013; Figure 3).

4.5.2 CDPKs

Recently, the *Arabidopsis* CALCIUM-DEPENDENT PROTEIN KINASE 29 (CPK29) has been reported to directly interpret Ca^{2+} signals from internal and external triggers to modulate PIN trafficking and polarity by targeting a specific Serine residue in the PIN HL not phosphorylated by other kinases (Lee et al., 2021). The *cpk29* loss-of-function mutant exhibits a decrease in polar PM localization and enhanced internal accumulation of PIN proteins, suggesting its involvement in Ca^{2+} -enhanced PIN exocytosis (Lee et al., 2021; Figure 3).

In tomato, StCDPK1 was reported to phosphorylate StPIN4 *in vitro*, suggesting a possible role in regulating the polarity of StPIN4 (Santin et al., 2017).

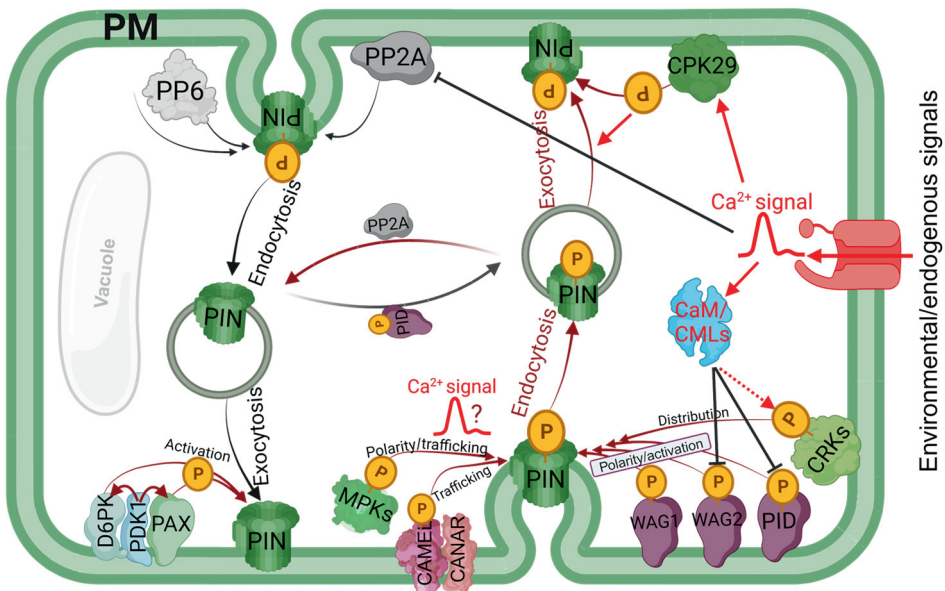


Figure 4. Model showing the role of Ca^{2+} signalling in protein kinase-mediated regulation of PIN polarity, activity or trafficking. Details are described in the main text. P: Phosphorylation. PM: Plasma membrane.

5. Feedback of auxin on its own transport: a role for Ca^{2+} signalling

The role of calcium as second messenger in auxin transport and signaling

In 1969, Tsvi Sachs proposed the canalization hypothesis, describing the feedback of auxin on its own transport (reviewed in Smith and Bayer, 2009). The subsequent identification of PIN proteins as determinants of the rate and direction of PAT in later years (reviewed in Marhava, 2022) has provided scientists with the molecular tools to understand the mechanism behind this feedback and its importance in auxin-dependent development.

Firstly, auxin was shown to feedback on PIN polarity through auxin signaling-mediated transcriptional changes in gene expression. Sauer et al. (2006) showed that local auxin application or auxin accumulation during de novo formation of vasculature and lateral roots leads to relocalization of PIN1 and PIN2 at the PM, which is cell-specific, *PIN* transcription-independent, but still involves the TIR1/AFB-Aux/IAA signaling pathway leading to ARF-dependent transcription. Prát et al. (2018) reported that the auxin responsive gene encoding the transcriptional activator WRKY23 acts downstream of IAA17-ARF7/19 to mediate this process, as *WRKY23* gain- and loss-of-function mutants showed altered auxin-mediated lateralization of PIN1 and PIN2. Hajný et al. (2020) reported that the CAMEL-CANAR RLKs, which phosphorylate PINs and regulates their polarity, act downstream of WRKY23. These findings represent an elegant mechanism of auxin feedback on its own transport machinery through the auxin signaling pathway.

Another mechanism of feedback of auxin on PIN polarity occurs through PIN membrane cycling dynamics. Paciorek et al. (2005) found that auxin acts as a general inhibitor of endocytosis, including PIN endocytosis, implying feedback of extracellular, apoplastic auxin on PIN trafficking and polarization. The signaling was recently found to be mediated by the controversial auxin receptor ABP1. Auxin facilitates the interaction of ABP1 and TMKs, which activates the ROP6/RIC1 pathway in root cells and the ROP2/RIC4 pathway in leaf pavement cells, leading to inhibition of clathrin-dependent PIN1 endocytosis (Xu et al., 2010; Xu et al., 2014; Pan et al., 2020). During gravistimulation, auxin-promoted

interaction with ABP1 leads to activation and stabilization of TMK1, which in turn enhances its interaction with and phosphorylation of PIN2, at the lower side of the root to reinforce asymmetry in PIN2-mediated auxin fluxes for gravitropic root bending (Rodriguez et al., 2022). ABP1-TMK mediated auxin perception is also required for a subset of auxin responses, such as the activation of PM H^+ -ATPases, global protein phosphorylation, regeneration of vasculature around the wound and formation of auxin-transporting channels for the development of vasculature originating from a local source of auxin (Friml et al., 2022).

Besides rapid auxin signaling via the ABP1-TMK receptors, calcium has been proposed to be involved in a swift auxin signaling system mediating rapid growth responses (Shishova and Lindberg, 2010; Plieth and Trewavas, 2002). It has been shown that exogenous auxin, via the AFB1-based auxin signalling pathway, triggers a rapid, transient increase in $[Ca^{2+}]_{cyt}$ in many plant species conducted by Ca^{2+} channels, in particular CNGC2 and CNGC14 (Verret et al., 2010; Vanneste and Friml, 2013; Wang et al., 2017; Dindas et al., 2018; Chakraborty et al., 2021; Yu et al., 2022a). In this way, local increases in auxin concentrations are translated into Ca^{2+} signals to regulate downstream targets.

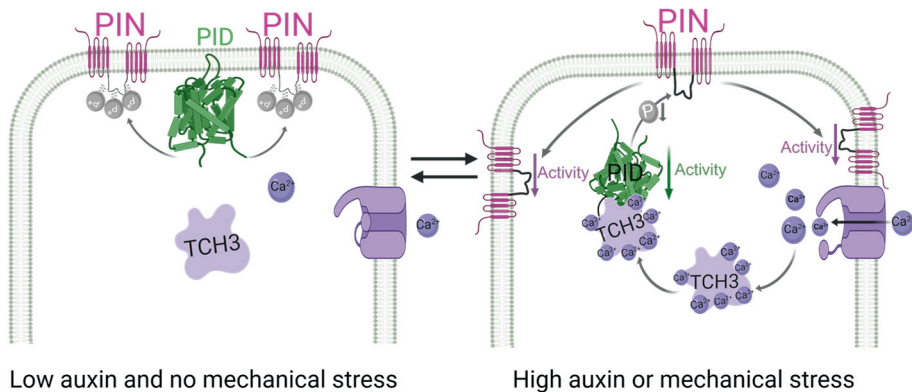


Figure 5. Model for feedback regulation of auxin or mechanical stress on PIN polarity and activity through Ca^{2+} -dependent binding of TCH3 to PID. Mechanical stress and auxin lead to elevated expression of *CML12/TCH3* and trigger elevation of $[Ca^{2+}]_{cyt}$, which activates the

The role of calcium as second messenger in auxin transport and signaling

CML/TCH3, leading to sequestration of PID from the PM to the cytosol and a decreased PID kinase activity. As a result, the attenuated PIN phosphorylation leads to reduced PIN polarity and activity.

The finding that the calcium sensors CML12/TCH3 and PBP1 interact with PID (Benjamins et al., 2003) provided an additional molecular link between Ca^{2+} signaling and PIN activity and polarity. CML12/TCH3 interacts with PID in a Ca^{2+} -dependent manner (Benjamins et al., 2003) and negatively regulates PID activity *in vivo* and *in vitro* (Robert, 2008; Galván-Ampudia, 2009). Moreover, *CML12/TCH3* expression was found to be rapidly up-regulated in response to mechanical stimuli, such as touch, as well as by other stimuli including darkness, temperature shocks or brassinosteroid or auxin signalling (reviewed in Braam et al., 1997). In *Arabidopsis* protoplasts and epidermis cells at the root tip, the interaction with CML12/TCH3 sequesters PID from the PM to the cytosol in the presence of Ca^{2+} and auxin (Fan, 2014). Based on these results, we propose an alternative model for the feedback of auxin on PIN activity and polarity (Figure 5): local increases in auxin levels or mechanical stress trigger a rapid and substantial up-regulated expression of *CML12/TCH3* and a transient increase in $[\text{Ca}^{2+}]_{\text{cyt}}$, leading to the activation of CML12/TCH3, which in turn sequesters PID, a crucial regulator of PIN protein polarity/activity, to the cytosol and inhibits its kinase activity. Consequently, PIN protein polarity and activity are decreased, leading to local changes in auxin transport and distribution.

5.1 The role of the Ca^{2+} /TCH3-PID pathway in plant growth and development

The Ca^{2+} -dependent TCH3-PID interaction provides an elegant mechanism how auxin or mechanical stress can modulate and fine tune PAT. The question remains in which plant growth or developmental process this mechanism plays a significant role. In view of the *PID* expression pattern and the phenotypes of *pid* loss-of-function mutants, it seems likely that this mechanism is involved in regulation of root growth and organ initiation in the embryo and inflorescence.

Previous studies in our group have indicated that the Ca^{2+} -dependent TCH3-PID interaction plays a role in the root gravitropic response (Fan, 2014). The gravitropic response of the root is driven by asymmetric redistribution of auxin in the root tip, which is coordinated by PIN proteins (reviewed in Han et al., 2021). Upon gravistimulation, PIN3 and PIN7 polarize to the lower sides of columella cells, thus driving the auxin flow from the auxin maximum towards the lower side of the root tip (Han et al., 2021). This additional auxin is subsequently transported by the apical/shootward localized PIN2 from the root tip, where gravity is perceived, to the elongation zone, where growth is regulated (Han et al., 2021). Simultaneously, the increased accumulation of auxin at the lower side of the root tip induces a transient increase in $[\text{Ca}^{2+}]_{\text{cyt}}$ (Monshausen et al., 2011) and a rapid and substantial up-regulated expression of *CML12/TCH3* (Antosiewicz et al., 1995; Benjamins et al., 2003). It is known that Ca^{2+} plays an essential role in gravitropism, as gravistimulation induces transient Ca^{2+} signals in many tissues and species (Vanneste and Friml, 2013) and blocking the Ca^{2+} channels inhibits the root gravitropic response, but not the asymmetric distribution of auxin, indicating that Ca^{2+} acts downstream of auxin (Fan, 2014). *PID* is co-expressed with *TCH3* in epidermis cells of the elongation zone of the root tip (Benjamins et al., 2001; Benjamins et al., 2003). Based on these data we proposed that the enhanced $[\text{Ca}^{2+}]_{\text{cyt}}$ and increased *TCH3* expression lead to TCH3-PID binding, which sequesters PID from the PM to the cytosol and decreases its kinase activity. This results in attenuated PIN2 phosphorylation and thus its apolar localization and reduced auxin efflux activity at the lower side of root tip, enhancing the asymmetric auxin distribution and thus the downward bending of the root tip. The importance of the asymmetric induction of *TCH3* expression during this process was confirmed by the delayed gravitropic response of *TCH3* overexpression seedlings. Not in line with this model is the finding that, *tch3* loss-of-function mutants did not show a significantly altered gravitropic root response, this may be caused by redundancy among the *CAM/CML* genes (Fan, 2014).

Auxin distribution and its polar transport mediated by the dynamic changes in PIN polarity patterns also underlies the initiation and patterning of new organs, for example, phyllotaxis (Yin, 2021). Aerial organs, such as leaves and flowers, are initiated at the shoot apical meristem (SAM) of a plant, and this process is triggered by local PIN1-driven accumulation of auxin (Yin, 2021). The continuous initiation and expansion of aerial organs through cell division and growth induces mechanical stress in the SAM, which has been identified as additional driver of phyllotaxis by regulating auxin transport (Heisler et al., 2010). Li et al. 2019 have shown that mechanical stimulation using laser ablation or drug treatment of the SAM cause transient increases in $[Ca^{2+}]_{cyt}$, leading to changes in PIN1 polarity (Li et al., 2019). By studying *SHOOT MERISTEMLESS* (*STM*), a mechanical stress-responsive gene encoding a master regulator and marker of meristematic identity in Arabidopsis, Landrein et al. (2015) observed that mechanical stress acts in parallel to auxin signalling, providing robustness to the regulation of gene activity in the shoot meristem (Landrein et al., 2015). So far, however, it remains unclear how exactly PIN1 polarity and activity are regulated to determine the next PIN1 convergence point where an organ primordium is initiated. Interestingly, *CML12/TCH3* has been shown to be highly upregulated in response to both mechanical stress and auxin (Braam and Davis, 1990; Benjamins et al., 2001; Benjamins et al., 2003; Fan, 2014). PID is a crucial regulator of PIN polarity, accumulating in the peripheral zone of the SAM and in newly formed leaf primordia, and known for its role in floral meristem outgrowth and floral organ development (Bennett et al., 1995; Friml et al., 2004; Wang et al., 2014). Moreover, providing mechanical stress to the SAM led to Ca^{2+} -dependent sequestration of PID from the PM to the cytosol (Fan, 2014). Based on this, we hypothesize that the Ca^{2+} -dependent TCH3-PID interaction presumably integrates hormonal and abiotic signals triggering elevations in $[Ca^{2+}]_{cyt}$, such as auxin and mechanical stress, to mediate the dynamic changes in PIN polarity and activity in

the SAM, thus providing robustness to the phyllotactic pattern. However, this hypothesis needs further validation.

6. Outline of the thesis

In **Chapter 1** of this thesis we review the state of the art of auxin signalling and transport and the involvement of Ca^{2+} as second messenger in these processes. We finalize by proposing a new model how, through the Ca^{2+} -dependent CML12/TCH3-PID interaction, auxin can feedback on PIN polarity and activity. However, the role of the Ca^{2+} -CML12/TCH3-PID module in plant growth and development is still unclear, as single *tch3* loss-of-function mutants do not show a clear phenotype, suggesting that other CMLs, and possibly CaMs, might act redundantly with CML12/TCH3.

To further confirm our hypothesis and identify whether other CaM/CMLs interact with PID, we selected the most closely related homologs of CML12/TCH3, including seven CaMs, CML8, 9, 10, 11, 13 and CML14 and the more distantly related CML24/TCH2 as candidates. In **Chapter 2**, we show that a confined clade comprising seven CaMs and four closely-related CMLs, including CML12/TCH3, interact with PID. In Arabidopsis protoplasts, co-transfection of these CaM/CMLs with PID in the presence of auxin resulted in sequestration of PID from the PM. A comparative study on the spatio-temporal expression of the corresponding *CaM/CML* genes and *PID* using *promoter:GUS* reporter fusions displayed differential but also largely overlapping expression patterns in most tissues throughout all the developmental stages. Interestingly, we observed that the *CaM2*, *CaM7*, *CML10* and *CML12/TCH3* genes are responsive to auxin treatment and gravistimulation. These results confirm our previous suggestion that CML12/TCH3 may acts redundantly with other CAM/CMLs in regulating PID activity, and explain why the *tch3* loss-of-function mutant does not show clear phenotypes.

In **Chapter 3**, to overcome the redundancy of the CaM/CMLs in regulating PID kinase and identify the biological function of the CaM/CML-PID interaction, we fine-mapped the CaM/CMLs binding domain in PID. We confirmed that PID associates to the PM by the insertion domain (ID) in the catalytic kinase core. Subsequent fine-mapping of the CaM/CML binding domain in PID showed that both CaM/CML binding and PM association converge at an amphipathic alpha helix in the PID ID. Disruption of this amphipathic alpha helix by substitution of several positively charged arginines by alanines (RtoA) interfered with both CaM/CML binding and PM association. Moreover, the PID(RtoA) versions showed the same overexpression phenotypes as wild-type PID and complemented the pin-like inflorescence phenotype of the *pid* loss-of-function mutant, when expressed under the *PID* promoter. This indicated that PM association is not essential for PID function and that the ‘untouchable’ PID(RtoA) versions enable us to finally unravel the role of the calcium-dependent PID-CaM/CML interaction in plant development.

In **Chapter 4**, we utilized the *pid-14* mutant lines expressing ‘untouchable’ PID(RtoA) versions to study the role of the calcium-dependent PID-CaM/CML interaction in plant development. Initial phenotypic analysis of these plants suggested that the mutant PID versions were fully functional, as they complemented the pin-like inflorescence phenotype of the *pid* mutant and did not alter seedling development or flowering time. However, closer inspection of the inflorescences of these plants showed clear defects in the spiral phyllotaxis, ranging from deviating divergence angles between subsequent flowers and fruits to the simultaneous initiation of flower primordia. These phenotypes were reflected in the increased number and randomized position of PIN convergence points and auxin maxima in the inflorescence meristems of the ‘untouchable’ PID expressing plants. Our data indicate that Ca^{2+} -dependent regulation of PID activity by CaM/CML binding is required for the accurate spatio-temporal positioning in the SAM of a single auxin maximum at a time.

Reference:

- Abas, L., Benjamins, R., Malenica, N., Paciorek, T., Wiśniewska, J., Moulinier–Anzola, J. C., ... & Luschnig, C.** (2006). Intracellular trafficking and proteolysis of the Arabidopsis auxin-efflux facilitator PIN2 are involved in root gravitropism. *Nat. Cell Biol.* 8: 249-256.
- Adamowski, M., & Friml, J.** (2015). PIN-dependent auxin transport: action, regulation, and evolution. *Plant Cell* 27: 20-32.
- Aloni, R., Schwalm, K., Langhans, M., & Ullrich, C. I.** (2003). Gradual shifts in sites of free-auxin production during leaf-primordium development and their role in vascular differentiation and leaf morphogenesis in Arabidopsis. *Planta* 216: 841-853.
- Antosiewicz, D. M., Polisensky, D. H., & Braam, J.** (1995). Cellular localization of the Ca^{2+} binding TCH3 protein of Arabidopsis. *Plant J.* 8: 623-636.
- Baba, A. I., Andrási, N., Valkai, I., Gorcsa, T., Koczka, L., Darula, Z., ... & Cséplő, Á.** (2019b). AtCRK5 protein kinase exhibits a regulatory role in hypocotyl hook development during skotomorphogenesis. *Int. J. Mol. Sci.* 20: 3432.
- Baba, A. I., Valkai, I., Labhane, N. M., Koczka, L., Andrási, N., Klement, É., ... & Cséplő, Á.** (2019a). CRK5 protein kinase contributes to the progression of embryogenesis of Arabidopsis thaliana. *Int. J. Mol. Sci.* 20: 6120.
- Bar, M., Aharon, M., Benjamin, S., Rotblat, B., Horowitz, M., & Avni, A.** (2008). AtEHDs, novel Arabidopsis EH-domain-containing proteins involved in endocytosis. *Plant J.* 55: 1025-1038.
- Barbosa, I. C., Zourelidou, M., Willige, B. C., Weller, B., & Schwechheimer, C.** (2014). D6 PROTEIN KINASE activates auxin transport-dependent growth and PIN-FORMED phosphorylation at the plasma membrane. *Dev. Cell* 29: 674-685.
- Baster, P., Robert, S., Kleine-Vehn, J., Vanneste, S., Kania, U., Grunewald, W., ... & Friml, J.** (2013). SCFTIR1/AFB-auxin signalling regulates PIN vacuolar trafficking and auxin fluxes during root gravitropism. *EMBO J.* 32: 260-274.
- Baum, G., Long, J. C., Jenkins, G. I., & Trewavas, A. J.** (1999). Stimulation of the blue light phototropic receptor NPH1 causes a transient increase in cytosolic Ca^{2+} . *Proc. Natl. Acad. Sci. U.S.A.* 96: 13554-13559.
- Benarroch, E. E.** (2013). Synaptic vesicle exocytosis: molecular mechanisms and clinical implications. *Neurology* 80: 1981-1988.
- Benjamins, R., Ampudia, C. S. G., Hooykaas, P. J., & Offringa, R.** (2003). PINOID-mediated signaling involves calcium-binding proteins. *Plant Physiol.* 132:1623-1630.

- Benjamins, R., Quint, A. B., Weijers, D., Hooykaas, P., & Offringa, R. (2001).** The PINOID protein kinase regulates organ development in Arabidopsis by enhancing polar auxin transport. *Development* 20: 4057-67.
- Benková, E., Michniewicz, M., Sauer, M., Teichmann, T., Seifertová, D., Jürgens, G., & Friml, J. (2003).** Local, efflux-dependent auxin gradients as a common module for plant organ formation. *Cell* 115: 591-602.
- Bennett, M. J., Marchant, A., Green, H. G., May, S. T., Ward, S. P., Millner, P. A., ... & Feldmann, K. A. (1996).** Arabidopsis AUX1 gene: a permease-like regulator of root gravitropism. *Science* 273: 948-950.
- Bennett, S. R., Alvarez, J., Bossinger, G., & Smyth, D. R. (1995).** Morphogenesis in pinoid mutants of Arabidopsis thaliana. *Plant J.* 8: 505-520.
- Blilou, I., Xu, J., Wildwater, M., Willemsen, V., Paponov, I., Friml, J., ... & Scheres, B. (2005).** The PIN auxin efflux facilitator network controls growth and patterning in Arabidopsis roots. *Nature* 433: 39-44.
- Bohn-Courseau, I. (2010).** Auxin: a major regulator of organogenesis. *C. R. Biol.* 333: 290-296.
- Braam, J., & Davis, R. W. (1990).** Rain-, wind-, and touch-induced expression of calmodulin and calmodulin-related genes in Arabidopsis. *Cell* 60: 357-364.
- Braam, J., Sistrunk, M. L., Polisensky, D. H., Xu, W., Purugganan, M. M., Antosiewicz, D. M., ... & Johnson, K. A. (1997).** Plant responses to environmental stress: regulation and functions of the Arabidopsis TCH genes. *Planta* 203: S35-S41.
- Cao, M., Chen, R., Li, P., Yu, Y., Zheng, R., Ge, D., Zheng, W., Wang, X., Gu, Y., Gelová, Z., Friml, J., Zhang, H., Liu, R., He, J., & Xu, T. (2019).** TMK1-mediated auxin signalling regulates differential growth of the apical hook. *Nature* 568: 240-243.
- Carroll, A. D., Moyen, C., Van Kesteren, P., Tooke, F., Battey, N. H., & Brownlee, C. (1998).** Ca^{2+} , annexins, and GTP modulate exocytosis from maize root cap protoplasts. *Plant Cell* 10: 1267-1276.
- Cavallari, N., Artner, C., & Benkova, E. (2021).** Auxin-regulated lateral root organogenesis. *Cold Spring Harb. Perspect. Biol.* 13: a039941.
- Ch, D., & Darwin, F. (1880).** The power of movement in plants. 407-408.
- Chakraborty, S., Toyota, M., Moeder, W., Chin, K., Fortuna, A., Champigny, M., ... & Yoshioka, K. (2021).** CYCLIC NUCLEOTIDE-GATED ION CHANNEL 2 modulates auxin homeostasis and signaling. *Plant Physiol.* 187: 1690-1703.

- Chen, J. G.** (2001). Dual auxin signaling pathways control cell elongation and division. *J. Plant Growth Regul.* 20(3).
- Cheng Y, Qin G, Dai X, Zhao Y.** (2008) NPY genes and AGC kinases define two key steps in auxin-mediated organogenesis in Arabidopsis. *Proc. Natl. Acad. Sci. U.S.A.* 105: 21017–21022.
- Cheng, S., & Wang, Y.** (2022). Subcellular trafficking and post-translational modification regulate PIN polarity in plants. *Front. Plant Sci.* 13: 923293.
- Chitwood, D. H., Headland, L. R., Ranjan, A., Martinez, C. C., Braybrook, S. A., Koenig, D. P., ... & Sinha, N. R.** (2012). Leaf asymmetry as a developmental constraint imposed by auxin-dependent phyllotactic patterning. *Plant Cell* 24: 2318-2327.
- Clark, G. B., Morgan, R. O., Fernandez, M. P., & Roux, S. J.** (2012). Evolutionary adaptation of plant annexins has diversified their molecular structures, interactions and functional roles. *New Phytol.* 196: 695-712.
- Cole, R. A., & Fowler, J. E.** (2006). Polarized growth: maintaining focus on the tip. *Curr. Opin. Plant Biol.* 9: 579-588.
- Craxton, M.** (2004). Synaptotagmin gene content of the sequenced genomes. *BMC Genomics* 5: 1-14.
- Dai, M., Zhang, C., Kania, U., Chen, F., Xue, Q., Mccray, T., ... & Wang, H.** (2012). A PP6-type phosphatase holoenzyme directly regulates PIN phosphorylation and auxin efflux in Arabidopsis. *Plant Cell* 24: 2497-2514.
- Dai, X., Zhang, Y., Zhang, D., Chen, J., Gao, X., Estelle, M., & Zhao, Y.** (2015). Embryonic lethality of Arabidopsis *abp1-1* is caused by deletion of the adjacent *BSM* gene. *Nat. Plants* 1: 1-4.
- Dal Bosco, C., Dovzhenko, A., & Palme, K.** (2012b). Intracellular auxin transport in pollen: PIN8, PIN5 and PILS5. *Plant Signal. Behav.* 7: 1504-1505.
- Dal Bosco, C., Dovzhenko, A., Liu, X., Woerner, N., Rensch, T., Eismann, M., ... & Palme, K.** (2012a). The endoplasmic reticulum localized PIN8 is a pollen-specific auxin carrier involved in intracellular auxin homeostasis. *Plant J.* 71: 860-870.
- Day, I. S., Reddy, V. S., Shad Ali, G., & Reddy, A. S. N.** (2002). Analysis of EF-hand-containing proteins in Arabidopsis. *Genome Biol.* 3: 1-24.
- De Smet, I., Voß, U., Lau, S., Wilson, M., Shao, N., Timme, R. E., ... & Beeckman, T.** (2011). Unraveling the evolution of auxin signaling. *Plant Physiol.* 155: 209-221.

- Deb, Y., Marti, D., Frenz, M., Kuhlemeier, C., & Reinhardt, D. (2015).** Phyllotaxis involves auxin drainage through leaf primordia. *Development* 142: 1992-2001.
- Dela Fuente, R. K. (1984).** Role of calcium in the polar secretion of indoleacetic acid. *Plant Physiol.* 76: 342-346.
- Dela Fuente, R. K., & Leopold, A. C. (1973).** A role for calcium in auxin transport. *Plant Physiol.* 51: 845-847.
- Dhonukshe, P., Huang, F., Galvan-Ampudia, C. S., Mähönen, A. P., Kleine-Vehn, J., Xu, J., ... & Offringa, R. (2010).** Plasma membrane-bound AGC3 kinases phosphorylate PIN auxin carriers at TPRXS (N/S) motifs to direct apical PIN recycling. *Development* 137: 3245-3255.
- Dhonukshe, P., Tanaka, H., Goh, T., Ebine, K., Mähönen, A. P., Prasad, K., ... & Friml, J. (2008).** Generation of cell polarity in plants links endocytosis, auxin distribution and cell fate decisions. *Nature* 456: 962-966.
- Dindas, J., Scherzer, S., Roelfsema, M. R. G., von Meyer, K., Müller, H. M., Al-Rasheid, K. A. S., ... & Hedrich, R. (2018).** AUX1-mediated root hair auxin influx governs SCFTIR1/AFB-type Ca^{2+} signaling. *Nat. Commun.* 9: 1174.
- Ding, Z., & Friml, J. (2010).** Auxin regulates distal stem cell differentiation in Arabidopsis roots. *Proc. Natl. Acad. Sci. U.S.A.* 107: 12046-12051.
- Ding, Z., Galván-Ampudia, C. S., Demarsy, E., Łangowski, Ł., Kleine-Vehn, J., Fan, Y., ... & Friml, J. (2011).** Light-mediated polarization of the PIN3 auxin transporter for the phototropic response in Arabidopsis. *Nat. Cell Biol.* 13: 447-452.
- Ding, Z., Wang, B., Moreno, I., Dupláková, N., Simon, S., Carraro, N., ... & Friml, J. (2012).** ER-localized auxin transporter PIN8 regulates auxin homeostasis and male gametophyte development in Arabidopsis. *Nat. Commun.* 3: 941.
- Ditengou, F. A., Gomes, D., Nziengui, H., Kochersperger, P., Lasok, H., Medeiros, V., ... & Palme, K. (2018).** Characterization of auxin transporter PIN 6 plasma membrane targeting reveals a function for PIN 6 in plant bolting. *New Phytol.* 217: 1610-1624.
- Dory, M., Hatzimasoura, E., Kállai, B. M., Nagy, S. K., Jäger, K., Darula, Z., ... & Dóczi, R. (2018).** Coevolving MAPK and PID phosphosites indicate an ancient environmental control of PIN auxin transporters in land plants. *FEBS Lett.* 592: 89-102.
- Dreher, K. A., Brown, J., Saw, R. E., & Callis, J. (2006).** The Arabidopsis Aux/IAA protein family has diversified in degradation and auxin responsiveness. *Plant Cell* 18: 699-714.

- Du, M., Spalding, E. P., & Gray, W. M. (2020).** Rapid auxin-mediated cell expansion. *Annu. Rev. Plant Biol.* 71: 379-402.
- Du, W., Wang, Y., Liang, S., & Lu, Y. T. (2005).** Biochemical and expression analysis of an Arabidopsis calcium-dependent protein kinase-related kinase. *Plant Sci.* 168: 1181-1192.
- Du, W., Wang, Y., Liang, S., & Lu, Y. T. (2005).** Biochemical and expression analysis of an Arabidopsis calcium-dependent protein kinase-related kinase. *Plant Sci.* 168: 1181-1192.
- Dubey, S. M., Han, S., Stutzman, N., Prigge, M. J., Medvecká, E., Platre, M. P., ... & Estelle, M. (2023).** The AFB1 auxin receptor controls the cytoplasmic auxin response pathway in Arabidopsis thaliana. *Mol. Plant* 7: 1120-1130.
- Eklund, L., & Eliasson, L. (1990).** Effects of calcium ion concentration on cell wall synthesis. *J. Exp. Bot.* 41: 863-867.
- Enders, T. A., Frick, E. M., & Strader, L. C. (2017).** An Arabidopsis kinase cascade influences auxin-responsive cell expansion. *Plant J.* 92: 68-81.
- Fan, Y. (2014).** The role of AGC3 kinases and calmodulins in plant growth responses to abiotic signals (Doctoral dissertation, Leiden University).
- Fendrych, M., Akhmanova, M., Merrin, J., Glanc, M., Hagihara, S., Takahashi, K., ... & Friml, J. (2018).** Rapid and reversible root growth inhibition by TIR1 auxin signalling. *Nat. Plants* 453–459 (2018).
- Fendrych, M., Akhmanova, M., Merrin, J., Glanc, M., Hagihara, S., Takahashi, K., ... & Friml, J. (2018).** Rapid and reversible root growth inhibition by TIR1 auxin signalling. *Nat. Plants* 4: 453-459.
- Friml, J., Benková, E., Blilou, I., Wisniewska, J., Hamann, T., Ljung, K., ... & Palme, K. (2002a).** AtPIN4 mediates sink-driven auxin gradients and root patterning in Arabidopsis. *Cell* 108: 661-673.
- Friml, J., Gallei, M., Gelová, Z., Johnson, A., Mazur, E., Monzer, A. et al. (2022)** ABP1-TMK auxin perception for global phosphorylation and auxin canalization. *Nature* 609: 575–581.
- Friml, J., Vieten, A., Sauer, M., Weijers, D., Schwarz, H., Hamann, T., ... & Jürgens, G. (2003).** Efflux-dependent auxin gradients establish the apical–basal axis of Arabidopsis. *Nature* 426: 147-153.
- Friml, J., Wiśniewska, J., Benková, E., Mendgen, K., & Palme, K. (2002b).** Lateral relocation of auxin efflux regulator PIN3 mediates tropism in Arabidopsis. *Nature* 415: 806-809.

- Friml, J., Yang, X., Michniewicz, M., Weijers, D., Quint, A., Tietz, O., ... & Offringa, R.** (2004). A PINOID-dependent binary switch in apical-basal PIN polar targeting directs auxin efflux. *Science* 306: 862-865.
- Gadeyne, A., Sánchez-Rodríguez, C., Vanneste, S., Di Rubbo, S., Zaubner, H., Vanneste, K., ... & Van Damme, D.** (2014). The TPLATE adaptor complex drives clathrin-mediated endocytosis in plants. *Cell* 156: 691-704.
- Galván-Ampudia, C. S.** (2009). Plant Agc protein kinases orient auxin-mediated differential growth and organogenesis (Doctoral dissertation, Leiden University).
- Galvan-Ampudia, C. S., Julkowska, M. M., Darwish, E., Gandullo, J., Korver, R. A., Brunoud, G., ... & Testerink, C.** (2013). Halotropism is a response of plant roots to avoid a saline environment. *Curr. Biol.* 23: 2044-2050.
- Galweiler, L., Guan, C., Muller, A., Wisman, E., Mendgen, K., Yephremov, A., & Palme, K.** (1998). Regulation of polar auxin transport by AtPIN1 in Arabidopsis vascular tissue. *Science* 282: 2226-2230.
- Gehring, C. A., Irving, H. R., & Parish, R. W.** (1990). Effects of auxin and abscisic acid on cytosolic calcium and pH in plant cells. *Proc. Natl. Acad. Sci. U.S.A.* 87: 9645-9649.
- Geisler, M. M.** (2021). A retro-perspective on auxin transport. *Front. Plant Sci.* 12: 756968.
- Gelová, Z., Gallei, M., Pernisová, M., Brunoud, G., Zhang, X., Glanc, M., ... & Friml, J.** (2021). Developmental roles of auxin binding protein 1 in Arabidopsis thaliana. *Plant Sci.* 303: 110750.
- Gerke, V., & Moss, S. E.** (2002). Annexins: from structure to function. *Physiol. Rev.* 82: 331-371.
- Goh, C. S., Lee, Y., & Kim, S. H.** (2012). Calcium could be involved in auxin-regulated maintenance of the quiescent center in the Arabidopsis root. *J. Plant Biol.* 55: 143-150.
- Goldsmith, M. H. M.** (1977). The polar transport of auxin. *Annu. Rev. Plant Physiol.* 28: 439-478.
- Grones, P., & Friml, J.** (2015). Auxin transporters and binding proteins at a glance. *J. Cell Sci.* 128: 1-7.
- Grunewald, W., & Friml, J.** (2010). The march of the PINs: developmental plasticity by dynamic polar targeting in plant cells. *EMBO J.* 29: 2700-2714.
- Guo, X., Qin, Q., Yan, J., Niu, Y., Huang, B., Guan, L., ... & Hou, S.** (2015). TYPE-ONE PROTEIN PHOSPHATASE4 regulates pavement cell interdigitation by modulating PIN-FORMED1 polarity and trafficking in Arabidopsis. *Plant Physiol.* 167: 1058-1075.

- Hajnó, J., Prát, T., Rydza, N., Rodriguez, L., Tan, S., Verstraeten, I., ... & Friml, J. (2020).** Receptor kinase module targets PIN-dependent auxin transport during canalization. *Science* 370: 550-557.
- Halliday, K. J., Martínez-García, J. F., & Josse, E. M. (2009).** Integration of light and auxin signaling. *Cold Spring Harb. Perspect. Biol.* 1: a001586.
- Han, H., Adamowski, M., Qi, L., Alotaibi, S. S., & Friml, J. (2021).** PIN-mediated polar auxin transport regulations in plant tropic responses. *New Phytol.* 232: 510-522.
- Harada, A., & Shimazaki, K. I. (2007).** Phototropins and blue light-dependent calcium signaling in higher plants. *J. Photochem. Photobiol.* 83: 102-111.
- Harada, A., Sakai, T., & Okada, K. (2003).** Phot1 and phot2 mediate blue light-induced transient increases in cytosolic Ca^{2+} differently in Arabidopsis leaves. *Proc. Natl. Acad. Sci. U.S.A.* 100: 8583-8588.
- Harmon, A. C. (2003).** Calcium-regulated protein kinases of plants. *Gravit. Space Biol.* 16: 83-91.
- Harper, J. F., Breton, G., & Harmon, A. (2004).** Decoding Ca^{2+} signals through plant protein kinases. *Annu. Rev. Plant Biol.* 55: 263-288.
- Hasenstein, K. H., & Evans, M. L. (1986).** Calcium dependence of rapid auxin action in maize roots. *Plant Physiol.* 81: 439-443.
- Hashimoto, K., & Kudla, J. (2011).** Calcium decoding mechanisms in plants. *Biochimie* 93: 2054-2059.
- He, F., Gao, C., Guo, G., Liu, J., Gao, Y., Pan, R., ... & Hu, J. (2019).** Maize annexin genes ZmANN33 and ZmANN35 encode proteins that function in cell membrane recovery during seed germination. *J. Exp. Bot.* 70: 1183-1195.
- Heisler, M. G., & Byrne, M. E. (2020).** Progress in understanding the role of auxin in lateral organ development in plants. *Curr. Opin. Plant Biol.* 53: 73-79.
- Hepler, P. K., & Wayne, R. O. (1985).** Calcium and plant development. *Annual review of Plant Physiol.* 36: 397-439.
- Hohm, T., Preuten, T., & Fankhauser, C. (2013).** Phototropism: translating light into directional growth. *Am. J. Bot.* 100: 47-59.
- Huang, F., Kemel Zago, M., Abas, L., van Marion, A., Galván-Ampudia, C. S., & Offringa, R. (2010).** Phosphorylation of conserved PIN motifs directs Arabidopsis PIN1 polarity and auxin transport. *Plant Cell* 22: 1129-1142.
- Ischebeck, T., Werner, S., Krishnamoorthy, P., Lerche, J., Meijón, M., Stenzel, I., ... & Heilmann, I. (2013).** Phosphatidylinositol 4, 5-bisphosphate influences PIN polarization by controlling clathrin-mediated membrane trafficking in Arabidopsis. *Plant Cell* 25: 4894-4911.

- Jenik, P. D., & Barton, M. K.** (2005). Surge and destroy: the role of auxin in plant embryogenesis. *Development* 16: 3577-85.
- Jia, W., Li, B., Li, S., Liang, Y., Wu, X., Ma, M., ... & Wang, Y.** (2016). Mitogen-activated protein kinase cascade MKK7-MPK6 plays important roles in plant development and regulates shoot branching by phosphorylating PIN1 in *Arabidopsis*. *PLoS Biol.* 14: e1002550.
- Jurado, S., Abraham, Z., Manzano, C., Lopez-Torrejon, G., Pacios, L. F., & Del Pozo, J. C.** (2010). The *Arabidopsis* cell cycle F-box protein SKP2A binds to auxin. *Plant Cell* 22: 3891-3904.
- Kim, S., Park, K., Kwon, C., & Yun, H. S.** (2022). Synaptotagmin 4 and 5 additively contribute to *Arabidopsis* immunity to *Pseudomonas syringae* DC3000. *Plant Signal. Behav.* 17: 2025323.
- Kimura, T., Haga, K., Shimizu-Mitao, Y., Takebayashi, Y., Kasahara, H., Hayashi, K. I., ... & Sakai, T.** (2018). Asymmetric auxin distribution is not required to establish root phototropism in *Arabidopsis*. *Plant Cell Physiol.* 59: 828-840.
- Kleine-Vehn, J., & Friml, J.** (2008). Polar targeting and endocytic recycling in auxin-dependent plant development. *Annu. Rev. Cell Dev. Biol.* 24: 447-473.
- Kleine-Vehn, J., Ding, Z., Jones, A. R., Tasaka, M., Morita, M. T., & Friml, J.** (2010). Gravity-induced PIN transcytosis for polarization of auxin fluxes in gravity-sensing root cells. *Proc. Natl. Acad. Sci. U.S.A.* 107: 22344-22349.
- Kleine-Vehn, J., Leitner, J., Zwiewka, M., Sauer, M., Abas, L., Luschnig, C., & Friml, J.** (2008). Differential degradation of PIN2 auxin efflux carrier by retromer-dependent vacuolar targeting. *Proc. Natl. Acad. Sci. U.S.A.* 105: 17812-17817.
- Kögl, F., Erxleben, H., & Haagen-Smit, A. J.** (1934). Über die Isolierung der Auxine a und b aus pflanzlichen Materialien. 9. Mitteilung über pflanzliche Wachstumsstoffe. *Physiologische Chemie.* 225: 215-229.
- Kohnen, M. V., Schmid-Siebert, E., Trevisan, M., Petrolati, L. A., Sénéchal, F., Müller-Moulé, P., ... & Fankhauser, C.** (2016). Neighbor detection induces organ-specific transcriptomes, revealing patterns underlying hypocotyl-specific growth. *Plant Cell* 28: 2889-2904.
- Křeček, P., Skůpa, P., Libus, J., Naramoto, S., Tejos, R., Friml, J., & Zažímalová, E.** (2009). The PIN-FORMED (PIN) protein family of auxin transporters. *Genome Biol.* 10: 1-11.

- Kuhn, A., Ramans Harborough, S., McLaughlin, H. M., Natarajan, B., Verstraeten, I., Friml, J., ... & Østergaard, L.** (2020). Direct ETTIN-auxin interaction controls chromatin states in gynoecium development. *Elife* 9: e51787.
- Landrein, B., Kiss, A., Sassi, M., Chauvet, A., Das, P., Cortizo, M., ... & Hamant, O.** (2015). Mechanical stress contributes to the expression of the STM homeobox gene in Arabidopsis shoot meristems. *Elife* 4: e07811.
- Leclercq, J., Ranty, B., Sanchez-Ballesta, M. T., Li, Z., Jones, B., Jauneau, A., ... & Bouzayen, M.** (2005). Molecular and biochemical characterization of LeCRK1, a ripening-associated tomato CDPK-related kinase. *J. Exp. Bot.* 56: 25-35.
- Lee, H. J., Kim, H. S., Park, J. M., Cho, H. S., & Jeon, J. H.** (2020). PIN-mediated polar auxin transport facilitates root– obstacle avoidance. *New Phytol.* 225: 1285-1296.
- Lee, J. S., Mulkey, T. J., & Evans, M. L.** (1984). Inhibition of polar calcium movement and gravitropism in roots treated with auxin-transport inhibitors. *Planta* 160: 536-543.
- Lešková, A., Zvarík, M., Araya, T., & Giehl, R. F.** (2020). Nickel toxicity targets cell wall-related processes and PIN2-mediated auxin transport to inhibit root elongation and gravitropic responses in Arabidopsis. *Plant Cell Physiol.* 61: 519-535.
- Li, P., Zhao, C., Zhang, Y., Wang, X., Wang, X., Wang, J., ... & Bi, Y.** (2016). Calcium alleviates cadmium-induced inhibition on root growth by maintaining auxin homeostasis in Arabidopsis seedlings. *Protoplasma* 253: 185-200.
- Li, Q., Zhu, X., Ishikura, S., Zhang, D., Gao, J., Sun, Y., ... & Niu, W.** (2014). Ca^{2+} signals promote GLUT4 exocytosis and reduce its endocytosis in muscle cells. *Am. J. Physiol. - Endocrinol. Metab.* 307: E209-E224.
- Li, T., Yan, A., Bhatia, N., Altinok, A., Afik, E., Durand-Smet, P., ... & Meyerowitz, E. M.** (2019). Calcium signals are necessary to establish auxin transporter polarity in a plant stem cell niche. *Nat. Commun.* 10: 726.
- Lichocka, M., Krzymowska, M., Górecka, M., & Hennig, J.** (2022). Arabidopsis annexin 5 is involved in maintenance of pollen membrane integrity and permeability. *J. Exp. Bot.* 73: 94-109.
- Lin, L., Wu, J., Jiang, M., & Wang, Y.** (2021). Plant mitogen-activated protein kinase cascades in environmental stresses. *Int. J. Mol. Sci.* 22: 1543.
- Luan, S., Kudla, J., Rodriguez-Concepcion, M., Yalovsky, S., & Gruissem, W.** (2002). Calmodulins and calcineurin B-like proteins: Calcium sensors for specific signal response coupling in plants. *Plant Cell* 14: S389-S400.

- Lv, B., Yu, Q., Liu, J., Wen, X., Yan, Z., Hu, K., Li, H., Kong, X., Li, C., Tian, H., De Smet, I., Zhang, X. S., & Ding, Z. (2020).** Non-canonical AUX/IAA protein IAA33 competes with canonical AUX/IAA repressor IAA5 to negatively regulate auxin signaling. *EMBO J.* 39: e101515.
- Mäkilä, R., Wybouw, B., Smetana, O., Vainio, L., Solé-Gil, A., Lyu, M., ... & Mähönen, A. P. (2023).** Gibberellins promote polar auxin transport to regulate stem cell fate decisions in cambium. *Nat. Plants* 1-14.
- Marcos, D., & Berleth, T. (2014).** Dynamic auxin transport patterns preceding vein formation revealed by live-imaging of Arabidopsis leaf primordia. *Front. Plant Sci.* 5: 235.
- Marhava, P. (2022).** Recent developments in the understanding of PIN polarity. *New Phytol.* 233: 624-630.
- Marhava, P., Bassukas, A. E. L., Zourelidou, M., Kolb, M., Moret, B., Fastner, A., ... & Hardtke, C. S. (2018).** A molecular rheostat adjusts auxin flux to promote root protophloem differentiation. *Nature* 558: 297-300.
- Marhavý, P., Duclercq, J., Weller, B., Feraru, E., Bielach, A., Offringa, R., ... & Benková, E. (2014).** Cytokinin controls polarity of PIN1-dependent auxin transport during lateral root organogenesis. *Curr. Biol.* 24: 1031-1037.
- Mattsson, J., Sung, Z. R., & Berleth, T. (1999).** Responses of plant vascular systems to auxin transport inhibition. *Development* 126: 2979-2991.
- Mazur, E., Benková, E., & Friml, J. (2016).** Vascular cambium regeneration and vessel formation in wounded inflorescence stems of Arabidopsis. *Sci. Rep.* 6: 1-15.
- McCormack, E., & Braam, J. (2003).** Calmodulins and related potential calcium sensors of Arabidopsis. *New Phytol.* 159: 585-598.
- McLaughlin, H. M., Ang, A. C. H., & Østergaard, L. (2021).** Noncanonical auxin signaling. *Cold Spring Harb. Perspect. Biol.* 13: a039917.
- Michalko, J., Dravecká, M., Bollenbach, T., & Friml, J. (2015).** Embryo-lethal phenotypes in early *abp1* mutants are due to disruption of the neighboring *BSM* gene. *F1000Research* 4.
- Michniewicz, M., Zago, M. K., Abas, L., Weijers, D., Schweighofer, A., Meskiene, I., ... & Friml, J. (2007).** Antagonistic regulation of PIN phosphorylation by PP2A and PINOID directs auxin flux. *Cell* 130: 1044-1056.
- Monshausen, G. B., Miller, N. D., Murphy, A. S., & Gilroy, S. (2011).** Dynamics of auxin-dependent Ca^{2+} and pH signaling in root growth revealed by integrating high-resolution imaging with automated computer vision-based analysis. *Plant J.* 65: 309-318.

- Monshausen, G. B., Miller, N. D., Murphy, A. S., & Gilroy, S. (2011).** Dynamics of auxin-dependent Ca^{2+} and pH signaling in root growth revealed by integrating high-resolution imaging with automated computer vision-based analysis. *Plant J.* 65: 309-318.
- Moulija, B., Coutand, C., & Julien, J. L. (2015).** Mechanosensitive control of plant growth: bearing the load, sensing, transducing, and responding. *Front. Plant Sci.* 6: 52.
- Mravec, J., Skůpa, P., Bailly, A., Hoyerová, K., Křeček, P., Bielach, A., ... & Friml, J. (2009).** Subcellular homeostasis of phytohormone auxin is mediated by the ER-localized PIN5 transporter. *Nature* 459: 1136-1140.
- Mroue, S., Simeunovic, A., & Robert, H. S. (2018).** Auxin production as an integrator of environmental cues for developmental growth regulation. *J. Exp. Bot.* 69: 201-212.
- Müller, C. J., Valdés, A. E., Wang, G., Ramachandran, P., Beste, L., Uddenberg, D., & Carlsbecker, A. (2016).** PHABULOSA mediates an auxin signaling loop to regulate vascular patterning in Arabidopsis. *Plant Physiol.* 170: 956-970.
- Nakayama, N., Smith, R. S., Mandel, T., Robinson, S., Kimura, S., Boudaoud, A., & Kuhlemeier, C. (2012).** Mechanical regulation of auxin-mediated growth. *Curr. Biol.* 22: 1468-1476.
- Naser, V., & Shani, E. (2016).** Auxin response under osmotic stress. *Plant Mol. Biol.* 91: 661-672.
- Okada, K., Ueda, J., Komaki, M. K., Bell, C. J., & Shimura, Y. (1991).** Requirement of the auxin polar transport system in early stages of Arabidopsis floral bud formation. *Plant Cell* 3: 677-684.
- Paciorek, T., & Friml, J. (2006).** Auxin signaling. *J. Cell Sci.* 119: 1199-1202.
- Paciorek, T., Zažímalová, E., Ruthardt, N., Petrášek, J., Stierhof, Y. D., Kleine-Vehn, J., ... & Friml, J. (2005).** Auxin inhibits endocytosis and promotes its own efflux from cells. *Nature* 435: 1251-1256.
- Page, E., Goings, G. E., Upshaw-Earley, J., & Hanck, D. A. (1994).** Endocytosis and uptake of lucifer yellow by cultured atrial myocytes and isolated intact atria from adult rats. Regulation and subcellular localization. *Circ. Res.* 75: 335-346.
- Pan, X., Fang, L., Liu, J., Senay-Aras, B., Lin, W., Zheng, S., ... & Yang, Z. (2020).** Auxin-induced signaling protein nanoclustering contributes to cell polarity formation. *Nat. commun.* 11: 3914.
- Pang, Z. P., & Südhof, T. C. (2010).** Cell biology of Ca^{2+} -triggered exocytosis. *Curr. Opin. Cell Biol.* 22: 496-505.

- Péret, B., Swarup, K., Ferguson, A., Seth, M., Yang, Y., Dhondt, S., ... & Swarup, R. (2012).** AUX/LAX genes encode a family of auxin influx transporters that perform distinct functions during Arabidopsis development. *Plant Cell* 24: 2874-2885.
- Pérez-Henríquez, P., & Yang, Z. (2023).** Extranuclear auxin signaling: a new insight into auxin's versatility. *New Phytol.* 237: 1115-1121.
- Perrot-Rechenmann, C. (2010).** Cellular responses to auxin: division versus expansion. *Cold Spring Harb. Perspect. Biol.* 2: a001446.
- Petrášek, J., Mravec, J., Bouchard, R., Blakeslee, J. J., Abas, M., Seifertová, D., ... & Friml, J. (2006).** PIN proteins perform a rate-limiting function in cellular auxin efflux. *Science* 312: 914-918.
- Plieth, C., & Trewavas, A. J. (2002).** Reorientation of seedlings in the earth's gravitational field induces cytosolic calcium transients. *Plant Physiol.* 129: 786-796.
- Prasad, K., & Dhonukshe, P. (2013).** Polar auxin transport: cell polarity to patterning. In *Polar auxin transport* 25-44.
- Prát, T., Hajný, J., Grunewald, W., Vasileva, M., Molnár, G., Tejos, R., Schmid, M., Sauer, M., & Friml, J. (2018).** WRKY23 is a component of the transcriptional network mediating auxin feedback on PIN polarity. *PLoS Genet.* 14: e1007177.
- Prigge, M. J., Platre, M., Kadakia, N., Zhang, Y., Greenham, K., Szutu, W., ... & Estelle, M. (2020).** Genetic analysis of the Arabidopsis TIR1/AFB auxin receptors reveals both overlapping and specialized functions. *eLife* 9: e54740.
- Qi, J., Wang, Y., Yu, T., Cunha, A., Wu, B., Vernoux, T., ... & Jiao, Y. (2014).** Auxin depletion from leaf primordia contributes to organ patterning. *Proc. Natl. Acad. Sci. U.S.A.* 111: 18769-18774.
- Qi, L., Kwiakowski, M., Chen, H., Hoermayer, L., Sinclair, S., Zou, M., ... & Friml, J. (2022).** Adenylate cyclase activity of TIR1/AFB auxin receptors in plants. *Nature* 611: 133-138.
- Raven, J. A. (1975).** Transport of indoleacetic acid in plant cells in relation to pH and electrical potential gradients, and its significance for polar IAA transport. *New Phytol.* 74: 163-172.
- Reddy, A., Caler, E. V., & Andrews, N. W. (2001).** Plasma membrane repair is mediated by Ca^{2+} -regulated exocytosis of lysosomes. *Cell* 106: 157-169.
- Reinhardt, D., Mandel, T., & Kuhlemeier, C. (2000).** Auxin regulates the initiation and radial position of plant lateral organs. *Plant Cell* 12: 507-518.

- Reinhardt, D., Pesce, E. R., Stieger, P., Mandel, T., Baltensperger, K., Bennett, M., ... & Kuhlmeier, C.** (2003). Regulation of phyllotaxis by polar auxin transport. *Nature* 426: 255-260
- Retzer, K., Akhmanova, M., Konstantinova, N., Malínská, K., Leitner, J., Petrášek, J., & Luschnig, C.** (2019). Brassinosteroid signaling delimits root gravitropism via sorting of the *Arabidopsis* PIN2 auxin transporter. *Nat. Commun.* 10: 5516.
- Rigo, G., Ayaydin, F., Tietz, O., Zsigmond, L., Kovács, H., Páy, A., ... & Cséplő, Á.** (2013). Inactivation of plasma membrane-localized CDPK-RELATED KINASE5 decelerates PIN2 exocytosis and root gravitropic response in *Arabidopsis*. *Plant Cell* 25: 1592-1608.
- Robert, H. S.** (2008). Calcium-and BTB domain protein-modulated PINOID protein kinase directs polar auxin transport. (Doctoral dissertation, Leiden University).
- Robert, H. S., Quint, A., Brand, D., Vivian-Smith, A., & Offringa, R.** (2009). BTB and TAZ domain scaffold proteins perform a crucial function in *Arabidopsis* development. *Plant J.* 58: 109-121.
- Roberts, D. M., & Harmon, A. C.** (1992). Calcium-modulated proteins: targets of intracellular calcium signals in higher plants. *Annu. Rev. Plant Biol.* 43: 375-414.
- Rodriguez, L., Fiedler, L., Zou, M., Giannini, C., Monzer, A., Gelova, Z., ... & Friml, J.** (2022). Cell surface auxin signalling directly targets PIN-mediated auxin fluxes for adaptive plant development. *bioRxiv*, 2022-11.
- Rubery, P. H., & Sheldrake, A. R.** (1973). Effect of pH and surface charge on cell uptake of auxin. *Nat. New Biol.* 244: 285-288.
- Ruiz Rosquete, M., Waidmann, S., & Kleine-Vehn, J.** (2018). PIN7 auxin carrier has a preferential role in terminating radial root expansion in *Arabidopsis thaliana*. *Int. J. Mol. Sci.* 19: 1238.
- Ruiz-Lopez, N., Pérez-Sancho, J., Del Valle, A. E., Haslam, R. P., Vanneste, S., Catalá, R., ... & Botella, M. A.** (2021). Synaptotagmins at the endoplasmic reticulum-plasma membrane contact sites maintain diacylglycerol homeostasis during abiotic stress. *Plant Cell* 33: 2431-2453.
- Saini, S., Sharma, I., Kaur, N., & Pati, P. K.** (2013). Auxin: a master regulator in plant root development. *Plant Cell Rep.* 32, 741-757.
- Sanders, D., Pelloux, J., Brownlee, C., & Harper, J. F.** (2002). Calcium at the crossroads of signaling. *Plant Cell* 14: S401-S417.

- Santin, F., Bhogale, S., Fantino, E., Grandellis, C., Banerjee, A. K., & Ulloa, R. M.** (2017). *Solanum tuberosum* StCDPK1 is regulated by miR390 at the posttranscriptional level and phosphorylates the auxin efflux carrier StPIN4 in vitro, a potential downstream target in potato development. *Physiol. Plant.* 159: 244-261.
- Sassi, M., & Vernoux, T.** (2013). Auxin and self-organization at the shoot apical meristem. *J. Exp. Bot.* 64: 2579-2592.
- Sato, A., & Yamamoto, K. T.** (2008). Overexpression of the non-canonical Aux/IAA genes causes auxin-related aberrant phenotypes in *Arabidopsis*. *Physiol. Plant.* 133: 397-405.
- Sauer, M., Balla, J., Luschig, C., Wiśniewska, J., Reinöhl, V., Friml, J., & Benková, E.** (2006). Canalization of auxin flow by Aux/IAA-ARF-dependent feedback regulation of PIN polarity. *Genes Dev.* 20: 2902-2911.
- Scarpella, E., Barkoulas, M., & Tsiantis, M.** (2010). Control of leaf and vein development by auxin. *Cold Spring Harb. Perspect. Biol.* 2: a001511.
- Schapire, A. L., Voigt, B., Jasik, J., Rosado, A., Lopez-Cobollo, R., Menzel, D., ... & Botella, M. A.** (2008). *Arabidopsis* synaptotagmin 1 is required for the maintenance of plasma membrane integrity and cell viability. *Plant Cell* 20: 3374-3388.
- Serre, N. B., Kralík, D., Yun, P., Slouka, Z., Shabala, S., & Fendrych, M.** (2021). AFB1 controls rapid auxin signalling through membrane depolarization in *Arabidopsis thaliana* root. *Nature Plants* 7: 1229–1238.
- Shih, H. W., DePew, C. L., Miller, N. D., & Monshausen, G. B.** (2015). The cyclic nucleotide-gated channel CNGC14 regulates root gravitropism in *Arabidopsis thaliana*. *Curr. Biol.* 23: 3119-25.
- Shishova, M., & Lindberg, S.** (2004). Auxin induces an increase of Ca^{2+} concentration in the cytosol of wheat leaf protoplasts. *J. Plant Physiol.* 161: 937-945.
- Shishova, M., & Lindberg, S.** (2010). A new perspective on auxin perception. *J. Plant Physiol.* 167: 417-422.
- Šimášková, M., O'Brien, J. A., Khan, M., Van Noorden, G., Ötvös, K., Vieten, A., ... & Benková, E.** (2015). Cytokinin response factors regulate PIN-FORMED auxin transporters. *Nat. Commun.* 6: 8717.
- Simon, S., Skůpa, P., Viaene, T., Zwiewka, M., Tejos, R., Klíma, P., ... & Friml, J.** (2016). PIN6 auxin transporter at endoplasmic reticulum and plasma membrane mediates auxin homeostasis and organogenesis in *Arabidopsis*. *New Phytol.* 211: 65-74.

- Simonini, S., Deb, J., Moubayidin, L., Stephenson, P., Valluru, M., Freire-Rios, A., Sorefan, K., Weijers, D., Friml, J., and Østergaard, L. (2016).** A noncanonical auxin-sensing mechanism is required for organ morphogenesis in *Arabidopsis*. *Genes Dev.* 30: 2286-2296.
- Simonini, S., Mas, P. J., Mas, C. M., Østergaard, L., & Hart, D. J. (2018).** Auxin sensing is a property of an unstructured domain in the Auxin Response Factor ETTIN of *Arabidopsis thaliana*. *Sci. Rep.* 8: 1-11.
- Sisi, N. A., & Růžicka, K. (2020).** ER-localized PIN carriers: regulators of intracellular auxin homeostasis. *Plants* 9: 1527
- Smith, R. S., & Bayer, E. M. (2009).** Auxin transport-feedback models of patterning in plants. *Plant Cell Environ.* 32: 1258-1271.
- Sukumar, P., Edwards, K. S., Rahman, A., DeLong, A., & Muday, G. K. (2009).** PINOID kinase regulates root gravitropism through modulation of PIN2-dependent basipetal auxin transport in *Arabidopsis*. *Plant Physiol.* 150:722-735.
- Sutter, J. U., Denecke, J., & Thiel, G. (2012).** Synthesis of vesicle cargo determines amplitude of Ca^{2+} -sensitive exocytosis. *Cell Calcium* 52: 283-288.
- Sutter, J. U., Homann, U., & Thiel, G. (2000).** Ca^{2+} -stimulated exocytosis in maize coleoptile cells. *Plant Cell* 12: 1127-1136.
- Swarup, K., Benková, E., Swarup, R., Casimiro, I., Péret, B., Yang, Y., ... & Bennett, M. J. (2008).** The auxin influx carrier LAX3 promotes lateral root emergence. *Nat. Cell Biol.* 10: 946-954.
- Swarup, R., Friml, J., Marchant, A., Ljung, K., Sandberg, G., Palme, K., & Bennett, M. (2001).** Localization of the auxin permease AUX1 suggests two functionally distinct hormone transport pathways operate in the *Arabidopsis* root apex. *Genes Dev.* 15: 2648-2653.
- Tan, S., Zhang, X., Kong, W., Yang, X. L., Molnár, G., Vondráková, Z., ... & Xue, H. W. (2020).** The lipid code-dependent phosphoswitch PDK1–D6PK activates PIN-mediated auxin efflux in *Arabidopsis*. *Nat. Plants* 6: 556-569.
- Tejos, R., Sauer, M., Vanneste, S., Palacios-Gomez, M., Li, H., Heilmann, M., ... & Friml, J. (2014).** Bipolar plasma membrane distribution of phosphoinositides and their requirement for auxin-mediated cell polarity and patterning in *Arabidopsis*. *Plant Cell* 26: 2114-2128.
- Tester, M., & Zorec, R. (1992).** Cytoplasmic calcium stimulates exocytosis in a plant secretory cell. *Biophysical J.* 63: 864-867.
- Toyota, M., Furuichi, T., Tatsumi, H., & Sokabe, M. (2008).** Critical consideration on the relationship between auxin transport and calcium transients in gravity perception of *Arabidopsis* seedlings. *Plant Signal. Behav.* 3: 521-524.

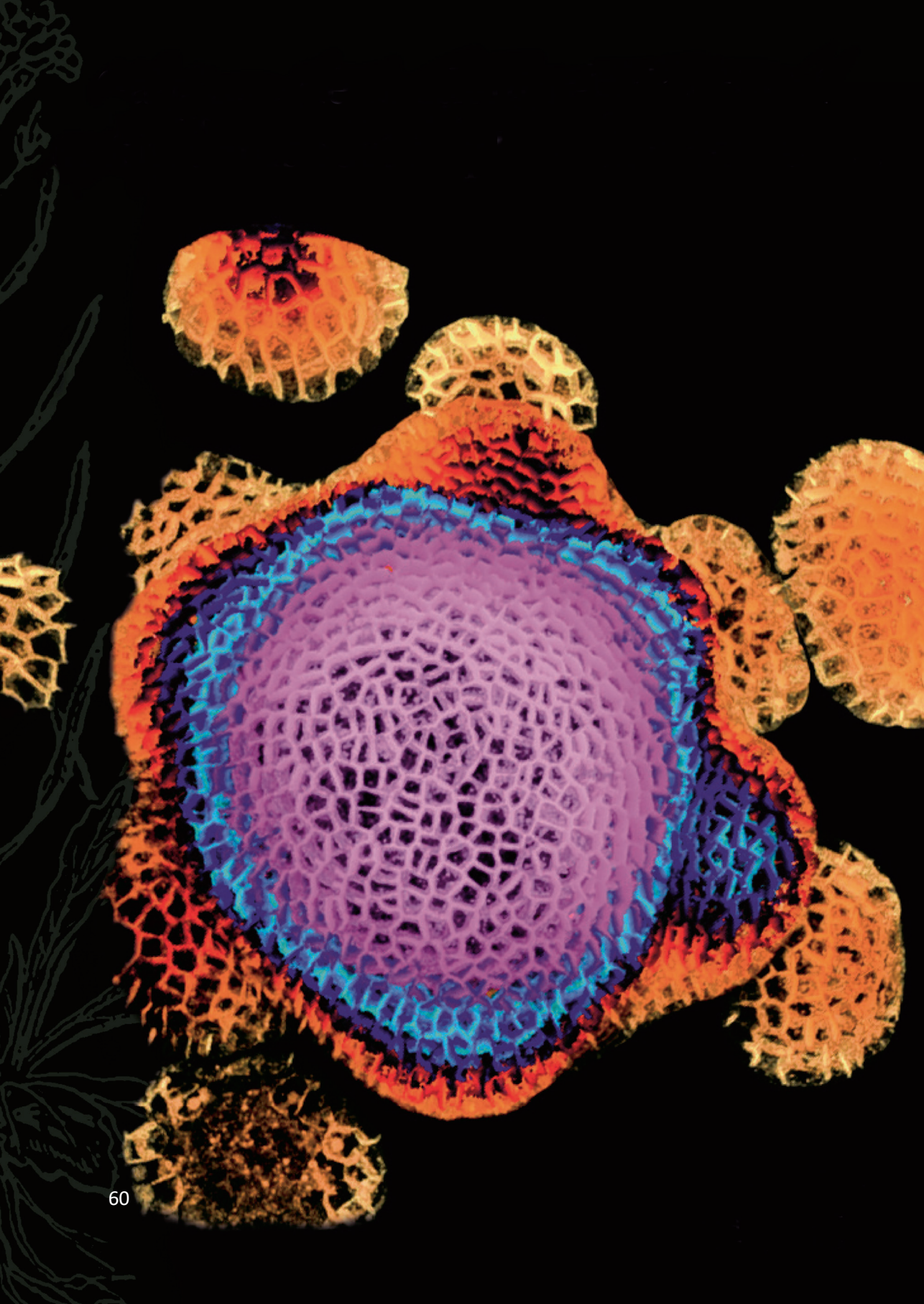
- Uyttewaal, M., Burian, A., Alim, K., Landrein, B., Borowska-Wykręt, D., Dedieu, A., ... & Hamant, O.** (2012). Mechanical stress acts via katanin to amplify differences in growth rate between adjacent cells in Arabidopsis. *Cell* 149: 439-451.
- Van Damme, D., Gadeyne, A., Vanstraelen, M., Inzé, D., Van Montagu, M. C., De Jaeger, G., ... & Geelen, D.** (2011). Adaptin-like protein TPLATE and clathrin recruitment during plant somatic cytokinesis occurs via two distinct pathways. *Proc. Natl. Acad. Sci. U.S.A.* 108: 615-620.
- Vanneste, S., & Friml, J.** (2013). Calcium: the missing link in auxin action. *Plants* 2: 650-675.
- Verret, F., Wheeler, G., Taylor, A. R., Farnham, G., & Brownlee, C.** (2010). Calcium channels in photosynthetic eukaryotes: implications for evolution of calcium-based signalling. *New Phytol.* 187: 23-43.
- Viaene, T., Delwiche, C. F., Rensing, S. A., & Friml, J.** (2013). Origin and evolution of PIN auxin transporters in the green lineage. *Trends Plant Sci.* 18: 5-10.
- Vieten, A., Vanneste, S., Wisniewska, J., Benková, E., Benjamins, R., Beeckman, T., ... & Friml, J.** (2005). Functional redundancy of PIN proteins is accompanied by auxin-dependent cross-regulation of PIN expression. *Development* 132: 4521-4531.
- Vogel, H. J.** (1994). Calmodulin: a versatile calcium mediator protein. *Biochem. Cell Biol.* 72: 357-376.
- Von Gersdorff, H., & Matthews, G.** (1994). Inhibition of endocytosis by elevated internal calcium in a synaptic terminal. *Nature* 370: 652-655.
- Wabnik, K., Govaerts, W., Friml, J., & Kleine-Vehn, J.** (2011). Feedback models for polarized auxin transport: an emerging trend. *Mol. Biosyst.* 7: 2352-2359.
- Wan, Y., Jasik, J., Wang, L., Hao, H., Volkmann, D., Menzel, D., ... & Lin, J.** (2012). The signal transducer NPH3 integrates the phototropin1 photosensor with PIN2-based polar auxin transport in Arabidopsis root phototropism. *Plant Cell* 24: 551-565.
- Wang, H. Z., Yang, K. Z., Zou, J. J., Zhu, L. L., Xie, Z. D., Morita, M. T., ... & Le, J.** (2015a). Transcriptional regulation of PIN genes by FOUR LIPS and MYB88 during Arabidopsis root gravitropism. *Nat. Commun.* 6: 8822.
- Wang, H., Han, S., Siao, W., Song, C., Xiang, Y., Wu, X., ... & Zhao, H.** (2015b). Arabidopsis synaptotagmin 2 participates in pollen germination and tube growth and is delivered to plasma membrane via conventional secretion. *Mol. Plant* 8: 1737-1750.

- Wang, P., Shen, L., Guo, J., Jing, W., Qu, Y., Li, W., ... & Zhang, W.** (2019). Phosphatidic acid directly regulates PINOID-dependent phosphorylation and activation of the PIN-FORMED2 auxin efflux transporter in response to salt stress. *Plant Cell* 31: 250-271.
- Wang, Q., Kohlen, W., Rossmann, S., Vernoux, T., & Theres, K.** (2014). Auxin depletion from the leaf axil conditions competence for axillary meristem formation in *Arabidopsis* and tomato. *Plant Cell* 26: 2068-2079.
- Wang, Y., Kang, Y., Ma, C., Miao, R., Wu, C., Long, Y., ... & Qi, Z.** (2017). CNGC2 is a Ca^{2+} influx channel that prevents accumulation of apoplastic Ca^{2+} in the leaf. *Plant Physiol.* 173: 1342-1354.
- Wang, Y., Liang, S., Xie, Q. G., & Lu, Y. T.** (2004). Characterization of a calmodulin-regulated Ca^{2+} -dependent-protein-kinase-related protein kinase, AtCRK1, from *Arabidopsis*. *Biochem. J.* 383: 73-81.
- Weller, B., Zourelidou, M., Frank, L., Barbosa, I. C., Fastner, A., Richter, S., ... & Schwechheimer, C.** (2017). Dynamic PIN-FORMED auxin efflux carrier phosphorylation at the plasma membrane controls auxin efflux-dependent growth. *Proc. Natl. Acad. Sci. U.S.A.* 114: E887-E896.
- Went, F.** (1926). On growth-accelerating substances in the coleoptile of *Avena sativa*. *Proc. Kon. Ned. Akad. Wetensch.* 30: 10-19.
- Willige, B. C., Ahlers, S., Zourelidou, M., Barbosa, I. C., Demarsy, E., Trevisan, M., ... & Schwechheimer, C.** (2013). D6PK AGCVIII kinases are required for auxin transport and phototropic hypocotyl bending in *Arabidopsis*. *Plant Cell* 25: 1674-1688.
- Willige, B. C., Isono, E., Richter, R., Zourelidou, M., & Schwechheimer, C.** (2011). Gibberellin regulates PIN-FORMED abundance and is required for auxin transport-dependent growth and development in *Arabidopsis thaliana*. *Plant Cell* 23: 2184-2195.
- Winnicki, K.** (2020). The winner takes it all: Auxin—The main player during plant embryogenesis. *Cells* 9: 606.
- Wiśniewska, J., Xu, J., Seifertová, D., Brewer, P. B., Ruzicka, K., Blilou, I., ... & Friml, J.** (2006). Polar PIN localization directs auxin flow in plants. *Science* 312: 883-883.
- Xiao, Y.** (2019). Novel factors modulating AGC kinase signaling-controlled polar auxin transport (Doctoral dissertation, Leiden University).
- Xiao, Y., & Offringa, R.** (2020). PDK1 regulates auxin transport and *Arabidopsis* vascular development through AGC1 kinase PAX. *Nat. Plants* 6: 544-555.

- Xiong, Y., & Jiao, Y.** (2019). The diverse roles of auxin in regulating leaf development. *Plants* 8: 243.
- Xu, H., & Heath, M. C.** (1998). Role of calcium in signal transduction during the hypersensitive response caused by basidiospore-derived infection of the cowpea rust fungus. *Plant Cell* 10: 585-597.
- Xu, T., Dai, N., Chen, J., Nagawa, S., Cao, M., Li, H., ... & Yang, Z.** (2014). Cell surface ABP1-TMK auxin-sensing complex activates ROP GTPase signaling. *Science* 343: 1025-1028.
- Xu, T., Dai, N., Chen, J., Nagawa, S., Cao, M., Li, H., ... & Yang, Z.** (2014). Cell surface ABP1-TMK auxin-sensing complex activates ROP GTPase signaling. *Science* 343: 1025-1028.
- Xu, T., Wen, M., Nagawa, S., Fu, Y., Chen, J. G., Wu, M. J., ... & Yang, Z.** (2010). Cell surface-and rho GTPase-based auxin signaling controls cellular interdigitation in *Arabidopsis*. *Cell* 143: 99-110.
- Xu, T., Wen, M., Nagawa, S., Fu, Y., Chen, J.G., Wu, M.J., Perrot-Rechenmann, C., Friml, J., Jones, A.M., and Yang, Z.** (2010). Cell surface- and Rho GTPase-based auxin signaling controls cellular interdigitation in *Arabidopsis*. *Cell* 143: 99–110.
- Yang, Y. D., Hammes, U. Z., Taylor, C. G., Schachtman, D. P., and Nielsen, E.** (2006). High-affinity auxin transport by the AUX1 influx carrier protein. *Curr. Biol.* 16: 1123-1127.
- Yin, X.** (2021). Phyllotaxis: From classical knowledge to molecular genetics. *J. Plant Res.* 134: 373-401.
- Yu, Y., Tang, W., Lin, W., Li, W., Zhou, X., Li, Y., ... & Yang, Z.** (2022a). ABLs and TMKs are co-receptors for extracellular auxin. *bioRxiv* 2022-11.
- Yu, Z., Zhang, F., Friml, J., & Ding, Z.** (2022b). Auxin signaling: Research advances over the past 30 years. *J. Integr. Plant Biol.* 64: 371-392.
- Žádníková, P., Petrášek, J., Marhavý, P., Raz, V., Vandenbussche, F., Ding, Z., ... & Benková, E.** (2010). Role of PIN-mediated auxin efflux in apical hook development of *Arabidopsis thaliana*. *Development* 137: 607-617.
- Žárský, V., Cvrčková, F., Potocký, M., & Hála, M.** (2009). Exocytosis and cell polarity in plants—exocyst and recycling domains. *New Phytol.* 183: 255-272.
- Zegzouti, H., Anthony, R. G., Jahchan, N., Bögre, L., & Christensen, S. K.** (2006). Phosphorylation and activation of PINOID by the phospholipid signaling kinase 3-phosphoinositide-dependent protein kinase 1 (PDK1) in *Arabidopsis*. *Proc. Natl. Acad. Sci. U.S.A.* 103: 6404-6409.

- Zhang, J., Mazur, E., Balla, J., Gallei, M., Kalousek, P., Medved'ová, Z., ... & Friml, J. (2020).** Strigolactones inhibit auxin feedback on PIN-dependent auxin transport canalization. *Nat. Commun.* 11: 3508.
- Zhang, J., Nodzyński, T., Pěňčík, A., Rolčík, J., & Friml, J. (2010).** PIN phosphorylation is sufficient to mediate PIN polarity and direct auxin transport. *Proc. Natl. Acad. Sci. U.S.A.* 107: 918-922.
- Zhang, J., Vanneste, S., Brewer, P. B., Michniewicz, M., Grones, P., Kleine-Vehn, J., ... & Friml, J. (2011).** Inositol trisphosphate-induced Ca^{2+} signaling modulates auxin transport and PIN polarity. *Dev. Cell* 20: 855-866.
- Zhang, K. X., Xu, H. H., Gong, W., Jin, Y., Shi, Y. Y., Yuan, T. T., ... & Lu, Y. T. (2014).** Proper PIN1 distribution is needed for root negative phototropism in *Arabidopsis*. *PLoS One* 9: e85720.
- Zhang, K. X., Xu, H. H., Yuan, T. T., Zhang, L., & Lu, Y. T. (2013).** Blue-light-induced PIN 3 polarization for root negative phototropic response in *Arabidopsis*. *Plant J.* 76: 308-321.
- Zhang, Y., & Friml, J. (2020).** Auxin guides roots to avoid obstacles during gravitropic growth. *New Phytol.* 225: 1049.
- Zhao, X., Wang, Y. L., Qiao, X. R., Wang, J., Wang, L. D., Xu, C. S., & Zhang, X. (2013).** Phototropins function in high-intensity blue light-induced hypocotyl phototropism in *Arabidopsis* by altering cytosolic calcium. *Plant Physiol.* 162: 1539-1551.
- Zhu, J., Wu, X., Yuan, S., Qian, D., Nan, Q., An, L., & Xiang, Y. (2014).** Annexin5 plays a vital role in *Arabidopsis* pollen development via Ca^{2+} -dependent membrane trafficking. *PloS one* 9: e102407.
- Zourelidou, M., Absmanner, B., Weller, B., Barbosa, I. C., Willige, B. C., Fastner, A., ... & Schwechheimer, C. (2014).** Auxin efflux by PIN-FORMED proteins is activated by two different protein kinases, D6 PROTEIN KINASE and PINOID. *Elife* 3: e02860.
- Zourelidou, M., Müller, I., Willige, B. C., Nill, C., Jikumaru, Y., Li, H., & Schwechheimer, C. (2009).** The polarly localized D6 PROTEIN KINASE is required for efficient auxin transport in *Arabidopsis thaliana*. *Development* 4: 627-36.

The role of calcium as second messenger in auxin transport and signaling



Chapter 2

CALMODULIN-LIKE 12/TOUCH 3 and closely related calmodulins and calmodulin-like proteins redundantly interact with the PINOID kinase

Xiaoyu Wei¹, Yuanwei Fan^{1,2}, Parjanya Kocherla¹, Linge Li^{1,3} and Remko Offringa^{1*}

¹ Plant Developmental Genetics, Institute of Biology Leiden, Leiden University, Sylviusweg 72, 2333 BE, Leiden, Netherlands

² Current address: Department of Biology and Center for Engineering Mechanobiology, Washington University in St. Louis, St. Louis, MO 63130, USA

³ Current address: Plant Ecophysiology, Institute of Environmental Biology, Utrecht University, Padualaan 8, 3584 CH Utrecht, The Netherlands

*Author for correspondence: r.offringa@biology.leidenuniv.nl

The results in this Chapter are included in the following publication: Fan, Y.W., **Wei, X.Y.**Offringa, R*. Auxin-induced regulation of PIN polarity by calcium-dependent binding of calmodulins and calmodulin-likes to the PINOID kinase (submitted).

Abstract

Plants have evolved an intricate system to survive in their changing and often unfavourable environment due to their sessile nature. Cross talk between the plant hormone auxin, a key regulator of plant growth and development, and Ca^{2+} , a universal second messenger, has been proposed to transduce various environmental and endogenous signals and modulate developmental plasticity. The *Arabidopsis thaliana* (Arabidopsis) AGC3 kinase PINOID (PID) is a key regulator of polar auxin transport, acting as a binary switch in apical-basal polar targeting of PIN FORMED (PIN) auxin efflux carriers and thereby determining the direction of auxin flow. Previously, we identified the calmodulin-like (CML) protein CALMODULIN-LIKE 12/TOUCH 3 (CML12/TCH3) as interacting partner of PID, suggesting that PID is one of the hubs in the Ca^{2+} -dependent regulation of auxin action. Here we found that a confined clade comprising seven CaMs and four closely-related CMLs, including CML12/TCH3, interact with PID. In *Arabidopsis* protoplasts, co-transfection of these CaM/CMLs with PID in the presence of auxin resulted in PID disassociation from the plasma membrane. A comparative study on the spatio-temporal expression of the corresponding *CaM/CML* genes and *PID* using *promoter:GUS* reporter fusions displayed differential but also largely overlapping expression patterns in most tissues throughout all the developmental stages. Interestingly, *CaM2*, *CaM7*, *CML10* and *CML12/TCH3* respond to auxin treatment and gravistimulation. These results confirm our previous conclusion that calcium is an important second messenger in regulating the direction of auxin transport by external but also internal signals, such as auxin itself.

Keywords: Auxin, PINOID (PID) kinase, Calmodulins/calmodulin-likes (CaM/CMLs), CALMODULIN-LIKE 12/TOUCH 3 (CML12/TCH3), Protein-protein interaction, *Arabidopsis thaliana*

Introduction

Due to their sessile nature, plants are constantly exposed to a changing and often unfavourable environment (Anderson et al., 2011). To survive, they have evolved an intricate system to sense various environmental cues, and to transduce these cues into intracellular signalling thereby activating downstream physiological responses (Raza et al., 2020). One of the core signal transduction components in this environmental sensing system is the second messenger calcium (Ca^{2+}) (Dong et al., 2022).

Ca^{2+} is an essential macronutrient that plays an important role in plant growth and development, such as in the formation of cell walls, cell membranes and other cellular processes (Hepler and Wayne, 1985; Eklund and Eliasson, 1990; Xu and Heath, 1998). On the other hand, Ca^{2+} is universally involved in responses to environmental changes (Xu et al., 2022). Many environmental cues (light, abiotic and biotic stresses), and internal signals (e.g. plant hormones) elicit signal-specific and tissue-specific changes in the concentration of cytosolic Ca^{2+} ($[\text{Ca}^{2+}]_{\text{cyt}}$), which is defined as the ‘calcium signature’ (Dong et al., 2022; Xu et al., 2022).

The stimulus-specific information encoded in the calcium signature is relayed and deciphered through the action of sensor proteins that bind Ca^{2+} (Hashimoto and Kudla, 2011). The majority of Ca^{2+} sensors are small proteins that reversibly bind Ca^{2+} with high affinity, with one or more highly conserved helix-loop-helix motifs termed “EF hands” (Day et al., 2002; Sanders et al., 2002). Ca^{2+} sensors can be sorted into two major groups: the sensor relays and the sensor responders (Sanders et al., 2002; Hashimoto and Kudla, 2011). The sensor relays function through bimolecular interactions and comprise calmodulins (CaMs), calmodulin-like proteins (CMLs) and calcineurin-B like proteins (CBLs). They undergo a conformational change after binding with Ca^{2+} , which allows them to interact with target proteins, such as the Ca^{2+} and CaM-dependent protein kinase (CCaMK) and the CBL-interacting protein kinases (CIPKs), which subsequently respond by

changes in structure and (enzyme) activity (Hashimoto and Kudla, 2011). In contrast, the Ca^{2+} -dependent protein kinase (CDPK) are sensor responders that function through intramolecular interactions between the sensor (EF hand) and the kinase (responder) domain. Binding of Ca^{2+} results in activation of the kinase domain, leading to the subsequent phosphorylation of target proteins (Hashimoto and Kudla, 2011).

Among the Ca^{2+} sensors, the CaMs are the most extensively studied. CaMs are highly conserved, small, acidic, relatively stable proteins that are ubiquitously expressed in eukaryotic cells (McCormack et al., 2005). The *Arabidopsis thaliana* (Arabidopsis) genome harbours seven *CaM* genes encoding four CaM isoforms: CaM1/4, CaM2/3/5, CaM6, and CaM7 (McCormack et al., 2005). They share a similar protein structure of two globular domains, each of them containing a pair of EF-hands, connected by an α -helical linker domain (McCormack et al., 2005). In addition, the Arabidopsis genome encodes an extended family of CaM-like proteins (CMLs). These CMLs have between one to six EF hand motifs and no other identifiable functional domains (La Verde et al., 2018). And the difference in target specificity, subcellular localization and Ca^{2+} affinity of CMLs compared to CaMs indicate that they have evolved to diverse roles in Ca^{2+} signalling (La Verde et al., 2018).

Another important player in plant responses to environmental stimuli is the plant hormone auxin, or indole-3-acetic acid (IAA). Through the dynamic distribution of auxin minima and maxima within plant tissues, this hormone is involved in an impressive variety of plant biological processes, ranging from regulating basic processes such as cell expansion and cell division to orchestrating embryogenesis, tissue specification, and organ development (Gomes and Scortecci, 2021). The differential distribution of auxin is established and maintained through the combined action of biosynthesis, metabolism, and cell to cell polar auxin transport (PAT) (Mroue et al., 2018). PAT is mediated by three auxin transporter families, namely the PIN-FORMED (PIN) efflux transporters, the ATP-binding cassette B

CALMODULIN-LIKE 12/TOUCH 3 and closely related calmodulins and calmodulin-like proteins redundantly interact with the PINOID kinase

(ABCB)-type efflux transporters, and AUXIN RESISTANT1/LIKE-AUX1 (AUX1/LAX) influx transporters (reviewed by Geisler, 2021). Among these transporters, the PIN auxin efflux carriers play a major role in determining the direction of auxin flow by their polar localization at the plasma membrane (PM) of the cell (Geisler, 2021). They are named after the *pin formed1* (*pin1*) loss-of-function mutant of one of the founding members, which shows severe defects in organ formation at the inflorescence meristem and as a result forms a needle-like inflorescences (Okada et al., 1991; Galweiler et al., 1998). The activity, polarity and trafficking of PINs are finely regulated by protein kinases that phosphorylate different residues in the central PIN hydrophilic loop (HL) (reviewed in Bassukas et al., 2022). Of these, the AGC3 kinases PINOID (PID), WAG1 and WAG2 instruct shootward/apical asymmetric PIN localisation by phosphorylating the serine residue in three conserved TPRXS motifs within the PIN-HL (Friml et al., 2004; Michniewicz et al., 2007; Huang et al., 2010; Dhonukshe et al., 2010). The *pid* loss-of-function mutant phenocopies the needle-like inflorescences of the *pin1* mutant, indicating that it is the dominant kinase regulating PIN1 polarity during organ formation in the inflorescence meristem (Bennett et al., 1995; Friml et al., 2004; Huang et al., 2010). More severe phenotypes, such as embryos without cotyledons and agravitropic roots, are only observed in the *pid wag1 wag2* triple mutant, showing that the three kinases act redundantly in these processes (Dhonukshe et al., 2010).

It has been reported that auxin acts in part through Ca^{2+} signalling, as cytoplasmic Ca^{2+} levels $[\text{Ca}^{2+}]_{\text{cyt}}$ rapidly increase after auxin application (Hasenstein and Evans, 1986; Gehring et al., 1990; Shishova and Lindberg, 2004; Monshausen et al., 2011). These changes in $[\text{Ca}^{2+}]_{\text{cyt}}$ were found to suppress PAT (Dela Fuente and Leopold, 1973) and to mediate gravitropic and phototropic growth responses (Baum et al., 1999; Plieth and Trewavas, 2002; Toyota et al., 2008a, b; Zhao et al., 2013) and organ formation at the shoot apical meristem (Li et al., 2019).

The finding that PID interacts with the CALMODULIN-LIKE 12/TOUCH 3 (CML12/TCH3) and the EF hand containing PID-BINDING PROTEIN 1 (PBP1) in a Ca^{2+} dependent manner provided a first molecular insight on how Ca^{2+} could possibly affect PAT (Benjamins et al., 2003). CML12/TCH3 is a negative regulator of PID kinase activity, both *in vitro*, as shown by phosphorylation assays, and in *planta* where *CML12/TCH3* overexpression reduces *PID* overexpression induced root meristem collapse (Robert, 2008; Galván-Ampudia, 2009). Moreover, when interacting with CML12/TCH3 in auxin-treated protoplasts, PID was sequestered from the PM to the cytosol (Galván-Ampudia, 2009). The same sequestration of PID was observed in root epidermis cells when roots were treated with auxin, and this sequestration was delayed, but not absent, in the *tch3* loss-of-function mutant. Moreover, the *tch3* loss-of-function mutant only shows a mild phenotype, strongly suggesting that CaMs and other CMLs function redundantly with CML12/TCH3. Here we observed that a confined clade comprising seven CaMs and the three CMLs (CML8, CML10, CML11) most closely related to CML12/TCH3 do also interact with PID. In Arabidopsis protoplasts, co-expression of these CaM/CMLs and PID in the presence of auxin resulted in dissociation of PID from PM. A systematic spatio-temporal expression study of the PID-interacting CaM/CMLs showed that their corresponding genes display a largely overlapping expression pattern with *PID* and that, like *PID*, *CaM2*, *CaM7*, *CML10* and *CML12/TCH3* are auxin responsive.

Results

PID interacts with CML12/TCH3 and 10 closely related CaMs and CMLs

CML12/TCH3 was previously identified as a PID interacting protein in a yeast-two hybrid screen, and the Ca^{2+} -dependent interaction was confirmed by *in vitro* pull-down assays (Benjamins et al., 2003; Galván-Ampudia, 2009). As the analysis of the *tch3* loss-of-function mutant suggested that other CMLs and possibly CaMs

might act redundantly with CML12/TCH3 (Robert, 2008; Fan, 2014), we selected the most closely related homologs of CML12/TCH3, including seven CaMs, CML8, 9, 10, 11, 13 and CML14 and the more distantly related CML24/TCH2 as candidates. *In vitro* pull-down assays using GST-tagged PID bound to glutathione beads as bait and His-tagged CaM/CMLs as prey indicated that the seven CaMs and CML8, 10 and CML11 interacted with PID, but that CML9, 13 and 14 and the more distantly related CML24 did not (Figure 1A; Figure S1).

Bimolecular fluorescence complementation (BiFC) was used to confirm these results for CaM1, CML10 and CML12/TCH3, using CML9 and CML24 as negative controls. Co-expression of PID-VYCE (having the C-terminus of Venus fused to PID) and CaM/CMLs-VYNE (N-terminus of Venus fluorescent protein fused to CaM1, CML9, CML10, CML12/TCH3 or CML24) in *Nicotiana benthamiana* leaf epidermis cells showed that CaM1, CML10 and CML12/TCH3 interact with PID, whereas CML9 and CML24 do not (Figure 1B). Subsequent co-transfection of *p35S:PID-GFP* and *p35S:CaM/CMLs-mRFP* in Arabidopsis protoplasts supplemented with auxin showed strong PID sequestration from the PM in protoplasts co-expressing one of the seven CaMs or the closely related CML8, 10 and CML11, whereas co-expression of the more distantly related CML9, 13, 14 and CML24 did not lead to sequestration of PID from the PM (Figure 1C).

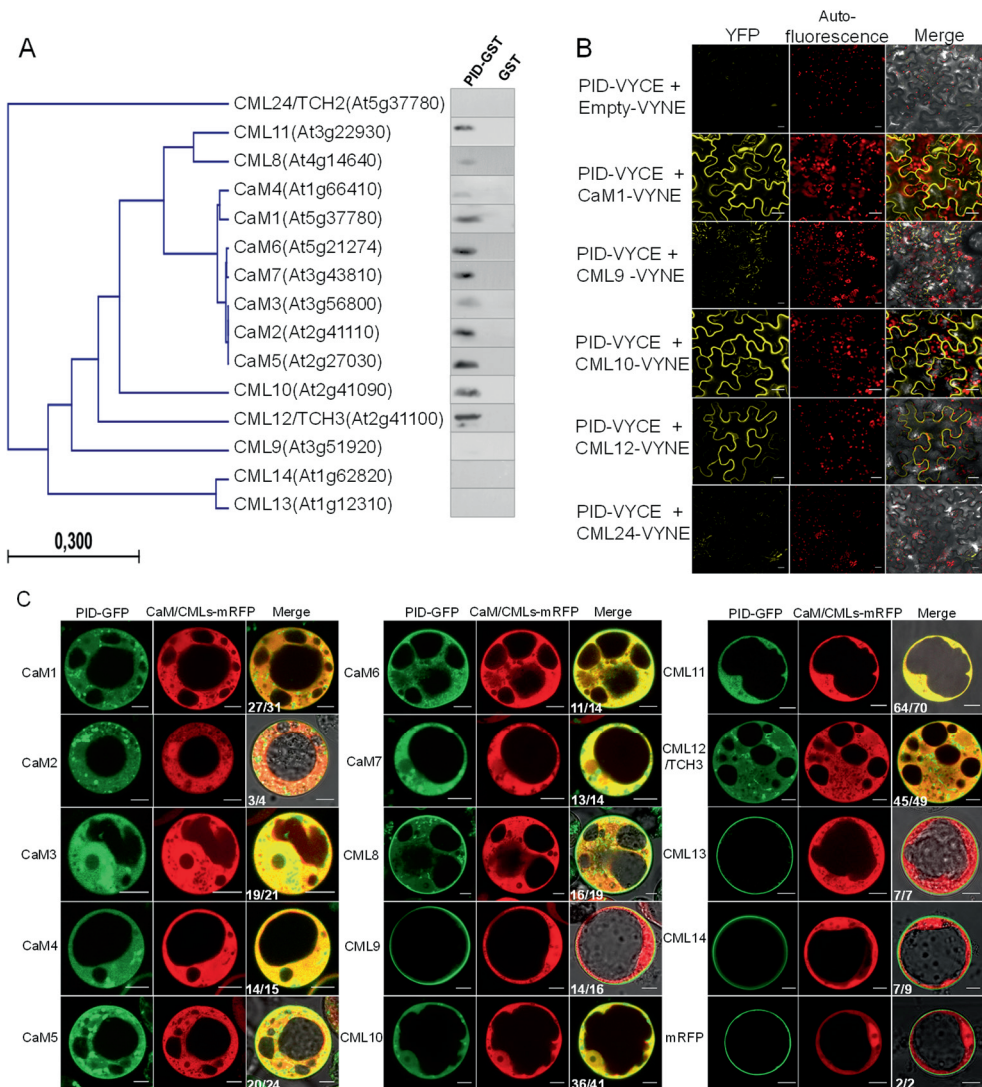


Figure 1. PID interacts with CML12/TCH3 and 10 closely related CaMs and CMLs. (A) Phylogenetic tree combined with the results of *in vitro* pull-down experiments using GST or GST-tagged PID bound to glutathione beads as bait and His-tagged CaMs or CMLs as prey. The phylogenetic tree was constructed based on the full-length protein sequences using the UPGMA method in CLC Main Workbench 6. Pulled down CaMs/CMLs are detected by hybridizing the Western blot with anti-His antibodies. (B) Bimolecular Fluorescence Complementation (BiFC) assay performed by co-expression of the indicated combination of fusion proteins (PID-VYCE: PID C-terminally fused to the C-terminal half of Venus; CaM/CML-VYNE: CaM/CML C-terminally fused to the N-terminal half of Venus) in leaf epidermis cells of three weeks old *Nicotiana benthamiana* plants after *Agrobacterium*-mediated DNA transfer. (C) 35S promoter-driven co-expression of PID-GFP and CaM/CML-mRFP fusions in Arabidopsis protoplasts in the presence of auxin. Sequestration

CALMODULIN-LIKE 12/TOUCH 3 and closely related calmodulins and calmodulin-like proteins redundantly interact with the PINOID kinase

of PID to the cytosolic is indicative of an interaction (CaM1-7, CML8, 10,11,12), whereas PM-localization of PID indicates that there is no interaction (CML9, 13 and 14 and the mRFP control). White numbers indicate how many of the total number of images show the same result. Scale bars indicate 10 μ m in **(B)** and **(C)**.

The above results validated our hypothesis and showed that a confined clade comprising the seven CaMs and four CMLs-CML8, 10, 11 and CML12/TCH3 act redundantly in interacting with and regulating the PID kinase, and that the more distantly related CMLs do not. The data explain why the *tch3* and other *cam/cml* single loss-of-function mutants do not present any eye-detectable phenotype (Figure S2).

Analysis of the structural diversity of both the interacting and non-interacting CaMs and CMLs using the online tool Multiple Em for Motif Elicitation (MEME) suite (<http://meme-suite.org/tools/meme>) showed that, except for CML12/TCH3, most proteins contain four Ca²⁺-binding EF-hands, each characterized by a conserved signature motif (1 to 4), and lack additional functional domains (Figure 2). CML12/TCH3 is exceptional as it contains six EF-hands due to a duplication of the first two EF-hands (Figure 2B). We did not detect a difference in EF-hand motif order or composition or a clear difference in the amino acid sequence that distinguishes the PID interacting from the non-interacting CaMs/CMLs.

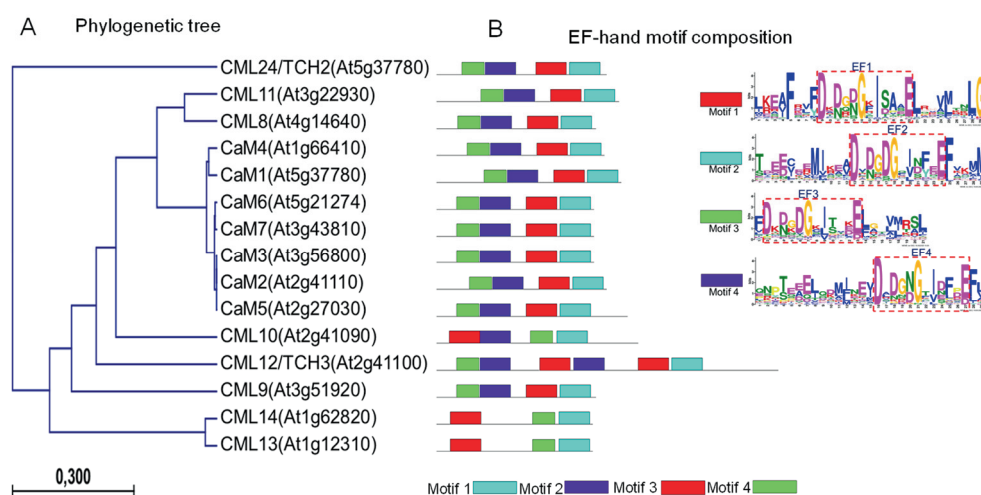
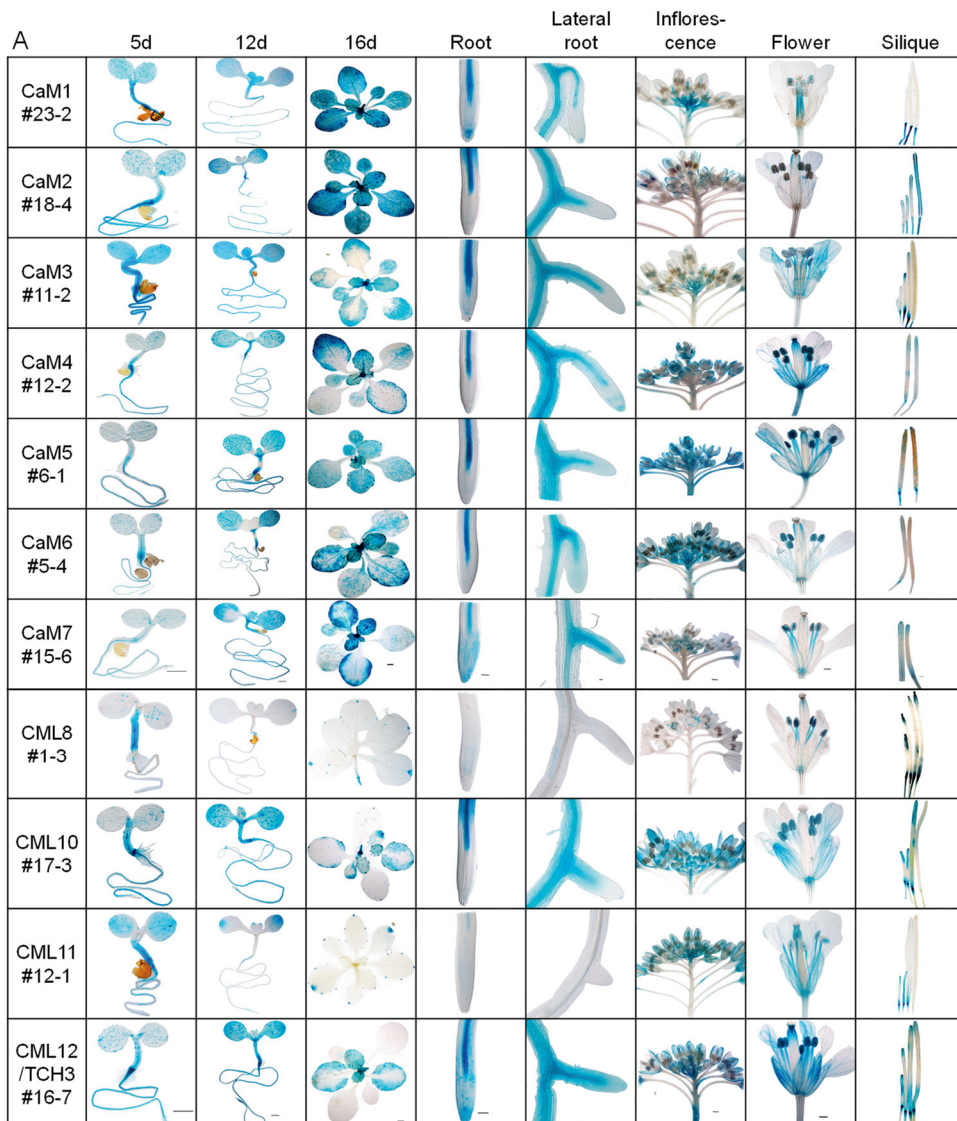


Figure 2. Phylogenetic tree and protein structure of the PID-interacting and not interacting CaM/CMLs in Arabidopsis. (A) A phylogenetic tree of PID-interacting and representative non-interacting CaMs and CMLs constructed based on the full-length protein sequences using the UPGMA method in CLC Main Workbench 6. (B) EF-hand motif composition of the CaM and CML proteins in (A). Four conserved motif signatures were identified in the EF-hands of Arabidopsis CaMs and CMLs using the Multiple Em for Motif Elicitation (MEME) suite (<http://meme-suite.org/tools/meme>) (Bailey and Elkan, 1994) with standard searching parameters, allowing a maximum of four different motifs and an optimum motif width between six and 30 amino acids.

PID interacting CaM/CMLs display a largely overlapping expression pattern



CALMODULIN-LIKE 12/TOUCH 3 and closely related calmodulins and calmodulin-like proteins redundantly interact with the PINOID kinase

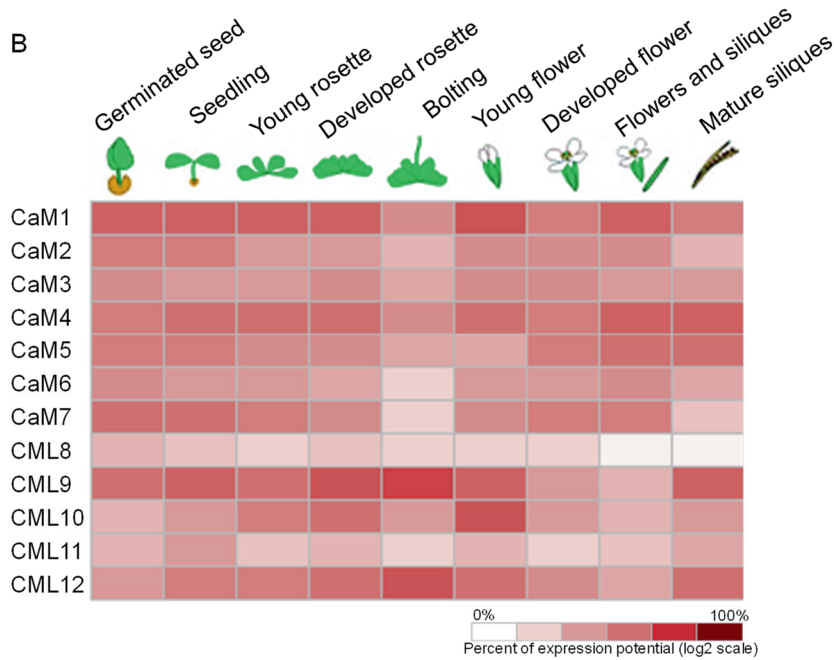


Figure 3. Spatio-temporal expression pattern of *CaM* and *CML* genes encoding PID-interacting proteins. (A) Histochemical staining for GUS activity in 5-, 12-, and 16-day-old *pCaM/CML:turboGFP-GUS* seedlings/plants and different tissues. # and number indicate the transgenic line number. Scale bars in 5-, 12-, and 16-day-old seedlings/plants, root, lateral root, inflorescence, flower, silique indicate 1 mm, 5 mm, 5 mm, 200 μ m, 50 μ m, 5 mm, 1 mm, 5 mm, respectively. (B) Relative expression heat map for the indicated Arabidopsis *CaMs* and *CMLs* in different tissues and developmental stages obtained from Genevestigator. Developmental stage from left to right: germinated seed, seedling, young rosette, developed rosette, bolting, young flower, developed flower, flowers and siliques, and mature siliques.

Previous analysis of the *CML12/TCH3* expression pattern has shown that the gene is expressed in the shoot apical meristem, vascular tissue and the pericycle at positions of lateral roots emergence, and in root and leaf cells undergoing cellular expansion (Sistrunk et al., 1994, Antosiewicz et al., 1995, Robert, 2008). In addition, *TCH3* expression was shown to be strongly induced by auxin and touch, especially in the root tip (Braam and Davis, 1990; Antosiewicz et al., 1995; Benjamins et al., 2001; Fan, 2014). It has also been reported that *PID* is co-expressed with *TCH3* in epidermis cells of the elongation zone of the root tip, vascular tissue and in the shoot apical meristem (Benjamins et al., 2001; Benjamins

et al., 2003), allowing a possible functional interaction between the two proteins in these tissues. In fact, auxin treatment has been shown to lead to Ca^{2+} -dependent sequestration of a functional PID:VENUS fusion from the PM to the cytosol in root epidermis cells. The sequestration was delayed in *tch3* loss-of-function mutant roots (Fan, 2014), suggesting that CML12/TCH3 does have a role in this.

To investigate which other PID interacting CaM/CMLs are also expressed in the PID expression domain, we studied the spatio-temporal expression patterns of these *CaM/CML* genes using lines transgenic for *pCaM/CMLs:turboGFP-GUS* fusions. Histochemical staining of different tissues at different developmental stages for GUS activity showed that the seven *CaM* genes share striking similarities in expression pattern. Although there is some variation in specific tissues, all genes are expressed in roots, hypocotyls, cotyledons and leaves, with predominant expression in vascular tissue, inflorescence meristems, flowers and siliques. Also in the root tip there is mild diversity in expression pattern, as *CaM1*, 3, 4, 5, and 7 show clear expression in the quiescent center (QC) of the root apical meristem (RAM) and in the columella cells to a varying extent. Additionally, *CaM7* is also expressed in the epidermis of the root tip (Figure 4A). In contrast, the *CMLs* show much more diversity compared to the *CaMs*. At the seedling stage, *CML8*, 10, 11, and *CML12/TCH3* are expressed in the cotyledons, hypocotyl, and the root vasculature, of which, *CML8* shows a relatively weak expression in cotyledons but stronger in the hypocotyl. However, in adult leaves, *CML8* and *CML11* specifically express in the tip of the leaves, while *CML10* and *CML12/TCH3* express in the young developing leaves. In roots, *CML8* and *CML11* are weakly expressed in the epidermis of the elongation zone, whereas *CML12/TCH3* expression here is much stronger and broader. Like the *CaM* genes, all four *CML* genes are expressed in flowers and siliques, but much weaker for *CML8*. Together with data compiled from the GENEVESTIGATOR database (Figure 3B), these results show that the genes encoding PID interacting

CALMODULIN-LIKE 12/TOUCH 3 and closely related calmodulins and calmodulin-like proteins redundantly interact with the PINOID kinase

CaM/CMLs display a largely overlapping expression pattern and are generally expressed in almost all tissues throughout all developmental stages.

Four genes encoding PID-interacting CaM/CMLs are auxin responsive and induced during gravitropic growth

Previous studies have indicated that both *PID* and *CML12/TCH3* are auxin responsive (Antosiewicz et al., 1995; Benjamins et al., 2001; Benjamins et al., 2003; Fan, 2014). In the case of *CML12/TCH3*, its auxin responsive expression in epidermis cells of the root tip would increase CML12/TCH3 levels and thereby potentiate its (auxin-induced) repressive effect on PID activity by binding to and sequestering PID from the plasma membrane (Fan, 2014). To test if the other genes encoding PID interacting *CaM/CMLs* are also auxin responsive, we treated 5-day-old seedlings of the corresponding *pCaM/CML:turboGFP-GUS* reporter lines for 1, 2, 3 and 5 hours with auxin and histochemically stained for GUS activity.

Four of the twelve *CaM/CML* genes showed a clear auxin responsive gene expression. In line with previous findings, *CML12/TCH3* expression was strongly induced in the entire root tip after one hour of auxin treatment, and the expression became more intense in the root tip, hypocotyl, shoot apex and cotyledons at later time points (Antosiewicz et al., 1995; Benjamins et al., 2001; Benjamins et al., 2003; Fan, 2014). *CaM2*, *CaM7* and *CML10* generally shared this pattern of auxin responsive gene expression, but the induction in root tips was less intense for *CaM7* and limited to the elongation zone of the root tip for *CaM2* and *CML10*.

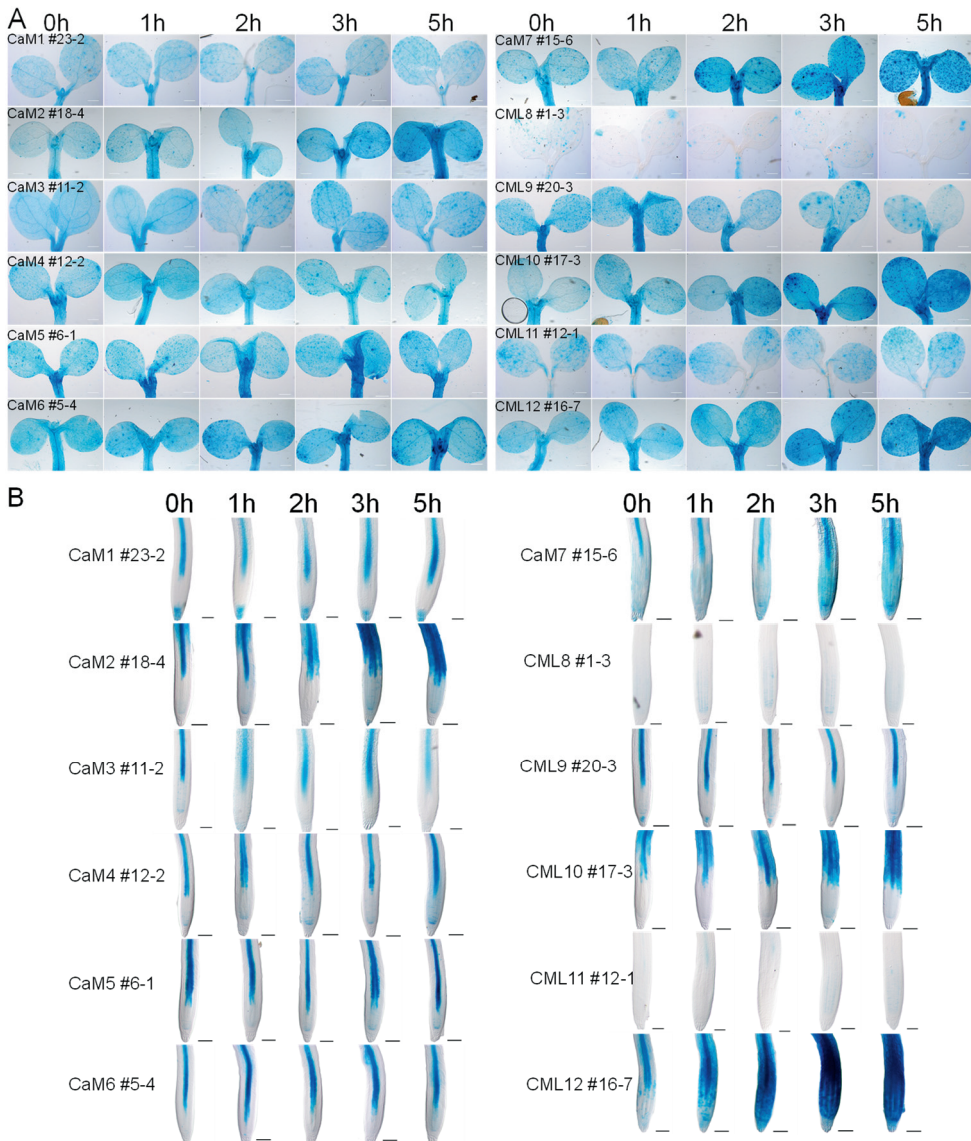


Figure 4. Four of the genes encoding PID-interacting CaM/CMLs are auxin responsive in seedling shoots and root tips. (A-B). Histochemical staining of the shoot (A) and root tip (B) of 5-day-old *pCaM/CMLs::turboGFP-GUS* seedlings treated with 5 μ M IAA for 0, 1, 2, 3, or 5 hours. Images representative of three to five replicates are shown. Scale bars in (A) and (B) indicate 50 mm, 50 μ m, respectively. # and number indicate the transgenic line number.

CALMODULIN-LIKE 12/TOUCH 3 and closely related calmodulins and calmodulin-like proteins redundantly interact with the PINOID kinase

Interestingly, the expression of the auxin responsive genes was also enhanced during root gravitropic growth (Figure 5). For *CAM2* and *CML10*, this enhancement was restricted to the root elongation zone with predominant induction in the vascular tissue, consistent with their limited auxin responsive expression in the root tip (Figure 4B). As previously shown for *CML12/TCH3* (Fan, 2014), during the gravitropic response *CAM7* expression was enhanced in the entire root tip with highest expression in the epidermal cells at the lower side of the root, in line with the transient asymmetric auxin distribution during the root gravitropic response (Band et al., 2012).

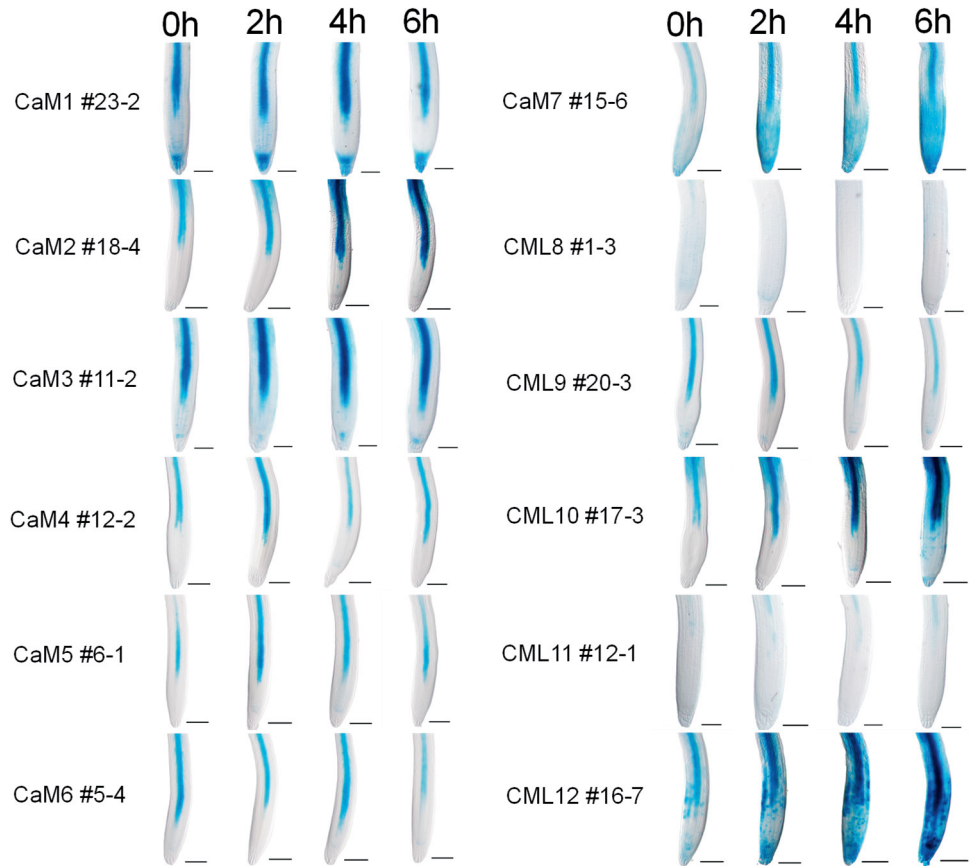


Figure 5. The expression of the auxin responsive CaM/CML genes is induced in the root tip during gravitropic growth. *pCaM/CMLs:turboGFP-GUS* seedlings were grown on vertical plates

containing agar medium for five days, transferred to new vertical agar medium plates, and gravi-stimulated by tilting the plates 90 degrees. Seedlings were histochemically stained for GUS activity after 0, 2, 4 or 6 hours incubation. # and number indicate the transgenic line number.

These results suggest that specifically CAM7 acts redundantly with CML12/TCH3 with respect to the previously observed PID sequestration in epidermis cells in the root tip. The stronger expression of CML12/TCH3 suggests that this is the more important CAM/CML in this process, which might explain the observed delay in auxin-induced PID sequestration in the *tch3* loss-of-function mutant background (Fan, 2014).

Discussion

The perception of environmental signals and internal cues such as gravity and auxin by plant cells generally leads to oscillations in the $[Ca^{2+}]_{cyt}$ (Felle, 1988; Gehring et al., 1990; Plieth and Trewavas, 2002; Toyota et al., 2007, 2008a, b; Verma et al., 2022). These stimulus-specific transient Ca^{2+} signatures are deciphered by Ca^{2+} sensors, such as CaMs and CMLs. Previously, we identified a possible mechanism by which auxin regulates its own polar transport. We observed that the AGC kinase PID, which regulates PAT by phosphorylating the PIN auxin efflux carriers, is inactivated and sequestered from the PM through an auxin-triggered, Ca^{2+} -dependent interaction with CML12/TCH3 (Benjamins et al., 2003; Galvan-Ampudia, 2009; Fan, 2014). As the *tch3* loss-of-function phenotype did not show clear phenotypes (Fan, 2014), we suspected that other CMLs and/or CaMs would act redundantly with CML12/TCH3. Here we found that seven CaMs and three other CMLs, all belonging to a confined clade that includes CML12/TCH3, also interact with PID and are able to sequester the kinase from the PM. The largely overlapping spatio-temporal, and for some auxin responsive, expression of the corresponding genes supports the notion that they may act redundantly in regulating the PID kinase.

Redundant action of CaM/CMLs in regulating target proteins seems a general concept

A protein microarray screen, genetic analysis and *in vivo* studies have shown that CaM/CMLs binding proteins generally interact with more than one CaM/CMLs (Popescu et al., 2007; Oh et al., 2012; Sun et al., 2022). In fact, the protein microarray screen has shown that about 25% (44 of 173) of the CaM/CML target proteins interact with all six CaM/CMLs that were used in this screen (CaM1, CaM6, CaM7, CML8, CML9, CML10), whereas 50% of the proteins bound to two or more of these CaM/CMLs (Popescu et al., 2007).

In the case of PID, there seems to be some specificity, as it interacts with a confined clade comprising CAMs and the four most closely related CMLs, and no interaction was observed between PID and the more distantly related CML9, 13, 14 and CML24 (TCH2). As a result, the non-interacting CMLs did not sequester PID from the PM to cytosol. The fact that the capacity to regulate PID kinase activity is limited to a specific subclade of the CaM/CMLs family suggests some structural conservation among the PID-interacting CaM/CMLs. Unfortunately, protein alignment and a careful search for differences in the conserved EF-hand motif type or order did not detect clear differences between the interacting and not-interacting CaM/CMLs. This indicates that functional studies on this interaction from the CaM/CML side will be difficult, if not impossible, also in view of the promiscuous interactions of CaM/CMLs with other target proteins (Popescu et al., 2007; Oh et al., 2012; Sun et al., 2022). Nonetheless, based on our expression analysis, only CAM7 and CML12/TCH3 show clear expression in epidermis cells of the differentiation zone of the root tip following auxin treatment or gravistimulation, suggesting that a *cam7 cml12/tch3* double mutant might reveal a mutant root phenotype. Unfortunately, time limitation did not allow to test this hypothesis. Based on the analysis presented in this Chapter, we decided to study the functional relevance of the PID CaM/CML interaction from the PID side. These follow-up studies are described in Chapter 3 and 4 of this thesis.

Limited functional diversification between genes encoding PID interacting CaM/CMLs

Our study on the spatio-temporal expression of the genes encoding PID-interacting CaM/CMLs showed that the seven *CaMs* are universally expressed in most organs (Figure 3A). On the one hand, this finding fits their role as the major Ca^{2+} sensors that regulate the activity of plentiful downstream target proteins involved in wide range of developmental processes and responses (La Verde et al., 2018). On the other hand, it is difficult to explain how these CaMs have maintained their high protein sequence identity combined with their largely overlapping spatio-temporal expression pattern under strict natural selection. One possibility is that, because of their promiscuous role, there is a requirement for a high CaM protein level in the cell beyond the capacity of one or a few *CaM* genes. The other possibility is that the seven *CaM* genes are the result of more recent gene duplication events and that there has not been sufficient time for their sub-functionalisation.

Compared to the *CaM* genes, the three genes encoding PID-interacting CMLs do show more diversification. *CML8* and *CML11* are highly expressed in the hypocotyl at early developmental stages, and later the expression becomes limited to the root-shoot junction, leaf tip and flowers. Our observations on the *CML8* expression pattern is similar to what was reported by Zhu et al. (2017). Here, the authors showed that *CML8* plays a role in plant immunity against *Pseudomonas syringae* in a salicylic acid dependent manner. *CML10* is strongly expressed in the root, hypocotyl and cotyledons of young seedlings and flowers. In rosette leaves, *CML10* is mainly accumulating in the newly formed leaves, indicating a possible role in early leaf development. *CML10* has been reported to be crucial in coping with biotic and abiotic stresses, and its expression is induced by bacterial (*Pseudomonas syringae*), fungal (*Plectosphaerella cucumerina*) and oomycetal (*Hyaloperonospora parasitica*) pathogens (Zimmermann et al., 2004; McCormack et al., 2005), H_2O_2 (McCormack et al., 2005; Cho et al., 2016), cold stress (Yu et al., 2022) and auxin (Figure 4). The expression pattern of *CML12/TCH3* is consistent

CALMODULIN-LIKE 12/TOUCH 3 and closely related calmodulins and calmodulin-like proteins redundantly interact with the PINOID kinase

with previous research, mainly in the vascular tissues of roots, cotyledons, hypocotyl, flowers and in the young developing rosette leaves. Additionally, *CML12/TCH3* is also expressed in the epidermis of the elongation zone of the root tip. As a touch-responsive gene, the expression of *CML12/TCH3* can be induced by touch, wind, rain, wounding, darkness (Braam and Davis, 1990; Sistrunk et al., 1994; Wright et al., 2002), gravity (Figure S3) and auxin (Antosiewicz et al., 1995; Benjamins et al., 2001; Benjamins et al., 2003; Fan, 2014; Figure 4). These results indicate that *CML12/TCH3* plays a crucial role in transducing both external and internal signals causing elevation of the $[Ca^{2+}]_{cyt}$. Recently, *CML12/TCH3*, *CAM1*, *CAM4* and *CAM6* have also been reported to cooperate with calcium-dependent protein kinases to trigger calcium-dependent activation of CaM-BINDING PROTEIN 60-LIKE G in the regulation of fungal resistance in Arabidopsis (Sun et al., 2022).

In conclusion, although the PID interacting CaMs and CMLs are seemingly redundant and involved in a plethora of responses, more detailed research is likely to reveal that they have sub-functionalized with both specific and overlapping roles in plant development and defence.

PID-CaM/CML-mediated Ca^{2+} signalling: another feedback loop by which auxin regulates its own action

Accumulating evidence has shown that PAT is regulated by various internal and external cues that trigger Ca^{2+} signalling, which in turn modulates PIN subcellular re-localization and trafficking. An inositol trisphosphate-induced increase in $[Ca^{2+}]_{cyt}$ was shown to modulate auxin transport by inducing apolarity of PIN1 but not of PIN2 (Zhang et al., 2011). Mechanical stimulation of SAM cells using glass needle-induced cell ablation triggers the increase of $[Ca^{2+}]_{cyt}$ and regulates the polarity of PIN protein, indicating the importance of Ca^{2+} in shoot development (Li et al., 2019). An auxin-induced increase in $[Ca^{2+}]_{cyt}$ has been reported in many species (Hasenstein and Evans, 1986; Felle, 1988; Shishova and Lindberg, 2004;

Monshausen et al., 2011), indicating the importance of Ca^{2+} in auxin physiology. It was shown to be required for the inhibition of auxin on root growth (Shih et al., 2015) and auxin-regulated root hair growth (Dindas et al., 2018). However, the downstream targets of auxin-induced Ca^{2+} signalling are still largely unknown.

The gravistimulation-induced increase in $[\text{Ca}^{2+}]_{\text{cyt}}$ in cells at the lower side of the root tip (Plieth and Trewavas, 2002; Toyota et al., 2007, 2008a, b) coincide with the asymmetric movement of auxin to this side (Lee et al., 1984; Band et al., 2012). At the same time the enhanced auxin levels result in the induction of *CML12/TCH3* expression (Antosiewicz et al., 1995; Monshausen et al., 2011; Chapters 3 and 4). Our results now suggest that CML12/TCH3 together with CAM7 are the receptors in the lower epidermis of the root tip that are activated by the elevated cytosolic Ca^{2+} , and as a result sequester PID and WAG2 from the PM to the cytosol (Figure 1C; Fan, 2014). Dissociation of these AGC kinases from the PM and their inactivation causes an apolarization of PIN2 at the lower side of root tip, thereby enhancing the asymmetric auxin distribution and thus the root gravitropic response (Fan, 2014). These results reveal yet another mechanism by which auxin regulates its own action.

Material and Methods

Molecular cloning and constructs

The constructs *pET16H-TCH3*, *pGEX-PID*, *pDONR207 PID* were described previously (Benjamins et al., 2003). *p35S:PID-GFP* was described in (Yao, 2019). To obtain the plasmids encoding His-tagged CaM/CMLs, the corresponding coding regions were amplified from cDNA of 5-day-old seedlings using the primer sets *CaM/CML attB F* and *CaM/CML attB R* (Table S1). The resulting DNA fragments were subsequently recombined into *pDONR207* (Invitrogen, Gateway cloning, BP reaction) and *pET16H* (LR reaction). To generate the constructs *p35S:CaM/CML-mRFP* and *pDEST-CaM/CML VYNE*, coding regions without stop codon were amplified from cDNA of 5-day-old seedlings using the primer set *CaM/CML- attB F* and *CaM/CML-stop attB R* (Table S1), the resulting fragments were first recombined into *pDONR207* (BP reaction) and subsequently into *p35S:mRFP* or *pDEST-^{GW}VYNE* (LR reaction). *pDEST-PID VYCE* resulted from the LR reaction of *pDONR207 PID* and *pDEST-^{GW}VYCE*. To generate the constructs *pCaM/CML:turboGFP-GUS*, the corresponding promoter regions of selected CaM/CMLs were cloned using the primer sets *pCaM/CMLs attB F* and *pCaM/CML attB R* (Table S1), and then recombined into *pDONR207* (BP reaction) and from there into *pMDC163(gateway):turboGFP-GUS* (reconstructed by Yao 2019) (LR reaction).

Primers used were designed with CLC Main Workbench (CLC bio) software and listed in the Table S1.

Plant material and growth conditions and phenotype analysis

All transgenic lines and mutants used in this study are in the Columbia (Col-0) background. T-DNA insertion lines *cam1-1* (*SALK_202076C*), *cam1-2* (*GK-533G05*), *cam2-1* (*SALK_114166C*), *cam2-2* (*SALK_089283C*), *cam3-1* (*SALK_149754C*), *cam4-1* (*SALK_021224*), *cam4-2* (*SAIL_736_D07*), *cam5-1*

(*SAIL_595_D04*), *cam5-2* (*SALK_007371C*), *cam6-1* (*SALK_033803C*), *cam7-1* (*SAIK_074336C*), *cml8-1* (*SALK_02252C*), *cml8-2* (*SALK_114570*), *cml10-1* (*SALK_058561C*), *cml11-1* (*SALK_083435C*), *cml12-1* (*SALK_098779*) were ordered from the Nottingham Arabidopsis Stock Centre.

To generate the *pCaM/CML:turboGFP-GUS* reporter lines, binary vectors were introduced into *Agrobacterium tumefaciens* strain AGL1 by electroporation (den Dulk-Ras and Hooykaas, 1995) and transformed in *Arabidopsis thaliana* Col-0 using the floral dip method (Clough and Bent, 1998).

For the seeds grown on plates, seeds were sterilized by 1min 70% ethanol, 10 min bleach solution containing 1% chlorine and washed three times with sterile H₂O. Sterilized seeds were kept in H₂O in the dark at 4 °C for two days for vernalization and germinated on vertical plates with 0.5x Murashige and Skoog (1/2 MS, Duchefa) medium containing 0.05% MES, 1% sucrose, solidified with 1% Daishin agar (Duchefa) at 22 °C and 16 hours photoperiod. *Arabidopsis thaliana* plants grown on soil were cultured at 21 °C, 16 hours photoperiod and 70% relative humidity. *Nicotiana benthamiana* seeds were germinated on soil and plants were grown at 25 °C, and 70% relative humidity and 16 hours photoperiod.

Histochemical staining and microscopy

For histochemical staining, 5- and 12-day-old *pCaM/CML:turboGFP-GUS* seedlings or tissues from plants at different developmental stages were collected and fixed in 90% acetone at -20 °C for 20 min, followed by two times 10 min in GUS-washing solution (0.1 M PhosphH-Pi buffer (0.1 M NaH₂PO₄ and 0.1 M Na₂HPO₄) pH 7.0, 10 mM EDTA, 2 mM K₃Fe(CN)₆) under vacuum and 10 minutes in GUS staining buffer (10 mM EDTA, 50 mM sodium phosphate pH 7.0, 1 mg/ml X-gluc, 0.1% (v/v) Triton X-100, 0.5 mM K₃Fe(CN)₆, 0.5 mM K₄Fe(CN)₆) under vacuum. Samples were subsequently stained for 3 hours at 37 °C in the dark. Staining was stopped by replacing the staining buffer for acetic acid/EtOH (3:1) for 60 minutes and by subsequent rehydration in a graded of ethanol series (75, 50,

CALMODULIN-LIKE 12/TOUCH 3 and closely related calmodulins and calmodulin-like proteins redundantly interact with the PINOID kinase

25%) for 30 min each time. For the final step, 25% ethanol was replaced by water. For microscopy, stained seedlings and tissues were prepared on slides with chloralhydrate solution (4 : 2 : 1 (w/w) chloral hydrate : glycerol : water) and pictures were taken using a Leica MZ16FA microscope equipped with a Leica DFC 420 C digital colour Camera. Images were processed using Image J and assembled into figures using Adobe Photoshop.

Auxin treatment

Seeds were germinated on vertical plates containing solid 1/2 MS medium for five days, then transferred to liquid 1/2 MS medium supplemented with 5 μ M IAA for 0, 1, 2, 3 or 5 hours. Because IAA was dissolved in DMSO at a 5 mM concentration, liquid medium containing 0.1% DMSO was used as control. Histochemical staining was performed, and pictures were taken as described above. Treatments were repeated three times.

Gravistimulation

Seeds were germinated on vertical plates containing solid 1/2 MS medium for five days, then transferred to fresh medium with the roots as straight as possible and allowed to recover for two hours. Gravistimulation was started by rotating the plates 90°. Seedlings were harvested at 0-, 2-, 4-, and 6-hours after the start of gravistimulation and histochemical staining was performed and pictures were taken as described above. Experiments were repeated three times.

Protoplast transformation

Protoplasts were obtained from *Arabidopsis thaliana* Col-0 cell suspension cultures and transfected as described (Schirawski et al., 2000). Plasmid DNAs were extracted using the Plasmid Midi Kit (QIAGEN, #12143). For PEG-mediated transfection 10 μ g of each plasmid (*p35S:CaM/CML-mRFP* and/or *p35S:PID-turboGFP*) was added per 0.5×10^6 protoplasts. The transfected protoplasts were

incubated for 16 hours at 21 °C in the dark. Pictures were taken using the Zeiss LSM5 Exciter/Axio Observer confocal microscope with either a 40x or 63x oil immersion objective (NA=1.2). The GFP signal was detected using an argon 488 nm laser for excitation and a 505 to 530 nm band pass emission filter. The RFP signal was detected using an argon 543 nm laser for excitation and a 560 to 615 nm band pass emission filter.

***In vitro* pull-down assay**

In vitro pull-down assays were performed as described (Robert, 2008) with some minor modifications. *E. coli* strain Rosetta (Novagen) was transformed with *pET16H-CaM/CML* or *pGEX-PID*. Single colonies were picked and grown overnight (o/n) at 37 °C in 2 ml liquid LC medium complemented with 15 µg/ml Kanamycin (Km) or 35 µg/ml Chloramphenicol (Cam), respectively. The 2 ml cultures were sub-cultured in 100 ml fresh LC medium containing Cam and Km and grown at 37°C until an OD₆₀₀ of 0.6. Protein expression was induced with 1 mM IPTG for 4h at 30°C. Bacteria were harvested by centrifugation at 4000 RPM for 20 minutes and frozen in liquid nitrogen. Frozen bacterial pellets were resuspended in 4 ml GST-tagged protein Extraction Buffer (20 mM Tris pH 7.5, 500 mM NaCl, 5 mM EDTA, 1 mM EGTA, 1 mM DTT, 0.2 % Triton X-100, 0.05 % Tween-20) or His-tagged protein Extraction/Binding Buffer (20 mM Tris pH 7.5, 500 mM NaCl, 5 mM MgCl₂, 2 mM CaCl₂, 1 mM DTT, 0.2 % Triton X-100, 0.05 % Tween-20) supplemented with 0.1 mM Phenylmethanesulfonylfluoride (PMSF) and a protease inhibitor tablet. The suspensions were sonicated for 2 minutes and centrifuged at 10000 g for 10 min at 4 °C. For pull-down, 200 µl GST-PID supernatants was added to 200 µl of pre-equilibrated Pierce™ Glutathione Agarose beads (#16100, Thermo Scientific™) and samples were incubated for 2 h at 4°C. Beads were washed twice with 1 ml Washing Buffer 1 (10 mM Tris pH 7.5, 150 mM NaCl, 5 mM EDTA, 1 mM EGTA, 1 mM DTT) after which 400 µl His-CaM/CML supernatants and 100 µl Extraction/Binding Buffer were added. The

84

CALMODULIN-LIKE 12/TOUCH 3 and closely related calmodulins and calmodulin-like proteins redundantly interact with the PINOID kinase

mixture was incubated at 4°C for 4 hours on a rotator, the beads were washed twice with 500 µl Washing Buffer 2 (10 mM Tris pH 7.5, 150 mM NaCl, 5 mM MgCl₂, 2 mM CaCl₂, 1 mM DTT) and associated proteins were released by adding 30 µl 2× SDS loading buffer (2 mL Tris (1 M, pH 6.8), 4.6 mL glycerol (50%), 1.6 mL SDS (10%), 0.4 mL bromophenol blue (0.5%), 0.4 mL β-mercaptoethanol)) and boiling for 10 minutes. 15 µl samples were loaded on a 15% SDS-PAGE gel and proteins were separated by electrophoresis, transferred onto a PVDF transfer membranes (#88520, Thermo Scientific™) using Trans-Blot® Turbo™ Transfer System (Bio-Rad) and detected by anti-GST immunoblotting (GST Antibody (B-14) HRP, sc-138 HRP, Santa Cruz Biotechnology) or anti-His immunoblotting (His-probe Antibody (H-3) HRP, sc-8036 HRP, Santa Cruz Biotechnology).

Bimolecular Fluorescence Complementation (BiFC) assay

For BiFC assays, 20 ml cultures of *Agrobacterium tumefaciens* strain AGL1 harbouring constructs *pDEST-PID-VYCE*, *pDEST-CaM1-VYNE*, *pDEST-CML9-VYNE*, *pDEST-CML10-VYNE*, *pDEST-CML12-VYNE*, *pDEST-CML24-VYNE* or *pDEST-VYCE* were incubated in a 28°C shaker until an OD₆₀₀ of 1.0 was reached. Bacteria were collected by centrifugation for 15 minutes at 4000 rpm, resuspended in 20 ml infiltration medium (10 mM MgCl₂, 10 mM MES/KOH, pH 5.7) supplemented with 200 µM Acetosyringone (Sigma-Aldrich, #D134406-5G), and incubated for at least 2 hours at 50 rpm at 28 °C on a table shaker in darkness. *Agrobacterium* strains each carrying one construct were mixed at equal volumes (5 ml each). Leaves of three weeks old *Nicotiana benthamiana* plants were infiltrated using a 5 ml syringe without needle. Two infiltrations per leaf, and a total of eight leaves from two plants were infiltrated. Two days later, infiltrated leaf parts were checked for YFP signal using the Zeiss LSM 5 Exciter 2C/1F Imager M1 (Zeiss, Oberkochen, Germany) confocal microscope, using a 20x objective. The YFP signal was detected using an argon 514 nm laser and a 530-600 nm band pass filter.

Accession numbers

Arabidopsis Genome Initiative locus identifiers for the genes mentioned are as follows: *CaM1/TCH1* (*At5g37780*), *CaM2* (*At2g41110*), *CaM3* (*At3g56800*), *CaM4* (*At1g66410*), *CaM5* (*At2g27030*), *CaM6* (*At5g21274*), *CaM7* (*At3g43810*), *CML8* (*At4g14640*), *CML9* (*At3g51920*), *CML10* (*At2g41090*), *CML11* (*At3g22930*), *CML12/TCH3* (*At2g41100*), *CML13* (*At1g12310*), *CML14* (*At1g62820*), *CML24/TCH2* (*At5g377770*), *PID* (*At2g34650*)

pCaM2 attB F	GGGGACAAGTTTGTACAAAAAAGCAGGCTCGGAATTCAGGGAAGCCTTCC
pCaM2 attB R	GGGGACCACTTTGTACAAGAAAGCTGGGTCTGTTTTTCTTTCTTTCT
pCaM3 attB F	GGGGACAAGTTTGTACAAAAAAGCAGGCTCGCCATTCATGACGTCATTTT
pCaM3 attB R	GGGGACCACTTTGTACAAGAAAGCTGGGTCTGTTTTTCTTCTCCTTTT
pCaM4 attB F	GGGGACAAGTTTGTACAAAAAAGCAGGCTCGAAATAGACATGGCCAGTTT
pCaM4 attB R	GGGGACCACTTTGTACAAGAAAGCTGGGTCTGCTTCTTCTCGTTTCT
pCaM5 attB F	GGGGACAAGTTTGTACAAAAAAGCAGGCTCGGACTAGACACAATAGTAGT
pCaM5 attB R	GGGGACCACTTTGTACAAGAAAGCTGGGTCTTTTTGGTTTAGATGAGAAA
pCaM6 attB F	GGGGACAAGTTTGTACAAAAAAGCAGGCTCGCACTCCGAATGTTACCTC
pCaM6 attB R	GGGGACCACTTTGTACAAGAAAGCTGGGTCTTTCCTTCTTACCTTTTTT
pCaM7 attB F	GGGGACAAGTTTGTACAAAAAAGCAGGCTCGAGACAGGTACCCACTTAAG
pCaM7 attB R	GGGGACCACTTTGTACAAGAAAGCTGGGTCTTTTTTGTCTTCTCGGAT
pCML8 attB F	GGGGACAAGTTTGTACAAAAAAGCAGGCTCGTGGTTCGTTAATTTGCTACG
pCML8 attB R	GGGGACCACTTTGTACAAGAAAGCTGGGTCTGTTTTCTGAGAATATTTT
pCML9 attB F	GGGGACAAGTTTGTACAAAAAAGCAGGCTCGGCGCATTTTCATTAATTCG
pCML9 attB R	GGGGACCACTTTGTACAAGAAAGCTGGGTCTCTTCGATCACAAAGAAAA
pCML10 attB F	GGGGACAAGTTTGTACAAAAAAGCAGGCTCGAATGCACTTGCGAATCCCT
pCML10 attB R	GGGGACCACTTTGTACAAGAAAGCTGGGTCTGTTTTTTATTTTCTGTGAT
pCML11 attB F	GGGGACAAGTTTGTACAAAAAAGCAGGCTCGATGCATCATTTTCTCCCT
pCML11 attB R	GGGGACCACTTTGTACAAGAAAGCTGGGTCCCAATTAATACTTGCTTAGT
pCML12 attB F	GGGGACAAGTTTGTACAAAAAAGCAGGCTCGAATGGTACATCAGTAACTT
pCML12 attB R	GGGGACCACTTTGTACAAGAAAGCTGGGTCTGTTTTTTTGTCTTCTGTG
CaM2 attB R	5'GGGGACCACTTTGTACAAGAAAGCTGGGTTACCTTAGCCATCATAACCTTCA3'
CaM2-stop attB R	5'GGGGACCACTTTGTACAAGAAAGCTGGGTCCTTAGCCATCATAACCTTCA3'
CaM3 attB F	GGGGACAAGTTTGTACAAAAAAGCAGGCTCGATGGCGGATCAGCTACCG
CaM3 attB R	GGGGACCACTTTGTACAAGAAAGCTGGGTCTCACTTAGCCATCATGACCT
CaM3-stop attB R	GGGGACCACTTTGTACAAGAAAGCTGGGTCCTTAGCCATCATGACCTTAA
CaM4 attB F	GGGGACAAGTTTGTACAAAAAAGCAGGCTCGATGGCGGATCAGCTAACTG
CaM4 attB R	GGGGACCACTTTGTACAAGAAAGCTGGGTCTCACTTAGCCATCATAATCT
CaM4-stop attB R	GGGGACCACTTTGTACAAGAAAGCTGGGTCCTTAGCCATCATAATCTTGA
CaM5 attB F	GGGGACAAGTTTGTACAAAAAAGCAGGCTCGATGGCAGATCAGCTACCG

CALMODULIN-LIKE 12/TOUCH 3 and closely related calmodulins and calmodulin-like proteins redundantly interact with the PINOID kinase

CaM5 attB R	GGGGACCACTTTGTACAAGAAAGCTGGGTCTCAGAGAATACGGCAGTGAC
CaM5-stop attB R	GGGGACCACTTTGTACAAGAAAGCTGGGTCGAGAATACGGCAGTGACTTT
CaM6 attB F	GGGGACAAGTTTGTACAAAAAAGCAGGCTCGATGGCGGATCAGCTCACCG
CaM6 attB R	GGGGACCACTTTGTACAAGAAAGCTGGGTCTCACTTAGCCATCATGACTT
CaM6-stop attB R	GGGGACCACTTTGTACAAGAAAGCTGGGTCCTTAGCCATCATGACTTTGA
CaM7 attB F	GGGGACAAGTTTGTACAAAAAAGCAGGCTCGATGGCGGATCAGCTAACCG
CaM7 attB R	GGGGACCACTTTGTACAAGAAAGCTGGGTCTCACTTTGCCATCATGACTT
CaM7-stop attB R	GGGGACCACTTTGTACAAGAAAGCTGGGTCCTTTGCCATCATGACTTTGA
CML8 attB F	GGGGACAAGTTTGTACAAAAAAGCAGGCTCGATGGAAGAAACAGCACTGA
CML8 attB R	GGGGACCACTTTGTACAAGAAAGCTGGGTC TCAGTCAATGTTGATCATCA
CML8-stop attB R	GGGGACCACTTTGTACAAGAAAGCTGGGTC GTCAATGTTGATCATCATCT
CML9 attB F	GGGACAAGTTTGTACAAAAAAGCAGGCTTCATGGCGGATGCTTTACAGATGAAG
CML9 attB R	GGGGACCACTTTGTACAAGAAAGCTGGGTCGTAATAAGAGGCAGCAATCATCA
CML9-stop attB R	GGGGACCACTTTGTACAAGAAAGCTGGGTCATAAGAGGCAGCAATCATCA
CML10 attB F	GGGGACAAGTTTGTACAAAAAAGCAGGCTTCATGGCGAATAAGTTCACTAG
CML10 attB R	GGGGACCACTTTGTACAAGAAAGCTGGGTCTCAAGAAAACAACGCTTCGAACA
CML10-stop attB R	GGGGACCACTTTGTACAAGAAAGCTGGGTCAGAAAACAACGCTTCGAACA
CML11 attB F	GGGGACAAGTTTGTACAAAAAAGCAGGCTTC ATGGCGGATCAGCTCACCG
CML11 attB R	GGGGACCACTTTGTACAAGAAAGCTGGGTCTTAACCAATTGATCATCATCAT
CML11-stop attB R	GGGGACCACTTTGTACAAGAAAGCTGGGTCACCATTGATCATCATCAT
CML13 attB F	GGGGACAAGTTTGTACAAAAAAGCAGGCTCG ATGGGGAAGATGGTCTGA
CML13 attB R	GGGGACCACTTTGTACAAGAAAGCTGGGTC TCACTTAGCAACCATCCTTG
CML13-stop attB R	GGGGACCACTTTGTACAAGAAAGCTGGGTC CTTAGCAACCATCCTTGCTA
CML14 attB F	GGGGACAAGTTTGTACAAAAAAGCAGGCTCG ATGAGCAAGGATGGTTTGA
CML14 attB R	GGGGACCACTTTGTACAAGAAAGCTGGGTC TTACTTAGCAACCATCTAG
CML14-stop attB R	GGGGACCACTTTGTACAAGAAAGCTGGGTC CTTAGCAACCATCTAGCAA
CML24 attB F	GGGGACAAGTTTGTACAAAAAAGCAGGCTTCATGTCATCGAAGAACGGAGTTG
CML24 attB R	GGGGACCACTTTGTACAAGAAAGCTGGGTCTCAAGCACCACCACCATTACTCA
CML24-stop attB R	GGGGACCACTTTGTACAAGAAAGCTGGGTCAGCACCACCACCATTACTCA
LBb1.3 for SALK lines	ATTTTGCCGATTTCGGAAC

Acknowledgements

The authors would like to thank Gerda Lamers and Joost Willemse for their help with the microscopy, Ward de Winter and Jan Vink for help with medium, tissue culture and plant caretaking. This author was supported by the China Scholarship Council.

Author contribution

Remko Offringa, Xiaoyu Wei designed the experiments, Xiaoyu Wei, Parjanya Kocherla, Linge Li, Yuanwei Fan performed the experiments and data analysis, Xiaoyu Wei and Remko Offringa wrote and finalization of the Chapter.

References

- Antosiewicz, D. M., Polisensky, D. H., & Braam, J.** (1995). Cellular localization of the Ca²⁺ binding TCH3 protein of Arabidopsis. *Plant J.* 8: 623-636.
- Bailey, T. L., & Elkan, C.** (1994). Fitting a mixture model by expectation maximization to discover motifs in biopolymers. *Proc. Int. Conf. Intell. Syst. Mol. Biol.* 2: 28-36.
- Band, L. R., Wells, D. M., Larrieu, A., Sun, J., Middleton, A. M., French, A. P., ... & Bennett, M. J.** (2012). Root gravitropism is regulated by a transient lateral auxin gradient controlled by a tipping-point mechanism. *Proc. Natl. Acad. Sci. U.S.A.* 109: 4668-4673.
- Bassukas, A. E. L., Xiao, Y., & Schwechheimer, C.** (2022). Phosphorylation control of PIN auxin transporters. *Curr. Opin. Plant Biol.* 65: 102146.
- Batistic, O., Waadt, R., Steinhorst, L., Held, K., and Kudla, J.** (2010). CBL-mediated targeting of CIPKs facilitates the decoding of calcium signals emanating from distinct cellular stores. *Plant J.* 61: 211-222.
- Baum, G., Long, J. C., Jenkins, G. I., & Trewavas, A. J.** (1999). Stimulation of the blue light phototropic receptor NPH1 causes a transient increase in cytosolic Ca²⁺. *Proc. Natl. Acad. Sci. U.S.A.* 96: 13554-13559.
- Benjamins, R., Ampudia, C.S., Hooykaas, P.J., & Offringa, R.** (2003). PINOID-mediated signaling involves calcium-binding proteins. *Plant Physiol.* 132: 1623-1630.
- Benjamins, R., Quint, A., Weijers, D., Hooykaas, P., & Offringa, R.** (2001). The PINOID protein kinase regulates organ development in Arabidopsis by enhancing polar auxin transport. *Development* 128: 4057-4067.
- Bennett, S. R., Alvarez, J., Bossinger, G., & Smyth, D. R.** (1995). Morphogenesis in *pinoid* mutants of Arabidopsis thaliana. *Plant J.* 8: 505-520.
- Boudsocq, M., & Sheen, J.** (2013). CDPKs in immune and stress signaling. *Trends Plant Sci.* 18: 30-40.
- Braam, J., & Davis, R. W.** (1990). Rain-, wind-, and touch-induced expression of calmodulin and calmodulin-related genes in Arabidopsis. *Cell* 60: 357-364.
- Cheng, H. Q., Han, L. B., Yang, C. L., Wu, X. M., Zhong, N. Q., Wu, J. H., Wang, F. X., Wang, H. Y., & Xia, G. X.** (2016). The cotton MYB108 forms a positive feedback regulation loop with CML11 and participates in the defense response against *Verticillium dahliae* infection. *J. Exp. Bot.* 67: 1935-1950.
- Cho, K. M., Nguyen, H. T. K., Kim, S. Y., Shin, J. S., Cho, D. H., Hong, S. B., ... & Ok, S. H.** (2016). CML 10, a variant of calmodulin, modulates ascorbic acid synthesis. *New Phytol.* 209: 664-678.

- Clough, S. J., & Bent, A. F.** (1998). Floral dip: a simplified method for *Agrobacterium*-mediated transformation of *Arabidopsis thaliana*. *Plant J.* 16: 735-743.
- Day, I. S., Reddy, V. S., Shad Ali, G., & Reddy, A. S. N.** (2002). Analysis of EF-hand-containing proteins in *Arabidopsis*. *Genome Biol.* 3: 1-24.
- Dela Fuente, R.K., and Leopold, A.C.** (1973). A role for calcium in auxin transport. *Plant Physiol.* 51: 845-847.
- den Dulk-Ras, A., & Hooykaas, P. J.** (1995). Electroporation of *Agrobacterium tumefaciens*. *Plant cell electroporation and electrofusion protocols*, 63-72.
- Dhonukshe, P., Huang, F., Galván-Ampudia, C. S., Mähönen, A. P., Kleine-Vehn, J., Xu, J., ... & Offringa, R.** (2010). Plasma membrane-bound AGC3 kinases phosphorylate PIN auxin carriers at TPRXS (N/S) motifs to direct apical PIN recycling. *Development* 137: 3245-3255.
- Dindas, J., Scherzer, S., Roelfsema, M. R. G., von Meyer, K., Müller, H. M., Al-Rasheid, K. A. S., ... & Hedrich, R.** (2018). AUX1-mediated root hair auxin influx governs SCFTIR1/AFB-type Ca^{2+} signaling. *Nat. Commun.* 9: 1-10.
- Dong, Q., Wallrad, L., Almutairi, B. O., & Kudla, J.** (2022). Ca^{2+} signaling in plant responses to abiotic stresses. *J. Integr. Plant Biol.* 64: 287-300.
- Eklund, L., & Eliasson, L.** (1990). Effects of calcium ion concentration on cell wall synthesis. *J. Exp. Bot.* 41: 863-867.
- Fan, Y.** (2014). The role of AGC3 kinases and calmodulins in plant growth responses to abiotic signals (Doctoral dissertation, Leiden University).
- Felle, H.** (1988). Auxin causes oscillations of cytosolic free calcium and pH in *Zea mays* coleoptiles. *Planta* 174: 495-499.
- Friml, J., Yang, X., Michniewicz, M., Weijers, D., Quint, A., Tietz, O., ... & Offringa, R.** (2004). A PINOID-dependent binary switch in apical-basal PIN polar targeting directs auxin efflux. *Science* 306: 862-865.
- Galván-Ampudia, C. S.** (2009). Plant Agc protein kinases orient auxin-mediated differential growth and organogenesis (Doctoral dissertation, Leiden University).
- Galván-Ampudia, C. S., & Offringa, R.** (2007). Plant evolution: AGC kinases tell the auxin tale. *Trends Plant Sci.* 12: 541-547.
- Galweiler, L., Guan, C., Muller, A., Wisman, E., Mendgen, K., Yephremov, A., & Palme, K.** (1998). Regulation of polar auxin transport by AtPIN1 in *Arabidopsis* vascular tissue. *Science* 282: 2226-2230.
- Gehl, C., Waadt, R., Kudla, J., Mendel, R. R., & Hänsch, R.** (2009). New GATEWAY vectors for high throughput analyses of protein-protein interactions by bimolecular fluorescence complementation. *Mol. Plant* 2: 1051-1058.

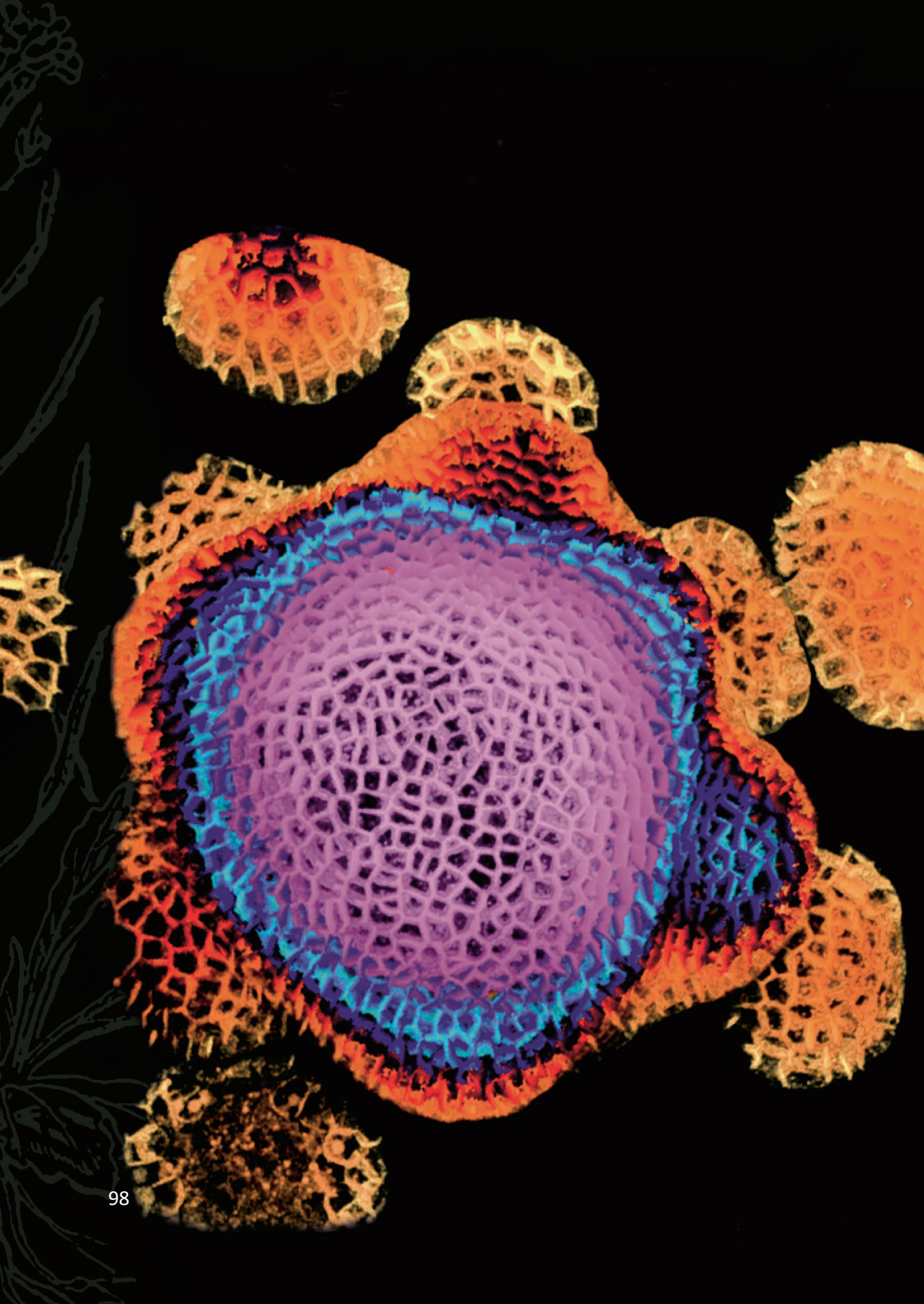
- Gehring, C. A., Irving, H. R., & Parish, R. W.** (1990). Effects of auxin and abscisic acid on cytosolic calcium and pH in plant cells. *Proc. Natl. Acad. Sci. U.S.A.* 87: 9645-9649.
- Geisler, M. M.** (2021). A retro-perspective on auxin transport. *Front. Plant Sci.* 12: 756968.
- Goh, C. S., Lee, Y., & Kim, S. H.** (2012). Calcium could be involved in auxin-regulated maintenance of the quiescent center in the Arabidopsis root. *J. Plant Biol.* 55: 143-150.
- Gomes, G. L. B., & Scortecci, K. C.** (2021). Auxin and its role in plant development: structure, signalling, regulation and response mechanisms. *Plant Biol.* 23: 894-904.
- Harmon, A. C., Gribskov, M., & Harper, J. F.** (2000). CDPKs—a kinase for every Ca^{2+} signal? *Trends Plant Sci.* 5: 154-159.
- Hasenstein, K. H., & Evans, M. L.** (1986). Calcium dependence of rapid auxin action in maize roots. *Plant Physiol.* 81: 439-443.
- Hepler, P.K. and Wayne, R.O.** (1985) Calcium and Plant Development. *Annual Review of Plant Physiol.* 36: 397-439.
- Huang, F., Kemel Zago, M., Abas, L., van Marion, A., Galván-Ampudia, C. S., & Offringa, R.** (2010). Phosphorylation of conserved PIN motifs directs Arabidopsis PIN1 polarity and auxin transport. *Plant Cell* 22: 1129-1142.
- Jing, X., Cai, C., Fan, S., Wang, L., & Zeng, X.** (2019). Spatial and temporal calcium signaling and its physiological effects in Moso Bamboo under drought stress. *Forests* 10: 224.
- Klee, C.B., Ren, H., and Wang, X.** (1998). Regulation of calmodulin stimulated protein phosphatase, calcineurin. *J. Biol. Chem.* 273: 13367-13370.
- La Verde, V., Dominici, P., & Astegno, A.** (2018). Towards understanding plant calcium signaling through calmodulin-like proteins: A biochemical and structural perspective. *Int. J. Mol. Sci.* 19: 1331.
- Lee, J. S., Mulkey, T. J., & Evans, M. L.** (1984). Inhibition of polar calcium movement and gravitropism in roots treated with auxin-transport inhibitors. *Planta* 160: 536-543.
- Lee, K., Thorneycroft, D., Achuthan, P., Hermjakob, H., and Ideker, T.** (2010). Mapping plant interactomes using literature curated and predicted protein-protein interaction data sets. *Plant Cell* 22: 997–1005.
- Lévy, J., Bres, C., Geurts, R., Chalhoub, B., Kulikova, O., Duc, G., ... & Debellé, F.** (2004). A putative Ca^{2+} and calmodulin-dependent protein kinase required for bacterial and fungal symbioses. *Science* 303: 1361-1364.

- Li, P., Zhao, C., Zhang, Y., Wang, X., Wang, X., Wang, J., ... & Bi, Y.** (2016). Calcium alleviates cadmium-induced inhibition on root growth by maintaining auxin homeostasis in *Arabidopsis* seedlings. *Protoplasma* 253: 185-200.
- Li, T., Yan, A., Bhatia, N., Altinok, A., Afik, E., Durand-Smet, P., ... & Meyerowitz, E. M.** (2019). Calcium signals are necessary to establish auxin transporter polarity in a plant stem cell niche. *Nat. Commun.* 10: 1-9.
- McCormack, E., Tsai, Y. C., & Braam, J.** (2005). Handling calcium signaling: *arabidopsis* CaMs and CMLs. *Trends Plant Sci.* 10: 383-389.
- Michniewicz, M., Zago, M. K., Abas, L., Weijers, D., Schweighofer, A., Meskiene, I., ... & Friml, J.** (2007). Antagonistic regulation of PIN phosphorylation by PP2A and PINOID directs auxin flux. *Cell* 130: 1044-1056.
- Monshausen, G. B., Miller, N. D., Murphy, A. S., & Gilroy, S.** (2011). Dynamics of auxin-dependent Ca^{2+} and pH signaling in root growth revealed by integrating high-resolution imaging with automated computer vision-based analysis. *Plant J.* 65: 309-318.
- Mroue, S., Simeunovic, A., & Robert, H. S.** (2018). Auxin production as an integrator of environmental cues for developmental growth regulation. *J. Exp. Bot.* 69: 201-212.
- Oh, M. H., Kim, H. S., Wu, X., Clouse, S. D., Zielinski, R. E., & Huber, S. C.** (2012). Calcium/calmodulin inhibition of the *Arabidopsis* BRASSINOSTEROID-INSENSITIVE 1 receptor kinase provides a possible link between calcium and brassinosteroid signalling. *Biochemical J.* 443: 515-523.
- Okada, K., Ueda, J., Komaki, M. K., Bell, C. J., & Shimura, Y.** (1991). Requirement of the auxin polar transport system in early stages of *Arabidopsis* floral bud formation. *Plant Cell* 3: 677-684.
- Olafsson, P., Wang, T., & Lu, B.** (1995). Molecular cloning and functional characterization of the *Xenopus* Ca^{2+} -binding protein frequenin. *Proc. Natl. Acad. Sci. U.S.A.* 92: 8001-8005.
- Patil, S., Takezawa, D., and Poovaiah, B. W.** (1995). Chimeric plant calcium/calmodulin-dependent protein kinase gene with a neural visin-like calcium-binding domain. *Proc. Natl. Acad. Sci. U.S.A.* 92: 4897-4901.
- Perochon, A., Aldon, D., Galaud, J. P., & Ranty, B.** (2011). Calmodulin and calmodulin-like proteins in plant calcium signaling. *Biochimie* 93: 2048-2053.
- Perochon, A., Dieterle, S., Pouzet, C., Aldon, D., Galaud, J. P., & Ranty, B.** (2010). Interaction of a plant pseudo-response regulator with a calmodulin-like protein. *Biochem. Biophys. Res. Commun.* 398: 747-751.

- Petrásek, J., Mravec, J., Bouchard, R., Blakeslee, J. J., Abas, M., Seifertová, D., ... & Friml, J.** (2006). PIN proteins perform a rate-limiting function in cellular auxin efflux. *Science* 312: 914-918.
- Plieth, C., & Trewavas, A. J.** (2002). Reorientation of seedlings in the earth's gravitational field induces cytosolic calcium transients. *Plant Physiol.* 129: 786-796.
- Popescu, S.C., Popescu, G.V., Bachan, S., Zhang, Z., Seay, M., Gerstein, M., Snyder, M., and Dinesh-Kumar, S.P.** (2007). Differential binding of calmodulin-related proteins to their targets revealed through high-density Arabidopsis protein microarrays. *Proc. Natl. Acad. Sci. U.S.A.* 104: 4730-4735.
- Raza, A., Ashraf, F., Zou, X., Zhang, X., & Tosif, H.** (2020). Plant adaptation and tolerance to environmental stresses: mechanisms and perspectives. *Plant Ecophysiology and Adaptation under Climate Change: Mechanisms and Perspectives I: General Consequences and Plant Responses*, 117-145.
- Robert, H.** (2008). Calcium- and BTB domain protein-modulated PINOID kinase directs polar auxin transport. (Doctoral dissertation, Leiden University).
- Rudd, J. J., & Franklin-Tong, V. E.** (1999). Calcium signaling in plants. *Cell. Mol. Life Sci.* 55: 214-232.
- Sanders, D., Pelloux, J., Brownlee, C., and Harper, J.F.** (2002). Calcium at the crossroads of signaling. *Plant Cell* 14 (suppl.): S401-S417.
- Sathyanarayanan, P. V., Cremo, C. R., & Poovaiah, B. W.** (2000). Plant chimeric Ca^{2+} /calmodulin-dependent protein kinase: role of the neural visinin-like domain in regulating autophosphorylation and calmodulin affinity. *J Biol. Chem.* 275: 30417-30422.
- Schirawski, J., Planchais, S., & Haenni, A. L.** (2000). An improved protocol for the preparation of protoplasts from an established Arabidopsis thaliana cell suspension culture and infection with RNA of turnip yellow mosaic tymovirus: a simple and reliable method. *J. Virol. Methods* 86: 85-94.
- Schulz, P., Herde, M., & Romeis, T.** (2013). Calcium-dependent protein kinases: hubs in plant stress signaling and development. *Plant Physiol.* 163: 523-530.
- Shih, H. W., DePew, C. L., Miller, N. D., & Monshausen, G. B.** (2015). The Cyclic Nucleotide-Gated Channel CNGC14 Regulates Root Gravitropism in Arabidopsis thaliana. *Curr. Biol.* 25: 3119–3125.
- Shishova, M., & Lindberg, S.** (2004). Auxin induces an increase of Ca^{2+} concentration in the cytosol of wheat leaf protoplasts. *J. Plant Physiol.* 161: 937-945.

- Sistrunk, M.L., Antosiewicz, D.M., Purugganan, M.M., & Braam, J. (1994).** Arabidopsis TCH3 encodes a novel Ca^{2+} binding protein and shows environmentally induced and tissue-specific regulation. *Plant Cell* 6: 1553-1565.
- Sun, L., Qin, J., Wu, X., Zhang, J., & Zhang, J. (2022).** TOUCH 3 and CALMODULIN 1/4/6 cooperate with calcium-dependent protein kinases to trigger calcium-dependent activation of CAM-BINDING PROTEIN 60-LIKE G and regulate fungal resistance in plants. *Plant Cell* 34: 4088-4104.
- Takezawa, D., Ramachandiran, S., Paranjape, V., and Poovaiah, B. W. (1996).** Dual regulation of a chimeric plant serine threonine kinase by calcium and calcium calmodulin. *J. Biol. Chem.* 271: 8126–8132.
- Tanaka, H., Dhonukshe, P., Brewer, P.B., and Friml, J. (2006).** Spatiotemporal asymmetric auxin distribution: a means to coordinate plant development. *Cell Mol. Life Sci.* 63: 2738-2754.
- Toyota, M., Furuichi, T., Tatsumi, H., & Sokabe, M. (2007).** Hypergravity stimulation induces changes in intracellular calcium concentration in Arabidopsis seedlings. *Adv. Space Res.* 7: 1190-1197.
- Toyota, M., Furuichi, T., Tatsumi, H., & Sokabe, M. (2008).** Critical consideration on the relationship between auxin transport and calcium transients in gravity perception of Arabidopsis seedlings. *Plant Signal. Behav.* 8: 521-524.
- Toyota, M., Furuichi, T., Tatsumi, H., & Sokabe, M. (2008).** Cytoplasmic calcium increases in response to changes in the gravity vector in hypocotyls and petioles of Arabidopsis seedlings. *Plant Physiol.* 2: 505-14.
- Ung, K. L., Winkler, M., Schulz, L., Kolb, M., Janacek, D. P., Dedic, E., ... & Pedersen, B. P. (2022).** Structures and mechanism of the plant PIN-FORMED auxin transporter. *Nature* 609: 605-610.
- Verma, S., Negi, N. P., Narwal, P., Kumari, P., Kisku, A. V., Gahlot, P., ... & Kumar, D. (2022).** Calcium signaling in coordinating plant development, circadian oscillations and environmental stress responses in plants. *Environ. Exp. Bot.* 201: 104935.
- Wang, J. P., Munyampundu, J. P., Xu, Y. P., & Cai, X. Z. (2015).** Phylogeny of Plant Calcium and Calmodulin-Dependent Protein Kinases (CCaMKs) and Functional Analyses of Tomato CCaMK in Disease Resistance. *Front. Plant Sci.* 6: 1075.
- Weinl, S., and Kudla, J. (2009).** The CBL-CIPK Ca^{2+} -decoding signaling network: Function and perspectives. *New Phytol.* 184: 517–528.

- Wright, A. J., Knight, H., & Knight, M. R.** (2002). Mechanically stimulated TCH3 gene expression in Arabidopsis involves protein phosphorylation and EIN6 downstream of calcium. *Plant Physiol.* 4: 1402-1409.
- Xiao, Y.** (2019). Novel factors modulating AGC kinase signaling controlled polar auxin transport. (Doctoral dissertation, Leiden University).
- Xu, H., Heath, M.C.** (1998). Role of calcium in signal transduction during the hypersensitive response caused by basidiospore-derived infection of the cowpea rust fungus. *Plant Cell* 4: 585–597.
- Xu, T., Niu, J., & Jiang, Z.** (2022). Sensing mechanisms: Calcium signaling mediated abiotic stress in plants. *Front. Plant Sci.* 13: 925863.
- Yang, C., Li, A., Zhao, Y., Zhang, Z., Zhu, Y., Tan, X., ... & Mao, L.** (2011). Overexpression of a wheat CCaMK gene reduces ABA sensitivity of Arabidopsis thaliana during seed germination and seedling growth. *Plant Mol. Biol. Rep.* 3: 681-692.
- Yu, S., Wu, J., Sun, Y., Zhu, H., Sun, Q., Zhao, P., ... & Guo, Z.** (2022). A calmodulin-like protein (CML10) interacts with cytosolic enzymes GSTU8 and FBA6 to regulate cold tolerance. *Plant Physiol.* 190: 1321-1333.
- Zhang, J., Vanneste, S., Brewer, P. B., Michniewicz, M., Grones, P., Kleine-Vehn, J., ... & Friml, J.** (2011). Inositol trisphosphate-induced Ca^{2+} signaling modulates auxin transport and PIN polarity. *Dev. Cell* 20: 855-866.
- Zhang, L., & Lu, Y. T.** (2003). Calmodulin-binding protein kinases in plants. *Trends Plant Sci.* 8: 123-127.
- Zhao, X., Wang, Y.L., Qiao, X.R., Wang, J., Wang, L.D., Xu, C.S., & Zhang, X.** (2013). Phototropins function in high-intensity blue light-induced hypocotyl phototropism in Arabidopsis by altering cytosolic calcium. *Plant Physiol.* 162: 1539-1551.
- Zhu, X., Dunand, C., Snedden, W., & Galaud, J. P.** (2015). CaM and CML emergence in the green lineage. *Trends Plant Sci.* 20: 483-48.
- Zhu, X., Robe, E., Jomat, L., Aldon, D., Mazars, C., & Galaud, J. P.** (2017). CML8, an Arabidopsis Calmodulin-Like protein, plays a role in Pseudomonas syringae plant immunity. *Plant Cell Physiol.* 58: 307-319.
- Zimmermann, P., Hirsch-Hoffmann, M., Hennig, L., & Gruissem, W.** (2004). GENEVESTIGATOR. Arabidopsis microarray database and analysis toolbox. *Plant Physiol.* 136: 2621-2632.



Chapter 3

PINOID plasma membrane association and CALMODULIN-LIKE 12/TOUCH 3 binding converge on an amphipathic alpha-helix in the kinase insertion domain

Xiaoyu Wei^{1,4}, Yuanwei Fan^{2,4}, Eike Rademacher^{3,4} and Remko Offringa^{1*}

¹ Plant Developmental Genetics, Institute of Biology Leiden, Leiden University, Sylviusweg 72, 2333 BE, Leiden, Netherlands

² Department of Biology and Center for Engineering Mechanobiology, Washington University in St. Louis, St. Louis, MO 63130, USA

³ Rijk Zwaan, 2678 KX De Lier, The Netherlands

⁴ These authors contributed equally to this manuscript

*Author for correspondence: r.offringa@biology.leidenuniv.nl

The results in this Chapter are included in the following publication: **Wei, X.Y.**, Fan, Y.W.,.....Offringa, R*. Calcium-regulated PINOID kinase activity is required for a robust spiral phyllotaxis in the Arabidopsis inflorescence (In preparation).

Abstract

The protein kinase PINOID (PID) is a plasma membrane (PM) associated AGC3 protein kinase that regulates auxin transport polarity by phosphorylating PIN auxin efflux carriers. Previous research and our results in Chapter 2 showed that a confined clade comprising seven CaMs and four closely-related calmodulin-like proteins (CMLs), including CALMODULIN-LIKE 12/TOUCH 3 (CML12/TCH3), interact with PID, and sequester PID from the PM to the cytosol. These PID interacting CaM/CMLs were found to be co-expressed with PID in many tissues, and the single loss-of-function mutants of the genes encoding PID interacting CaM/CMLs did not show a clear phenotype, suggesting that there is functional redundancy. In order to identify the biological function of the CaM/CML-PID interaction, we mapped the CaM/CMLs binding domain in PID. First, we confirmed that PID associates to the PM by the insertion domain (ID) in the catalytic kinase core. Subsequent fine mapping of the CaM/CML binding domain in PID showed that both CaM/CML binding and PM association converge at an amphipathic alpha helix in the PID ID. Disruption of this amphipathic alpha helix by substitution of several positively charged arginines by alanines (RtoA) interfered with both CaM/CML binding and PM association. Surprisingly, the PID(RtoA) versions showed the same overexpression phenotypes as wild-type PID and complemented the pin-like inflorescence phenotype of the *pid* mutant, when expressed under the *PID* promoter. Our results indicate that PM association is not essential for PID function and that the ‘untouchable’ PID(RtoA) versions are useful tools to study the role of the PID-CaM/CML interaction in plant development.

Keywords: PINOID (PID), AGC protein serine/threonine kinase, Calmodulin (CaM), Calmodulin-like (CML), Plasma membrane association, Amphipathic alpha helix, Arabidopsis

Introduction

The plant hormone auxin is a well-established inducer of Ca^{2+} signalling (Hasenstein and Evans, 1986; Felle, 1988; Gerring et al., 1990; Irving et al., 1992; Shishova and Lindberg, 1999; Monshausen et al., 2011). In fact, several reports indicate the involvement of Ca^{2+} signalling in the regulation of auxin transport during gravitropism (Dela Fuente and Leopold, 1973; Lee et al., 1984; Plieth and Trewavas, 2002; Toyota et al., 2008) and phototropism (Baum et al., 1999; Harada et al., 2003; Harada and Shimazaki, 2007; Zhao et al., 2013), and its requirement for the inhibitory effect of auxin on root and root hair growth via the nonselective cation channel CYCLIC NUCLEOTIDE-GATED CHANNEL 14 (CNGC14) (Shih et al., 2015; Dindas et al., 2018). Surprisingly, despite all these findings, molecular details about the role of Ca^{2+} signalling downstream of auxin and its cellular targets have remained elusive for a long time.

Previously, we identified the calmodulin-like protein CALMODULIN-LIKE 12/TOUCH 3 (CML12/TCH3) as interacting partner of the protein kinase PINOID (PID) (Benjamins et al., 2003). As PID is known to regulate polar auxin transport (PAT) by phosphorylating PIN proteins (Friml et al., 2004; Michniewicz et al., 2007; Huang et al., 2010), our findings provided one of the first molecular links between auxin and Ca^{2+} signalling. Calmodulins (CaMs) and calmodulin-like proteins (CMLs) are well-defined calcium sensors and central to the activation of calcium signalling pathways (Yang and Tsai, 2022). The crystal structure of CaM has revealed two globular domains, each containing two EF-hand Ca^{2+} -binding sites, connected by a linker (Babu et al., 1985; Chattopadhyaya et al., 1992; Kretsinger et al., 1986; Babu et al., 1988; Tidow and Nissen, 2013). CMLs have a similar structure and only vary in the number of EF hands (McCormack and Braam, 2003). CaM/CMLs respond rapidly to oscillations in the cytosolic Ca^{2+} levels ($[\text{Ca}^{2+}]_{\text{cyt}}$). Binding of Ca^{2+} to the EF-hands triggers a more open conformation, exposing the methionine-rich hydrophobic pockets in each globular

domain (Crivici and Ikura, 1995; Zhang et al., 1995). These stretches of methionines have high polarizability and flexibility, and their increased accessibility allows CaM/CMLs to undergo extensive protein-protein interactions (Gellman, 1991; Zhang et al., 1994; Zhang and Vogel, 1994; Yamniuk and Vogel, 2004).

PID belongs to the AGC3 subclade of plant-specific AGCVIII protein serine-threonine kinase family (Galvan-Ampudia and Offringa, 2007). AGCVIII kinases distinguish themselves from other (non-plant) AGC kinases by an insertion domain (ID) between catalytic subdomain VII and VIII, ranging in size from 36 to 90 amino acid residues (Bögre et al., 2003; Galván-Ampudia and Offringa, 2007; Rademacher and Offringa, 2012). Previous data already indicated that the insertion domain (ID) is responsible for PID plasma membrane (PM) association (Zegzouti et al., 2006). The results in Chapter 2 showed that PID not only interacts with CML12/TCH3 but also with all seven CaMs and three other CMLs (CML8, CML10, CML11), all belonging to a confined clade of closely related CaM/CMLs in *Arabidopsis*. Through this interaction PID is sequestered from the PM to the cytosol, suggesting that these CaM/CMLs bind to the insertion domain and thereby disrupt its PM association. In addition, we have shown that these PID interacting CaM/CMLs are co-expressed with PID in many tissues, such as the shoot apical meristem, vascular tissues, young developing leaves and flowers, enabling a functional interaction between PID and these CaM/CMLs in these tissues. Unfortunately, the single loss-of-function mutants for *CML12/TCH3* or for the other genes encoding PID interacting CaM/CMLs did not show a clear phenotype, and together with their overlapping expression pattern this suggests that they act redundantly (Chapter 2). With the current CRISPR-Cas tool-box, it would be easy to generate multiple CaM/CML mutants to investigate the role of the CaM/CML-PID interaction in plant growth and development. However, CaM/CMLs generally interact with and regulate multiple proteins and are thus involved in many calcium-dependent signalling pathways (Perochon et al., 2011).

Therefore, a knock-out of all the genes encoding PID-interacting CaM/CMLs is very likely to lead to severe defects. In fact, knocking out the single *CaM* gene in *Saccharomyces cerevisiae* (Davis et al., 1986), *Schizosaccharomyces pombe* (Takeda and Yamamoto, 1987), *Aspergillus nidulans* (Lu et al., 1992) and *Drosophila melanogaster* (Heiman et al., 1996) appeared to be lethal. Therefore, we decided to map the CaM/CMLs-binding domain in PID in order to identify the key amino acids responsible for CaM/CMLs-binding, with the final aim to generate an ‘untouchable’ but still fully functional version of PID. Complementation of the *pid* loss-of-function mutant should then reveal the role of the calcium-dependent CaM/CML binding to PID.

In this Chapter, we fine mapped the CaM/CML binding domain in PID through amino acid deletions and substitutions. Subsequent protein domain modelling identified an amphipathic alpha helix in the ID of PID that mediates both PM association and the interaction with the CaM/CMLs. Substitution of the positively charged arginines in this alpha helix resulted in the desired ‘untouchable’ PID, which will enable us to finally unravel the role of the calcium-dependent PID-CaM/CML interaction in plant development (see Chapter 4).

Results

PID PM association and CML12/TCH3 interaction are both mediated by the ID in the catalytic kinase core

To confirm the initial observations that PM association of PID is mediated by the ID (Zegzouti et al., 2006), we fused the ID (AA 227 to 280) to YFP. Expression of this fusion under the 35S promotor in Arabidopsis protoplasts showed similar PM association as the PID-YFP fusion (Figure 1A, B), thereby confirming that the ID is responsible for PM association. Moreover, expression of a PID-YFP fusion lacking the ID (PID(-ID)-YFP) resulted in cytosolic localisation, whereas a fusion with the ID reintroduced (PID(+ID)-YFP) showed again the same PM association

as the PID-YFP and ID-YFP fusions (Figure 1A, B). To verify our hypothesis that CaM/CMLs bind to the ID of PID, *in vitro* pull-down assays were performed with GST-tagged PID, PID(-ID), PID(+ID) and ID alone bound to glutathione beads as bait and His-tagged CML12/TCH3 as prey. These experiments showed that CML12/TCH3 can be pulled down by GST-PID when the ID is present and even more efficient by the GST-ID fusion, but not by the GST-PID version lacking the ID. (Figure 1C). These results indicated that both the PM association and the CaM/CML binding domains are located in the ID of PID.

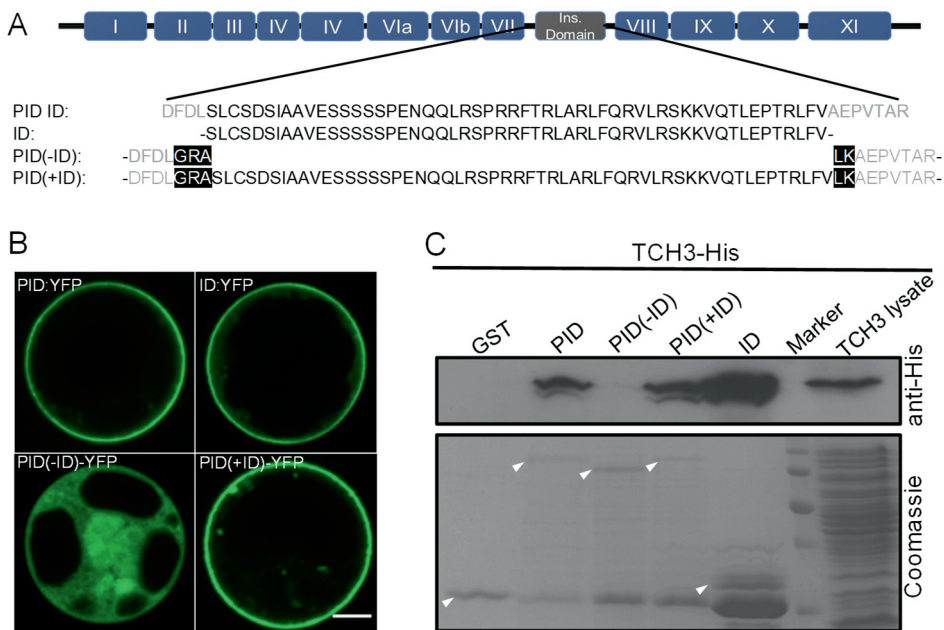


Figure 1. The ID in the catalytic core of the PID kinase mediates both PM association and CaM/CML binding. (A) Schematic structure of the PID kinase with the 12 conserved domains of the catalytic core and the ID indicated (above) and amino acid sequence of the PID ID and PID mutant versions. (B). Arabidopsis protoplasts transfected with *p35S::PID-YFP*, *p35S::ID-YFP*, *p35S::PID(-ID)-YFP*, *p35S::PID(+ID)-YFP*. The scale bar indicates 10 μ m. (C) *In vitro* pull-down using GST, GST-PID (PID), GST-PID(-ID) (PID(-ID)), GST-PID with the ID placed back (PID(+ID)) or GST-ID (ID) bound to glutathione beads as bait and His-tagged TCH3 as prey. Upper image: pulled down TCH3-His detected by hybridizing the Western blot with anti-His antibodies. Lower image: Coomassie stained gel showing the loading of glutathione beads with GST-tagged proteins. White arrowheads indicate the positions of the respective GST-tagged proteins.

Central segment in the PID ID is sufficient for PM association and CML12/TCH3 binding

Previous studies on CaM/CML binding domains have indicated that CaM/CMLs interact with two types of motifs: the amphipathic alpha helix and the IQ or IQ-like motif (O'Neil and DeGrado, 1990; Clore et al., 1993; Rhoads and Friedberg, 1997; Bähler and Rhoads, 2002; Yamniuk and Vogel, 2004; Ranty et al., 2006; Andrews et al., 2020). To our surprise, analysis of the PID ID detected an alpha helix (amino acid residues 249 to 266) that partially overlapped with an IQ-like motif (amino acid residues 261 to 273) (Figure 2A). Visualization of the predicted alpha helix in the central segment using helical wheel projection software indicated the presence of a perfect amphipathic alpha helix comprising amino acid residues 249 to 266 (RSPRRFTRLARLFQRVLR), with the key features of seven positively charged amino acids on one side, and six hydrophobic amino acids on the other side (Figure 2B, C).

A segment containing this amphipathic alpha helix and IQ-like motif (amino acid residues 244 to 275) was fused to GST (ID₂₄₄₋₂₇₅) for *in vitro* pull-down and to YFP (ID₂₄₄₋₂₇₅-YFP) for expression in protoplasts under the 35S promoter. The pull-down result indicated that the short segment is sufficient for interacting with CML12/TCH3 (Figure 2D), and expression of the ID₂₄₄₋₂₇₅-YFP fusion in Arabidopsis protoplasts showed that it was sufficient for PM association (Figure 2E). In Chapter 2 we showed that PID was sequestered from the PM to the cytosol when co-expressed in Arabidopsis protoplasts with CML12/TCH3 in an auxin-dependent manner. Co-expression of either the full length ID-YFP or the shorter ID₂₄₄₋₂₇₅-YFP fusion with CML12/TCH3 in Arabidopsis protoplast showed that, like the full-length ID, also the shorter ID₂₄₄₋₂₇₅ fragment could be sequestered from the PM to the cytosol when auxin was added to the protoplasts (Figure 2F). Together these data suggest that the ID₂₄₄₋₂₇₅ segment comprising the amphipathic alpha helix and IQ-like motif mediates both PM association and CaM/CML binding.

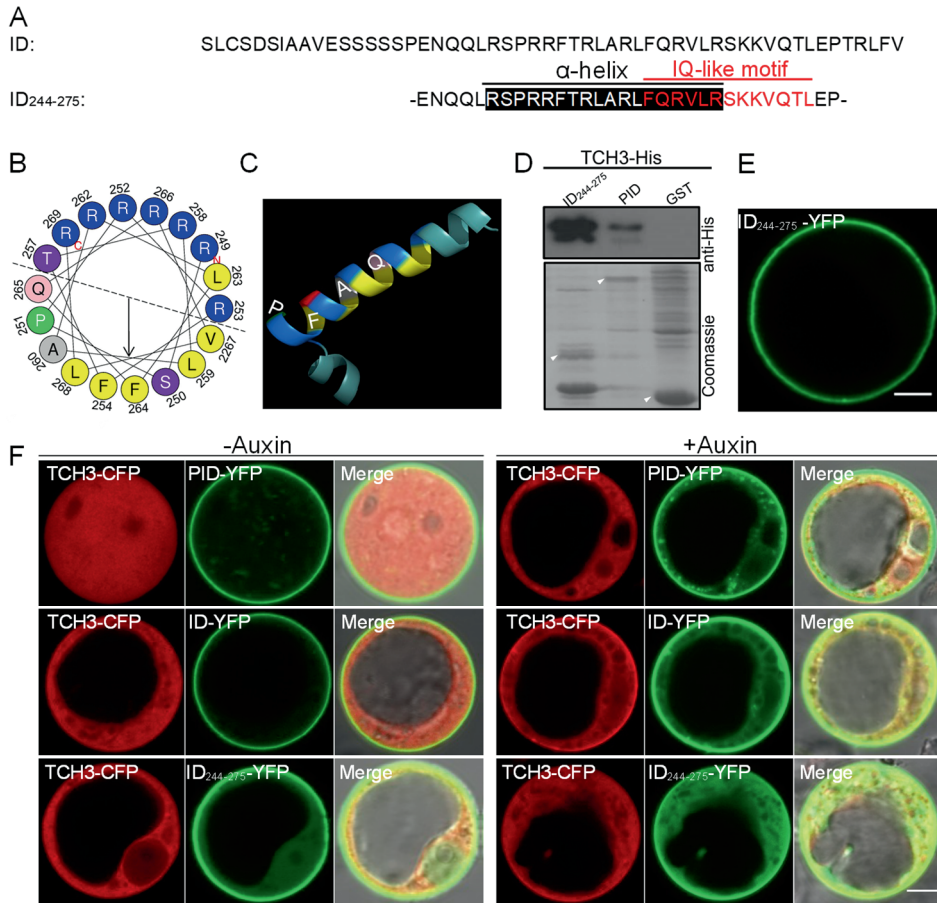


Figure 2. Central segment in the PID ID containing an alpha-helix and an IQ-like domain is sufficient for PM association and CaM/CML binding. (A) Amino acid sequence of the PID ID and the central segment (AA 244-275) containing the alpha-helix (white letters on a black background) and IQ-like motif (red letters). (B, C) Alpha helix projection (B) and protein structure prediction (C) indicate that amino acid residues 249 to 266 in the PID ID contain a perfect amphipathic alpha helix. Positively charged residues are in blue, hydrophobic residues are in yellow or grey, serine (S) and threonine (T) are in purple, green for proline (P) and pink for glutamic acid (Q). The numbers in (B) indicate the order of the amino acids in the sequence. Color coding in (C): blue indicates basic/hydrophilic residues, yellow indicates hydrophobic residues, red indicates the threonine residue. (D). *In vitro* pull-down using GST, GST-PID (PID), or GST-ID (ID) bound to glutathione beads as bait and His-tagged TCH3 as prey. Pulled down TCH3-His was detected by Western blot hybridized with anti-His antibodies. White arrowheads indicate the positions of the respective GST-tagged proteins. (E) Arabidopsis protoplast expressing ID₂₄₄₋₂₇₅-YFP. (F) Auxin-starved (left panel) and auxin-supplemented (right panel) Arabidopsis protoplasts co-transfected with *p35S::PID-YFP*, *p35S::ID-YFP*, *p35S::ID₂₄₄₋₂₇₅-YFP* and *p35S::TCH3-CFP*. The scale bar in (E) and (F) indicates 10 μm.

PINOID plasma membrane association and CALMODULIN-LIKE 12/TOUCH 3 binding converge on an amphipathic alpha-helix in the kinase insertion domain

Apart from binding CaM/CMLs, amphipathic alpha helices are also known for mediating PM association of proteins (Zhukovsky et al., 2019), whereas IQ-like motifs are specific for CaM/CML binding. The presence of an overlapping amphipathic alpha helix and an IQ-like motif in the PID ID suggested that the first might be involved in PM association, whereas the latter mediated the CaM/CML binding. To test this, we generated PID mutant versions with amino acid substitutions at the C-terminus of the IQ-like motif that did not disrupt the amphipathic alpha helix (Figure S1A). The substitutions were selected based on previous findings that CaM/CMLs bind their target proteins either through hydrophobic interactions (e.g. V, L) or through electrostatic interactions (e.g. K) (O'Neil and DeGrado, 1990; Crivici and Ikura, 1995; Bähler and Rhoads, 2002; Rhoads and Friedberg, 1997; Poovaiah et al., 2013; Andrews et al., 2020). In the mutant PID versions PID K268A, PID K269A and PID K268269A the positively charged lysines (K) were therefore substituted with neutral alanines (A), and in mutant PID versions PID V270D, PID V270D/L273E, the hydrophobic amino acids valine (V) and leucine (L) were substituted with the hydrophilic/negatively charged amino acids aspartic acid (D) or glutamic acid (E), respectively.

In vitro pull-downs showed that all these mutants (PID(K268A), PID(K269A), PID (K268,269A), PID(V270D), PID(V270D/L273E) could still interact with CML12/TCH3 (Figure S1C). Expression of the YFP fusions of these mutant PID versions in Arabidopsis protoplasts showed mainly PM localization (Figure S1B). These results suggest that the IQ-like motif may not be involved in CML12/TCH3 binding nor in PM association.

To confirm these results and further map the CaM/CML binding domain, we replaced the PID ID with three smaller segments: PID(+ID₂₂₇₋₂₅₃), PID(+ID₂₄₀₋₂₆₆) or PID(+ID₂₅₄₋₂₈₀) (Figure 3A). *In vitro* pull-downs and Arabidopsis protoplast transfection assays showed that only the PID(+ID₂₄₀₋₂₆₆) version (including amphipathic alpha helix, but excluding the C-terminal half of the IQ-like motif) was able to interact with CML12/TCH3 and show PM association (Figure 3B, C).

Taken together, these results indicate that the central segment of the PID ID harbouring an amphipathic alpha helix is sufficient and necessary for both PM association and CML12/TCH3 binding.

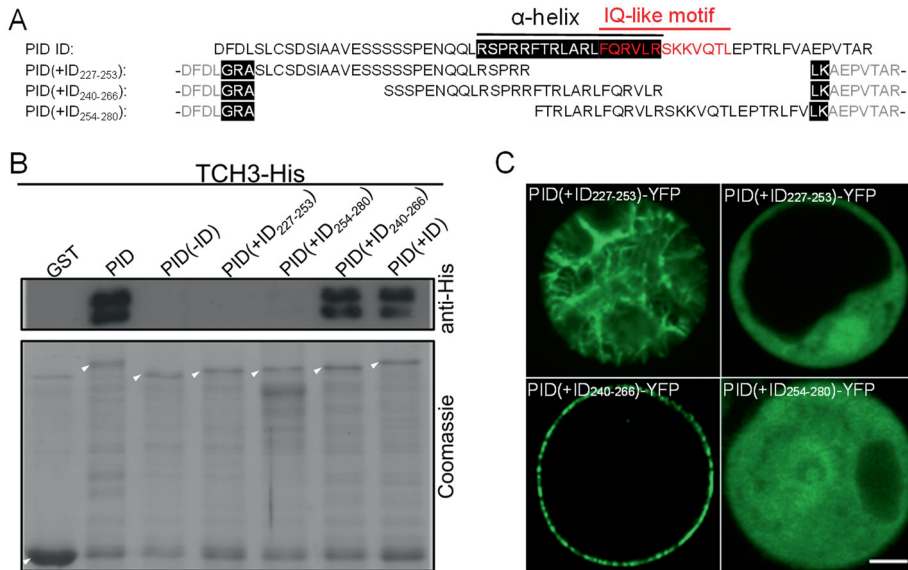


Figure 3. Central segment of the PID ID containing the amphipathic alpha-helix is sufficient and necessary for both PM association and CaM/CML binding. (A) Amino acid sequence of PID ID and different PID mutant versions. (B) *In vitro* pull-down using GST, GST-PID (PID), GST-PID without ID (PID-ID), GST-PID minus ID with three smaller segments replaced back (PID(+ID₂₂₇₋₂₅₃), PID(+ID₂₄₀₋₂₆₆), and PID(+ID₂₅₄₋₂₈₀)) bound to glutathione beads as bait and His-tagged TCH3 as prey. Pulled down TCH3-His was detected by Western blot hybridized with anti-His antibodies. White arrowheads indicate the positions of the respective GST-tagged proteins. (C) Arabidopsis protoplasts transfected with *p35S: PID(+ID₂₂₇₋₂₅₃)-YFP*, *p35S: PID(+ID₂₄₀₋₂₆₆)-YFP*, *p35S: PID(+ID₂₅₄₋₂₈₀)-YFP*. The scale bar indicates 10 μm.

PM association and CML12/TCH3 binding converge at the amphipathic alpha helix in the PID ID

Alanine scanning has been widely employed as a method of exploration of protein-protein binding interfaces (Lefèvre et al., 1997). To further analyse the central segment in the PID ID and validate the importance of the predicted amphipathic alpha helix in CaM/CMLs binding and PM association, three successive stretches of seven amino acids in the central segment were substituted with alanines, resulting in respectively PID Ala1 (QLRSPRR), PID Ala2 (FTRLARL) and PID 108

PINOID plasma membrane association and CALMODULIN-LIKE 12/TOUCH 3 binding converge on an amphipathic alpha-helix in the kinase insertion domain

Ala3 (FQRVLRS) (Figure 4A). The N-terminal part of the central fragment (SSSPENQ) was ignored, as it did not contain amino acids typical for CaM/CML binding or PM association. Interestingly, none of the three PID alanine mutant versions showed *in vitro* interaction with CML12/TCH3 (Figure 4C), nor did they associate with the PM (Figure 4B). These data confirmed that the complete predicted amphipathic alpha helix is crucial for CaM/CMLs binding and PM association.

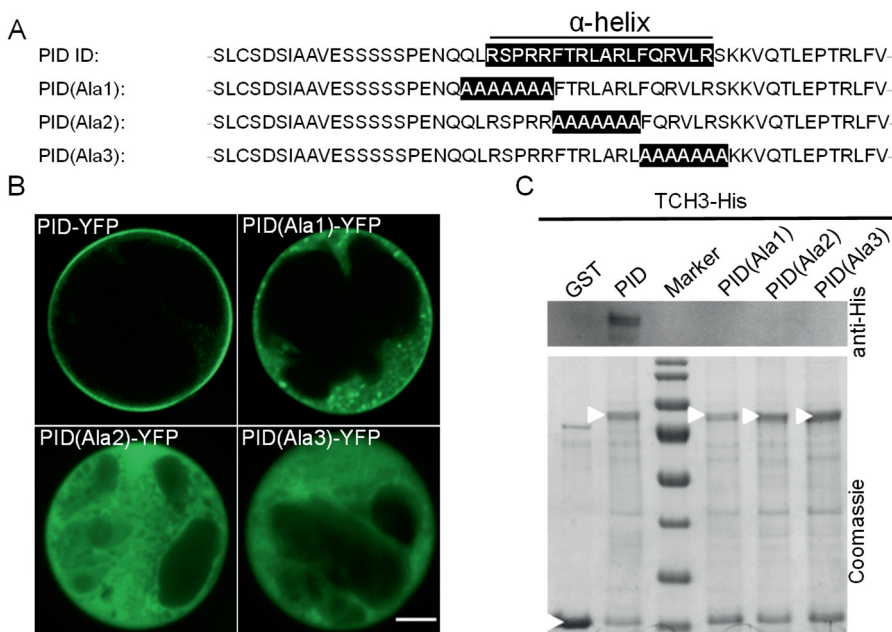


Figure 4. The complete amphipathic alpha-helix in the PID ID is required for PM association and CML12/TCH3 binding. (A). Amino acid sequence of the PID ID and the three PID Ala mutant versions. The amphipathic alpha helix and the alanine substitutions are indicated with white letters on a black background. (B) Arabidopsis protoplasts transfected with *p35S::PID Ala1-YFP*, *p35S::PID Ala2-YFP* and *p35S::PID Ala3-YFP*. The scale bar indicates 10 μm. (C) *In vitro* pull-down using GST, GST-PID (PID), GST-PID with alanine scanned ID (PID(Ala1), PID(Ala2), PID(Ala3)) bound to glutathione beads as bait and His-tagged TCH3 as prey. Pulled down TCH3-His was detected by Western blot hybridized with anti-His antibodies. White arrowheads indicate the positions of the respective GST-tagged proteins.

Positively charged arginines in the amphipathic alpha helix mediate PM association and CML12/TCH3 binding

It has been reported that positively charged amino acids in the binding domains are crucial for interaction with CaM/CMLs (O'Neil and DeGrado., 1990; Clore et al., 1993; Arazi et al., 1995; Xu et al., 2012). To identify the key amino acids that are responsible for CaM/CML binding, we generated PID mutant versions in which some of the arginines that make up the amphipathic alpha helix in the PID ID were substituted with alanines (i.e. PID(R3)A, PID(R2A) and PID (R5A), see Figure 5A). *In vitro* pull-downs and BiFC assays showed that all three PID mutant versions cannot interact with CML12/TCH3 anymore (Figure 5B, C). Expression of these mutant versions in Arabidopsis protoplasts showed that their PM association was disrupted as they showed predominant cytosolic localization (Figure 5D).

These results indicated that the positively charged arginines in the predicted amphipathic alpha helix are vital for both PM association and CML12/TCH3 binding.

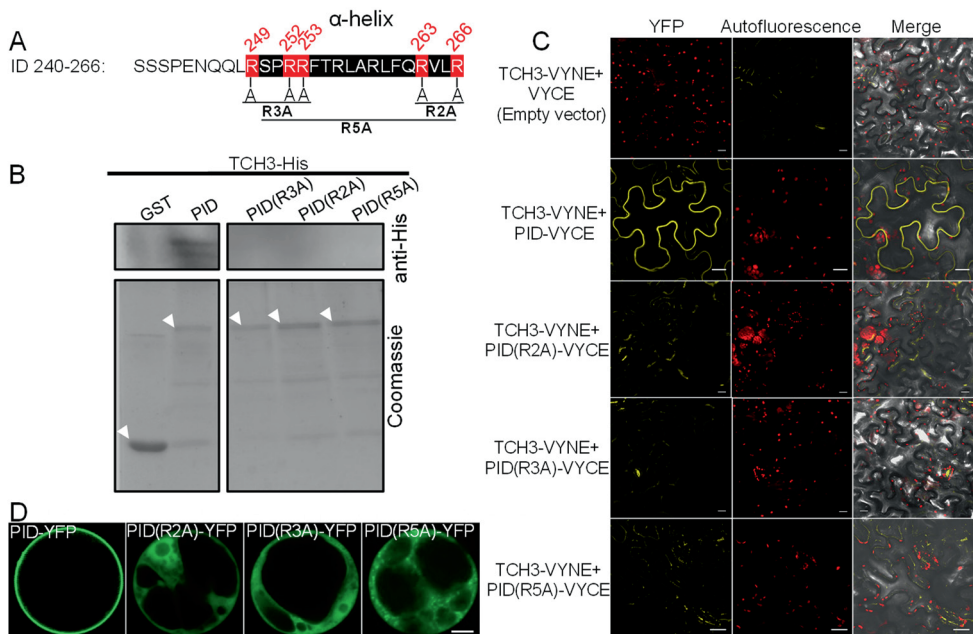


Figure 5. Positively charged arginines in the amphipathic alpha helix in the PID ID are essential for PM association and CaM/CML binding. (A). The amino acid sequence of the central part of the

PINOID plasma membrane association and CALMODULIN-LIKE 12/TOUCH 3 binding converge on an amphipathic alpha-helix in the kinase insertion domain

PID ID, with the predicted amphipathic alpha helix indicated with white letters on a black background. The alanine substituted arginines are indicated in red, and the three PID mutant versions PID(R3A), PID(R2A) and PID(R5A) are indicated below the sequence. **(B)** *In vitro* pull-down using GST, GST-PID (PID), GST-PID(R2A), GST-PID(R3A) or GST-PID(R5A) (respectively PID(R2A), PID(R3A) or PID(R5A)) bound to glutathione beads as bait and His-tagged TCH3 as prey. Pulled down TCH3-His was detected by hybridizing the Western blot with anti-His antibodies (upper panel). White arrowheads indicate the positions of the respective GST-tagged proteins in a Coomassie stained gel (lower panel). **(C)** Bimolecular Fluorescence Complementation (BiFC) assay performed by transient *Agrobacterium*-mediated expression of the C-terminal half of YFP C-terminally fused to PID (PID - VYCE) or to the PID(R to A) mutants and the N-terminal half of YFP C-terminally fused to TCH3 (TCH3-VYNE) in leaf epidermis cells of three weeks old *Nicotiana benthamiana* plants. An empty vector expressing the N-terminal half of YFP (VYCE) was used as negative control. **(D)** Arabidopsis protoplasts transfected with *p35S::PID-YFP*, *p35S::PID(R2A)-YFP*, *p35S::PID(R3A)-YFP* or *p35S::PID(R5A)-YFP*. The scale bar in (C) and (D) indicates 10 μ m.

Overexpression of arginine to alanine PID mutants show strong phenotypes resembling overexpression of wild type PID

By mapping the PM association and CaM/CML binding domains we aimed to separate these two activities in order to be able to generate an ‘untouchable’ PID version, which would overcome the anticipated functional redundancy among the 11 genes encoding PID interacting CaM/CMLs (see Chapter 2) and allow to study the role of the calcium-dependent regulation of PID activity. The above data suggests, however, that PM association and CaM/CML binding are tightly linked, as they converge at an amphipathic alpha helix in the PID ID. As PM association of PID was considered important for its role in phosphorylating PIN proteins (Dhonukshe et al., 2010), we set out to test the activity of the PID(R3A), PID(R2A) and PID(R5A) mutant versions by overexpressing them as YFP fusions in Arabidopsis.

Previously, we have shown that overexpression of wild-type *PID* causes strong seedling phenotypes, such as agravitropic root and shoot growth and collapse of the main root meristem. Moreover, flowering *PID* overexpression plants frequently develop pin-like inflorescences (Benjamins et al., 2001; Friml et al., 2004). Similar phenotypes were observed when we overexpressed a PID-YFP fusion in Arabidopsis (*p35S::PID-YFP*). Around 82% of the flowering T1 plants developed pin-like inflorescences (Figure 6A) and T3 seedlings of selected homozygous

single locus lines showed agravitropic growth and root meristem collapse (Figure 6B, D). Analysis of the root tips before meristem collapse by confocal microscopy showed clear PM association of the PID-YFP fusion protein (Figure 6D). Similar results were obtained for YFP fusions of PID versions in which part of the IQ-like motif was disrupted ((PID(K268A), PID(K269A), PID(K268,269A), PID(V270D) and PID(V270D/L273E)), which did not affect PM association or CML12/TCH3 binding (Figure S2A, B). Unexpectedly, overexpression of the three PID(R→A)-YFP fusions still resulted in a high percentage of T1 plants (between 72% and 86%) showing pin-like inflorescence (Figure 6A; Figure S2B). Moreover, T3 seedlings of selected homozygous single locus lines showed agravitropic growth and root meristem collapse (Figure 6B; Figure S2A). The severity of agravitropic growth and the occurrence of root meristem collapse corresponded to the level of overexpression in each line (Figure 6I). As observed in *Arabidopsis* protoplasts (Figure 5D), the PID(R3A), PID(R2A) and PID(R5A) versions showed predominant cytosolic localization in root tip cells (Figure 6F, H). Taken together, these results suggest that the three PID(R→A) versions are still functional kinases despite their predominant cytosolic localisation.

PINOID plasma membrane association and CALMODULIN-LIKE 12/TOUCH 3 binding converge on an amphipathic alpha-helix in the kinase insertion domain

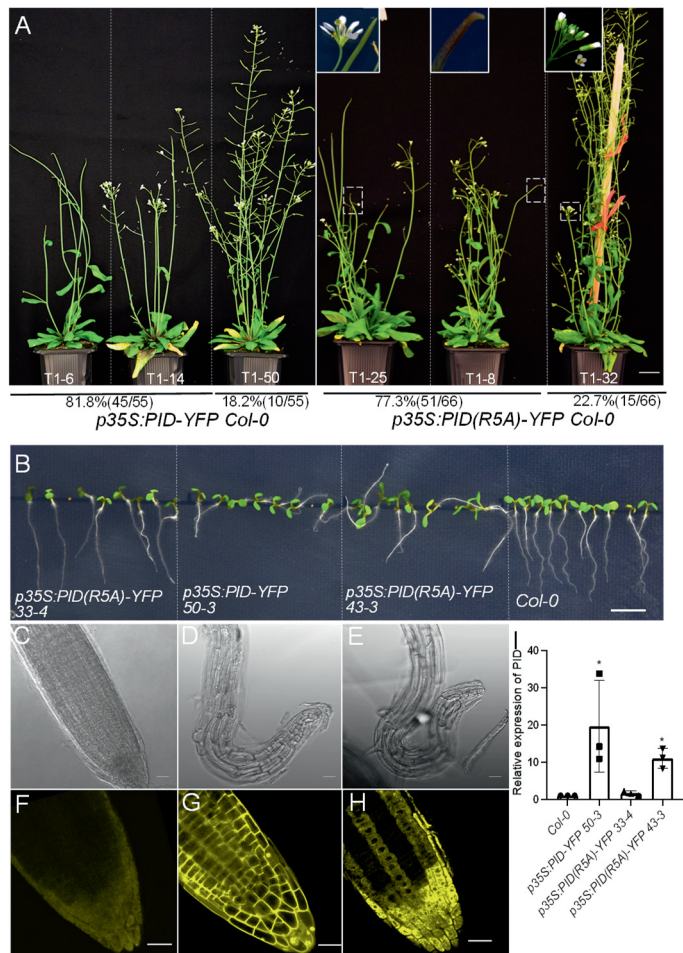
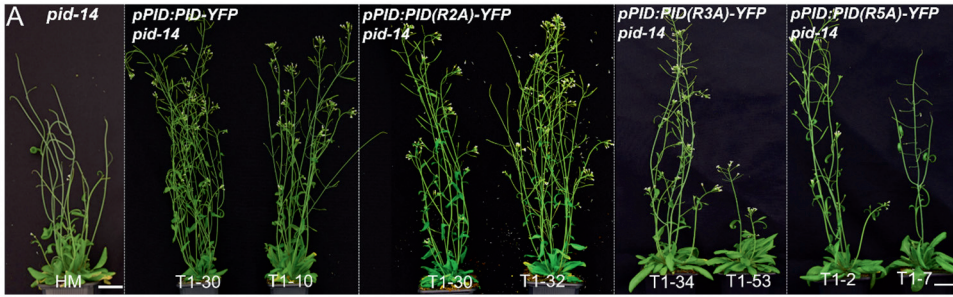


Figure 6. Overexpression studies indicate that PID(R5A) is a functional kinase. (A) Phenotypes of flowering T1 plants transgenic for *p35S::PID-YFP* or *p35S::PID(R5A)-YFP*. Below the percentage and number of T1 plants showing pin-like or wild-type inflorescences are indicated. (B) Phenotype of 5-day-old vertically grown seedlings of wild-type Arabidopsis (Col-0) or of selected *p35S::PID-YFP* and *p35S::PID(R5A)-YFP* T3 lines. (C-E). Root tip phenotype of a weak expressing *p35S::PID(R5A)-YFP* seedling (C) or of a strong expressing *p35S::PID-YFP* (D) or *p35S::PID(R5A)-YFP* (E) seedling in (B). (F-H). Representative confocal images showing YFP signal in the root tips of *35S::PID-YFP* and *35S::PID(R5A)-YFP* seedlings in (B). (I) Relative expression levels of PID, as determined by qRT-PCR analysis on RNA isolated from the seedlings of the indicated lines presented in (B). Different dots indicate the values of three biological replicates per plant line, bar indicates the mean, and error bars indicate the SEM. The asterisk indicates a significant difference from wild type ($P < 0.05$), as determined by Student's *t*-test. Size bars indicate 2 cm in (A), 1 cm in (B), 20 μ m in (C-H).

Complementation of *pid* loss-of-function mutant defects by PID(R→A) versions confirms their functionality.

To further validate the kinase activity of the PID(R→A) versions, we generated *pPID:PID-YFP* and *pPID:PID(R→A)-YFP* fusion constructs and transformed those to plants heterozygous for the strong *pid-14* loss-of-function mutant allele. T1 plants homozygous for the *pid-14* allele were selected for phenotyping (Figure 7A). The wild-type *pPID:PID-YFP* construct fully restored the severe shoot defects of *pid-14* in 12 of the 14 (85,7%) selected T1 plants, whereas two T1 plants showed incomplete rescue as they still developed pin-like inflorescences (Figure 7A, B). For the *pPID:PID(RtoA)-YFP* constructs a similar percentage of T1 plants (75, 88 or 80%, respectively) showed full rescue of the mutant phenotype (Figure 7A, B). These results confirm the conclusions from the overexpression experiments that the PID(R→A) mutant versions are still functional despite their loss of PM association. On the one hand, this implies that the PM association of PID, unlike what was previously assumed (Dhonukshe et al., 2010), is not essential for its function. This suggests that the key effect of the calcium-dependent binding of CaM/CMLs to PID is the reduced kinase activity rather than the sequestration from the PM. On the other hand, we can conclude that with the PID(R→A) versions we have generated the desired ‘untouchable’ PID mutants and that the *pPID:PID(RtoA)-YFP pid-14* lines now should give us the possibility to identify the role of the PID-CaM/CMLs complex in plants growth and development.

PINOID plasma membrane association and CALMODULIN-LIKE 12/TOUCH 3 binding converge on an amphipathic alpha-helix in the kinase insertion domain



B

Constructs	T1 plants (<i>pid-14</i> HM)	Inflorescence	
		WT-like	pin-like
<i>pPID::PID-YFP pid-14</i>	14	85.7%(12/14)	14.3%(2/14)
<i>pPID::PID(R3A)-YFP pid-14</i>	16	75.0%(12/16)	25.0%(4/16)
<i>pPID::PID(R2A)-YFP pid-14</i>	25	88.0%(22/25)	12.0%(3/25)
<i>pPID::PID(R5A)-YFP pid-14</i>	15	80.0%(12/15)	20.0%(3/15)

Figure 7. PID(R→A) variants complement the *pid-14* mutant inflorescence defects. (A) Flowering plants phenotypes of the *pid-14* mutant and of selected *pPID::PID-YFP pid-14*, *pPID::PID(R2A)-YFP pid-14*, *pPID::PID(R3A)-YFP pid-14*, *pPID::PID(R5A)-YFP pid-14* T1 plants. Size bar indicates 2 cm in (A). (B). Table depicting the total number of T1 plants homozygous for the *pid-14* allele (*pid-14* HM) that were used for phenotyping, and the number and percentage of T1 plants showing either a wild-type-like (WT-like) or a pin-like inflorescence phenotype.

Discussion

Ca²⁺ signalling has for a long time been reported to play a role in the action of the plant hormone auxin, in part by regulating its polar cell-to-cell transport (Dela Fuente and Leopold, 1973; Dela Fuente, 1984). The serine/threonine kinase PID also regulates PAT by phosphorylating the PIN auxin efflux carriers and thereby directing their polarity and enhancing their activity (Friml et al., 2004, Huang et al., 2010; Dhonukshe et al., 2010; Zourelidou et al., 2014). The finding that the calcium binding proteins CML12/TCH3 and PBP1 interact with PID and regulate its kinase activity *in vitro* provided the first molecular link between Ca²⁺ signalling and PAT (Benjamins et al., 2003). Auxin-induced and calcium-dependent binding of CML12/TCH3 reduced the kinase activity of PID *in vitro* and sequestered PID from the PM to the cytosol in Arabidopsis protoplasts and root and shoot epidermal

cells (Galvan-Ampudia, 2009; Fan, 2014; Chapter 2). Our study in Chapter 2 of this thesis showed that, besides CML12/TCH3, the closely related three CMLs (CML8, CML10, CML11) and all seven Arabidopsis CaMs act redundantly in binding PID. The genes encoding these PID interacting CaM/CMLs share a largely overlapping expression pattern, and single *cam/cml* T-DNA insertion mutants we did not see a phenotype distinguishable from wild-type Arabidopsis. Therefore, to overcome the likely functional redundancy of these PID interacting CaM/CML genes in our attempt to reveal the role of the PID-CaM/CML interaction in plant development, we mapped the CaM/CMLs binding domain in PID. This resulted in the identification of an amphipathic alpha helix in the PID insertion domain that mediates both PM association and CaM/CML binding. Disruption of this amphipathic alpha helix by substituting some of the positively charged arginines to alanins resulted in PID(R→A) mutant versions that were no longer PM associated and did not interact with CaM/CMLs anymore, but were still functional based on overexpression phenotypes and complementation of the *pid* loss-of-function mutant. In Chapter 4 of this thesis, these ‘untouchable’ PID mutant versions are used to investigate the role of the PID-CaM/CML interaction in plant growth and development.

CaM/CML binding and PM association domain converge on an amphipathic alpha helix in the PID ID

Our results show that both PM association and CaM/CML binding converge at an amphipathic alpha helix in the ID located in the middle of the catalytic core of the PID kinase. Previous research has already shown that CaM/CMLs do bind to amphipathic alpha helices with high affinity and broad specificity (O'Neil and DeGrado, 1990), and that this structural feature is frequently found in CaM/CML binding proteins (Persechini and Kretsinger, 1988; O'Neil and DeGrado, 1990; Crivici and Ikura, 1995; Komolov et al., 2021). In our case, the identified amphipathic alpha helix has seven positively charged amino acids on one side, and

six hydrophobic amino acids on the other side, which is perfectly in accordance with the features previously described for such an alpha helix (O'Neil and DeGrado, 1990).

Interestingly, we also identified an IQ-like motif in the PID ID that partially overlaps with the amphipathic alpha helix. The IQ/IQ-like motif was identified using the consensus sequences that were based on a large group of calmodulin binding proteins, including unconventional myosins (Bähler and Rhoads, 2002), ion channels (sodium, potassium, calcium channels and etc.) (Schumacher et al., 2004; Fallon et al., 2005; Mori et al., 2008; Fallon et al., 2009; Reddy Sarhan et al., 2012; Wang et al., 2012; Chichili et al., 2013) and PM Ca^{2+} -ATPases (Tidow et al., 2012). It has been reported for several animal proteins, including utrophin, Ras guanine nucleotide-releasing factor, Nina C myosins and calcium vector target protein, that CaM/CMLs can bind to IQ-motifs in a calcium-dependent manner (Bähler and Rhoads, 2002). But exceptions were also found, for example, some CaMs or CaM-related proteins serve as myosin light chains to interact with the IQ domains of myosin independently of Ca^{2+} (Cheney and Mooseker, 1992; Atcheson et al., 2011; Heissler and Sellers, 2014). The IQ-like motif is similar to the IQ-motif, but can bind to a broader range of proteins in a calcium-dependent manner (Houdusse and Cohen, 1995). The IQ-like motif we identified in the PID ID lacks the conserved central G residue and the second basic residues. Substitution of some positively charged or hydrophobic amino acids in this IQ-like motif did not affect CML12/TCH3 binding or the function of PID based on overexpression phenotypes and complementation of the *pid* loss-of-function mutant. In addition, the central segment PID ID₂₄₀₋₂₆₆, in which the C-terminal part of the IQ-like motif was lacking, could still interact with CML12/TCH3. These data suggest that this putative IQ-like motif is not involved in binding with CaM/CMLs.

Results by Zegzouti and co-authors (2006) already indicated that the PID ID is involved in PM association of the kinase. Our results confirmed this and are in line with a more recent report on the interactions of the positive arginine residues in the

PID ID with the negative electrostatic field generated especially by the phosphatidylinositol-4-phosphate (PI4P)-enriched PM (Simon et al., 2016). These negative charges in the PM contribute to the localization of many proteins containing polybasic clusters or cationic domains through electrostatic interactions (Heo et al., 2006; McLaughlin and Murray, 2005). This supports our findings that the amphipathic alpha helix in the PID ID has a positively charged face and that the arginine residues responsible for this positive charge are crucial for the electrostatic association of PID with the PM. These findings are also in line with the observation that the mutant version PID(R/K9Q), in which all nine positively charged amino acids (arginines and lysines) in the PID ID₂₄₈₋₂₇₀ are substituted by the uncharged glutamine (Q), does not associate anymore with the PM (Simon et al., 2016).

The dual role of the amphipathic alpha helix in the PID ID also explains why CaM/CMLs sequester PID from the PM to the cytosol. CaM/CML binding is likely to shield the positively charged arginines in the amphipathic alpha helix from the negatively charged PM and thereby prevent PM association. According to previous studies, CaM/CMLs have a much higher affinity to target proteins when the EF-hands are occupied with Ca²⁺ than the lipid bilayer, but this situation is reversed in the absence of Ca²⁺ (Gillette et al., 2015; Agamasu et al., 2019; Grant et al., 2020).

Predominant PM association is not important for PID function

PID is known as a protein kinase that localizes predominantly at the PM of epidermis cells in the embryo, root tip (including root hairs) and the shoot apical meristem (Lee and Cho, 2006; Michniewicz et al., 2007; Dhonukshe et al., 2010; Landrein et al., 2015; Simon et al., 2016) and in Arabidopsis protoplasts (Galvan-Ampudia, 2009; Chapter 2). The PM association of PID makes sense in view of its role as regulator of PIN polarity by direct phosphorylation of these auxin efflux carriers (Friml et al., 2004; Huang et al., 2010; Dhonukshe et al., 2010; Zourelidou

et al., 2014). However, PID localization is dynamic, as it has also been observed localized to the cytoplasm and some subcellular compartments, indicating that it cycles between the PM and the cytoplasm or intracellular compartments. Treatments with brefeldin A (BFA), which targets GNOM-mediated basal PIN recycling, the kinase inhibitor staurosporine (ST), NaCl or the PI4-kinase (PI4K) inhibitor phenylarsine oxide (PAO) all cause strong PID internalization from the PM to the cytosol (Lee and Cho, 2006; Dhonukshe et al., 2010; Simon et al., 2016; Wang et al., 2019). Our data show that auxin can induce internalization of PID in a Ca^{2+} -dependent manner in epidermis cells in the root tip and shoot meristem and in Arabidopsis protoplasts (Galvan-Ampudia, 2009; Fan, 2014; Chapter 2) and that abiotic signals such as gravity and mechanical stress are also able to cause the internalization of PID (Fan, 2014). The latter makes sense in view of the PID-CaM/CML interaction, since both auxin and abiotic signals cause elevations in the $[\text{Ca}^{2+}]_{\text{cyt}}$.

However, our results on the activity of the ‘untouchable’ PID versions suggest that its PM localization is not important for its activity. This implies that recruitment of PID from the PM by the CaM/CML interaction is rather a side effect, and that reduced activity or inactivation of the kinase by CaM/CML binding is more important. This is seemingly in contrast to a previous report, showing that inhibition of PID activity by the kinase inhibitors staurosporine (ST) restores the root hair growth in *PID* overexpression lines, but that PID localization at the PM is disrupted and that the kinase is internalized to the cytosol (Lee and Cho, 2006). In the same publication also shown that overexpression of the kinase dead PID(D225G) or PID(D205N) mutant versions (Christensen et al., 2000) has no inhibitory effect on root hair growth and that the mutant proteins show largely dispersed cytoplasmic distribution (Lee and Cho, 2006). These results indicate that kinase activity and PM association of PID are tightly linked. Recently, we have provided evidence that PID is in a complex at the PM with MACCHI-BOU 4/MAB4(ENP1)-LIKE (MAB4/MEL) and PIN proteins and that this complex is

self-reinforced by PID-mediated PIN phosphorylation (Glanc et al., 2021). The formation of this complex could be important to initiate PID PM localization and require PID activity (hence the cytosolic localization of kinase dead versions), whereas the amphipathic alpha helix in the PID ID would be subsequently needed to maintain PM localization for a longer period. This model would also explain why our PID(R→A) versions, despite their cytosolic localization, are not disrupted in their activity, as their short term/transient recruitment to the PM localized PIN phospho-targets would still be promoted by the MAB4/MEL scaffold proteins. The above model explains that predominant PM association is not essential for PID function, which is corroborated by our observation that PID(R→A) versions do not need higher expression levels to induce overexpression phenotypes or complement *pid* loss-of-function defects compared to wild-type PID.

PINOID plasma membrane association and CALMODULIN-LIKE 12/TOUCH 3 binding converge on an amphipathic alpha-helix in the kinase insertion domain

Material and Methods

Molecular cloning and constructs

The constructs *pDEST-PID-VYCE*, *pDEST-TCH3-VYNE*, *pET16H-TCH3*, *pGEX-PID*, *pART7-TCH3-CFP*, *pART7-PID-YFP*, *pDONR-PID* are described in Chapter 2.

For construct *pDONR207-PID(-ID)*, the entire *pDONR-PID* plasmid excluding the ID (AA 227 to 280) segment, but including the rest of the PID cDNA and the vector backbone was amplified using primers *PID Deletion 2 S* and *PID Deletion 2 AS* (Table S1). The PCR product was digested with *Bsp*TI and self-ligated, yielding *pDONR207-PID(-ID)*.

For construct *pDONR207-PID(+ID)*, the ID was amplified using primers PID InsDom S and PID InsDom AS (Table S1), the resulting fragment was digested with *Sgs*I and *Bsp*TI and inserted by ligation into *pDONR207-PID(-ID)* digested with *Sgs*I and *Bsp*TI.

For construct *pDONR207-PID(+ID₂₂₇₋₂₅₃)*, *pDONR207-PID(+ID₂₄₀₋₂₆₆)* and *pDONR207-PID(+ID₂₅₄₋₂₈₀)*, DNA fragments coding for the ID segments 227-253, 240-266 and 254-280 with *Sgs*I and *Bsp*TI restriction sites added were generated by annealing the corresponding oligonucleotides indicated in Table S1, following the protocol from Sigma-Aldrich. The resulting fragments were digested with *Sgs*I and *Bsp*TI and inserted by ligation into *pDONR207-PID(-ID)* digested with *Sgs*I and *Bsp*TI.

The constructs *pDONR207-PID(Ala1)*, *pDONR207-PID(Ala2)*, *pDONR207-PID(Ala3)* *pDONR-PID(R2A)*, *pDONR-PID(R3A)*, *pDONR-PID(R5A)*, *pDONR-PID(K268A)*, *pDONR-PID(K269A)*, *pDONR-PID(K268,269A)*, *pDONR-PID(V270D)*, *pDONR-PID(V270D/L273E)* were obtained using the Agilent QuickChange II XL site directed mutagenesis kit and the corresponding primer sets listed in Table S1 with *pDONR-PID* or *pDONR-PID(R3A)* (for *pDONR-PID(R5A)*) as template.

The constructs *pDEST-PID(R2A)-VYCE*, *pDEST-PID(R3A)-VYCE*, *pDEST-PID(R5A)-VYCE* were obtained by recombining the coding region from the corresponding *pDONR* plasmid (see above) by LR reaction into *pDEST-GWVYCE*.

For the binary plasmids *p35S::PID-YFP*, *p35S::PID(R2A)-YFP*, *p35S::PID(R3A)-YFP*, *p35S::PID(R5A)-YFP*, *p35S::PID(K268A)-YFP*, *p35S::PID(K269A)-YFP*, *p35S::PID(K268,269A)-YFP*, *p35S::PID(V270D)-YFP* and *p35S::PID(V270D/L273E)-YFP*, the corresponding coding region was first recombined by LR reaction from the *pDONR* plasmid (see above) into the *pART7-p35S-Gateway-YFP* Entry plasmid (Galvan-Ampudia, 2009). Subsequently, the *p35S::PID-YFP* expression cassette was ligated as *NotI* fragment in the T-region of the *NotI* digested binary vector *pART27* (Gleave, 1992).

The constructs *pPID::PID-YFP*, *pPID::PID(R2A)-YFP*, *pPID::PID(R3A)-YFP*, *pPID::PID(R5A)-YFP*, *pPID::PID(K268A)-YFP*, *pPID::PID(K269A)-YFP*, *pPID::PID(K268,269A)-YFP*, *pPID::PID(V270D)-YFP* and *pPID::PID(V270D/L273E)-YFP* were obtained by recombining the coding region by LR reaction from the corresponding *pDONR207* vector (see above) to *pGreenII0179 PID3.2kb::Gateway-YFP-HA* (Galvan-Ampudia, 2009).

Primers used were designed with CLC Main Workbench (CLC bio) software and listed in the Table S1.

Plant material, growth conditions and phenotype analysis

All *Arabidopsis thaliana* transgenic lines and mutants used in this study are in the Columbia (Col-0) background.

For *Arabidopsis* transgenic lines the binary plasmids *p35S::PID-YFP*, *p35S::PID(R2A)-YFP*, *p35S::PID(R3A)-YFP*, *p35S::PID(R5A)-YFP*, *p35S::PID(K268A)-YFP*, *p35S::PID(K269A)-YFP*, *p35S::PID(K268,269A)-YFP*, *p35S::PID(V270D)-YFP* and *p35S::PID(V270D/L273E)-YFP* were electroporated into *Agrobacterium* strain AGL1 (Lazo et al., 1991; Chassy et al., 1988) and T-DNA constructs were transformed to Col-0 using the floral dip method (Clough

and Bent., 1998). Primary transformants (T1) were selected on 0.5× Murashige and Skoog (1/2 MS) medium (Duchefa) containing 0.05% MES, 0.8% Daishin agar (Duchefa) and 1% sucrose, supplemented with 50 µg/ml kanamycin the constructs and with 100 µg/ml timentin to inhibit *Agrobacterium* growth, and the phenotypes were recorded. Single locus insertion and homozygous lines were used for further analysis.

Binary plasmids *pPID:PID-YFP*, *pPID:PID(R2A)-YFP*, *pPID:PID(R3A)-YFP*, *pPID:PID(R5A)-YFP*, *pPID:PID(K268A)-YFP*, *pPID:PID(K269A)-YFP*, *pPID:PID(K268,269A)-YFP*, *pPID:PID(V270D)-YFP* and *pPID:PID(V270D/L273E)-YFP* were electroporated into *Agrobacterium* strain AGL1 (Lazo et al., 1991; Chassy et al., 1988) and T-DNA constructs were transformed to heterozygous *pid-14/+* (*Salk_049736*) plants using the floral dip method (Clough and Bent., 1998). Primary transformants (T1) were selected on medium supplemented with 25 µg/ml hygromycin for the constructs, 50 µg/ml kanamycin for the *pid-14* mutant allele and 100 µg/ml timentin to inhibit *Agrobacterium* growth. Homozygous *pid-14* plants were selected by genotyping with primers *PID LP* and *LBb1.3* (for SALK lines) and subsequently used for phenotyping. T3 lines with single locus homozygous T-DNA insertion were used for further analysis.

Seeds were surface sterilized by incubating for 1 min. in 70% ethanol and 10 min. in bleach solution containing 1% chlorine and subsequently washed three times with sterile dH₂O. Sterilized seeds were kept in the dark at 4 °C for two days for vernalization and subsequently germinated on vertical plates containing 0.5× Murashige and Skoog (1/2 MS) Duchefa medium containing 0.05% MES, 1% Daishin agar (Duchefa) and 1% sucrose at 22 °C and 16 hours photoperiod. Plants grown on soil were cultured at 21 °C, 16 hours photoperiod, and 70% relative humidity.

Seedlings on plates, potted plants were photographed with a Nikon D5300 camera. Primary root length was measured with ImageJ (Fiji) and analysed with GraphPad Prism 5.

Protein structure prediction and helix wheel projection

The structure of the PID ID was analysed by web protein structure prediction tools <http://zhanglab.ccmb.med.umich.edu/QUARK/> (Xu and Zhang, 2012; Mortuza et al., 2021) and <http://bioserv.rpbs.univ-paris-diderot.fr/PEP-FOLD/> (Thevenet et al., 2012; Shen et al., 2014). The helix wheel projection was made by <http://heliquest.ipmc.cnrs.fr/>. The consensus sequences for an IQ motif ([FILV]Qxxx[RK]Gxxx[RK]xx[FILVWY]) or an IQ-like motif ([FILV]Qxxx[RK]xxxxxxxx) were used to identify such a motif in PID.

RNA extraction and (q)RT-PCR

Vertically grown 5-day-old seedlings were collected and total RNA was extracted using the NucleoSpin RNA Plant kit (Macherey Nagel, #740949). Reverse transcription (RT) was performed using the RevertAid Reverse Transcription Kit (Thermo Scientific™, #K1691). qRT-PCR was performed in the CFX96 Touch™ Real-Time PCR Detection System (Bio-Rad) using TB Green® Premix Ex Taq™ II (Tli RNase H Plus) (Takara, #RR820B).

Protoplast transformation

Protoplasts of *Arabidopsis thaliana* Col-0 cell suspension cultures were obtained and transfected as described (Schirawski et al., 2000). Plasmid DNAs were extracted using the Plasmid Midi Kit (QIAGEN, #12143), 10µg per plasmid was added to 0.5×10^6 cells for PEG-mediated protoplast transfection. Auxin (NAA, 1 µM) was removed from the media during protoplast isolation and transfection, and either left out or added to the recovery medium after transfection. The transfected protoplasts were incubated for 16 hours at 21 °C in the dark. Pictures were taken

PINOID plasma membrane association and CALMODULIN-LIKE 12/TOUCH 3 binding converge on an amphipathic alpha-helix in the kinase insertion domain

using the Zeiss LSM5 Exciter/Axio Observer confocal microscope with either a 40x or 63x oil immersion objective (NA=1.2). The CFP signal was detected using an argon 458 nm laser and a 475-525 nm band pass filter, and the YFP signal was detected using an argon 514 nm laser and a 530-600 nm band pass filter.

***In vitro* pull-down assay**

In vitro pull-down assays were performed as described in Chapter 2.

Bimolecular Fluorescence Complementation (BiFC) assay

To perform the BiFC assays, 20 ml cultures of *Agrobacterium tumefaciens* strain AGL1 harbouring either *pDEST-PID-VYCE*, *pDEST-PID(R2A)-VYCE*, *pDEST-PID(R3A)-VYCE*, *pDEST-PID(R5A)-VYCE*, *pDEST-TCH3/CML12-VYNE* or *pDEST-VYCE* were incubated in a 28°C shaker until an OD₆₀₀ of 1.0 was reached. Bacteria were collected by centrifugation for 15 minutes at 4000rpm, resuspended in 20 ml infiltration medium (10 mM MgCl₂, 10 mM MES/KOH, pH 5.7) supplemented with 200µM Acetosyringone (Sigma-Aldrich, #D134406-5G), and cultured for at least 2 hours at 50 rpm on a table shaker in darkness. Equal volumes of the agrobacteria carrying two constructs (5 ml each) were mixed. Leaves of three-week-old *Nicotiana benthamiana* plants were infiltrated using a 5 ml syringe without needle. Two days later, infiltrated leaf parts were checked for YFP signal using the Zeiss LSM 5 Exciter 2C/1F Imager M1 (Zeiss, Oberkochen, Germany) confocal microscope, using a 20x objective. The YFP signal was detected using an argon 514 nm laser and a 530-600 nm band pass filter.

Accession numbers

Arabidopsis Genome Initiative locus identifiers for the genes mentioned are as follows: CaM1/TCH1 (At5g37780), CaM2 (At2g41110), CaM3 (At3g56800), CaM4 (At1g66410), CaM5 (At2g27030), CaM6 (At5g21274), CaM7 (At3g43810),

CML8 (At4g14640), CML9 (At3g51920), CML10 (At2g41090), CML11 (At3g22930), CML12/TCH3 (At2g41100), PID (At2g34650).

Acknowledgements

The authors would like to thank Gerda Lamers and Joost Willemse for their help with the microscopy, Ward de Winter and Jan Vink for help with medium, tissue culture and plant caretaking. This author was supported by the China Scholarship Council.

Author contribution

Remko Offringa, Xiaoyu Wei designed the experiments, Yuanwei Fan and Eike Rademacher performed experiments presented Figure 1-4 and figure 5 (A, B, D), Xiaoyu Wei performed the rest of the experiments and data analysis, Xiaoyu Wei and Remko Offringa wrote and finalized of the Chapter.

PINOID plasma membrane association and CALMODULIN-LIKE 12/TOUCH 3 binding converge on an amphipathic alpha-helix in the kinase insertion domain

Supplementary data:

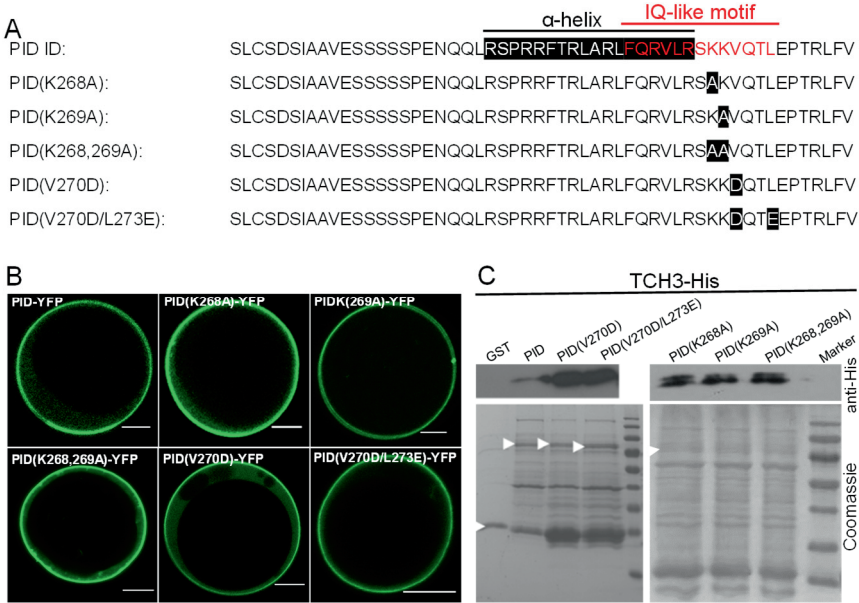


Figure S1. Disruption of the IQ-like motif does affect either PM association or CaM/CML binding. (A). The amino acid sequence of PID ID and the amino acid substitutions in different PID mutant versions. (B). Expression of PID-YFP, PID(K268A)-YFP, PID(K269A)-YFP, PID(K268,269A)-YFP, PID(V270D)-YFP or PID(V270D/L273E)-YFP fusions from the 35S promoter in Arabidopsis protoplasts. (C) *In vitro* pull down using GST, GST-tagged PID (PID) or GST-tagged PID mutant versions PID(K268A), PID(K269A), PID(K268,269A), PID(V270D), PID(V270D/L273E) bound to glutathione beads as bait and His-tagged TCH3 as prey. Pulled down TCH3-His was detected by hybridizing the Western blot with anti-His antibodies (upper panel). White arrowheads in lower panel indicate the positions of the respective GST-tagged proteins in a Coomassie stained gel. The scale bar in (B) indicates 10 μ m.

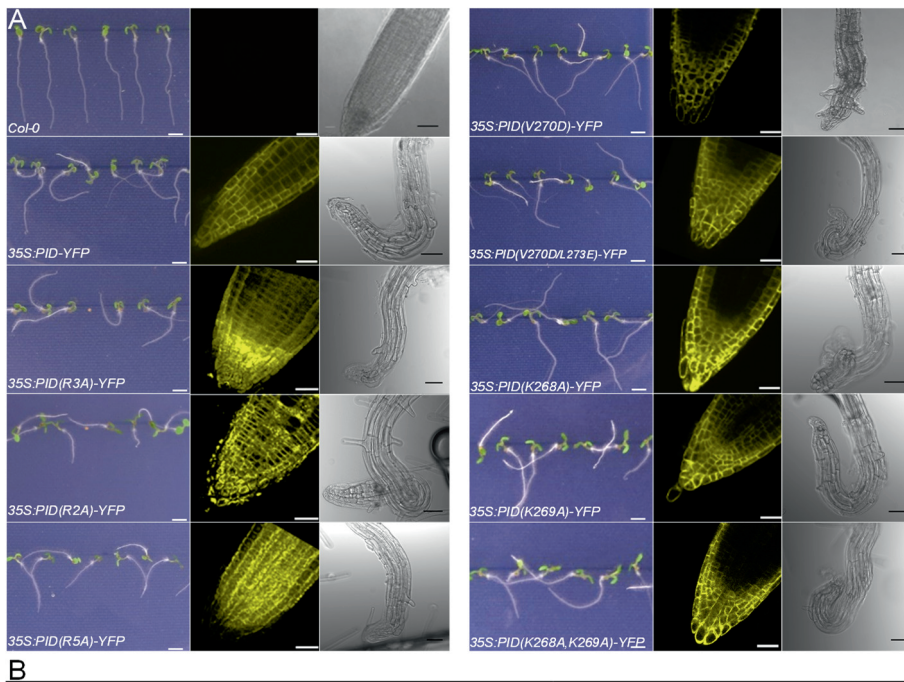
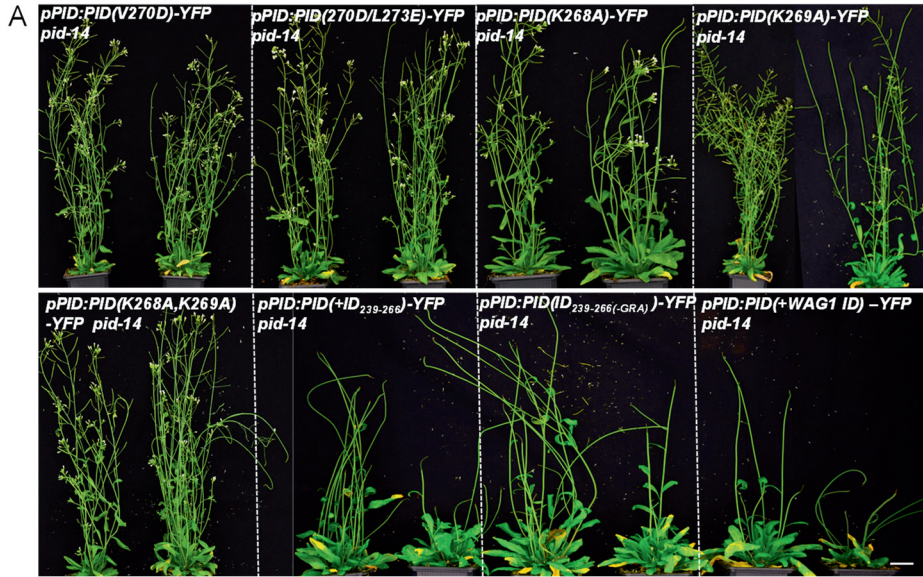


Figure S2. Seedling phenotypes of lines overexpressing wild-type PID or mutant PID versions. (A). Phenotype of 5-day-old vertically grown seedlings (left image) and confocal microscopy analysis of the root tip showing the YFP signal (middle image) or the transmitted light (right image) of wild-type Arabidopsis (Col-0) or of T3 lines homozygous for a single locus insertion of the *p35S::PID-YFP*, *p35S::PID(R2A)-YFP*, *p35S::PID(R3A)-YFP*, *p35S::PID(R5A)-YFP*, *p35S::PID(K268A)-YFP*,

PINOID plasma membrane association and CALMODULIN-LIKE 12/TOUCH 3 binding converge on an amphipathic alpha-helix in the kinase insertion domain

p35S::PID(K269A)-YFP, *p35S::PID(K268A,K269A)-YFP*, *p35S::PID(V270D)-YFP* or *p35S::PID(V270D/L273E)-YFP* T-DNA construct. **(B)**. Table depicting the number of primary transformants (T1) phenotyped at the flowering plant level and the number and percentage of plants developing either wild-type or pin-like inflorescences. Size bar indicates 0.2 cm in the left panel, 20 μ m in the middle panel and 50 μ m in the right panel of (A).



B

Constructs	T1 plants (<i>pid-14</i> HM)	Inflorescence	
		WT	pin-like
<i>pPID::PID-YFP pid-14</i>	14	85.7%(12/14)	14.3%(2/14)
<i>pPID::PID(V270D)-YFP pid-14</i>	15	80.0%(12/15)	20.0%(3/15)
<i>pPID::PID(V270D/L273E)-YFP pid-14</i>	17	94.1%(16/17)	5.9%(1/17)
<i>pPID::PID(K268A)-YFP pid-14</i>	10	80.0%(8/10)	20.0%(2/10)
<i>pPID::PID(K269A)-YFP pid-14</i>	14	85.7%(12/14)	14.3%(2/14)
<i>pPID::PID(K268A,K269A)-YFP pid-14</i>	9	77.8%(7/9)	22.2%(2/9)
<i>pPID::PID(+ID₂₃₉₋₂₆₆)-YFP pid-14</i>	31	19.4%(6/31)	80.6%(25/31)
<i>pPID::PID(ID₂₃₉₋₂₆₆(-GRA))-YFP pid-14</i>	6	16.7%%(1/6)	83.3%(5/6)
<i>pPID::PID(+WAG1 ID) -YFP pid-14</i>	17	0.0%(0/17)	100%(17/17)

Figure S3. Complementation analysis of mutant PID versions expressed under the *PID* promoter in the *pid-14* mutant background. (A) Flowering plant phenotype of primary transformants (T1) homozygous for the *pid-14* loss-of-function allele and transgenic for the

pPID:PID-YFP, *pPID:PID(R2A)-YFP*, *pPID:PID(R3A)-YFP*, *pPID:PID(R5A)-YFP*, *pPID:PID(K268A)-YFP*, *pPID:PID(K269A)-YFP*, *pPID:PID(K268A,K269A)-YFP*, *pPID:PID(V270D)-YFP*, *pPID:PID(V270D/L273E)-YFP*. (B). Table depicting the number of phenotyped primary transformants (T1) with the indicated T-DNA construct and homozygous for the *pid-14* allele (*pid-14* HM), and the number and percentage of transformants showing wild-type or pin-like inflorescences. Size bar indicates 2 cm in (A).

Table S1. Oligonucleotides used for cloning, genotyping or qRT-PCR.

AttB1 InsDom AA229 S	5'GGGGACAAGTTTGTACAAAAAGCAGGCTTAATGCTATGCTCCGACTCAATCG3'
AttB2 InsDom AA279 AS	5'GGGGACCACCTTTGTACAAGAAAGCTGGGTCAAAGAGACGGGTGG3'
AttB1 InsDom AA248 S	5'GGGGACAAGTTTGTACAAAAAGCAGGCTTAATGGGAATCAACAACCTC3'
AttB2 InsDom AA274 AS	5'GGGGACCACCTTTGTACAAGAAAGCTGGGTGTTCTAAAGTCTGAACC3'
PID Deletion 2 S	<i>Bsp</i> TI <i>Sgs</i> I 5'AAACTTAAGGCGCGCCGAGGTCAAAGTCAGAGAGC3'
PID Deletion 2 AS	<i>Bsp</i> TI 5'GACCTTAAGGCTGAACCGTTACTGC3'
PID InsDom S	<i>Sgs</i> I 5'TGGCGCGCCTCTCTATGCTCCGACTCAAT3'
PID InsDom AS	<i>Bsp</i> TI 5'CGTCTTAAGAACAAAGAGACGGGTGG3'
PID InsDom R249,252,253A AS	5'GTGAATGCTGCAGGTGAAGCGAGTTGTTG 3'
PID InsDom R263,266A	5'CTTTTCCAAGCAGTACTGGCGTCTAAAAAGG3'
PID InsDom R268A	5'TCCAACGAGTCTTGCAGTCTGCAAGGTTACAGACTTTAGAAC3'
PID InsDom R269A	5'GGTTGGTTCTAAAGTCTGAACAGCTTTAGACCGCAAGACTCGTTGG3'
PID InsDom R268,269A	5'GACGGGTTGGTTCTAAAGTCTGAACAGTGCAGACCGCAAGACTCGTTGAAAAAGT3'
PID-ALA1 S	5'GAATCTTCTCGTCTTCGCCGAGAAATCAAGCAGCCGCTGCAGCGGCAGCATTC ACTCGTCTCGCTAGACTTTTCCAACG3'
PID-ALA1 AS	5'CGTTGGAAAAAGTCTAGCGAGACGAGTGAATGCTGCCGCTGCAGCGGCTGCTTGA TTCTCCGGCGAAGACGAGGAAGATTC3'
PID-ALA2 S	5'GAGAATCAACAACCTCCGTTACCGCGACGAGCCGCTGCTGCCGCTGCAGCTTTC CAACGAGTCTTGCGGTCTAAAAAGGT3'
PID-ALA2 AS	5'ACCTTTTAGACCGCAAGACTCGTTGGAAAGCTGCAGCGGCAGCAGCGGCTCGT CGCGGTGAACGGAGTTGTTGATTCTC3'
PID-ALA3 S	5'CACCGCGACGATTCACTCGTCTCGCTAGACTTGCCGACGAGCCGCGGCGGCTA AAAAGGTTTCAGACTTTAGAACCAACCCGT3'
PID-ALA3 AS	5'ACGGGTTGGTTCTAAAGTCTGAACCTTTTAGCCGCCGCGGCTGCTGCCGCAAGT CTAGCGAGACGAGTGAATCGTCGCGGTG3'
PID InsDom AA227-253 S	5'CGGCCTCTCTATGCTCCGACTCAATCGACGCCGTTGAATCTTCTCTGCTTCG CCGGAGAATCAACAACCTCCGTTACCGCGACGAC3'
PID InsDom AA227-253 AS	5'TTAAGTCGTCGCGTGAACGGAGTTGTTGATTCTCCGGCGAAGACGAGGAAGATTCAACGGCTGC GATTGAGTCGGAGCATAGAGAGG3'
PID InsDom AA254-280 S	5'CGCGCTTCACTCGTCTCGCTAGACTTTTCCAACGAGTCTTGCGGTCTAAAAA GGTTCAGACTTTAGAACCAACCCGTCTTTGTTC3'
PID InsDom AA254-280 AS	5'TTAAGAACAAAGAGACGGGTTGGTTCTAAAGTCTGAACCTTTTAGACCGCA AGACTCGTTGAAAAAGTCTAGCGAGACGAGTGAAGG3'
PID InsDom AA240-266 S	5'CGCGCTCTGCTTCGCCGAGAAATCAACAACCTCCGTTACCGCGACGATTCA CTCGTCTCGCTAGACTTTTCCAACGAGTCTTGCGGC3'
PID InsDom AA240-266 AS	5'TTAAGCCGAAGACTCGTTGAAAAAGTCTAGCGAGACGAGTGAATCGTCGCG

PINOID plasma membrane association and CALMODULIN-LIKE 12/TOUCH 3 binding converge on an amphipathic alpha-helix in the kinase insertion domain

	GTGAACGGAGTTGTTGATTCTCCGGCGAAGACGAGG3'
PP2A-3-qRT-FP	5'GATGGATACAAC TGGGCTCACG3'
PP2A-3-qRT-RP	5'TCGGTGCTGGTTCAAAC TGG3'
PID-qRT-FP	5'ATTTAACTCTCTCCGTCATAGACAAC3'
PID -qRT-RP	5'ACATGTGTAGATATTCTAACGCCACTA3'
LBb1.3 (for SALK lines)	5'ATTTTGCCGATTTCGGAAC3'
PID LP	5'CTGTAACCAAAAACAAAATAAA3'

Reference:

- Agamasu, C., Ghirlando, R., Taylor, T., Messing, S., Tran, T. H., Bindu, L., ... & Stephen, A. G.** (2019). KRAS prenylation is required for bivalent binding with calmodulin in a nucleotide-independent manner. *Biophys. J.* 116: 1049-1063.
- Andrews, C., Xu, Y., Kirberger, M., & Yang, J. J.** (2020). Structural aspects and prediction of calmodulin-binding proteins. *Int. J. Mol. Sci.* 22: 308.
- Arazi, T., Baum, G., Snedden, W. A., Shelp, B. J., & Fromm, H.** (1995). Molecular and biochemical analysis of calmodulin interactions with the calmodulin-binding domain of plant glutamate **decarboxylase**. *Plant Physiol.* 108: 551-561.
- Atcheson, E., Hamilton, E., Pathmanathan, S., Greer, B., Harriott, P., & Timson, D. J.** (2011). IQ-motif selectivity in human IQGAP2 and IQGAP3: binding of calmodulin and myosin essential light chain. *Biosci. Rep.* 31: 371-379.
- Babu, Y. S., Bugg, C. E., & Cook, W. J.** (1988). Structure of calmodulin refined at 2.2 Å resolution. *J. Mol. Biol.* 204: 191-204.
- Bähler, M., & Rhoads, A.** (2002). Calmodulin signaling via the IQ motif. *FEBS Lett.* 513: 107-113.
- Baum, G., Long, J. C., Jenkins, G. I., & Trewavas, A. J.** (1999). Stimulation of the blue light phototropic receptor NPH1 causes a transient increase in cytosolic Ca^{2+} . *Proc. Natl. Acad. Sci. U.S.A.* 96: 13554-13559.
- Benamins, R., Quint, A., Weijers, D., Hooykaas, P., & Offringa, R.** (2001). The PINOID protein kinase regulates organ development in Arabidopsis by enhancing polar auxin transport. *Development* 128: 4057-4067.
- Black, D. J., & Persechini, A.** (2011). In calmodulin-IQ domain complexes, the Ca^{2+} -free and Ca^{2+} -bound forms of the calmodulin C-lobe direct the N-lobe to different binding sites. *Biochemistry* 50: 10061-10068.
- Chassy, B. M., Mercenier, A., & Flickinger, J.** (1988). Transformation of bacteria by electroporation. *Trends Biotechnol.* 6: 303-309.
- Chattopadhyaya, R., Meador, W. E., Means, A. R., & Quiocho, F. A.** (1992). Calmodulin structure refined at 1.7 Å resolution. *J. Mol. Biol.* 228: 1177-1192.
- Cheney, R. E., & Mooseker, M. S.** (1992). Unconventional myosins. *Curr. Opin. Cell Biol.*
- Chichili, V. P. R., Xiao, Y., Seetharaman, J., Cummins, T. R., & Sivaraman, J.** (2013). Structural basis for the modulation of the neuronal voltage-gated sodium channel NaV1. 6 by calmodulin. *Sci. Rep.* 3: 2435.
- Christensen, S. K., Dagenais, N., Chory, J., & Weigel, D.** (2000). Regulation of auxin response by the protein kinase PINOID. *Cell* 100: 469-478.

- Clore, G. M., Bax, A., Ikura, M., & Gronenborn, A. M.** (1993). Structure of calmodulin-target peptide complexes: *Curr. Opin. Struct. Biol.* 3: 838–845.
- Clough, S. J., & Bent, A. F.** (1998). Floral dip: a simplified method for *Agrobacterium*-mediated transformation of *Arabidopsis thaliana*. *Plant J.* 16: 735–743.
- Crivici, A., & Ikura, M.** (1995). Molecular and structural basis of target recognition by calmodulin. *Annu. Rev. Biophys. Biomol. Struct.* 24: 85–116.
- Davis, T. N., Urdea, M. S., Masiarz, F. R., & Thorner, J.** (1986). Isolation of the yeast calmodulin gene: calmodulin is an essential protein. *Cell* 47: 423–431.
- Dela Fuente, R. K.** (1984). Role of calcium in the polar secretion of indoleacetic acid. *Plant Physiol.* 76: 342–346.
- Dela Fuente, R. K., & Leopold, A. C.** (1973). A role for calcium in auxin transport. *Plant Physiol.* 51: 845–847.
- Dhonukshe, P., Huang, F., Galvan-Ampudia, C. S., Mähönen, A. P., Kleine-Vehn, J., Xu, J., ... & Offringa, R.** (2010). Plasma membrane-bound AGC3 kinases phosphorylate PIN auxin carriers at TPRXS (N/S) motifs to direct apical PIN recycling. *Development* 137: 3245–3255.
- Dindas, J., Scherzer, S., Roelfsema, M. R. G., von Meyer, K., Müller, H. M., Al-Rasheid, K. A. S., ... & Hedrich, R.** (2018). AUX1-mediated root hair auxin influx governs SCFTIR1/AFB-type Ca^{2+} signaling. *Nat. Commun.* 9: 1174.
- Fallon, J. L., Baker, M. R., Xiong, L., Loy, R. E., Yang, G., Dirksen, R. T., ... & Quijcho, F. A.** (2009). Crystal structure of dimeric cardiac L-type calcium channel regulatory domains bridged by Ca^{2+} -calmodulins. *Proc. Natl. Acad. Sci. U.S.A.* 106: 5135–5140.
- Fallon, J. L., Halling, D. B., Hamilton, S. L., & Quijcho, F. A.** (2005). Structure of calmodulin bound to the hydrophobic IQ domain of the cardiac Cav1.2 calcium channel. *Structure* 13: 1881–1886.
- Fan, Y.** (2014). The role of AGC3 kinases and calmodulins in plant growth responses to abiotic signals (Doctoral dissertation, Leiden University).
- Felle, H.** (1988). Auxin causes oscillations of cytosolic free calcium and pH in *Zea mays* coleoptiles. *Planta* 174: 495–499.
- Friml, J., Yang, X., Michniewicz, M., Weijers, D., Quint, A., Tietz, O., ... & Offringa, R.** (2004). A PINOID-dependent binary switch in apical-basal PIN polar targeting directs auxin efflux. *Science* 306: 862–865.
- Galván Ampudia, C. S.** (2009). Plant AGC protein kinases orient auxin-mediated differential growth and organogenesis. (Doctoral dissertation, Leiden University).

- Galvan-Ampudia, C. S. and R. Offringa.** (2007). Plant evolution: AGC kinases tell the auxin tale. *Trends Plant Sci.* 12: 541-547.
- Gehring, C. A., Irving, H. R., & Parish, R. W.** (1990). Effects of auxin and abscisic acid on cytosolic calcium and pH in plant cells. *Proc. Natl. Acad. Sci. U.S.A.* 87(24), 9645-9649.
- Gellman, S. H.** (1991). On the role of methionine residues in the sequence-independent recognition of nonpolar protein surfaces. *Biochemistry* 30: 6633-6636.
- Gillette, W. K., Esposito, D., Abreu Blanco, M., Alexander, P., Bindu, L., Bittner, C., ... & Stephen, A. G.** (2015). Farnesylated and methylated KRAS4b: high yield production of protein suitable for biophysical studies of prenylated protein-lipid interactions. *Sci. Rep.* 5: 1-13.
- Glanc, M., Van Gelderen, K., Hoermayer, L., Tan, S., Naramoto, S., Zhang, X., ... & Friml, J.** (2021). AGC kinases and MAB4/MEL proteins maintain PIN polarity by limiting lateral diffusion in plant cells. *Curr. Biol.* 31: 1918-1930.
- Gleave, A. P.** (1992). A versatile binary vector system with a T-DNA organisational structure conducive to efficient integration of cloned DNA into the plant genome. *Plant Mol. Biol.* 20: 1203-1207.
- Grant, B. M., Enomoto, M., Back, S. I., Lee, K. Y., Gebregiorgis, T., Ishiyama, N., ... & Marshall, C. B.** (2020). Calmodulin disrupts plasma membrane localization of farnesylated KRAS4b by sequestering its lipid moiety. *Sci. Signal.* 13: eaaz0344.
- Harada, A., & Shimazaki, K. I.** (2007). Phototropins and blue light-dependent calcium signaling in higher plants. *J. Photochem. Photobiol.* 83:102-111.
- Harada, A., Sakai, T., & Okada, K.** (2003). Phot1 and phot2 mediate blue light-induced transient increases in cytosolic Ca^{2+} differently in Arabidopsis leaves. *Proc. Natl. Acad. Sci. U.S.A.* 100: 8583-8588.
- Hasenstein, K. H., & Evans, M. L.** (1986). Calcium dependence of rapid auxin action in maize roots. *Plant Physiol.* 81: 439-443.
- Heiman, R. G., Atkinson, R. C., Andruss, B. F., Bolduc, C., Kovalick, G. E., & Beckingham, K.** (1996). Spontaneous avoidance behavior in *Drosophila* null for calmodulin expression. *Proc. Natl. Acad. Sci. U.S.A.* 93: 2420-2425.
- Heissler, S. M., & Sellers, J. R.** (2014). Myosin light chains: Teaching old dogs new tricks. *Bioarchitecture* 4: 169-188.
- Heo, W. D., Inoue, T., Park, W. S., Kim, M. L., Park, B. O., Wandless, T. J., & Meyer, T.** (2006). PI (3, 4, 5) P3 and PI (4, 5) P2 lipids target proteins with polybasic clusters to the plasma membrane. *Science* 314: 1458-1461.

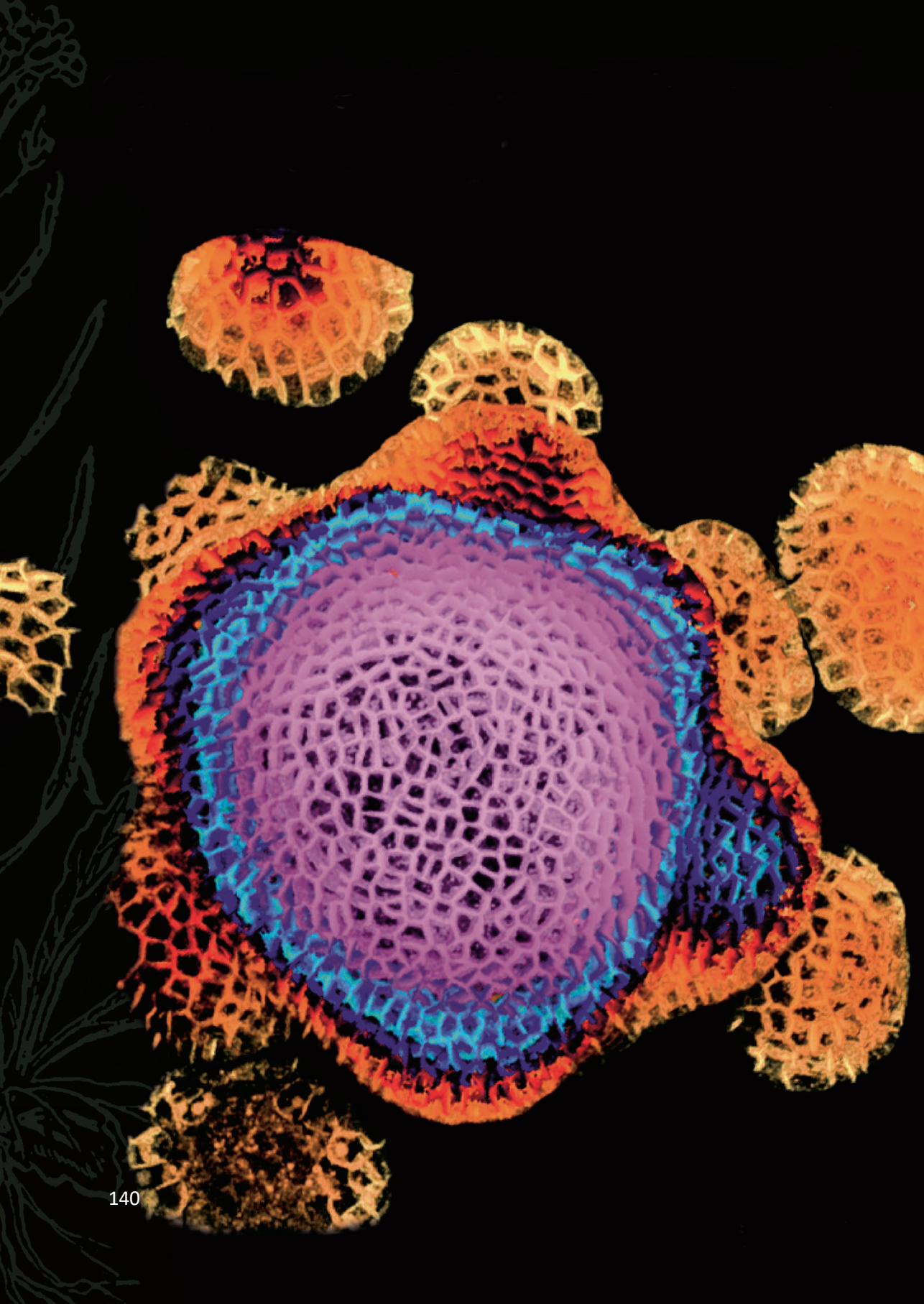
- Houdusse, A., & Cohen, C.** (1995). Target sequence recognition by the calmodulin superfamily: implications from light chain binding to the regulatory domain of scallop myosin. *Proc. Natl. Acad. Sci. U.S.A.* 92: 10644-10647.
- Huang, F., Kemel Zago, M., Abas, L., van Marion, A., Galván-Ampudia, C. S., & Offringa, R.** (2010). Phosphorylation of conserved PIN motifs directs Arabidopsis PIN1 polarity and auxin transport. *Plant Cell* 22: 1129-1142.
- Ikura, M., & Ames, J. B.** (2006). Genetic polymorphism and protein conformational plasticity in the calmodulin superfamily: two ways to promote multifunctionality. *Proc. Natl. Acad. Sci. U.S.A.* 103: 1159-1164.
- Irving, H. R., Gehring, C. A., & Parish, R. W.** (1992). Changes in cytosolic pH and calcium of guard cells precede stomatal movements. *Proc. Natl. Acad. Sci. U.S.A.* 89: 1790-1794.
- Komolov, K. E., Sulon, S. M., Bhardwaj, A., van Keulen, S. C., Duc, N. M., Laurinavichyute, D. K., ... & Benovic, J. L.** (2021). Structure of a GRK5-calmodulin complex reveals molecular mechanism of GRK activation and substrate targeting. *Mol. Cell* 81: 323-339.
- Kretsinger, R. H., Rudnick, S. E., & Weissman, L. J.** (1986). Crystal structure of calmodulin. *J. Inorg. Biochem.* 28: 289-302.
- Krupnick, J. G., & Benovic, J. L.** (1998). The role of receptor kinases and arrestins in G protein-coupled receptor regulation. *Annu. Rev. Pharmacol. Toxicol.* 38: 289-319.
- Landrein, B., Kiss, A., Sassi, M., Chauvet, A., Das, P., Cortizo, M., ... & Hamant, O.** (2015). Mechanical stress contributes to the expression of the STM homeobox gene in Arabidopsis shoot meristems. *Elife* 4: e07811.
- Lazo, G. R., Stein, P. A., & Ludwig, R. A.** (1991). A DNA transformation-competent Arabidopsis genomic library in Agrobacterium. *Biotechnology* 9: 963-967.
- Lee, J. S., Mulkey, T. J., & Evans, M. L.** (1984). Inhibition of polar calcium movement and gravitropism in roots treated with auxin-transport inhibitors. *Planta* 160: 536-543.
- Lefèvre, F., Rémy, M. H., & Masson, J. M.** (1997). Alanine-stretch scanning mutagenesis: a simple and efficient method to probe protein structure and function. *Nucleic Acids Res.* 25: 447-448.
- Lu, K. P., Rasmussen, C. D., May, G. S., & Means, A. R.** (1992). Cooperative regulation of cell proliferation by calcium and calmodulin in *Aspergillus nidulans*. *Mol Endocrinol.* 6: 365-374.

- McCormack, E., & Braam, J.** (2003). Calmodulins and related potential calcium sensors of Arabidopsis. *New Phytol.* 159: 585-598.
- McLaughlin, S., & Murray, D.** (2005). Plasma membrane phosphoinositide organization by protein electrostatics. *Nature* 438: 605-611.
- Michniewicz, M., Zago, M. K., Abas, L., Weijers, D., Schweighofer, A., Meskiene, I., ... & Friml, J.** (2007). Antagonistic regulation of PIN phosphorylation by PP2A and PINOID directs auxin flux. *Cell* 130: 1044-1056.
- Monshausen, G. B., Miller, N. D., Murphy, A. S., & Gilroy, S.** (2011). Dynamics of auxin-dependent Ca^{2+} and pH signaling in root growth revealed by integrating high-resolution imaging with automated computer vision-based analysis. *Plant J.* 65: 309-318.
- Mori, M. X., Vander Kooi, C. W., Leahy, D. J., & Yue, D. T.** (2008). Crystal structure of the CaV2 IQ domain in complex with Ca^{2+} /calmodulin: high-resolution mechanistic implications for channel regulation by Ca^{2+} . *Structure* 16: 607-620.
- Mortuza, S. M., Zheng, W., Zhang, C., Li, Y., Pearce, R., & Zhang, Y.** (2021). Improving fragment-based ab initio protein structure assembly using low-accuracy contact-map predictions. *Nat. Commun.* 12: 5011.
- O'Neil, K. T., & DeGrado, W. F.** (1990). How calmodulin binds its targets: sequence independent recognition of amphiphilic α -helices. *Trends Biochem. Sci.* 15: 59-64.
- Perochon, A., Aldon, D., Galaud, J. P., & Ranty, B.** (2011). Calmodulin and calmodulin-like proteins in plant calcium signaling. *Biochimie* 93: 2048-2053.
- Persechini, A., & Kretsinger, R. H.** (1988). Toward a model of the calmodulin-myosin light-chain kinase complex: implications for calmodulin function. *J. Cardiovasc. Pharmacol.* 12: 1-12.
- Plieth, C., & Trewavas, A. J.** (2002). Reorientation of seedlings in the earth's gravitational field induces cytosolic calcium transients. *Plant Physiol.* 129: 786-796.
- Poovaiah, B. W., Du, L., Wang, H., & Yang, T.** (2013). Recent advances in calcium/calmodulin-mediated signaling with an emphasis on plant-microbe interactions. *Plant Physiol.* 163: 531-542.
- Ranty, B., Aldon, D., & Galaud, J. P.** (2006). Plant calmodulins and calmodulin-related proteins: multifaceted relays to decode calcium signals. *Plant Signal. Behav.* 1: 96-104.
- Rhoads, A. R., & Friedberg, F.** (1997). Sequence motifs for calmodulin recognition. *FASEB J.* 11: 331-340.

- Sack, J. S., Greenhough, T. J., Bugg, C. E., Means, A. R., & Cook, W. J.** (1985). Three-dimensional structure of calmodulin. *Nature* 315: 37-40.
- Sarhan, M., Van Petegem, F., & Ahern, C. A.** (2012). Crystallographic basis for calcium regulation of sodium channels. *Biophys. J.* 102: 325a.
- Shen, Y., Maupetit, J., Derreumaux, P., & Tufféry, P.** (2014). Improved PEP-FOLD approach for peptide and miniprotein structure prediction. *J. Chem. Theory Comput.* 10: 4745-4758.
- Shih, H. W., DePew, C. L., Miller, N. D., & Monshausen, G. B.** (2015). The cyclic nucleotide-gated channel CNGC14 regulates root gravitropism in *Arabidopsis thaliana*. *Curr. Biol.* 25: 3119-3125.
- Shishova, M., & Lindberg, S.** (1999). Auxin-induced cytosol acidification in wheat leaf protoplasts depends on external concentration of Ca^{2+} . *Journal of Plant Physiol.* 155: 190-196.
- Simon, M. L., Platre, M. P., Marquès-Bueno, M. M., Armengot, L., Stanislas, T., Bayle, V., Caillaud, M. C., & Jaillais, Y.** (2016). A PtdIns(4)P-driven electrostatic field controls cell membrane identity and signalling in plants. *Nat. Plants* 2: 16089.
- Takeda, T., & Yamamoto, M.** (1987). Analysis and in vivo disruption of the gene coding for calmodulin in *Schizosaccharomyces pombe*. *Proc. Natl. Acad. Sci. U.S.A.* 84: 3580–3584.
- Thevenet, P., Shen, Y., Maupetit, J., Guyon, F., Derreumaux, P., & Tuffery, P.** (2012). PEP-FOLD: an updated de novo structure prediction server for both linear and disulfide bonded cyclic peptides. *Nucleic Acids Res.* 40: W288-W293
- Tidow, H., & Nissen, P.** (2013). Structural diversity of calmodulin binding to its target sites. *FEBS J.* 280: 5551-5565.
- Tidow, H., Poulsen, L. R., Andreeva, A., Knudsen, M., Hein, K. L., Wiuf, C., ... & Nissen, P.** (2012). A bimodular mechanism of calcium control in eukaryotes. *Nature* 491: 468-472.
- Toyota, M., Furuichi, T., Tatsumi, H., & Sokabe, M.** (2008). Critical consideration on the relationship between auxin transport and calcium transients in gravity perception of *Arabidopsis* seedlings. *Plant Signal. Behav.* 3: 521-524.
- Wang, C., Chung, B. C., Yan, H., Lee, S. Y., & Pitt, G. S.** (2012). Crystal structure of the ternary complex of a NaV C-terminal domain, a fibroblast growth factor homologous factor, and calmodulin. *Structure* 20: 1167-1176.
- Wang, P., Shen, L., Guo, J., Jing, W., Qu, Y., Li, W., ... & Zhang, W.** (2019). Phosphatidic acid directly regulates PINOID-dependent phosphorylation and activation of the PIN-FORMED2 auxin efflux transporter in response to salt stress. *Plant Cell* 31: 250-271.

- Xu, B., Chelikani, P., & Bhullar, R. P.** (2012). Characterization and functional analysis of the calmodulin-binding domain of Rac1 GTPase. *PloS one* 7: e42975.
- Xu, D., & Zhang, Y.** (2012). Ab initio protein structure assembly using continuous structure fragments and optimized knowledge-based force field. *Proteins*. 80: 1715-1735.
- Yamniuk, A. P., & Vogel, H. J.** (2004). Calmodulin's flexibility allows for promiscuity in its interactions with target proteins and peptides. *Mol. Biotechnol.* 27: 33-57.
- Yang, C. F., & Tsai, W. C.** (2021). Calmodulin: The switch button of calcium signaling. *Tzu Chi Med. J.* 34: 15-22.
- Zegzouti, H., Li, W., Lorenz, T. C., Xie, M., Payne, C. T., Smith, K., ... & Christensen, S. K.** (2006). Structural and functional insights into the regulation of Arabidopsis AGC VIIa kinases. *J. Biol. Chem.* 281: 35520-35530.
- Zhang, M., & Vogel, H. J.** (1994). Two-dimensional NMR studies of selenomethionyl calmodulin. *J. Mol. Biol.* 239: 545-554.
- Zhang, M., Li, M., Wang, J. H., & Vogel, H. J.** (1994). The effect of Met→Leu mutations on calmodulin's ability to activate cyclic nucleotide phosphodiesterase. *J. Biol. Chem.* 269: 15546-15552.
- Zhang, M., Tanaka, T., & Ikura, M.** (1995). Calcium-induced conformational transition revealed by the solution structure of apo calmodulin. *Nat. Struct. Mol. Biol.* 2: 758-767.
- Zhao, X., Wang, Y.L., Qiao, X.R., Wang, J., Wang, L.D., Xu, C.S., & Zhang, X.** (2013). Phototropins function in high-intensity blue light-induced hypocotyl phototropism in Arabidopsis by altering cytosolic calcium. *Plant Physiol* 162: 1539-1551.
- Zhukovsky, M. A., Filograna, A., Luini, A., Corda, D., & Valente, C.** (2019). Protein amphipathic helix insertion: A mechanism to induce membrane fission. *Front. Cell Dev. Biol.* 7: 291.
- Zourelidou, M., Absmanner, B., Weller, B., Barbosa, I. C., Willige, B. C., Fastner, A., ... & Schwechheimer, C.** (2014). Auxin efflux by PIN-FORMED proteins is activated by two different protein kinases, D6 PROTEIN KINASE and PINOID. *Elife* 3: e02860.

PINOID plasma membrane association and CALMODULIN-LIKE 12/TOUCH 3 binding converge on an amphipathic alpha-helix in the kinase insertion domain



Chapter 4

Calcium-regulated PINOID kinase activity is required for a robust spiral phyllotaxis in the Arabidopsis inflorescence

Xiaoyu Wei¹ and Remko Offringa^{1*}

¹Plant Developmental Genetics, Institute of Biology Leiden, Leiden University, Sylviusweg 72, 2333 BE, Leiden, Netherlands

*Author for correspondence: r.offringa@biology.leidenuniv.nl

The results in this Chapter are included in the following publication: **Wei, X.Y.**, Fan, Y.W.,.....Offringa, R*. Calcium-regulated PINOID kinase activity is required for a robust spiral phyllotaxis in the Arabidopsis inflorescence (In preparation).

Abstract

Plant leaves and flowers are generated by the shoot apical meristem (SAM) following a precise spatio-temporal pattern, leading to a regular organ arrangement on a plant stem, also known as phyllotaxis. The plant hormone auxin plays a central role in establishing this pattern, as PIN-FORMED1 (PIN1) carrier-generated auxin maxima in the L1 layer of the SAM are the sites of organ initiation. The PINOID (PID) kinase is an important factor in this process, as it activates PIN proteins and directs their polarity to form convergence points where auxin maxima and organs are initiated. In the previous two Chapters of this thesis, we showed that PID interacts in a Ca^{2+} -dependent manner with CALMODULIN-LIKE 12/TOUCH 3 (CML12/TCH3) and 10 closely related calmodulins (CaMs) and CMLs. To study the role of PID-CaM/CML binding in plant development, we expressed ‘untouchable’ PID versions, specifically disrupted in their CaM/CML binding domain, in the *pid* loss-of-function mutant background. Initial phenotypic analysis of these plants suggested that the mutant PID versions were fully functional, as they complemented the pin-like inflorescence phenotype of the *pid* mutant. However, closer inspection of the inflorescences of these plants showed clear defects in the spiral phyllotaxis, ranging from deviating divergence angles between subsequent flowers and fruits to the simultaneous initiation of flower primordia. These phenotypes were reflected in the increased number and randomized position of PIN convergence points and auxin maxima in the inflorescence meristems of the ‘untouchable’ PID expressing plants. Together our data indicate that Ca^{2+} -dependent regulation of PID activity by CaM/CML binding is required for the accurate spatio-temporal positioning in the SAM of one auxin maximum at a time. We hypothesise that the PID – CAM/CML interaction integrates hormonal and abiotic signals that trigger elevations in $[\text{Ca}^{2+}]_{\text{cyt}}$, such as auxin and mechanical stress, to generate robustness in the spiral phyllotaxis that is typical for the Arabidopsis inflorescence.

Calcium-regulated PINOID kinase activity is required for a robust spiral phyllotaxis in the *Arabidopsis* inflorescence

Keywords: *Arabidopsis thaliana*, polar auxin transport, calcium signalling, mechanical stress, PINOID (PID) kinase, Calmodulin (CaM), Calmodulin-like (CML), phyllotaxis, inflorescence meristem (IM)

Introduction

Phyllotaxis is the regular arrangement of aerial organs, such as leaves and flowers, around the stem of a plant. These organs are generated from the shoot apical meristems (SAMs) of the plant, which includes the vegetative shoot apical meristem (SAM) generating leaves and the SAM-derived inflorescence meristem (IM) and floral meristem (FM) respectively generating flowers and floral organs. These SAMs comprise four functional zones: the central zone (CZ), peripheral zone (PZ), organizing center (OC), and rib zone (RZ) (Lyndon, 1998; Xue et al., 2020). Lateral organ primordia are initiated from the PZ and this process is triggered by local accumulation of the plant hormone auxin (Kuhlemeier and Reinhardt, 2001). Thus, phyllotaxis is determined by the dynamic and patterned auxin distribution at SAMs (Reinhardt et al., 2000; Reinhardt et al., 2003).

Auxin accumulation and distribution are for an important part mediated by polar auxin transport (PAT), which depends on the “long” PIN-FORMED (PIN) auxin efflux carriers, as their polar subcellular localization determines the directionality of PAT (Petrasek et al., 2006; Wisniewska et al., 2006; Zwiewka et al., 2019). It has been reported that the distribution of auxin in the L1 layer of SAMs through PIN1 is pivotal to the establishment of stable phyllotactic patterns (Jönsson et al., 2006; Smith et al., 2006; Stoma et al., 2008; Bhatia and Heisler, 2018). In the *Arabidopsis thaliana* (*Arabidopsis*) *pin-formed1* (*pin1*) mutant, aberrant inflorescences develop, characterized by the absence of flowers and a naked “pin-like” stem (Okada et al., 1991). PIN1 is strongly expressed in the SAMs, where it is

mainly found in the L1 layer, especially at the sites of incipient primordia formation (Reinhardt et al., 2003; Benková et al., 2003; Heisler et al., 2005). PIN1 polarizes towards the initiation site, forming a convergence pattern to generate an auxin maximum that triggers organ initiation. Together with the *pin1* mutant phenotype, this supports a direct role for PIN1 polarity in phyllotactic patterning (Reinhardt et al., 2003; Benková et al., 2003; Heisler et al., 2005; Bhatia et al., 2016). The polarization of PIN1 is regulated by the protein kinase PINOID (PID), a well-characterized regulator of PIN1 polarity. PID belongs to the AGC3 clade of the plant-specific family of AGCVIII protein kinases (Rademacher and Offringa, 2012). Together with its homologs WAG1 and WAG2, PID can induce a rootward(basal)-to-shootward(apical) shift in PIN polarity by phosphorylating serine residues in three conserved TPRXS motifs within the large central hydrophilic loop (PIN-HL) of “long” PIN proteins (Friml et al., 2004; Michniewicz et al., 2007; Huang et al., 2010; Dhonukshe et al., 2010). Interestingly, MITOGEN-ACTIVATED PROTEIN KINASES (MPK) 4 and 6 have been reported to phosphorylate the threonines in the same three TPRXS motifs of PIN1, leading to reduced plasma membrane (PM) abundance of PIN1 (Dory et al., 2018). Next to the three AGC3 clade kinases, members from the AGC1 clade of AGCVIII protein kinases, such as D6PK and PAX, have been shown to phosphorylate PIN proteins at different but also overlapping serine residues. Unlike the AGC3 kinases, phosphorylation by the AGC1 kinases does not cause a shift in polarity, but like AGC3 kinase-mediated phosphorylation it was reported to trigger PIN auxin efflux activity (Zourelidou et al., 2014; Barbosa et al., 2018; Marhava et al., 2018).

In addition to these kinases, various external stimuli (Heisler et al., 2010; Goh et al., 2012; Zhang et al., 2011; Li et al., 2019) and endogenous cues (Friml et al., 2003; Benková et al., 2003; Kleine-Vehn et al., 2011) have been reported to influence PIN polarity. The mechanism behind these influences is still largely unclear. External and endogenous cues cause signal-specific and tissue-specific changes in the concentration of cytosolic Ca^{2+} ($[\text{Ca}^{2+}]_{\text{cyt}}$), which are deciphered through the

action of Ca^{2+} sensors (Roberts and Harmon, 1992; Vogel, 1994). These sensors can be classified into two major groups: sensor relays, including Calmodulin/CaM-like proteins (CaM/CMLs) and Calcineurin B-like proteins (CBLs), and sensor responders, such as calcium-dependent protein kinases (CPKs) (Sanders et al., 2002).

Surprisingly, studies reporting molecular evidence for the involvement of Ca^{2+} signalling in the modulation of PAT are still limited. Recently, CPK29 was found to directly interpret Ca^{2+} signals from internal and external triggers, modulating PIN trafficking and polarity by phosphorylating another serine than the AGC or MAPK kinases in the PIN1-HL (Lee et al., 2021). In tomato, StCDPK1 has been reported to phosphorylate *StPIN4* *in vitro*, suggesting a possible role in regulating StPIN4 polarity (Santin et al., 2017). Moreover, the CDPK related kinase CRK5 translates Ca^{2+} oscillations into altered PIN2 polarity by direct phosphorylation of the PIN2-HL (Rigó et al., 2013). Previously, we identified CALMODULIN-LIKE 12/TOUCH 3/ (CML12/TCH3) and the small EF-Hand protein, PID-BINDING PROTEIN 1 (PBP1) as interacting partners of PID (Benjamins et al., 2003). These findings provided one of the first molecular clues how Ca^{2+} signalling might modulate auxin transport polarity. Later, the inositol triphosphate (IP_3)-dependent $[\text{Ca}^{2+}]_{\text{cyt}}$ was implied in apical-basal PIN polarity and the activity of the AGC3 kinases (Zhang et al., 2011), which strengthened our model that the AGC3 kinases link Ca^{2+} signalling to PIN polarity.

In Chapter 2 of this thesis, we focussed on the PID-CML12/TCH3 interaction, showing that PID interacts with all seven *Arabidopsis* Calmodulins (CaMs) and with the four most closely related CMLs, CML8, CML10, CML11 and CML12/TCH3. Mutant and expression analyses indicated that there is considerable functional redundancy among the genes encoding the PID-interacting CaM/CMLs. This, together with the promiscuous interaction of CaM/CMLs with many different proteins, makes it very unlikely that (multiple) *cam/cml* loss-of-function mutants will specifically reveal the role of the PID-CaM/CML interaction in plant

development. Considering the observation that the PID-CaM/CML interaction leads to sequestration of PID from the PM, we fine mapped the CaM/CML interaction domain in PID to an amphipathic alpha helix in the insertion domain (ID) in the catalytic core of the kinase. Substitution of several of the positively charged arginines in the helix by alanines resulted in functional but ‘untouchable’ PID kinase versions (Chapter 3).

Here we used lines expressing the ‘untouchable’ PID version from the *PID* promoter in the *pid* loss-of-function mutant background to reveal the role of Ca^{2+} -regulation of PID activity in plant development. Our results show that disruption of the Ca^{2+} -dependent PID-CaM/CML interaction leads to significant defects in the spiral phyllotaxis generated by the Arabidopsis IM. Typically, more flower primordia were initiated at the same time, correlating with the simultaneous occurrence of multiple PIN1-generated auxin maxima. Based on these results we propose a model where the Ca^{2+} -dependent PID-CaM/CML interaction, possibly induced by local mechanical stress in the IM, is required to limit organ initiation by PIN1-mediated generation of a single auxin maximum at a time, thereby maintaining the regular spiral phyllotaxis.

Results

‘Untouchable’ PID does not alter seedling development or flowering time

In Chapter 3 we showed that disruption of the amphipathic alpha helix in the PID ID by substitution of arginines by alanines gave rise to PID versions (PID(R2A), PID(R3A) and PID(R5A)) that failed to interact with the CaM/CMLs (‘untouchable’), but were functional based on the overexpression phenotypes and a rescue of the pin-like inflorescence phenotype of the *pid-14* loss-of-function mutant, when expressed as PID-YFP fusion under the *PID* promoter. At least 43 transgenic lines were obtained for each construct (*pPID:PID-YFP* and three

Calcium-regulated PINOID kinase activity is required for a robust spiral phyllotaxis in the *Arabidopsis* inflorescence

pPID::PID(R→A)-YFP constructs), and at least two single locus homozygous lines in *pid-14* homozygous background were used for further analysis.

A systematic phenotypic study showed no obvious differences between the *pPID::PID(R→A)-YFP pid-14* lines and the *pPID::PID-YFP pid-14* line or wild-type *Arabidopsis* (Col-0) at early developmental stages e.g. with respect to gravitropic growth, primary root length or rosette phenotype (Figure 1A-C, Figure S1A, B). Also, there was no clear difference between the flowering time of the tested lines (Figure 1C, Figure S1C), which showed a similar *PID* expression level (Figure 1D). A low percentage of the *pPID::PID(R→A)-YFP pid-14* or *pPID::PID-YFP pid-14* seedlings developed three cotyledons, a phenotype that was not linked to the R→A substitutions, but most likely to the promoter-cDNA-YFP construct design. The lack of an intron in the coding region of the *PID* gene probably altered the spatio-temporal expression, leading to insufficient expression in the embryo and thus to incomplete complementation of the *pid* mutant.

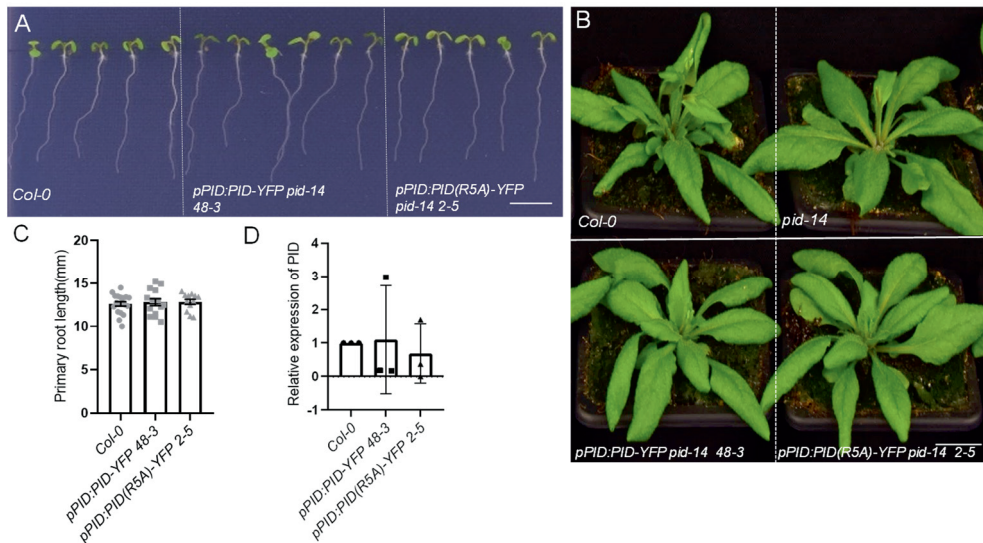


Figure 1. Seedlings and bolting plants of *pPID::PID(R5A)-YFP pid-14* lines show no obvious phenotypic differences from wild-type *Arabidopsis* (Col-0) or *pPID::PID-YFP pid-14* control lines. (A) 5-day-old seedlings of wild-type *Arabidopsis* (Col-0), and representative lines containing *pPID::PID-YFP* or *pPID::PID(R5A)-YFP* in the homozygous *pid-14* mutant background. (B) 6-week-

old bolting plants of wild-type Arabidopsis (Col-0), and representative lines containing *pPID:PID-YFP* or *pPID:PID(R5A)-YFP* in the homozygous *pid-14* mutant background. See also Figure S1. (C) Quantification of primary root length of 5-day-old seedlings ($n = 11-14$) in (A). (D) Quantitative RT-PCR analysis of PID expression for the lines presented in (A). Bars in (C and D) represent means, error bars the SEM, and dots the values of the biological repeats. The experiment was repeated three times. A one-way ANOVA with Tukey's test was used to test for statistically significant differences. Size bar indicates 5 mm in (A), 2 cm in (B).

‘Untouchable’ PID leads to abnormal inflorescence phyllotaxis

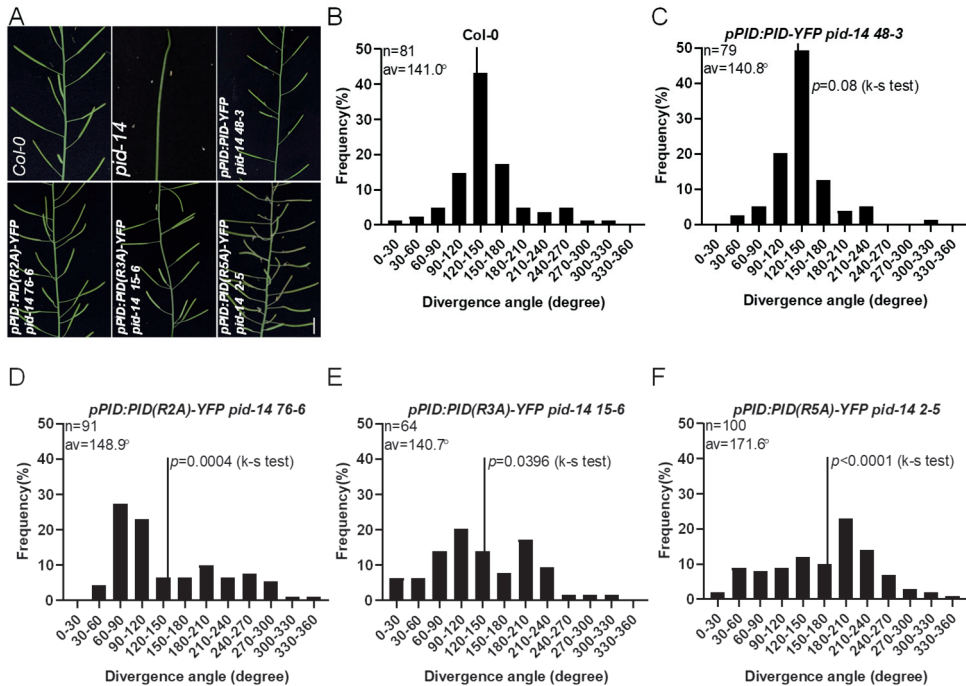


Figure 2. Expression of ‘untouchable’ PID versions in the *pid* mutant background leads to severe inflorescence phyllotaxis defects. (A) Representative inflorescences of 8-week-old wild-type Arabidopsis (Col-0) or *pid-14*, *pPID:PID-YFP pid-14* or *pPID:PID(R→A)-YFP pid-14* plants. (B-F) Distribution of divergence angles between two successive siliques along the inflorescences of wild-type Arabidopsis (Col-0) (B), *pPID:PID-YFP pid-14* (C), *pPID:PID(R2A)-YFP pid-14* (D), *pPID:PID(R3A)-YFP pid-14* (E) or *pPID:PID(R5A)-YFP pid-14* (F). Divergence angles were classified into 12 classes of 30°, and the percentages per class over the total number measured (n) are indicated in each graph. The average (av) divergence angle is shown and indicated as black line in the graph. For each construct, inflorescences of at least five lines were measured. The Kolmogorov–Smirnov test showed significant difference between Col-0 wild type and *pPID:PID(R2A)-YFP pid-14* ($p=0.0004$), *pPID:PID(R3A)-YFP pid-14* ($p=0.0396$) or *pPID:PID(R5A)-YFP pid-14* ($p<0.0001$). Size bar in (A) indicates 1 cm.

Initial observations suggested that the *pPID:PID(R→A)-YFP* construct complemented the pin like inflorescence phenotype of the *pid-14* mutant. More close inspection of the *pPID:PID(R→A)-YFP pid-14* inflorescences, however, showed clear defects in the spiral phyllotaxis that is typically observed in inflorescences of wild-type *Arabidopsis* (Col-0) (Figure 2A, B). In the latter inflorescences and also in those of *pPID:PID-YFP pid-14* plants, successive flowers arose and diverged by average angles of 141° (n=81) and 140.8° (n=79), respectively, statistically approximating the so-called the ‘golden’ angle of 137.5°. In contrast, the flowers of the *pPID:PID(R→A)-YFP pid-14* plants initiated in a disordered, almost randomized, fashion, with average divergence angles significantly deviating from the golden angle, or with angle value frequencies that deviated from a normal distribution (Figure 2D-F). We did not observe a specific pattern in the deviations from the spiral phyllotaxis. The data suggests that the role of the PID CaM/CML interaction is to prevent randomized organ initiation and promote positioning of subsequent organ primordia at a regular distance leading to the ‘golden’ divergence angle that is typical for spiral phyllotaxis in *Arabidopsis*.

‘Untouchable’ PID causes simultaneous flower primordium initiation and increases the variation in IM size

The IM generates the inflorescence and is the major determinant of the final phyllotactic pattern. However, the divergence angle in spiral phyllotaxis can also be modulated by post-meristematic growth such as internode elongation or stem torsion (Byrne et al., 2003; Peaucelle et al., 2007; Landrein et al., 2013). To investigate the cause of the observed irregular inflorescence phyllotaxis in more detail, we partially dissected the inflorescences of wild-type *Arabidopsis* (Col-0) and the wild-type PID or ‘untouchable’ PID complemented lines (Figure 3A).

In wild-type plants, each flower was attached by its pedicel to a single node, and nodes were separated by an internode, of which the length decreased gradually with each higher position on the inflorescence stem. The *pPID:PID-YFP pid-14*

plants showed the same flower, node, internode pattern (Figure 2A, 3A). In contrast, in *pid-14* mutant lines expressing ‘untouchable’ PID we frequently observed short internodes in between two longer ones, coinciding with an aberrant divergence angle, or two or even more flowers with their pedicels attached to the same node (Figure 2A, 3A). In some cases, two flowers were attached via the same pedicel to a node, or via their own pedicel to the same node but at a divergence angle of 180°. These data indicates that the irregular inflorescence phyllotaxis is not caused by defects of internode growth, but rather by the irregular and sometimes simultaneous initiation of flower primordia at the IM, subsequently causing irregular internode lengths.



Figure 3. ‘Untouchable’ PID expression leads to simultaneous flower primordium initiation. (A) Partially dissected inflorescences of 8-week-old wild-type Arabidopsis (Col-0) or *pPID:PID-YFP pid-14*, *pPID:PID(R2A)-YFP pid-14*, *pPID:PID(R3A)-YFP pid-14* or *pPID:PID(R5A)-YFP pid-14* plants. White arrows indicate positions where flower primordia were simultaneously initiated. **(B)** Subsequent fruits and flowers picked from the top part of a wild-type Arabidopsis (Col-0) inflorescence, showing a nice developmental series (upper panel), and clusters of co-initiated flowers picked from the top of *pPID:PID(R2A)-YFP pid-14*, *pPID:PID(R3A)-YFP pid-14* or *pPID:PID(R5A)-YFP pid-14* inflorescences. Size bar indicates 2 mm in (A).

To further confirm these results, we checked the developmental stages of subsequent fruits and flowers picked from the top part of an inflorescence. In wild-type Arabidopsis (Col-0) or the *pid-14* mutant complemented with wild-type PID

(*pPID:PID-YFP pid-14*) we observed a perfect developmental series, with each subsequent fruit or flower being at an earlier developmental stage, reflecting their sequential and regular timing of initiation at the IM (Figure 3B). In contrast, when we did the same for the *pid-14* mutants complemented with the ‘untouchable’ PID versions (*pPID:PID(R → A)-YFP pid-14*), we observed clusters of the flowers at the same developmental stage, indicating that they were simultaneously initiated at the IM (Figure 3A, B).

To validate that flower primordia were initiated simultaneously and to gain more mechanistic insight, we studied the anatomy of the IMs by scanning electron microscopy (SEM). At Col-0 IMs, flower primordia were initiated gradually in a regular clockwise or counter-clockwise spiral pattern (Figure 4A). The order from the youngest to the oldest primordium could be easily identified based on their developmental stage, with a divergence angle between successive primordia close to 137.5°, the so-called “golden angle” (Jean and Barab, 1998; Figure 4A). The IMs of *pid-14* mutant plants generally failed to initiate flower primordia organs and thus formed the typical ‘pin-like’ apical structures (Figure 4B). When the *pid-14* mutant was complemented with wild-type PID (*pPID:PID-YFP pid-14*), the IM showed the normal spiral pattern of primordium initiation that was also observed in Col-0 (Figure 4C). Markedly, the IMs of the *pid-14* mutant complemented with ‘untouchable’ PID versions (*pPID:PID(R → A)-YFP pid-14*) displayed a more random and variable pattern of flower primordium initiation, with simultaneous primordium initiation occurring frequently (Figure 4D-F). In some cases, two or even more primordia were initiated at one site of the SAM (e.g., P2? and P4? in Figure 4D and E), in line with the observed clusters of flowers and fruits (Figure 2A, Figure 3B).

Irregular phyllotactic patterns and simultaneous primordium initiation have previously been associated with an increased meristem size (Landrein et al., 2015; Yin, 2021). We used the SEM images to measure and compare the size of the IM of wild-type versus the *pid-14* complemented lines. Unexpectedly, the average IM

size of *pPID:PID(R→A)-YFP pid-14* plants was not significantly larger than that of wild-type Arabidopsis or *pPID:PID-YFP pid-14* plants, but we did observe a significant increase in the variation in size of the individual IMs (Figure 4G).

Together, our data shows that the Ca^{2+} -dependent regulation of PID activity by the CaM/CMLs is required to perfectly arrange newly formed organs by generating the regular spiral phyllotaxis and to prevent the simultaneous initiation of flower primordia at the IM. As PID function is not directly linked to the regulation of meristem size, we hypothesize that the latter is an indirect consequence of the phyllotaxis defects.

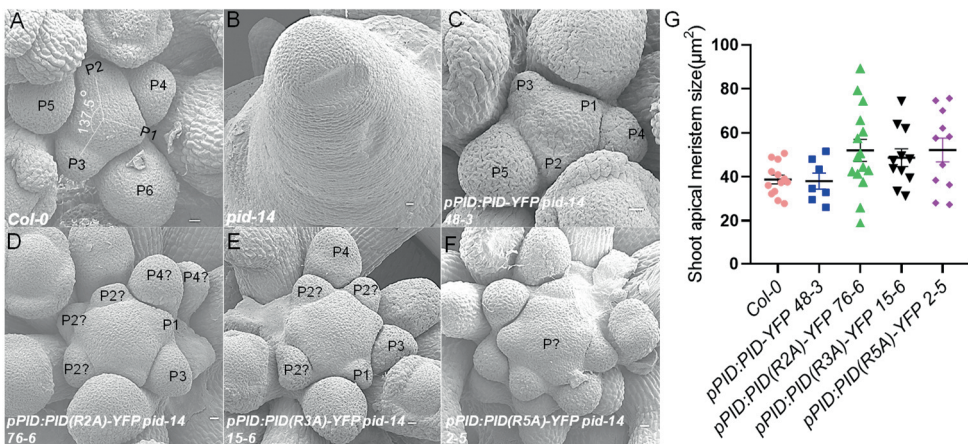


Figure 4. ‘Untouchable’ PID leads to simultaneous flower primordium initiation and increases the variation in IM size. (A-F) Scanning electron microscopy images of dissected inflorescence meristems of 7-week-old wild-type Arabidopsis (Col-0) (A) or *pid-14* (B), *pPID:PID-YFP pid-14* (C), *pPID:PID(R2A)-YFP pid-14* (D), *pPID:PID(R3A)-YFP pid-14* (E) or *pPID:PID(R5A)-YFP pid-14* (F) plants. The flower primordia are indicated with a P and the number indicates the developmental order from young to older. P? in (F) indicates that for this IM it was difficult to stage the different primordia. (G) Quantitative analysis of IM size (in μm^2) of the plant lines presented in (A). Dots, squares, triangles or diamonds indicate the sizes of individual IMs, the black line indicates the average size. A one-way ANOVA with Tukey’s test showed no significant difference in the average IM size between plant lines. However, an F-test indicated a significant increase in the variation in IM sizes in line *pPID:PID(R2A)-YFP pid-14* 76-6 ($p=0.0008$), *pPID:PID(R3A)-YFP pid-14* 15-6 ($p=0.028$), or *pPID:PID(R5A)-YFP pid-14* 2-5 ($p=0.023$), compared to Col-0, but not in line *pPID:PID-YFP pid-14* 48-3 ($p=0.192$). Size bar in (A-F) indicates 10 μm .

‘Untouchable’ PID leads to mis-positioning of PIN-generated auxin maxima in the IM.

It is well-established that auxin maxima generated by PIN1-driven PAT are the initiation points of flower primordia in the IM (Kuhlemeier and Reinhardt, 2001; Reinhardt et al., 2003; Jonsson et al., 2006; Sassi and Vernoux, 2013). More recent microscopy analysis combined with computational modelling suggests that these maxima are not fixed in space, but rather are waves of high auxin travelling through the IM in a centrifugal (outward directed) manner. The duration of exposure to high auxin was suggested to be the decisive trigger for primordium initiation (Galvan-Ampudia et al., 2020). Like PIN1, also PID has an important role in this process, as it allows the generation of auxin maxima by directing apical PIN1 localization, resulting in upward PAT through the epidermis of the IM (Friml et al., 2004; Huang et al., 2010).

In both wild-type *Arabidopsis* (Col-0) and the *pid-14* mutant complemented with wild-type PID (*pPID:PID-YFP pid-14*), the *pDR5:GFP* reporter indicated three strong auxin response maxima marking the positions of incipient primordium i(1) and primordia P1 and P2, respectively. In addition, weaker signals were observed colocalizing with the initiated primordia P3, P4 and P5, respectively (Figure 5A, C). The developmental order of the primordia, as indicated by the auxin maxima, was clear and they appeared at a divergence angle typical for the spiral phyllotaxis in *Arabidopsis*. In the *pid-14* loss-of-function mutant, no auxin response maxima were observed in the IM (Figure 5B), in line with the rootward/basal polarity of PIN1 (Figure 5F, J) and the absence of flower primordia on the pin-like inflorescences of this mutant (Figure 4B). In the *pid-14* mutant lines complemented with ‘untouchable’ PID (*pPID:PID(R5A)-YFP pid-14*) we observed a more dispersed distribution of auxin response maxima in the IM (Figure 5D). At least 6 auxin response maxima were observed, which is significantly more than the 3 to 4 observed in wild-type *Arabidopsis* (Figure 5M). Moreover, the developmental order of the incipient primordia that are marked by these auxin maxima could not be distinguished, as a clear spiral pattern of incipient primordia was absent. These results indicate that the main role of the Ca^{2+} -dependent regulation of PID kinase

activity is to control the position of primordium initiation by limiting the number of auxin response maxima in the IM.

As *PIN1* expression is auxin responsive and PID regulates PIN1 polarity, we compared *PIN1* expression and PIN1 polarity in Arabidopsis wild-type with that in the *pid-14* mutant or the different complemented lines. In wild-type Arabidopsis or in *pid-14* mutant lines complemented with wild-type PID *PIN1* was expressed throughout the L1 layer of the IM, but most strongly in flower primordia P1 to P3, where its polar localization converged towards the primordium tip (Figure 5E, G). Conversely, in the *pid-14* loss-of-function mutant we observed weaker but even *PIN1* expression in the L1 layer of the pin-like IM and predominant rootward/basal localisation of the protein (Figure 5F, J). No PIN1 convergence points were observed, in line with the absence of flower primordia (Figure 5F, J). In *pid-14* mutant lines complemented with ‘untouchable’ PID, PIN1 was also expressed throughout the L1 layer of the IM, with stronger expression at sites of incipient and young primordia. As observed for the *pDR5:GFP* reporter, the number of PIN1 convergence points was markedly higher than in wild-type IMs (Figure 5H). The confocal images did not allow us to detect obvious differences in PIN1 polarity between wild-type Arabidopsis or wild-type PID complemented lines and the ‘untouchable’ PID complemented lines. Confocal sections of IMs below the L1 layer showed 3-4 stronger signals corresponding to the convergence points in wild-type Arabidopsis or wild-type PID complemented lines, representing the pro-vascular cells with rootward-oriented PIN1 that will later form the vascular tissue connecting the newly formed organs to the existing vascular system of the plant. In the ‘untouchable’ PID complemented lines we observed 6 to 7 signals (Figure 5L), in line with the increase of the number of *pDR5:GFP* signals and PIN1 marked convergence points (Figure 5M).

These results indicate that, the altered auxin distribution in the IM is driven by the marked change of PIN1 expression pattern.

Calcium-regulated PINOID kinase activity is required for a robust spiral phyllotaxis in the Arabidopsis inflorescence

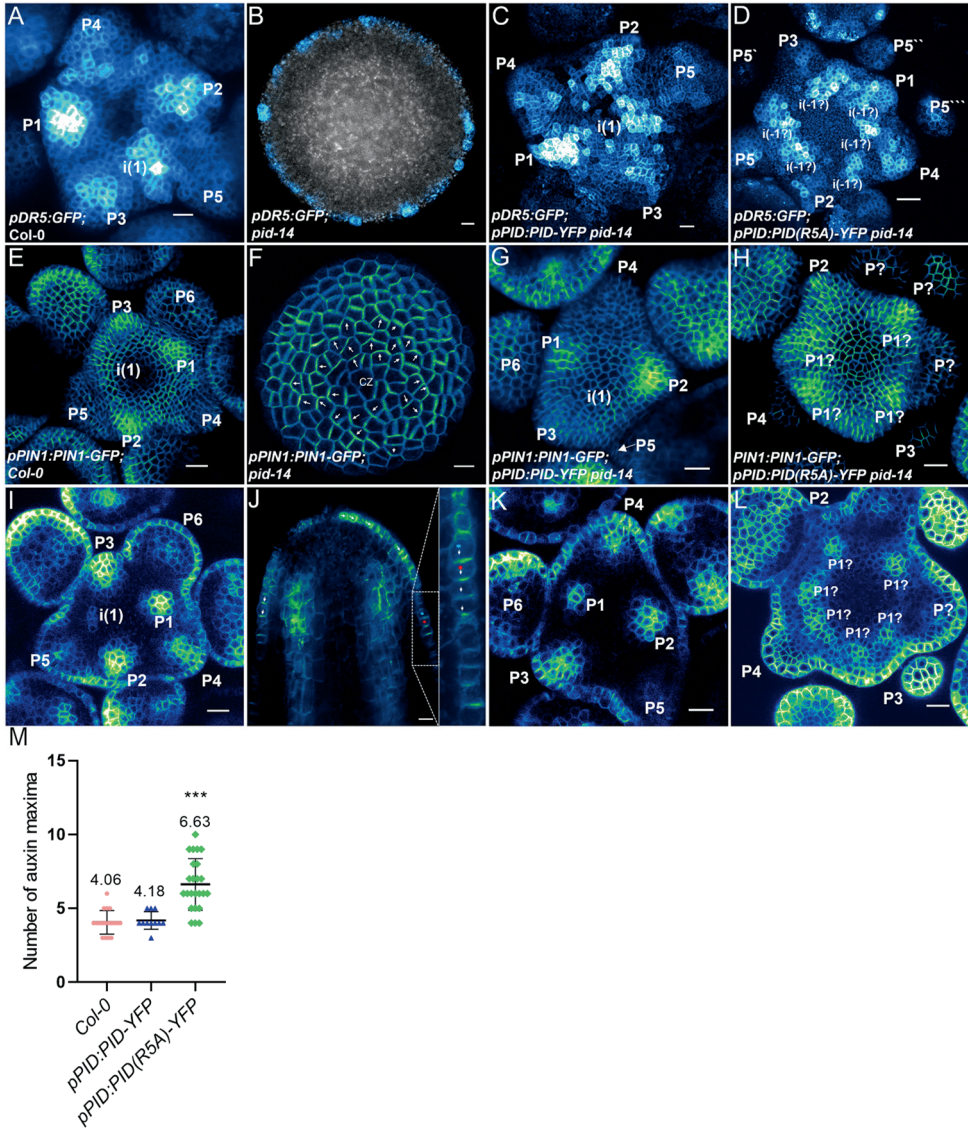


Figure 5. ‘Untouchable’ PID results in more auxin response maxima and in mis-positioned PIN1 convergence points. (A-D). Expression of *pDR5:GFP* in Col-0 (A), *pid-14* (B) and ‘untouchable’ PID mutant complementary line: *pPID:PID-YFP* (C) or *pPID:PID R5A-YFP* (D) in the homozygous *pid-14* mutant background. (E-H) 3D reconstructed top view of Arabidopsis SAMs showing the expression of *PIN1:PIN1-GFP* in Col-0 (E), *pid-14* (F), and lines containing *pPID:PID-YFP* (G), or *pPID:PID R5A-YFP* (H) in the homozygous *pid-14* mutant background. Confocal stacks obtained from *pPIN1:PIN1-GFP* expressing plants were converted into 3D. (I-L) Horizontal or longitudinal section view in (E-H) respectively. (M) Quantitative analysis of auxin maxima in the SAM of the plants presented in (A, C, D). One-way ANOVA with Tukey’s test showed significant

difference between Col-0 and *pPID:PID R5A-YFP* (***p*<0.001), but not with line *pPID:PID-YFP*. White letter P stands for primordia, the number indicates the developmental order of the primordia. CZ: central zone of SAM. i: incipient primordia. White arrow indicates the PIN1 polarity. Stars in same color indicate the same cell. Size bar indicates 10 nm in (A-D) and 20 nm in (E-L).

Discussion

Plant organs are repetitively generated at the SAM in a precise spatio-temporal pattern, known as phyllotaxis (Yin, 2021). The phytohormone auxin and its polar transport play a pivotal role in organogenesis at the SAM. Accumulating evidence suggests that calcium signalling is involved in modulating auxin responses and PAT (Dela Fuente and Leopold, 1973; Lee et al., 1984; Plieth and Trewavas, 2002; Toyota et al., 2008). In this study, we found that Ca^{2+} -dependent binding of CaM/CMLs regulates the activity of the PID kinase, an important regulator of PAT, and modulates the distribution of PIN-driven auxin maxima and patterns phyllotaxis at the SAM.

The CaM/CML-PID interaction confirms the importance of Ca^{2+} signalling in phyllotaxis

It is well established that auxin and its polar transport are necessary and sufficient for organ formation at the SAM. This is supported by the findings that inhibition of PAT, either by treatment with the PAT inhibitor N-1-naphthylphthalamic acid (NPA) or by mutations in PIN1 or PID, terminates organ initiation at the flanks of the SAM and results in the formation of pin-like inflorescences lacking flowers (Okada et al., 1991; Bennett et al., 1995; Vernoux et al., 2000; Reinhardt et al., 2000; Bohn-Courseau, 2010). Moreover, application of exogenous auxin to these pin-like apices has been shown to restore organ initiation, indicating that they are deprived of auxin and that auxin is sufficient for organ initiation at the IM (Reinhardt et al., 2000; Reinhardt et al., 2003). PIN1 is predominantly expressed in the L1 layer and in the provascular cells in the IM (Figure 5; Benková et al., 2003; Reinhardt et al., 2003; Heisler et al., 2005), where it directs auxin flux through its highly dynamic expression and polarity patterns, forming convergence points that trigger

primordium initiation by generating auxin maxima in a regular pattern (Figure 5A and E; Heisler et al., 2005; Bhatia and Heisler, 2018; Galvan-Ampudia et al., 2020). How this PIN1 dynamics is coordinated to form these convergences points in a regular pattern was still not fully understood. Several lines of evidence indicate that both exogenous and endogenous signals triggering rapid changes in $[Ca^{2+}]_{cyt}$ are involved (Zhang et al., 2011; Goh et al., 2012; Shih et al., 2015; Li et al., 2019). Our findings now provide a clear molecular basis connecting Ca^{2+} signaling to the dynamic action of the two key players in phyllotaxis, the PIN1 auxin efflux carriers and the PID protein kinase regulating their polarity and activity.

The Ca^{2+} -dependent regulation of PID activity integrates auxin and mechanical stress signaling during phyllotactic patterning.

The dynamic PIN1 convergence patterns are the result of feedback between auxin and the expression and polarity of PIN1 on the one hand, and mechanical stress in the IM caused by the continuous initiation and outgrowth of new organs on the other (Smith et al., 2006; Heisler et al., 2010; Bhatia et al., 2016; Kareem et al., 2022).

New organs in the meristem are initiated through accumulation of auxin at specific sites in the peripheral zone, and accumulation of auxin starting from the earlier steps of organ initiation (Vernoux et al., 2011; Brunoud et al., 2012). Mechanisms acting downstream of auxin that regulated PIN1 convergences have been reported, for example the AUXIN RESPONSE FACTOR 5/MONOPTEROS (ARF5/MP) (Bhatia et al., 2016; Garrett et al., 2012; Fal et al., 2017). MP positions the auxin-responsive *PIN1* expression, thereby facilitating a positive feedback loop that results in periodic organ formation (Bhatia et al., 2016). Disruption of MP-mediated auxin signalling or the auxin positive feedback loop causes ectopic PIN1 expression, thereby disturbing the position of auxin maxima leading to altered floral phyllotaxis (Garrett et al., 2012; Fal et al., 2017).

The initiation of primordia at the SAM is associated with the presence of high mechanical stress levels (Lyndon, 1998; Uyttewaal et al., 2012). Of the genes encoding CaM/CML sensor proteins, particularly *CaM1/TCH1* and *CML12/TCH3* are of interest, as these genes have been shown to be highly upregulated in response to mechanical stress and auxin and mechanical stress, respectively (Braam and Davis, 1990; Braam et al., 1997; McCormack et al., 2005; Chapter 2). Based on these findings and the results presented in this chapter we hypothesize that the continuous organ initiation and growth at the SAM leads to dynamic local increases in mechanical stress that trigger elevation of $[Ca^{2+}]_{cyt}$ together with an increased Ca^{2+} sensing capacity by in the elevated expression of *CaM/CML* genes. Binding of Ca^{2+} activates the CaM/CMLs (Ca^{2+} -CaM/CMLs), which in turn inhibit PID activity by binding to this kinase, leading to reduced PIN1 phosphorylation and resulting in local changes in PIN1 polarity and activity. This local inactivation of PIN1 is required to pin point the position of the next PIN1 convergence point directing auxin maxima-induced organ initiation (Figure 6). In the *pid* mutant lines expressing ‘untouchable’ PID, this controlled positioning as a result of the feedback of auxin and mechanical stress on PAT processes in the SAM is absent, leading to mispositioning and erroneous timing of organ initiation. Phenotypes of the Arabidopsis *katanin1* mutant provide support for this hypothesis. KATANIN1 (KTN1) is a microtubule severing protein, and the *ktn1* mutant is defective in cortical microtubule bundling, which prevents oriented cellulose deposition (Bichet et al., 2001; Burk and Ye, 2002), resulting in a reduced global response to mechanical stress at the SAM (Uyttewaal et al., 2012) and thus in a perturbed phyllotaxis (Jackson et al., 2019). Where exactly in the SAM auxin feedback and mechanical stress come together to decrease PID activity still needs to be established. The most likely position is just distal to where the new convergence point should be established. As the reduction in PID activity is likely to be very transient, changes in PIN polarity may not reveal this position. Instead, the use of

more recently developed Ca^{2+} reporters combined with reporters that show the PID-CaM/CML interaction itself may provide more insight into this matter.

In summary, our results reveal a novel mechanism by which Ca^{2+} -dependent control of PID activity through the CaM/CML sensor proteins plays a crucial role in coordinating auxin distribution at the SAM and maintaining the normal phyllotaxis pattern through regulation of PIN1 convergence points (Figure 6). In the absence of PID, basal polarity of PIN1 deprives the SAM of auxin, resulting in pin-like inflorescences that lack organ initiation. When the Ca^{2+} -dependent control of PID activity is removed, this leads to mispositioning of primordium initiation and often to co-initiation of primordia, resulting in inflorescences with aberrant phyllotactic patterns and more flowers compared to wild type (Figure 6).

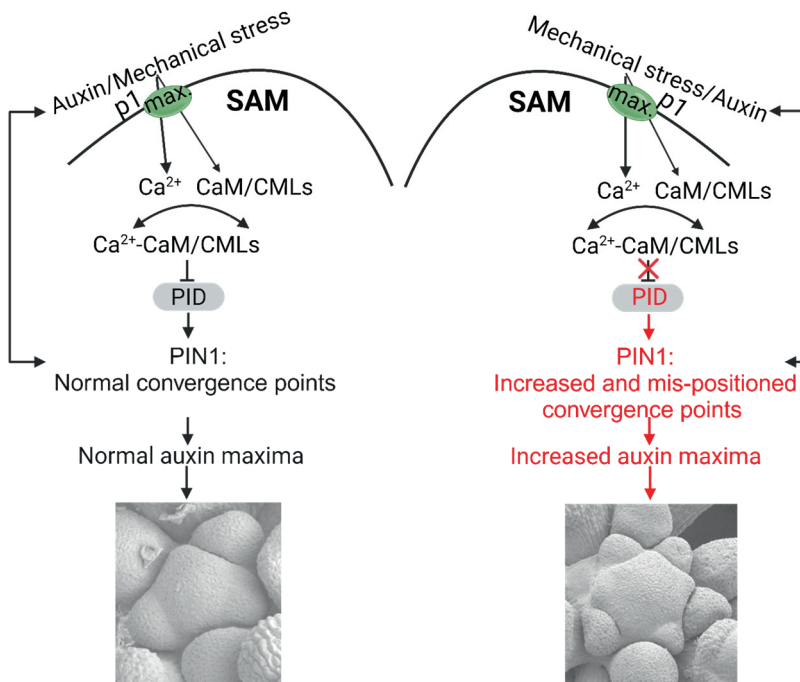


Figure 6. A model showing the involvement of CaM/CMLs-PID complex in patterning phyllotaxis. Mechanical stress and auxin induce the high expression of the major Ca^{2+} sensors *CaM/CMLs* and trigger elevation of $[\text{Ca}^{2+}]_{\text{cyt}}$, which activates the *CaM/CMLs* (Ca^{2+} -*CaM/CMLs*). Ca^{2+} -*CaM/CMLs* suppresses PID kinase activity and thereby affect the expression pattern of its phosphorylation target, PIN1 protein. Expression pattern of PIN1 then instructs the auxin distribution at the SAM thus patterning phyllotaxis.

Material and Methods

Arabidopsis lines and plant growth

All Arabidopsis lines are in the Col-0 background. The *pid-14* loss-of-function mutant and the *pPIN1:PIN1-GFP* and *pDR5:GFP* reporter lines were described previously (Friml et al., 2004; Benkova et al., 2003). Arabidopsis transgenic lines in the homozygous *pid-14* mutant background, *pPID:PID-YFP pid-14*, *pPID:PID(R2A)-YFP pid-14*, *pPID:PID(R3A)-YFP pid-14* and *pPID:PID(R5A)-YFP pid14* are described in Chapter 3.

For the seed germination on sterile medium, seeds were surface sterilized by incubating 1 min in 70% ethanol and 10 min in bleach solution containing 1% chlorine. Sterilized seeds were subsequently washed three times with sterile dH₂O, kept in the dark at 4°C for two days for vernalization and germinated on vertical plates containing 0.5× Murashige and Skoog (1/2 MS) Duchefa medium with 0.05% MES, 1% Daishin agar (Duchefa) and 1% sucrose at 22 °C and 16 hours photoperiod. Plants grown on soil were cultured at 21°C, 16 hours photoperiod and 70% relative humidity.

Phenotypic analysis and microscopy

Seedlings on plates, soil grown plants and inflorescence details were photographed with a Nikon D5300 camera. The primary root length of seedlings was measured with ImageJ (Fiji) and analysed with GraphPad Prism 5.

The phyllotactic pattern was assessed on fully grown inflorescences of 8-week-old plants. Divergence angles were measured as described in Peaucelle et al. (2007). IMs were dissected from inflorescences of 5-week-old plants and placed with the bottom internode in a drop of 1% low melting point agarose and observed with a Nikon AX Confocal microscope using a 40x long working distance water dipping objective. The fluorescent signal from the *pDR5:GFP* or *pPIN1:PIN1-GFP* reporters was monitored using an argon laser for excitation at 488 nm and a 505-160

Calcium-regulated PINOID kinase activity is required for a robust spiral phyllotaxis in the *Arabidopsis* inflorescence

530nm band pass emission filter. Images were processed using Image J. For scanning electron microscopy (SEM) imaging, IMs were dissected from inflorescences of 7-week-old plants and fixed in 2% paraformaldehyde (PFA) and 1% glutaraldehyde in 1× phosphate-buffer saline (PBS) for two hours at 21 °C and subsequently overnight at 4 °C. Fixed IMs were washed twice with 1× PBS and dehydrated using an acetone series (70%, 80%, 90%, 100%) under vacuum. The samples were subsequently transferred to a Bal-Tec CDP030 critical point drier, where the acetone was replaced by liquid carbon dioxide. IMs were fixed to stubs and sputter coated with gold using SEM Coating unit 5100 (Polaron Equipment Ltd.). Gold was discharged by admitting pressurized argon in a low vacuum environment. Coated IMs were kept in dry under vacuum and were imaged with a JEOL SEM 6400 scanning electron microscope.

The size of IMs was measured using scanning electron microscopy (SEM) SAM images with the method as described in (Shi et al., 2018), the number of auxin maxima were counted using confocal microscope images. All data were analyzed and plotted into graphs in GraphPad Prism 8.

RNA extraction and RT-PCR

Vertically grown 5-day-old seedlings were collected and total RNA was extracted using the NucleoSpin RNA Plant kit (Macherey Nagel, #740949). Reverse transcription (RT) was performed using the RevertAid Reverse Transcription Kit (Thermo Scientific™, #K1691). qRT-PCR was performed in the CFX96 Touch™ Real-Time PCR Detection System (Bio-Rad) using TB Green® Premix Ex Taq™ II (Tli RNase H Plus) (Takara, #RR820B). primers used are: PP2A-3-qRT-FP: GATGGATACAACTGGGCTCACG3; PP2A-3-qRT-RP: TCGGTGCTGGTTCAAACCTGG3; PID-qRT-FP: ATTTACACTCTCTCCGTCATAGACAAC3; PID-qRT-RP: ACATGTGTAGATATTCTAACGCCACTA

Accession numbers

Arabidopsis Genome Initiative locus identifiers for the genes mentioned are as follows: CML12/TCH3 (At2g41100), PID (At2g34650), PIN1(AT1G73590)

Acknowledgements

The authors would like to thank Gerda Lamers and Joost Willemse for their help with the microscopy, Ward de Winter and Jan Vink for help with medium, tissue culture and plant caretaking. This author was supported by the China Scholarship Council.

Author contribution

Remko Offringa, Xiaoyu Wei designed the experiments, Xiaoyu Wei performed the experiments and data analysis, Xiaoyu Wei and Remko Offringa wrote and finalized the Chapter.

Calcium-regulated PINOID kinase activity is required for a robust spiral phyllotaxis in the Arabidopsis inflorescence

Supplementary data:

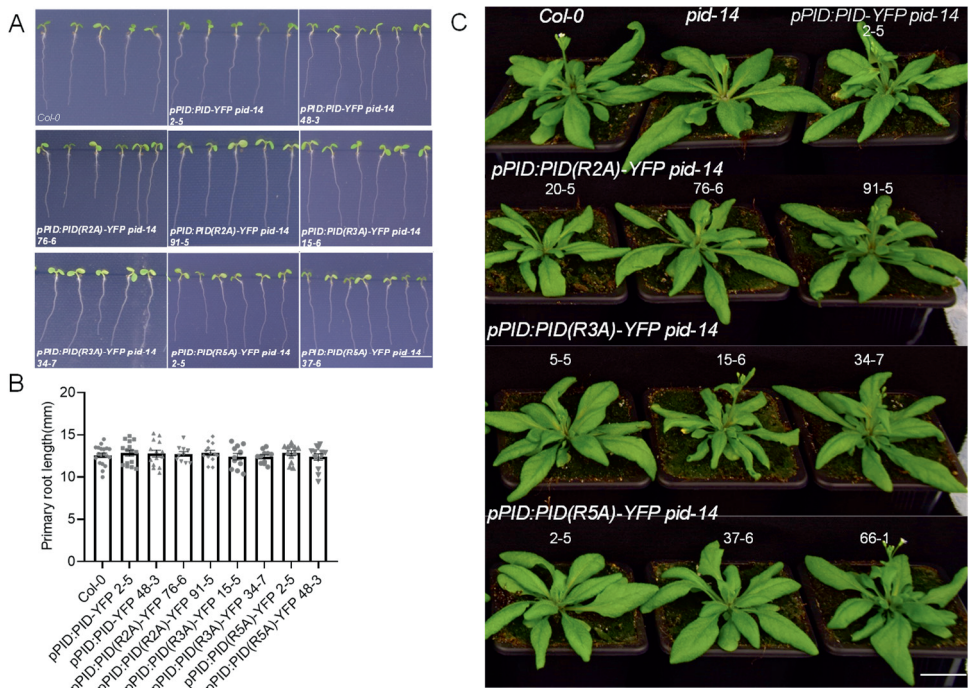


Figure S1. Seedlings and bolting plants of *pPID:PID(R→A)-YFP pid-14* lines show no obvious phenotypic differences from wild-type Arabidopsis (Col-0) or *pPID:PID-YFP pid-14* control lines. . (A) 5-day-old seedlings of wild-type Arabidopsis (Col-0) or *pPID:PID-YFP pid-14*, *pPID:PID(R2A)-YFP pid-14*, *pPID:PID(R3A)-YFP pid-14* or *pPID:PID(R5A)-YFP pid-14* plants. (B) Quantification of primary root length of 5-day-old seedlings in (A). Results of a representative triplicate experiment are shown. Bars represent means, error bars the SEM, and dots the values of the individual seedlings (n=11-14). A one-way ANOVA with Tukey's test detected no significant differences between the tested plant lines. (C) 6-week-old bolting plants of wild-type Arabidopsis (Col-0) or or *pPID:PID-YFP pid-14*, *pPID:PID(R2A)-YFP pid-14*, *pPID:PID(R3A)-YFP pid-14* or *pPID:PID(R5A)-YFP pid-14* plants. Size bar in indicates 5 mm in (A), 2 cm in (B).

Reference:

- Adamowski, M., & Friml, J. (2015).** PIN-dependent auxin transport: action, regulation, and evolution. *Plant Cell* 27: 20–32.
- Barbosa, I. C., Hammes, U. Z., & Schwechheimer, C. (2018).** Activation and polarity control of PIN-FORMED auxin transporters by phosphorylation. *Trends Plant Sci.* 23: 523-538.
- Benjamins, R., Ampudia, C.S., Hooykaas, P.J., & Offringa, R. (2003).** PINOID-mediated signaling involves calcium-binding proteins. *Plant Physiol.* 132: 1623-1630.
- Benková, E., Michniewicz, M., Sauer, M., Teichmann, T., Seifertová, D., Jürgens, G., & Friml, J. (2003).** Local, efflux-dependent auxin gradients as a common module for plant organ formation. *Cell* 115: 591-602.
- Benková, E., Michniewicz, M., Sauer, M., Teichmann, T., Seifertová, D., Jürgens, G., & Friml, J. (2003).** Local, efflux-dependent auxin gradients as a common module for plant organ formation. *Cell* 115: 591-602.
- Bennett, S. R., Alvarez, J., Bossinger, G., & Smyth, D. R. (1995).** Morphogenesis in *pinoid* mutants of *Arabidopsis thaliana*. *Plant J.* 8: 505-520.
- Bhatia, N., & Heisler, M. G. (2018).** Self-organizing periodicity in development: organ positioning in plants. *Development* 145: dev149336.
- Bhatia, N., Bozorg, B., Larsson, A., Ohno, C., Jönsson, H., & Heisler, M. G. (2016).** Auxin acts through MONOPTEROS to regulate plant cell polarity and pattern phyllotaxis. *Curr. Biol.* 26: 3202-3208.
- Bichet, A., Desnos, T., Turner, S., Grandjean, O., & Höfte, H. (2001).** BOTERO1 is required for normal orientation of cortical microtubules and anisotropic cell expansion in *Arabidopsis*. *Plant J.* 25: 137-148.
- Bohn-Courseau, I. (2010).** Auxin: a major regulator of organogenesis. *C. R. Biol.* 333: 290-296.
- Braam, J., & Davis, R. W. (1990).** Rain-, wind-, and touch-induced expression of calmodulin and calmodulin-related genes in *Arabidopsis*. *Cell* 60: 357-364.
- Braam, J., Sistrunk, M. L., Polisensky, D. H., Xu, W., Purugganan, M. M., Antosiewicz, D. M., ... & Johnson, K. A. (1997).** Plant responses to environmental stress: regulation and functions of the *Arabidopsis* TCH genes. *Planta* 203: S35-S41.
- Brunoud, G., Wells, D. M., Oliva, M., Larrieu, A., Mirabet, V., Burrow, A. H., ... & Vernoux, T. (2012).** A novel sensor to map auxin response and distribution at high spatio-temporal resolution. *Nature* 482: 103-106.

- Burk, D. H., & Ye, Z. H.** (2002). Alteration of oriented deposition of cellulose microfibrils by mutation of a katanin-like microtubule-severing protein. *Plant Cell* 14: 2145-2160.
- Byrne, M. E., Groover, A. T., Fontana, J. R., & Martienssen, R. A.** (2003). Phyllotactic pattern and stem cell fate are determined by the *Arabidopsis* homeobox gene *BELLRINGER*. *Development* 17: 3941-50.
- Dela Fuente, R.K., and Leopold, A.C.** (1973). A role for calcium in auxin transport. *Plant Physiol.* 51: 845-847.
- Dhonukshe, P., Huang, F., Galvan-Ampudia, C. S., Mähönen, A. P., Kleine-Vehn, J., Xu, J., ... & Offringa, R.** (2010). Plasma membrane-bound AGC3 kinases phosphorylate PIN auxin carriers at TPRXS (N/S) motifs to direct apical PIN recycling. *Development* 137: 3245-3255.
- Dory, M., Hatzimasoura, E., Kállai, B. M., Nagy, S. K., Jäger, K., Darula, Z., ... & Dóczi, R.** (2018). Coevolving MAPK and PID phosphosites indicate an ancient environmental control of PIN auxin transporters in land plants. *FEBS Lett.* 592: 89-102.
- Fal, K., Liu, M., Duisembekova, A., Refahi, Y., Haswell, E. S., & Hamant, O.** (2017). Phyllotactic regularity requires the Paf1 complex in *Arabidopsis*. *Development* 144: 4428-4436.
- Friml, J., Vieten, A., Sauer, M., Weijers, D., Schwarz, H., Hamann, T., ... & Jürgens, G.** (2003). Efflux-dependent auxin gradients establish the apical-basal axis of *Arabidopsis*. *Nature* 426: 147-153.
- Friml, J., Yang, X., Michniewicz, M., Weijers, D., Quint, A., Tietz, O., ... & Offringa, R.** (2004). A PINOID-dependent binary switch in apical-basal PIN polar targeting directs auxin efflux. *Science* 306: 862-865.
- Furutani, M., Nakano, Y., & Tasaka, M.** (2014). MAB4-induced auxin sink generates local auxin gradients in *Arabidopsis* organ formation. *Proceedings of the National Academy of Sciences* 111: 1198-1203.
- Galvan-Ampudia, C. S., Cerutti, G., Legrand, J., Brunoud, G., Martin-Arevalillo, R., Azais, R., ... & Vernoux, T.** (2020). Temporal integration of auxin information for the regulation of patterning. *Elife* 9: e55832.
- Galvan-Ampudia, C. S., Cerutti, G., Legrand, J., Brunoud, G., Martin-Arevalillo, R., Azais, R., ... & Vernoux, T.** (2020). Temporal integration of auxin information for the regulation of patterning. *Elife* 9: e55832.
- Garrett, J. J., Meents, M. J., Blackshaw, M. T., Blackshaw, L. C., Hou, H., Styranko, D. M., ... & Schultz, E. A.** (2012). A novel, semi-dominant allele of

MONOPTEROS provides insight into leaf initiation and vein pattern formation. *Planta* 236: 297-312.

Goh, C. S., Lee, Y., & Kim, S. H. (2012). Calcium could be involved in auxin-regulated maintenance of the quiescent center in the Arabidopsis root. *J. Plant Biol.* 55: 143-150.

Heisler, M. G., Hamant, O., Krupinski, P., Uyttewaal, M., Ohno, C., Jönsson, H., ... & Meyerowitz, E. M. (2010). Alignment between PIN1 polarity and microtubule orientation in the shoot apical meristem reveals a tight coupling between morphogenesis and auxin transport. *PLoS Biol.* 8: e1000516.

Heisler, M. G., Ohno, C., Das, P., Sieber, P., Reddy, G. V., Long, J. A., & Meyerowitz, E. M. (2005). Patterns of auxin transport and gene expression during primordium development revealed by live imaging of the Arabidopsis inflorescence meristem. *Curr. Biol.* 15: 1899-1911.

Huang, F., Kemel Zago, M., Abas, L., van Marion, A., Galván-Ampudia, C. S., & Offringa, R. (2010). Phosphorylation of conserved PIN motifs directs Arabidopsis PIN1 polarity and auxin transport. *Plant Cell* 22: 1129-1142.

Jackson, M. D., Duran-Nebreda, S., Kierzkowski, D., Strauss, S., Xu, H., Landrein, B., ... & Bassel, G. W. (2019). Global topological order emerges through local mechanical control of cell divisions in the Arabidopsis shoot apical meristem. *Cell Syst.* 8: 53-65.

Jean, R. V., & Barab, D. (1998). Symmetry in plants . *J. Plant Physiol.* 157: 356.

Jia, W., Li, B., Li, S., Liang, Y., Wu, X., Ma, M., ... & Wang, Y. (2016). Mitogen-activated protein kinase cascade MKK7-MPK6 plays important roles in plant development and regulates shoot branching by phosphorylating PIN1 in Arabidopsis. *PLoS Biol.* 14: e1002550.

Jönsson, H., Heisler, M. G., Shapiro, B. E., Meyerowitz, E. M., & Mjolsness, E. (2006). An auxin-driven polarized transport model for phyllotaxis. *Proc. Natl. Acad. Sci. U.S.A.* 103: 1633-1638.

Kareem, A., Bhatia, N., Ohno, C., & Heisler, M. G. (2022). PIN-FORMED1 polarity in the plant shoot epidermis is insensitive to the polarity of neighboring cells. *Iscience* 25: 105062.

Keinath, N. F., Waadt, R., Brugman, R., Schroeder, J. I., Grossmann, G., Schumacher, K., & Krebs, M. (2015). Live cell imaging with R-GECO1 sheds light on flg22-and chitin-induced transient [Ca²⁺] cyt patterns in Arabidopsis. *Mol. Plant* 8: 1188-1200.

Kleine-Vehn, J., Wabnik, K., Martiniere, A., Langowski, L., Willig, K., Naramoto, S., ... & Friml, J. (2011). Recycling, clustering, and endocytosis

jointly maintain PIN auxin carrier polarity at the plasma membrane. *Mol. Syst. Biol.* 7: 540.

Kuhlemeier, C., & Reinhardt, D. (2001). Auxin and phyllotaxis. *Trends Plant Sci.* 6: 187-189.

Landrein, B., Lathe, R., Bringmann, M., Vouillot, C., Ivakov, A., Boudaoud, A., ... & Hamant, O. (2013). Impaired cellulose synthase guidance leads to stem torsion and twists phyllotactic patterns in Arabidopsis. *Curr. Biol.* 23: 895-900.

Landrein, B., Refahi, Y., Besnard, F., Hervieux, N., Mirabet, V., Boudaoud, A., ... & Hamant, O. (2015). Meristem size contributes to the robustness of phyllotaxis in Arabidopsis. *J. Exp. Bot.* 66: 1317-1324.

Lee, H., Ganguly, A., Baik, S., & Cho, H. T. (2021). Calcium-dependent protein kinase 29 modulates PIN-FORMED polarity and Arabidopsis development via its own phosphorylation code. *Plant Cell* 33: 3513-3531.

Lee, J. S., Mulkey, T. J., & Evans, M. L. (1984). Inhibition of polar calcium movement and gravitropism in roots treated with auxin-transport inhibitors. *Planta* 160: 536-543.

Li, T., Yan, A., Bhatia, N., Altinok, A., Afik, E., Durand-Smet, P., ... & Meyerowitz, E. M. (2019). Calcium signals are necessary to establish auxin transporter polarity in a plant stem cell niche. *Nat. Commun.* 10: 726.

Lyndon, R. F. (1998). The shoot apical meristem: its growth and development. Cambridge University Press.

Marhava, P., Bassukas, A. E. L., Zourelidou, M., Kolb, M., Moret, B., Fastner, A., ... & Hardtke, C. S. (2018). A molecular rheostat adjusts auxin flux to promote root protophloem differentiation. *Nature* 558: 297-300.

McCormack, E., Tsai, Y. C., & Braam, J. (2005). Handling calcium signaling: arabidopsis CaMs and CMLs. *Trends Plant Sci.* 10: 383-389.

Monshausen, G. B., Miller, N. D., Murphy, A. S., & Gilroy, S. (2011). Dynamics of auxin-dependent Ca²⁺ and pH signaling in root growth revealed by integrating high-resolution imaging with automated computer vision-based analysis. *Plant J.* 65: 309-318.

Nakayama, N., Smith, R. S., Mandel, T., Robinson, S., Kimura, S., Boudaoud, A., & Kuhlemeier, C. (2012). Mechanical regulation of auxin-mediated growth. *Curr. Biol.* 22: 1468-1476.

Okada, K., Ueda, J., Komaki, M. K., Bell, C. J., & Shimura, Y. (1991). Requirement of the auxin polar transport system in early stages of Arabidopsis floral bud formation. *Plant Cell* 3: 677-684.

- Peaucelle, A., Morin, H., Traas, J., & Laufs, P.** (2007). Plants expressing a miR164-resistant CUC2 gene reveal the importance of post-meristematic maintenance of phyllotaxy in Arabidopsis. *Development* 6: 1045-50.
- Petrásek, J., Mravec, J., Bouchard, R., Blakeslee, J. J., Abas, M., Seifertová, D., ... & Friml, J.** (2006). PIN proteins perform a rate-limiting function in cellular auxin efflux. *Science* 312: 914-918.
- Plieth, C., & Trewavas, A. J.** (2002). Reorientation of seedlings in the earth's gravitational field induces cytosolic calcium transients. *Plant Physiol.* 129: 786-796.
- Rademacher, E. H., & Offringa, R.** (2012). Evolutionary adaptations of plant AGC kinases: from light signaling to cell polarity regulation. *Front. Plant Sci.* 3: 250.
- Reinhardt, D., Mandel, T., & Kuhlemeier, C.** (2000). Auxin regulates the initiation and radial position of plant lateral organs. *Plant Cell* 12: 507-518.
- Reinhardt, D., Pesce, E. R., Stieger, P., Mandel, T., Baltensperger, K., Bennett, M., ... & Kuhlemeier, C.** (2003). Regulation of phyllotaxis by polar auxin transport. *Nature* 426: 255-260.
- Rigó, G., Ayaydin, F., Tietz, O., Zsigmond, L., Kovács, H., Páy, A., ... & Cséplő, Á.** (2013). Inactivation of plasma membrane-localized CDPK-RELATED KINASE5 decelerates PIN2 exocytosis and root gravitropic response in Arabidopsis. *Plant Cell* 25: 1592-1608.
- Roberts, D. M., & Harmon, A. C.** (1992). Calcium-modulated proteins: targets of intracellular calcium signals in higher plants. *Annu. Rev. Plant Biol.* 43: 375-414.
- Rudd, J. J., & Franklin-Tong, V. E.** (1999). Calcium signaling in plants. *Cell. Mol. Life Sci.* 55: 214-232.
- Santin, F., Bhogale, S., Fantino, E., Grandellis, C., Banerjee, A. K., & Ulloa, R. M.** (2017). Solanum tuberosum StCDPK1 is regulated by miR390 at the posttranscriptional level and phosphorylates the auxin efflux carrier StPIN4 in vitro, a potential downstream target in potato development. *Physiol. Plant.* 159: 244-261.
- Sassi, M., & Vernoux, T.** (2013). Auxin and self-organization at the shoot apical meristem. *J. Exp. Bot.* 64: 2579-2592.
- Shi, B., Guo, X., Wang, Y., Xiong, Y., Wang, J., Hayashi, K. I., ... & Jiao, Y.** (2018). Feedback from lateral organs controls shoot apical meristem growth by modulating auxin transport. *Dev. Cell* 44: 204-216.

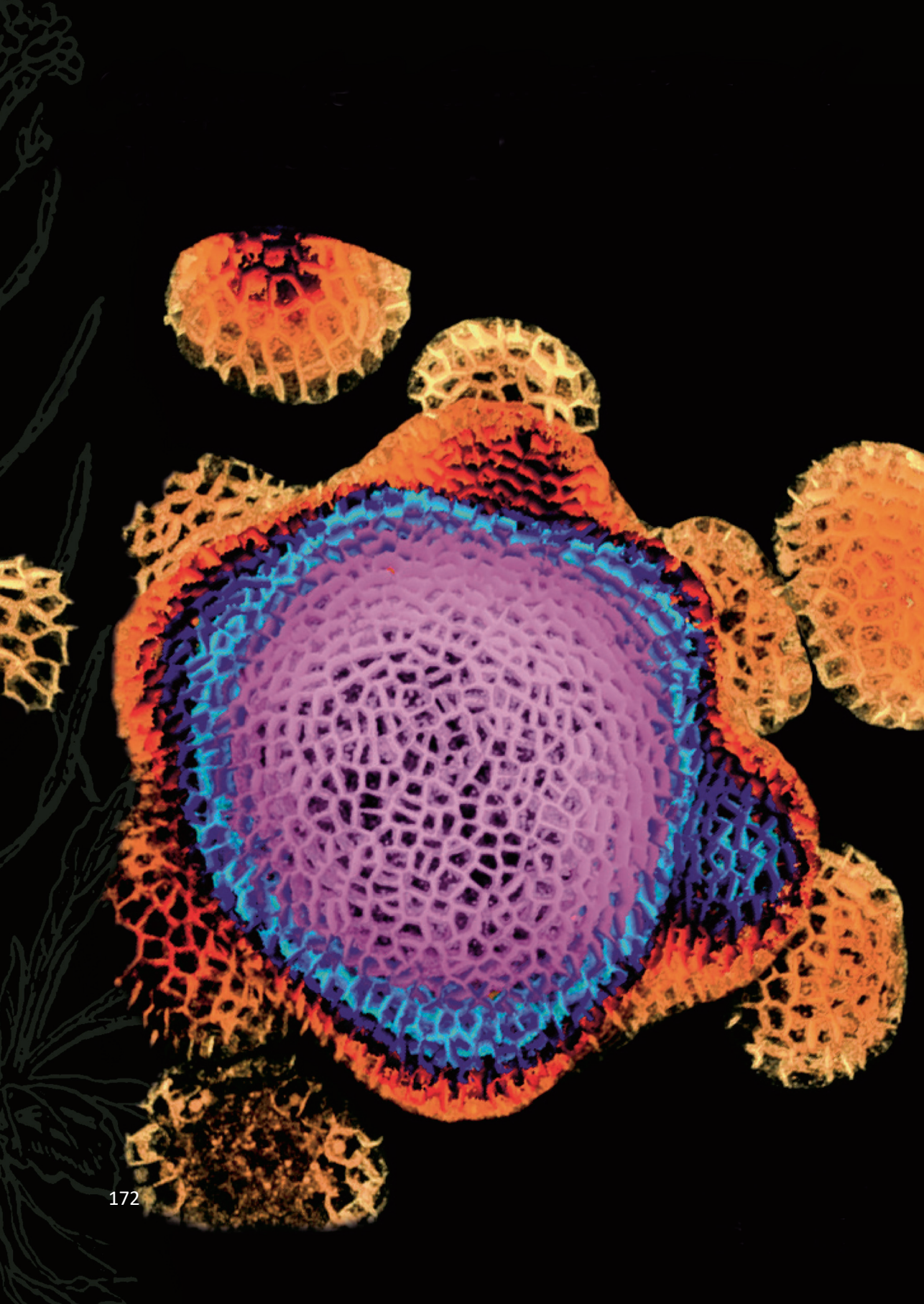
- Shih, H. W., DePew, C. L., Miller, N. D., & Monshausen, G. B.** (2015). The Cyclic Nucleotide-Gated Channel CNGC14 Regulates Root Gravitropism in *Arabidopsis thaliana*. *Curr. Biol.* 25: 3119–3125.
- Smith, R. S., Guyomarc'h, S., Mandel, T., Reinhardt, D., Kuhlemeier, C., & Prusinkiewicz, P.** (2006). A plausible model of phyllotaxis. *Proc. Natl. Acad. Sci. U.S.A.* 103: 1301–1306.
- Stoma, S., Lucas, M., Chopard, J., Schaedel, M., Traas, J., & Godin, C.** (2008). Flux-based transport enhancement as a plausible unifying mechanism for auxin transport in meristem development. *PLoS Comput. Biol.* 4: e1000207.
- Toyota, M., Furuichi, T., Tatsumi, H., & Sokabe, M.** (2008). Critical consideration on the relationship between auxin transport and calcium transients in gravity perception of *Arabidopsis* seedlings. *Plant Signal. Behav.* 3: 521-524.
- Uyttewaal, M., Burian, A., Alim, K., Landrein, B., Borowska-Wykręć, D., Dedieu, A., ... & Hamant, O.** (2012). Mechanical stress acts via katanin to amplify differences in growth rate between adjacent cells in *Arabidopsis*. *Cell* 149: 439-451.
- Vanneste, S., & Friml, J.** (2009). Auxin: a trigger for change in plant development. *Cell* 136: 1005–1016.
- Vernoux, T., Brunoud, G., Farcot, E., Morin, V., Van den Daele, H., Legrand, J., ... & Traas, J.** (2011). The auxin signalling network translates dynamic input into robust patterning at the shoot apex. *Mol. Syst. Biol.* 7: 508.
- Vernoux, T., Kronenberger, J., Grandjean, O., Laufs, P., & Traas, J.** (2000). PIN-FORMED 1 regulates cell fate at the periphery of the shoot apical meristem. *Development* 127: 5157-5165.
- Vogel, H. J.** (1994). Calmodulin: a versatile calcium mediator protein. *Biochem. Cell Biol.* 72: 357-376.
- Wisniewska, J., Xu, J., Seifertová, D., Brewer, P. B., Ruzicka, K., Blilou, I., ... & Friml, J.** (2006). Polar PIN localization directs auxin flow in plants. *Science* 312: 883-883.
- Xu, T., Niu, J., & Jiang, Z.** (2022). Sensing mechanisms: Calcium signaling mediated abiotic stress in plants. *Front. Plant Sci.* 13: 925863.
- Xue, Z., Liu, L., & Zhang, C.** (2020). Regulation of shoot apical meristem and axillary meristem development in plants. *Int. J. Mol. Sci.* 21: 2917.
- Yin, X.** (2021). Phyllotaxis: From classical knowledge to molecular genetics. *J. Plant Res.* 134: 373-401.

Zhang, J., Vanneste, S., Brewer, P. B., Michniewicz, M., Grones, P., Kleine-Vehn, J., ... & Friml, J. (2011). Inositol trisphosphate-induced Ca^{2+} signaling modulates auxin transport and PIN polarity. *Dev. Cell* 20: 855-866.

Zourelidou, M., Absmanner, B., Weller, B., Barbosa, I. C., Willige, B. C., Fastner, A., ... & Schwechheimer, C. (2014). Auxin efflux by PIN-FORMED proteins is activated by two different protein kinases, D6 PROTEIN KINASE and PINOID. *Elife* 3: e02860.

Zwiewka, M., Bilanovičová, V., Seifu, Y. W., & Nodzyński, T. (2019). The nuts and bolts of PIN auxin efflux carriers. *Front. Plant Sci.* 10: 985.

Calcium-regulated PINOID kinase activity is required for a robust spiral phyllotaxis in the
Arabidopsis inflorescence



Summary

Due to their sessile nature, plants have evolved an intricate system to survive in their ever-changing and often unfavourable environment. The plant hormone auxin plays a central role in this system, as it regulates very basic cellular processes, including cell division, growth and differentiation. As a result, it is involved in an extraordinarily broad variety of biological mechanisms to promote and influence plant growth and development in response to a wide range of endogenous and environmental signals.

Over the past decades, a wealth of information has been produced on the biosynthesis, metabolism, transport and signalling of this hormone. In **Chapter 1**, we review some of these mechanisms, focussing on auxin perception and signal transduction, its distribution by polar auxin transport (PAT) driven by the PIN-FORMED (PIN) auxin efflux carriers, and how the bivalent cation calcium (Ca^{2+}), a universal second messenger, is involved in translating both endogenous and environmental signals into auxin-mediated developmental and growth responses. Intensive research in the last decades has revealed several signalling routes for auxin. Firstly, there is the canonical nuclear auxin signalling pathway, involving the TRANSPORT INHIBITOR RESPONSE 1 (TIR1)/AUXIN-SIGNALING F-BOX (AFB) F-box proteins that through auxin-mediated recruitment and ubiquitination of Aux/IAA repressors liberate AUXIN RESPONSE FACTORS (ARFs) to activate auxin responsive gene transcription. Secondly, the AUXIN BINDING PROTEIN 1 (ABP1) signalling pathway has been revamped by the finding that coordinated binding of auxin to ABP1 and the receptor-like TRANSMEMBRANE KINASE 1 (TMK1) activates signalling at the PM, leading to e.g. cell wall acidification by activation of H^+ -ATPases. Moreover, identification of the role of the S-Phase Kinase-Associated Protein 2A (SKP2A), ARF3, and IAA32/33/34 has provided a better understanding of the complexity of the cellular auxin response machinery. Subsequently, we review the current advances and

understanding of PIN-driven PAT. The directionality and rate of intercellular auxin flow is mainly dependent on the asymmetric localisation and activity of PIN proteins at the PM, which involves Ca^{2+} signalling and is regulated by phosphorylation of their central hydrophilic loop by plant-specific AGC protein kinases.

One of these protein kinases in *Arabidopsis thaliana* (Arabidopsis), the AGC3 kinase PINOID (PID), is a key regulator of PAT, acting as a binary switch in apical-basal polar targeting of PIN auxin efflux carriers, thereby determining the direction of auxin flow. PID was found to interact with CALMODULIN-LIKE 12/TOUCH 3 (CML12/TCH3) and the EF hand containing PID-BINDING PROTEIN 1 (PBP1) in a Ca^{2+} dependent manner, providing one of the first molecular insights into how Ca^{2+} could possibly affect PAT. CML12/TCH3 binding negatively regulates PID kinase activity both *in vitro* and *in vivo*, and its interaction with CML12/TCH3 sequesters PID from the plasma membrane (PM) to the cytosol, in a Ca^{2+} - and auxin-dependent manner. Moreover, increased local auxin levels trigger a transient increase in cytosolic Ca^{2+} levels ($[\text{Ca}^{2+}]_{\text{cyt}}$) and a rapid and substantial up-regulation of *CML12/TCH3* expression. Therefore, building upon these previous findings, at the end of **Chapter 1** an alternative model for auxin feedback regulation of PIN polarity is proposed, involving Ca^{2+} -CML12/TCH3-PID signalling.

In **Chapter 2**, we conducted further studies on the Ca^{2+} -regulated PID kinase. The *tch3* loss-of-function mutant showed only a mild phenotype, strongly suggesting that CaMs and other CMLs function redundantly with CML12/TCH3. Consequently, our first step was to test the interaction of the closely related homologs of CML12/TCH3 with PID.

Through *in vitro* pull-downs and Bimolecular Fluorescence Complementation (BiFC) assays, we showed that a confined clade comprising seven CaMs and three CMLs (CML8, CML10, CML11) most closely related to CML12/TCH3 also interact with PID. In Arabidopsis protoplasts, co-expression of these CaM/CMLs

and PID in the presence of auxin resulted in dissociation of PID from the plasma membrane (PM). To gain a deeper understanding, we conducted a comparative study on the spatio-temporal expression of the corresponding *CaM/CML* genes and *PID* using *promoter:GUS* reporter fusions. This analysis revealed differential but largely overlapping expression patterns in most tissues throughout all developmental stages.

These results suggested functional redundancy among these CaM/CMLs in regulating PID kinase. To overcome the redundancy and identify the biological function of the CaM/CML-PID interaction, in **Chapter 3** we mapped the CaM/CMLs-binding domain in PID in order to identify the key amino acids responsible for CaM/CMLs-binding, with the final aim to generate an ‘untouchable’ but still fully functional version of PID. Complementation of the *pid* loss-of-function mutant should then reveal the role of the calcium-dependent CaM/CML binding to PID. First, we confirmed that PID associates to the PM by the insertion domain (ID) in the catalytic kinase core. Subsequent fine mapping of the CaM/CML binding domain in PID showed that both CaM/CML binding and PM association converge at an amphipathic alpha helix in the PID ID. Disruption of this amphipathic alpha helix by substitution of several positively charged arginines by alanines (RtoA) interfered with both CaM/CML binding and PM association. Surprisingly, the PID(RtoA) versions showed the same overexpression phenotypes as wild-type PID and complemented the pin-like inflorescence phenotype of the *pid* mutant, when expressed under the *PID* promoter. These results indicate that dominant PM association is not essential for PID function and that the ‘untouchable’ PID(RtoA) versions enable us to finally unravel the role of the calcium-dependent PID-CaM/CML interaction in plant development.

In **Chapter 4**, we utilized the *pid-14* mutant lines expressing ‘untouchable’ PID(RtoA) versions to study the role of the calcium-dependent PID-CaM/CML interaction in plant development. Initial phenotypic analyses of these plants suggested that the mutant PID versions were fully functional, as they did not alter

seedling development or flowering time and complemented the *pin*-like inflorescence phenotype of the *pid* mutant. However, closer inspection of the inflorescences of these plants showed clear defects in the spiral phyllotaxis, ranging from deviating divergence angles between subsequent flowers and fruits to the simultaneous initiation of flower primordia. These phenotypes were reflected in the increased number and randomized position of PIN convergence points and resulting auxin maxima in the inflorescence meristems (IMs) of the ‘untouchable’ PID expressing plants.

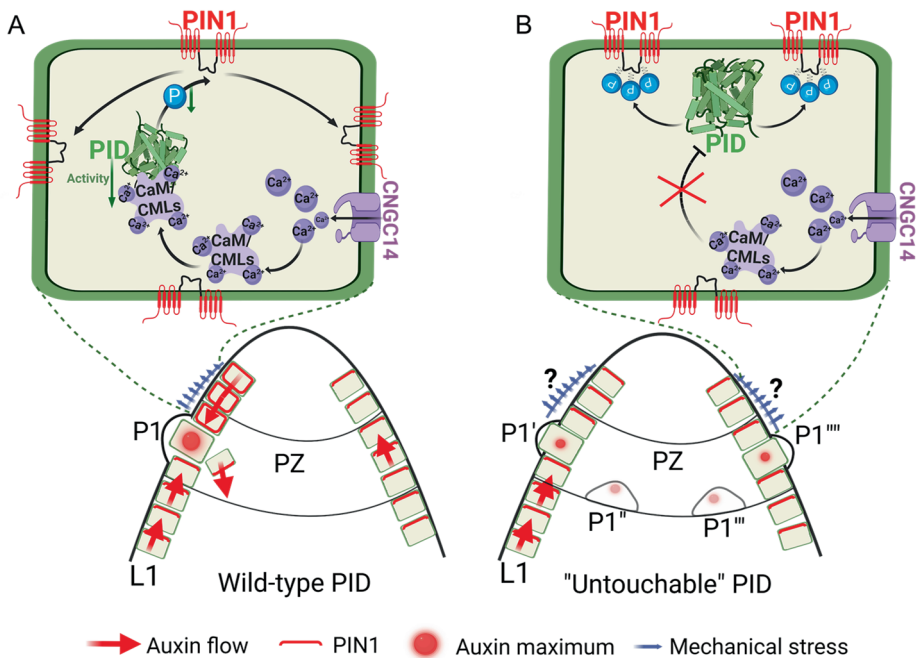


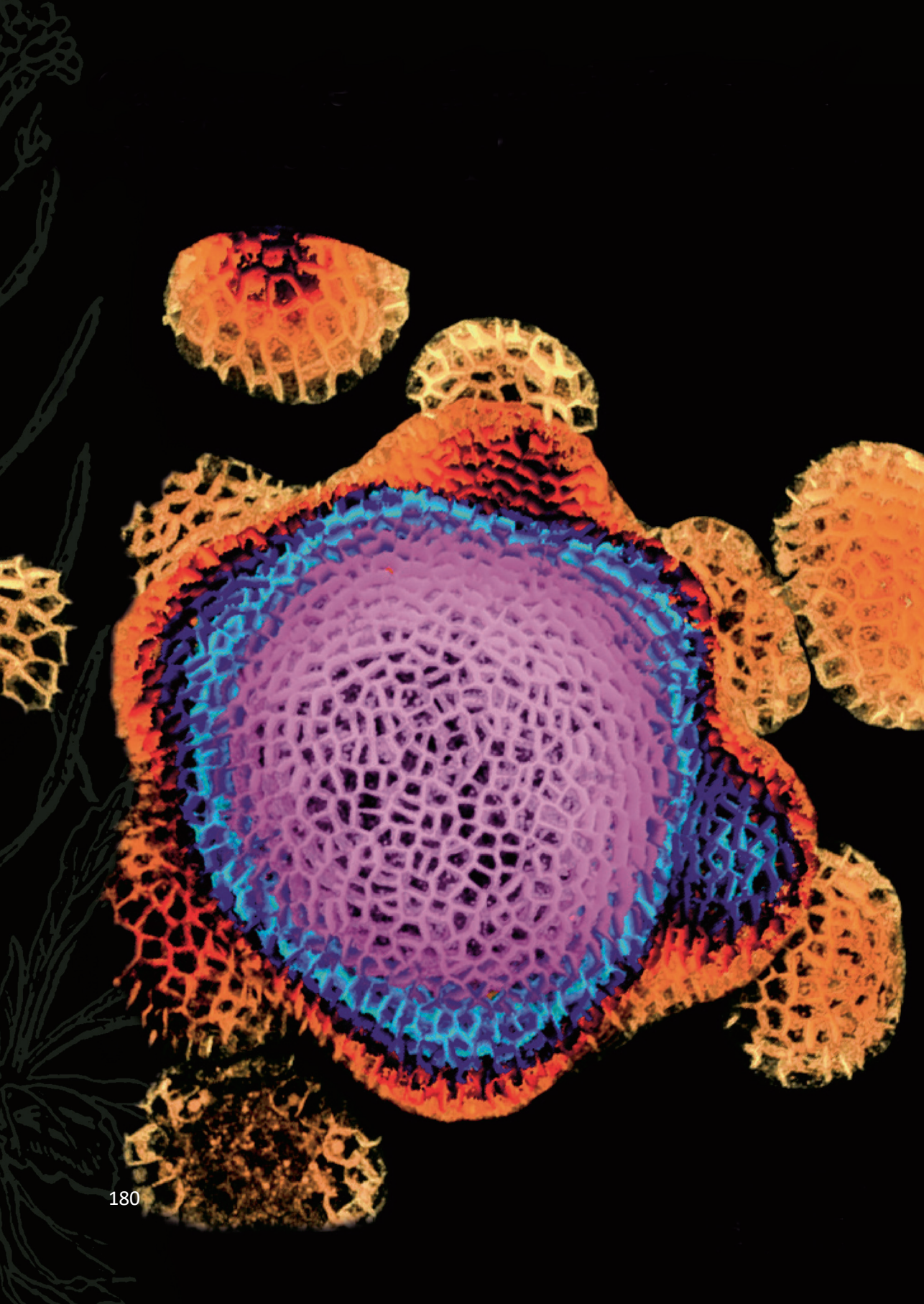
Figure 1. Model for the involvement of the CaM/CMLs-PID interaction in positioning primordia in the Arabidopsis IM. A) A single strong, perfectly positioned auxin maximum appearing in a wild-type Arabidopsis IM. **B)** The stochastic, simultaneous appearance of weaker auxin maxima in Arabidopsis lines expressing “untouchable” PID. L1 indicates the epidermis; PZ = peripheral zone; P1 = newly initiated floral primordia. ? = indicates that due to irregular phyllotaxis the position of mechanical stress will be unclear.

Previous research has indicated that the spiral phyllotaxis observed in Arabidopsis inflorescence meristems (IMs) is the result of an interplay between PIN1-generated auxin maxima and mechanical stress imposed on (cells in) the IM by the

continuous initiation and outgrowth of new floral primordia. Ca^{2+} signalling has been proposed as mediator connecting the auxin and mechanical stress pathways, however, the signalling components involved have remained elusive. Based on the results presented in this thesis, we now propose a model in which the previously discovered Ca^{2+} -dependent regulation of PID activity by CaM/CML binding provides the missing link (Figure 1). In this model, PID phosphorylation-directed apical PIN1 causes cell-to-cell transport of auxin through the shoot epidermis to the peripheral zone of the IM. The growth of the regularly positioned young floral primordia impose mechanical stress on the IM, resulting in a stress maximum in cells just above the position where the next primordium will be initiated. This stress maximum triggers PM-localized Ca^{2+} channels, resulting in elevated cytosolic Ca^{2+} levels and the subsequent activation of CaM/CMLs and their binding to the PID kinase. Due to the inhibited kinase activity, PIN1 proteins become dephosphorylated and their reduced apical polarity results in auxin accumulation in the cells below. The enhanced auxin levels in these cells again lead to elevated cytosolic Ca^{2+} levels and CaM/CML-mediated depolarization of PIN1, finally resulting in a single strong auxin maximum and thus in the initiation of a perfectly positioned floral organ (Figure 1A). In the lines expressing “untouchable” PID, the mechanical stress-induced depolarization of PIN1 does not occur, causing auxin maxima to appear, regularly simultaneous, in a stochastic manner, resulting in the observed defects in spiral phyllotaxis (Figure 1B). The irregular phyllotaxis is likely to have an effect on the mechanical stress in the IM, and thus positions of stress maxima will also be stochastic.

The results described in thesis provide new insights into how organ initiation at the Arabidopsis IM is coordinated and how the spiral phyllotaxis pattern is maintained. Still, there are some unanswered questions. Firstly, in **Chapter 2** we show that a confined clade of the CaM/CMLs gene family interact with and regulate the PID kinase. However, the precise expression pattern of the CaM/CMLs in the IM has to be determined to know which of the PID interacting CaM/CMLs are responsible

for translating mechanical stress and auxin induced Ca^{2+} peaks into changes in PIN1 polarity. Secondly, an intriguing finding in **Chapter 3** of this thesis is that, despite the predominant cytosolic localization of the “untouchable” PID versions, they were able to complement most defects of the *pid* mutant, showing that these mutants version are functional kinase *in vivo*. A more detailed study on how this happened would gain a much better understanding on the significance of the PM-association of PID as one of the key regulators of polar auxin transport. Thirdly, our model in Figure 1 relies on a few assumptions, an important one being the occurrence of a mechanical stress maximum above the epidermal cells in the peripheral zone of the IM where the new primordium will be initiated. Such a stress maximum could possibly be detected by temporary PIN1 depolarization event. Another option would be to use recently designed molecular probes to detect mechanical stress in cell walls. We have tried both options, but they appeared technically challenging. Currently we are trying to use the sequestration of PID to the cytosol to localize the mechanical stress maxima. An alternative option would be to generate a fluorescent probe based on the interaction between PID and CaM/CML. Hopefully, one of the approaches mentioned above will allow us to obtain a better understanding of how the Ca^{2+} -dependent CaM/CML-PID interaction integrates hormonal and abiotic signals that trigger elevations in $[\text{Ca}^{2+}]_{\text{cyt}}$, such as auxin and mechanical stress, to generate robustness in the spiral phyllotaxis that is typical for the Arabidopsis inflorescence.



Samenvatting

Vanwege hun sessiele levenswijze hebben planten een vernuftig systeem ontwikkeld om te overleven in hun steeds veranderende en vaak ongunstige omgeving. Het plantenhormoon auxine speelt daarbij een centrale rol, mede omdat het zeer basale cellulaire processen reguleert, zoals celdeling, groei en differentiatie. Het is daardoor betrokken bij een grote verscheidenheid aan biologische processen die de groei en ontwikkeling van planten bevorderen en beïnvloeden in reactie op een breed scala aan endogene en omgevingssignalen.

De afgelopen decennia is er een schat aan informatie over de biosynthese, het metabolisme, het transport en de signalering van auxine beschikbaar gekomen. In **Hoofdstuk 1** worden een aantal van deze processen besproken, met de nadruk op auxineperceptie en signaaltransductie, de distributie van het hormoon door PIN-FORMED (PIN) auxine-efflux carrier-gedreven polair auxinetransport (PAT), en hoe het bivalente kation calcium (Ca^{2+}), een universele tweede boodschapper, betrokken is bij het vertalen van zowel endogene als omgevingssignalen in auxine-gemedieerde ontwikkeling en groei. Intensief onderzoek heeft de afgelopen jaren verschillende signaaltransductieroutes voor auxine aan het licht gebracht. De standaard auxine-signalering vindt plaats in de kern, waarbij de TRANSPORT INHIBITOR RESPONSE 1 (TIR1)/AUXIN-SIGNALING F-BOX (AFB) F-box-eiwitten, door auxine-gemedieerde rekrutering en ubiquitinering van Aux/IAA-repressoreiwitten, AUXINE RESPONS FACTOREN (ARF) vrijmaken om gentranscriptie te activeren. Daarnaast is er de herontdekte AUXIN BINDING PROTEIN 1 (ABP1) signaalroute, waarbij gecoördineerde binding van auxine aan ABP1 en het plasmamembraan (PM) gelokaliseerde TRANSMEMBRANE KINASE 1 (TMK1) onder andere leidt tot celwandverzuring door activering van H^+ -ATPasen. Bovendien heeft identificatie van de rol van S-Phase Kinase-Associated Protein 2A (SKP2A), ARF3 en IAA32/33/34 in auxinesignaaltransductie een beter begrip opgeleverd van de complexiteit van de

cellulaire auxine responsen. Vervolgens wordt de huidige kennis over het PIN-gedreven PAT behandeld. De richting en snelheid van de intercellulaire auxinestroom is voornamelijk afhankelijk van de asymmetrische lokalisatie en activiteit van PIN eiwitten aan het PM, waarbij Ca^{2+} -signalering betrokken is, en die wordt gereguleerd door fosforylering van de centrale hydrofiele lus in PIN eiwitten door plant-specifieke AGC proteïnekinasen.

Eén van deze AGC proteïnekinasen in *Arabidopsis thaliana* (Arabidopsis), het membraan-geassocieerde AGC3-kinase PINOID (PID), is een belangrijke regulator van PAT en fungeert als een binaire schakelaar in de apicaal-basale polaire targeting van PIN auxine-effluxcarriers naar het PM, die daarmee de richting van de auxinestroom bepalen. Eerder was gevonden dat PID op een Ca^{2+} -afhankelijke wijze interacteert met CALMODULIN-LIKE 12/TOUCH 3 (CML12/TCH3) en met het EF-hand-bevattende PID-BINDING PROTEIN 1 (PBP1). Deze vinding leverde één van de eerste moleculaire inzichten hoe Ca^{2+} mogelijk betrokken is bij de regulering van PAT. CML12/TCH3-binding inhibeert de activiteit van het PID-kinase, zowel *in vitro* als *in vivo*, en de interactie met CML12/TCH3 zorgt ervoor dat het PID kinase van het PM naar het cytosol beweegt. Bovendien veroorzaken verhoogde lokale auxineconcentraties een transiënte toename van de Ca^{2+} niveaus in het cytosol en een snelle en significante toename in *CML12/TCH3* expressie. Voortbouwend op deze eerdere bevindingen, wordt aan het einde van **Hoofdstuk 1** een alternatief model voor de rol van Ca^{2+} -afhankelijke CML12/TCH3-PID-signalering in de terugkoppeling van auxine op PIN polariteit voorgesteld.

In **Hoofdstuk 2** is de Ca^{2+} -afhankelijke regulering van het PID kinase door CML12/TCH3 verder onderzocht. De *tch3* verlies-van-functie mutant vertoont slechts een mild fenotype, wat suggereert dat andere CMLs en mogelijk ook CaMs redundant functioneren met CML12/TCH3. De eerste stap was daarom te testen of andere CMLs of CaMs met PID interacteren. Door middel van *in vitro* pull-downs en de Bimolecular Fluorescence Complementation (BiFC)-assay is aangetoond dat een specifieke groep bestaande uit zeven CaMs en drie CMLs (CML8, CML10,

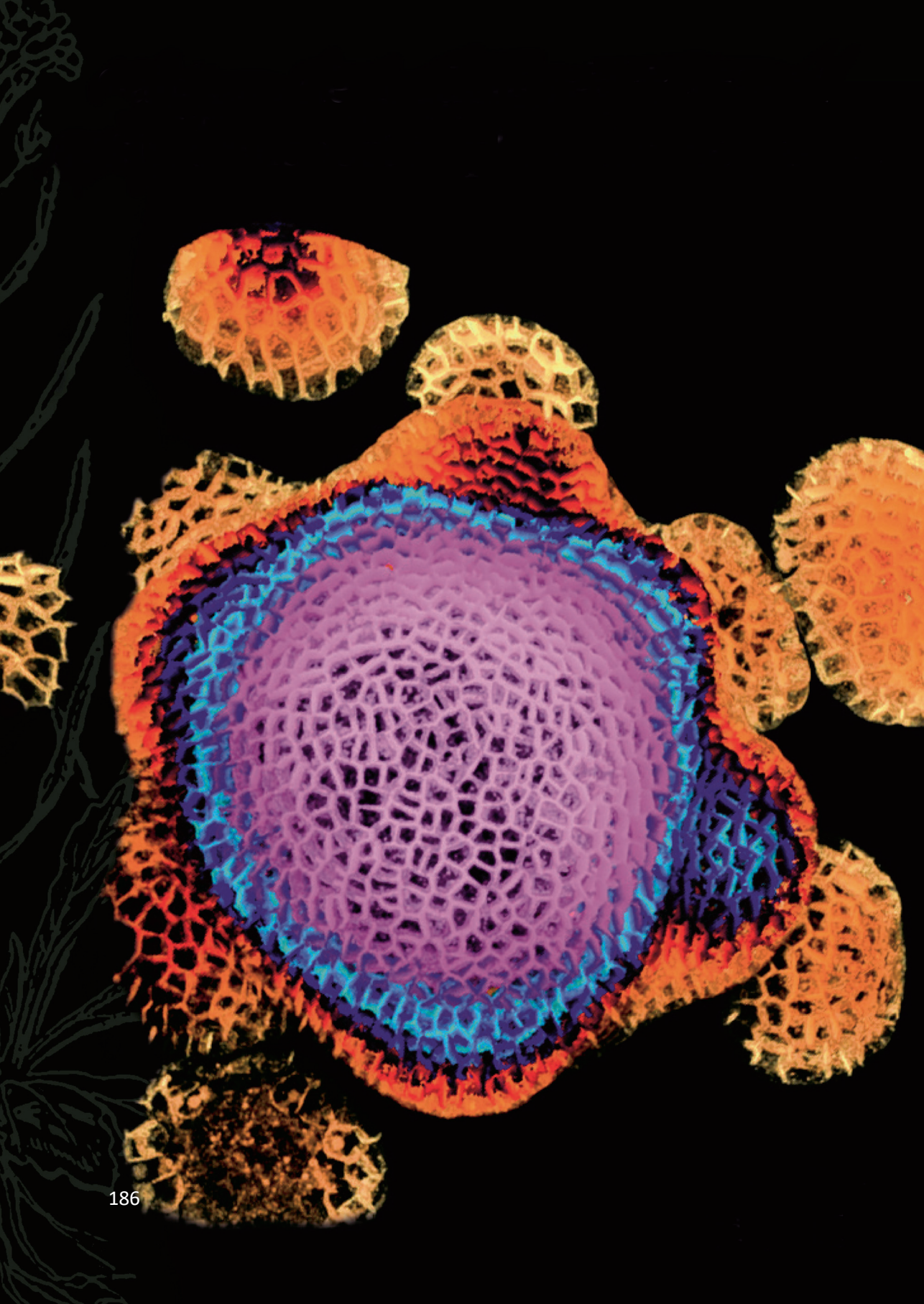
CML11), die het nauw verwant zijn aan CML12/TCH3, ook interacteren met PID. Co-expressie in *Arabidopsis* protoplasten van PID met deze CaM/CMLs in de aanwezigheid van auxine resulteerde in dissociatie van PID van het PM. Vervolgens is met behulp van *promoter:GUS* reporterfusies de spatio-temporele expressie van de overeenkomstige *CaM/CML* genen en *PID* met elkaar vergeleken. Deze analyse liet zien dat de betreffende *CaM/CML* genen in de meeste weefsels gedurende alle ontwikkelingsstadia tot expressie komen, en dat de expressiepatronen naast duidelijke verschillen ook grotendeels overlappen.

De resultaten suggereren dat er functionele redundantie bestaat tussen de CaM/CMLs die met het PID kinase interacteren. Om deze redundantie te omzeilen en daarmee de biologische functie van de CaM/CML-PID-interactie te kunnen bestuderen, is in **Hoofdstuk 3** het CaM/CML-bindend domein in PID in kaart gebracht. Het hoofddoel was aminozuren te identificeren die verantwoordelijk zijn voor CaM/CML-binding, om met deze kennis door middel van aminozuursubstituties 'untouchable' maar nog steeds functionele versies van PID te genereren. Complementatie van de *pid* verlies-van functie mutant met deze versies zou dan de rol van de Ca^{2+} -afhankelijke CaM/CML-binding aan PID moeten onthullen. Allereerst hebben we bevestigd dat PID zich associeert met het PM via het insertiedomein (ID) in het katalytische kinase domein. Vervolgens is het CaM/CML-bindende domein in PID in kaart gebracht. Het onderzoek toonde aan dat zowel CaM/CML-binding als PM-associatie plaats vindt via een amfipatische alfa-helix in het ID van PID. Verstoring van deze amfipatische alfa-helix door substitutie van positief geladen arginines door alanines (R-naar-A) verstoorte zowel CaM/CML-binding als PM-associatie. Verrassend genoeg resulteerde overexpressie van deze PID(R-naar-A) versies in dezelfde fenotypes als wildtype PID en complementeerden ze, wanneer tot expressie gebracht onder de *PID* promotor, het pin-achtige bloeiwijzefenotype van de *pid* mutant. Deze resultaten geven aan dat PM-associatie niet essentieel is voor PID functie en dat de 'untouchable' PID(R-naar-A) versies ons in staat stellen om eindelijk de rol van de

Ca²⁺-afhankelijke PID-CaM/CML interactie in de ontwikkeling van planten te ontrafelen.

In **Hoofdstuk 4** zijn de plantenlijnen die ‘untouchable’ PID(R-naar-A) versies onder de *PID* promoter in de *pid* mutante achtergrond tot expressie brengen in meer detail geanalyseerd. De zaailingontwikkeling en bloeitijd van deze planten bleek vergelijkbaar met wildtype Arabidopsis. Nadere inspectie van de bloeiwijzen bracht echter duidelijke afwijkingen in de spiraalvormige phyllotaxis aan het licht, variërend van afwijkende divergentiehoeken tussen opeenvolgende bloemen en vruchten tot de gelijktijdige initiatie van bloemprimordia. Deze fenotypes kwamen overeen met een toename in het aantal en de gerandomiseerde positie van PIN-convergentiepunten en de resulterende auxinemaxima in de bloeiwijzemeristemen van deze planten.

De resultaten beschreven in dit proefschrift geven nieuwe inzichten in hoe signalen zoals auxine en mechanische stress, die orgaanvorming in het Arabidopsis bloeimeristeem sturen, via Ca²⁺-signalering worden geïntegreerd door de CaM/CML-PID module, die daarmee zorg draagt voor een robuuste spiraal fyllotaxis die typisch is voor de Arabidopsis bloeiwijze.



Curriculum Vitae

Xiaoyu Wei was born on July 15th, 1989, in Yan'an city, Shaanxi province, China. In 2008, he started his Bachelor's study at the College of Plant Science & Technology, Huazhong Agricultural University (Wuhan, China). In 2012 he obtained his Bachelor's degree in Agriculture, and started his Master study at the College of Horticulture, Northwest Agriculture and Forestry University (Xi'an, China), under the supervision of Prof. dr. Li Mingjun. His Master project focused on "Genome-based expression analysis and function identification of sugar transporter genes in apple." In 2015, he obtained his Master's degree in pomology, and in the same year he obtained a fellowship from the China Scholarship Council to support his doctoral research in the laboratory of Prof. dr. Remko Offringa at the Institute of Biology of Leiden University, The Netherlands. During his PhD research, he focussed on the role of calcium-dependent regulation of auxin transport polarity in plant development as is described in this thesis.

